The Biological Role of Extracellular Matrix in Ovarian Cancer Metastasis.

Miranda Ween (B.Sc. (Biomedical Science) (Hons))

For the Degree of Doctor of Philosophy

University of Adelaide

From the Research Centre for Reproductive Health, Robinson Institute, Discipline of Obstetrics and Gynaecology, Faculty of Health Sciences, University of Adelaide.

October 2010

TABLE OF CONTENTS

TABLE OF FIGURES

TABLE OF TABLES

SUMMARY

Ovarian cancer metastasis is characterized by the shedding of malignant cells from the surface of the ovary and their implantation onto the peritoneal surface which lines the abdominal cavity. As the factors promoting this process are poorly understood, we investigated the ovarian cancer–peritoneal interaction by means of *in vitro* co-culture experiments with ovarian cancer (OVCAR-3, OVCAR-5, and SKOV-3) and peritoneal (LP-9) cells. In this system, we identified by mass spectrometry that levels of transforming growth factor β inducible protein (TGFBIp), periostin, fibronectin, plasminogen activator inhibitor-1, cytokeratins 1, 5, 6C, 9, 10, 14, and 16, transketolase, annexin A2, annexin A6, and elongation factor-2 were modulated as a result of direct contact between peritoneal and ovarian cancer cells or through interactions via shared media.

We went on to investigate the functional role of the extracellular matrix (ECM) protein, TGFBIp in ovarian cancer. Immunohistochemistry showed high TGFBIp levels in normal surface ovarian epithelial and peritoneal cells whilst in comparison, TGFBIp levels in primary serous ovarian carcinomas and matching metastatic implants were greatly reduced. In functional *in vitro* experiments, rTGFBIp significantly increased the motility and invasion of OVCAR-5 and SKOV-3 cells and significantly increased ovarian cancer cell (OVCAR-5, OVCAR-3 and SKOV-3) adhesion to peritoneal (LP-9) cells which was reversed by addition of a neutralizing TGFBIp antibody. We also demonstrated that the increases in OVCAR-5 cell adhesion, motility, and invasion, were independent of the Arg-Gly-Asp (RGD) motif in the C-terminal domain of TGFBIp. We conclude that TGFBIp expressed by peritoneal cells increases the metastatic potential of ovarian cancer cells. TGFBIp is therefore a potential novel therapeutic target against ovarian cancer.

Further investigation determined that secreted TGFBIp was processed at both the N- and C-terminal domains during ovarian cancer–peritoneal cell co-culture in the same amino acid range as that of TGFBIp cleaved by plasmin. Plasmin was found to be upregulated within 1 hr of co-culture and TGFBIp processing in the *in vitro* co-culture system could be blocked by a plasmin inhibitor, 6-aminocaproic acid (ε-ACA) and a broad spectrum protease inhibitor which inhibits plasmin but not matrix metalloproteinases (MMPs). Furthermore, the processing was not blocked by an MMP inhibitor, GM6001. We therefore conclude that TGFBIp is cleaved by plasmin and not an MMP during peritoneal-ovarian cancer co-culture.

In summary, these studies have shown, that when peritoneal cells are allowed to interact with ovarian cancer cells, whether by direct contact or by shared growth media which occurs at different steps of ovarian cancer metastasis, a proteolytic response is triggered.

We also investigated the expression of other ECM components in ovarian cancer; the proteoglycan versican, the polysaccharide hyaluronan (HA), and one of its receptors, CD44, in ovarian cancer tissues and their role in the metastatic behaviour of ovarian cancer cells. We found that a higher proportion of serous ovarian carcinoma had high stromal versican when compared with normal ovary and high stromal CD44 when compared with normal and benign serous tumours. Although high stromal versican was positively correlated with high stromal HA, stromal HA was not increased in serous ovarian carcinoma when compared with normal ovary or benign serous tumours.

We determined that the assembly of a HA-versican pericellular sheath around ovarian cancer cells could promote the motility of metastatic CD44 expressing OVCAR-5 and

SKOV-3 cells, but not by low-metastatic OVCAR-3 cells which lack CD44. The motility of OVCAR-5 and SKOV-3 cells was significantly increased in scratch wound and chemotaxis assays following treatment with recombinant versican. We demonstrated that small HA oligosaccharides (6-10) were able to significantly block formation of pericellular sheath, motility, and invasion of OVCAR-5 cells following treatment with versican. Treatment with exogenous HA increased ovarian cancer cell adhesion to peritoneal cells, and this increase was successfully blocked by the addition of HA oligosaccharides or treatment of the LP-9 monolayer with hyaluronidase. These novel findings indicate that the acquisition of a HA-versican pericellular sheath by ovarian cancer cells may aid their peritoneal dissemination and metastasis. Our results suggest that HA oligosaccharides may be effective at inhibiting the invasion of CD44 positive ovarian cancers and warrants further study as a potential therapy.

Overall, the studies in this thesis indicate a very strong role for the tumour microenvironment, and in particular the proteolysis of proteins in the tumour microenvironment. Further investigation will increase our understanding of the mechanisms and pathways involved in the proteolytic cascade which is triggered during ovarian cancer metastasis.

DECLARATION

I certify that this thesis contains no material which has been accepted for the award of any other degree or diploma in any univeristy or other tertiary institution to Miranda Ween and, to the best of my knowledge and belief, contains no material previously published or written by another person, except where due reference has been made in the text.

I give consent for this copy of my thesis, when deosited in the University Library, being made available for loan and photocopying, subject to the provisions of the Copyright Act 1968.

I also give permission for the digital version of my thesis to be made available on the web, via the University's digital research repository, the Library catalogue, the Australasian Digital Theses Program (ADTP) and also through web search engines, unless permission has been granted by the University to restrict access for a period of time.

Miranda Ween

October 2010

ACKNOWLEDGEMENTS

I have been fortunate enough to work in an environment full of generous people who have shared their time and expertise with me. I wish to acknowledge the following people in particular:

Professor Richard LeBaron (University of Texas at San Antonio, USA), for his donation of CHO K1, CHO V1 cells as well as his versican Vc Antibody.

Dr. Stephen Williams (Fox Chase Cancer Center, Philadelphia, USA), for his donation of OVCAR-5 cells.

Dr. Judith Clements (Queensland University of Technology, Brisbane, Australia), for her donation of OVCAR-3 and SKOV-3 cells.

Associate Professor Margaret Davy and Dr. Tom Dodd (Department of Gynaecological Oncology, Royal Adelaide Hospital), for providing ovarian tissue samples.

Mark Condina, Dr. Alex Collella, Chris Cusaro, Chris Bagley, and Dr. Peter Hoffmann, for performing the proteomic screening and mass spectrometry presented in chapters 2 and 3 and their unlimited patience in explaining the data to me.

Aleksandra Ochink, Shalini Jindal, and Helen Hughes (Dame Roma Mitchell Laboratory at the Hanson Institute, Adelaide), for their assistance in gathering of ovarian cancer tissues and formation of tissue micro-arrays used for all of the immunohistochemistry work in this thesis.

Ang Zhou, for happily teaching me his invasion model.

Kate Frewin, for scanning my numerous slides on the Nanozoomer with little notice.

Noor Lokman, for her enthusiasm and for performing the annexin A2 western and the plasmin assay.

Dr. Martin Oehler (Department of Gynaecological Oncology, Royal Adelaide Hospital), for collecting ovarian cancer samples from his patients and for his supervision of my

PhD. In particular I would like to thank the generous women of Adelaide who donated their tissue and serum for this project.

Professor Raymond Rodgers, for his expert advice, both scientific, and of university administrative processes throughout his supervision of my PhD.

Dr. Carmela Ricciardelli for her unending patience with me over the past 6 years as she taught me everything she knows both about science and work/life balance, for her unceasing enthusiasm for this project, and for her committed supervision of this PhD.

Finally, I thank my fellow PhD students, for their companionship and willingness to lend an ear when things weren't their best and their words of encouragement.

PUBLICATIONS ARISING DURING PHD CANDIDATURE

Ricciardelli C, Russell DL, Ween MP, Mayne K, Byers S, VR Marshall Tilley WD and Horsfall DJ. Formation of hyaluronan-and versican- rich pericellular matrix by prostate cancer cells promotes cell motility (J Biol Chem 2007)

Invited Review article - Ricciardelli C, Sakko AJ, Ween MP, Russell DL, Horsfall DJ. The biological role and regulation of versican levels in cancer. (Cancer Metastasis Rev 2009)

Invited Book chapter - Ricciardelli C, Sakko AJ, Ween MP, l Russell DL & Horsfall DJ. The proteoglycan versican: an important regulator of cell locomotion in development and disease. In "Cell Movement: New Research Trends". Nova Science Publishers, Inc. Hauppauge, NY. (Accepted 1st August 2008) Pub. Date: 2009 - 3rd Quarter, ISBN: 978-1-60692-570-6)

Ween MP, Hoffmann P, Rodgers RJ, Ricciardelli C and Oehler MK. Transforming growth factor beta-induced protein (TGFBIp) secreted by peritoneal mesothelial cells increases the metastatic potential of ovarian cancer cells (Accepted 12th of May 2010 for publication in the *International Journal of Cancer* Feb 2010).

Ween MP, Rodgers RJ, Oehler MK & Ricciardelli C. HA oligosaccharides inhibit pericellular matrix formation and ovarian cancer cell motility and invasion induced by the extracellular matrix protein versican. (In revision, Clinical and Experimental Metastasis).

Lokman N, Ween MP, Hoffmann P, Oehler MK & Ricciardelli C. Annexin A2 in ovarian cancer metastasis (In preparation).

PRESENTATIONS AT SCIENTIFIC MEETINGS

Reid K, Ween MP, Dodd T, Davy M, Rodgers R, Oehler MK & Ricciardelli C. Extracellular matrix proteins as prognostic markers for serous ovarian cancer. Australian Gynaecological Society meeting, Melbourne, VIC, May 2008.

Ween MP, Oehler MK, Rodgers RJ & Ricciardelli C. Formation of HA and versican rich pericellular matrix aids ovarian cancer motility. Australian Society for Medical Research, SA Meeting, Adelaide, South Australia, June 2008.

Ween MP, Oehler MK, Rodgers RJ & Ricciardelli C. Versican induces pericellular sheath formation and motility by ovarian cancer cells expressing CD44. Matrix Biology Society of Australia and New Zealand, Ettalong, NSW, October 2008.

Oehler MK, Ween MP, Hoffmann P, & Ricciardelli C. Proteomics of Ovarian Cancer Implantation. Australian and New Zealand Gynaecological Oncology group, Noosa, QLD April 2009 (Selected for oral presentation).

Ween MP, Hoffmann P, Rodgers RJ, Ricciardelli C, & Oehler MK. Transforming growth factor induced protein TGFBIp promotes ovarian cancer cell motility and adhesion to peritoneal cells Australian Society for Medical Research, SA Meeting, Adelaide, South Australia, June 2009 (Selected for oral presentation).

Ween MP, Hoffmann P, Rodgers RJ, Ricciardelli C, & Oehler MK. Transforming growth factor induced protein TGFBIp promotes ovarian cancer cell motility and adhesion to peritoneal cells. Society of Reproductive Biology, Adelaide, South Australia, August 2009.

Ween MP, Hoffmann P, Rodgers RJ, Ricciardelli C, & Oehler MK. Transforming growth factor induced protein TGFBIp promotes ovarian cancer cell motility and adhesion to

peritoneal cells. Matrix Biology Society of Australia and New Zealand, Barossa Valley, South Australia, October 2009 (Selected for oral presentation).

Ween MP, Hoffmann P, Rodgers RJ, Ricciardelli C, & Oehler MK. Transforming growth factor induced protein TGFBIp promotes ovarian cancer cell motility and adhesion to peritoneal cells. 5th International Conference on Tumour Microenvironment, Versailles, France, October 2009 (Selected for oral presentation).

Ween MP. The role of extracellular matrix proteins versican and TGFBIp in ovarian cancer metastasis. Invited speaker at the School of Biosciences at Cardiff University, Wales, October 2009.

ABBREVIATIONS

ACN	–	Acetonitrile
ADAMTS	–	Adamalysin with Thrombospondin type 1 Motifs
AR	–	Androgen Receptor
BK	–	Bradykinin
CA125	–	Cancer Antigen 125
CD44s	–	Standard CD44
CD44v	–	CD44 variants
ChABC	–	Chondroitinase ABC
CK-1	–	Cytokeratin-1/Keratin Type II Cytoskeletal 1
CK-5	–	Cytokeratin-5/Keratin Type II Cytoskeletal 5
CK-6C	–	Cytokeratin-6C/Keratin Type II Cytoskeletal 6C
CK-9	–	Cytokeratin-9/Keratin Type I Cytoskeletal 9
CK-10	–	Cytokeratin-10/Keratin Type I Cytoskeletal 10
CK-14	–	Cytokeratin-14/Keratin Type I Cytoskeletal 14
CK-16	–	Cytokeratin-16/Keratin Type I Cytoskeletal 16
CM	–	Conditioned Medium
CS	–	Chondroitin Sulphate
C-Terminal Domain	–	Carboxy Terminus Domain
DB	–	Dilution Buffer
DCIS	–	Ductal carcinoma *in situ*
ε-ACA	–	6-Aminocaproic Acid
ECL	–	Enhanced Chemiluminesence
ECM	–	Extracellular Matrix
EGF	–	Epidermal Growth Factor
EHS	–	Engelbreth-Holm-Swarm
ELISA	–	Enzyme Linked Immunosorbent Assay
EMI	–	Emilin and Multimerin
EPHX	–	Epoxide Hydrolase
ER	–	Oestrogen Receptor
FAS	–	Fasciclin
FIGO	–	International Federation of Gynaecologists and Obstetricians
GM6001	–	Galardin
H & E	–	Haematoxylin and Eosin
HA	–	Hyaluronan
HAase	–	Hyaluronidase
HER	–	Human Epidermal Growth Factor Receptor
HK	–	High Molecular Weight Kininogen
HMEC	–	Human Mammary Epithelial Cell
IPG	–	Immobilized pH Gradient
KO	–	Knockout

LC-ESI	–	Liquid Chromatography-Electrospray Ionisation
LMP	–	Low Malignant Potential
MALDI-TOF/TOF	–	Matrix Assistant Laser Desorption/Ionisation Time of Flight/Time of Flight
MMP	–	Matrix Metalloproteinase
MPNST	–	Malignant Peripheral Nerve Sheath Tumour
MS	–	Mass Spectrometry
N-Terminal Domain	–	Amino Terminus Domain
Oligo	–	Oligosaccharide
OSE	–	Normal Ovarian Surface Epithelial Cells
PAGE	–	Polyacrylamide Gel Electrophoresis
PAI-1	–	Plasminogen Activator Inhibitor-1
PBCA	–	Poly Butyl Cyanoacrylate
PBS	–	Phosphate Buffered Saline
PBS-T	–	Phosphate Buffered Saline with 0.05% Tween-20
PDGF	–	Platelet Derived Growth Factor
PEI	–	Polyethylenimine
PI	–	Broad Spectrum Protease Inhibitor
PR	–	Progesterone Receptor
RAAS	–	Renin Angiotensin Aldosterone System
RAH	–	Royal Adelaide Hospital
RGD	–	Arg-Gly-Asp
RT	–	Room Temperature
rTGFBIp	–	Recombinant TGFBIp
rV1	–	Recombinant Versican Isoform V1
SDS	–	Sodium Dodecyl Sulphate
SMCs	–	Smooth Muscle Cells
SNP	–	Single Nucleotide Polymorphism
TGFβ	–	Transforming Growth Factor β
TGFBIp	–	Transforming Growth Factor Inducible Protein
TKT	–	Transketolase
tPA	–	Tissue Type Plasminogen Activator
uPA	–	Urokinase Type Plasminogen Activator
uPAR	–	Urokinase Plasminogen Activator Surface Receptor
VEGF	–	Vascular Endothelial Growth Factor

CHAPTER 1 - GENERAL INTRODUCTION

1.1. BACKGROUND

1.1.1. Introduction to ovarian cancer

One hundred thousand cancer cases are diagnosed in Australia each year and approximately 1,100 of these are ovarian cancer. Ovarian cancer is the ninth most common cancer in women and has a frequency of 2.7% and has an overall lifetime risk of 1 in 77 [1]. However, it has the sixth highest mortality rate and accounts for 5.2% of all cancer related deaths [1]. This is due to more than 50% of ovarian cancers being detected at an advanced stage (III or IV). Ovarian cancer is diagnosed at an advanced stage predominantly due to non specific symptoms, and lack of a regular screening test available to the public, such as those currently available for other cancers such as breast cancer (mammograms), prostate cancer (prostate examination and prostate specific antigen blood test), and cervical cancer (pap-smears). Late stage ovarian cancer presents with widespread intra-abdominal disease and metastases, and has a much lower 5-year survival rate of only 12-30% compared with 50-90% for those diagnosed with an earlier stage of the disease [2].

The International Federation of Gynaecologists and Obstetricians (FIGO) classify ovarian tumours based on their level of progression of the primary tumour. Stage I – confined to the ovary, Stage II – extended from the ovary into the pelvic tissue, Stage III – extended from the ovary to the peritoneal lining, and stage IV – invaded through the peritoneum

and metastasised outside of the abdomen. The World Health Organisation (WHO) categorizes ovarian tumours based upon their derivation from coelomic surface epithelium, germ cells, and mesenchyme [3]. These three subsets of ovarian tumours are often known more commonly as epithelial, germ cell (which arise from the oocyte and give rise to teratomas) and stromal tumours (which includes granulosa cell tumours). Epithelial tumours account for approximately 80% of ovarian tumours (Table 1) [3-6] and are thought to arise from ovarian surface epithelial cells (OSE, Figure 1.1a). Ovarian epithelial tumours only occur in humans, and ageing hens [7]. Histopathologically and immunocytochemically, epithelial ovarian cancers are among the most complex of all human carcinomas [8]. During carcinogenesis they can acquire characteristics of the oviduct, endometrium, fallopian tubes, or the uterine cervix. Classification of these epithelial tumours (Table 1.1) is broken down into serous (fallopian tube-like), endometrioid (endometrium-like), and mucinous (endocervical-like) adenocarcinomas and the much rarer types of mixed epithelial carcinomas, squamous carcinomas, carcinosarcomas, and transitional (Brenner) tumours. Of these, serous tumours are the most common and comprise approximately 50% of all epithelial ovarian cancers [9-11].

Serous epithelial cancers morphologically exhibit a mixture of cystic, papillary, and solid growth patterns (Figure 1.1d). The key feature of malignancy is stromal invasion by the epithelial cells [3], whilst benign tumours, representing a third of all epithelial tumours, show some proliferation of the epithelial cells, but no invasion (Figure 1.1b). During progression, the cancer usually grows through the ovarian capsule and spread directly to other pelvic organs or the peritoneum.

There also exists a third category of tumours, the low malignant potential (LMP), or borderline tumours. These are classified as such by pathologists as they share common features with both the benign and malignant tumour types (Figure 1.1c). Serous borderline ovarian tumours represent up to 17% of all serous epithelial ovarian tumours. Whilst the majority of them are benign, 20% present with extra ovarian disease [4]. Affecting a much younger age group than ovarian cancer, borderline tumours have a much higher survival rate. Serous borderline tumours are often large with cystic and papillary growth areas and are present on the external surface of the ovary (Figure 1.1c). Peritoneal implants can occur in borderline ovarian tumours [12] although these implants are usually non-invasive [3].

A new model for the development and classification of epithelial ovarian cancer has been suggested [11, 13] (Figure 1.2). In this model all ovarian epithelial tumours are divided into 2 groups designated type I and type II. Type I tumours have a tendency to present as low-grade neoplasms which develop slowly from well-recognised precursors. They include low-grade micropapillary serous carcinoma, mucinous, endometrioid, and clear cell carcinoma. In contrast, type II tumours nearly always present as advanced stage, high-grade tumours, and are more aggressive. Included in this group are high-grade serous carcinomas, malignant mixed mesodermal tumours, and undifferentiated carcinomas. Apart from the clinical and pathologic differences, there are also genetic differences between these two groups summarised in Figure 1.2 and Section 1.1.2 [14].

Table 1.1. *Histological Types and subtypes of ovarian cancer and their frequencies*.

Adapted from [9-11].

Types	Frequency %
Epithelial Tumours	**80**
Serous	~50
Endometrioid	10-20
Mucinous	5-20
Clear Cell	3-10
Transitional cell/Brenner	Rare
Squamous cell	Rare
Mixed epithelial	Rare
Carcinosarcoma	Rare
Germ Cell Tumours	**10-15**
Dysgerminoma	50
Yolk sac tumours	20
Embryonal carcinoma	Low
Immature teratomas	Low
Choriocarcinoma	Rare
Polyembryomas	Rare
Mixed germ cell tumours	Rare
Stromal Tumours	**5-10**
Granulosa cell tumour	Low
Sertoli-Leydig cell tumour	Low

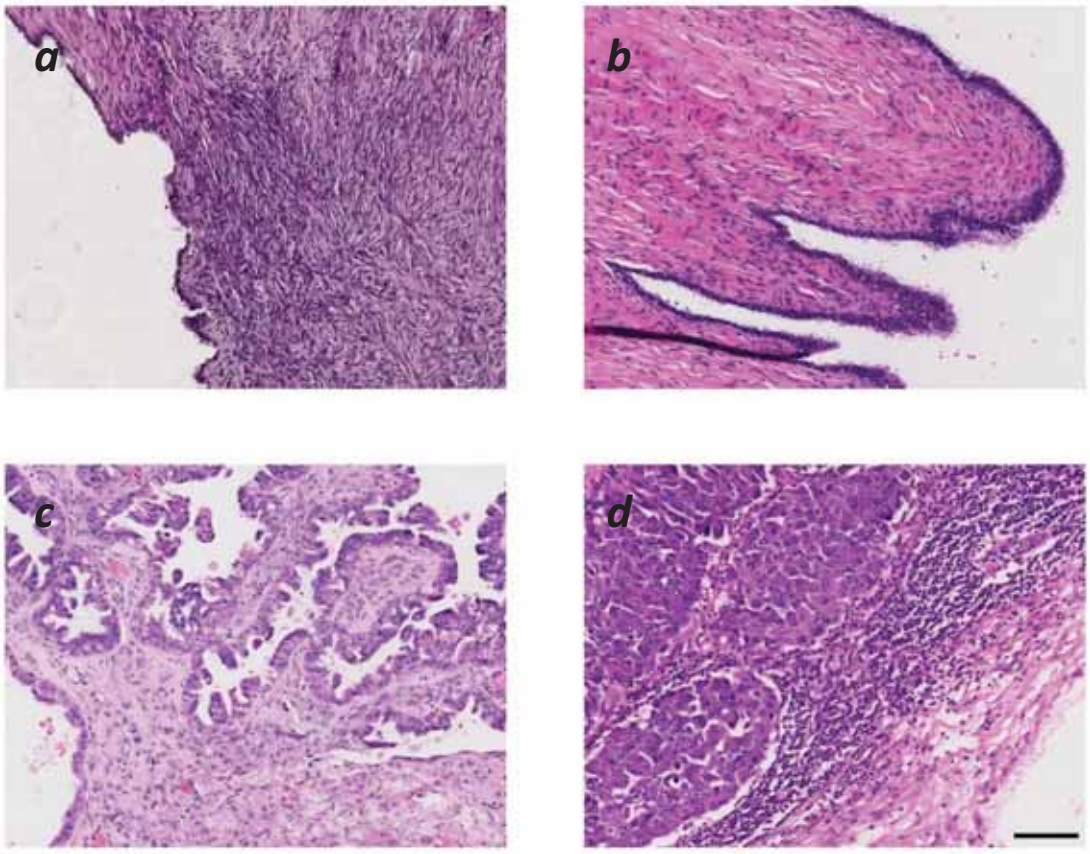

Figure 1.1. E*pithelial ovarian tumours (H & E staining).*

(a) Normal ovarian tissue (*b*) Benign serous ovarian tumour *(c)* Serous borderline tumour *(d)* Serous carcinoma. Magnification bar = 100 µm. All images are at the same magnification.

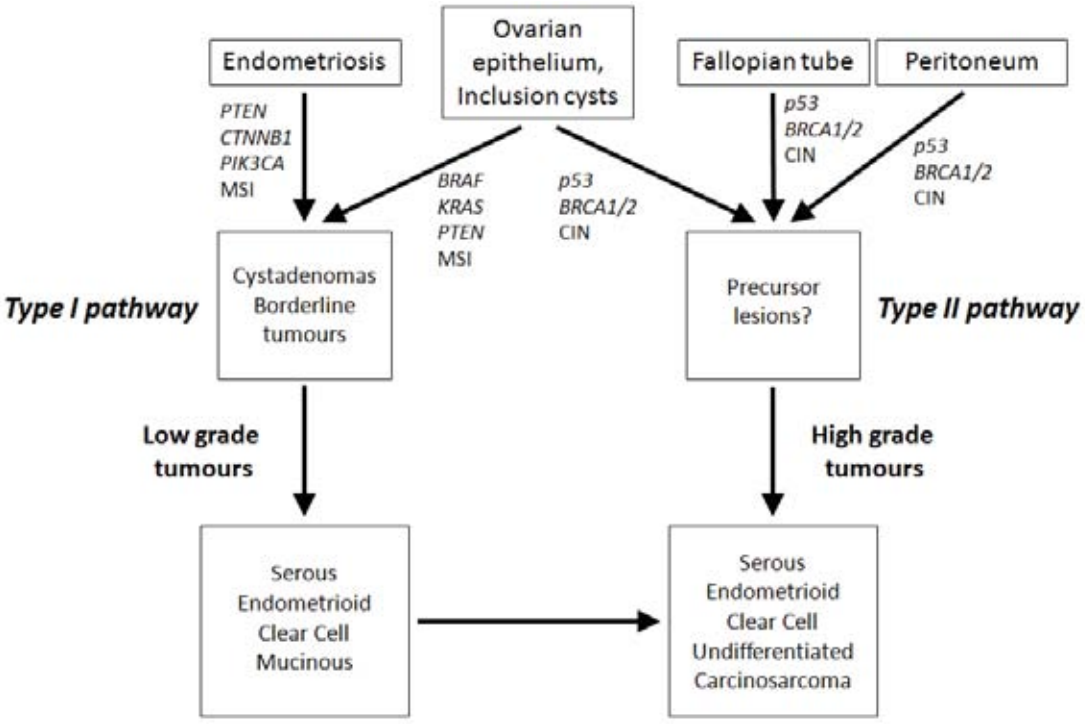

Figure 1.2. *Two-pathway concept of ovarian cancer development and potential genes involved.*

Ovarian cells progress through two possible pathways to become ovarian tumours [11].

1.1.2. Ovarian cancer risk factors

With the ever increasing development of technology in the medical and genetic field, and a growing appreciation for prospective studies, both the scientific community and the public are eager to determine exactly what puts a woman at risk of developing ovarian cancer. Is it genetic, environmental, or is it related to diet? Familial history of any type of cancer is well documented to increase the risk of developing cancer. It has been shown that occurrence of ovarian cancer in a first-degree relative (mother or sister) significantly increases the risk of ovarian cancer by greater than 5-fold [15]. Ovarian cancer in a first-degree relative also appeared to be a stronger risk factor for early-onset (≤ 50 years) ovarian cancer rather than late-onset [16].

Many genes have been investigated in relation to ovarian cancer risk. In regards to genes, the *BRCA1* and *2* genes were investigated as their mutation is very strongly associated with breast cancer [17, 18]. In a study of the *BRCA* gene and ovarian cancer association, only 1.7% of controls had a *BRCA1* or *BRCA2* mutation, whereas 29% of patients with ovarian cancer had a *BRCA1* or *BRCA2* mutation [19]. *BRCA1* in particular has been shown to play a major role in ovarian cancer susceptibility, but due to the large number of possible mutations, screening for this mutations is difficult [20]. Alterations in expression or copy number has been seen in the *TP53*, *RB1*, *OPCML*, *PIK3CA*, and *EEF1A2* genes in ovarian cancer [21-24]. The high-activity genotype of microsomal epoxide hydrolase (EPHX) has been shown to be associated with an increased ovarian cancer risk [25]. *P53,* a tumour suppressor gene, is mutated in 50% of late stage ovarian tumours, but rarely in early stage or borderline tumours [26], making

it an unlikely candidate for genetic screening. Other genes which are over-expressed or amplified in serous epithelial cancers include *cMYC* [27], *EGF-R,* and *CFMS* which are associated with poor outcome [28-30].

Currently, analysis of single nucleotide polymorphisms (SNPs) in genes which causes variations in the allelic distribution in the population is an accepted technique to find genetic association with diseases. This has also been used to predict cancer occurrence. SNPs in some of the metalloproteinases (MMPs) have been analysed and the frequency of the C allele and the C/C genotype of the *MMP2* C-735T SNP were significantly higher in epithelial ovarian cancer patients than those in healthy controls. Compared with the T/T and C/T genotypes, the C/C genotype was significantly associated with increased risk of ovarian cancer [31]. The A/G genotype and the G allele frequency of the *MMP-12* A-82G SNP was significantly higher in epithelial ovarian cancer patients than in controls. The A/A genotype of *MMP-13* 77A/G was also found to be associated with increased risk of mucinous ovarian cancer [32]. The progesterone receptor (PR) SNP known as PROGINS showed a higher incidence of the T2/T2 genotype in ovarian cancer and women carrying a mutated allele showed approximately 2-fold higher risk of ovarian cancer development [33]. There was also a significant correlation between PROGINS and patients with a familial history [33]. Androgens have also been linked with cancer outcome [34-36], Goodman et al. investigated the A allele of the rs749292 SNP of the *CYP19A1* gene which encodes the cytochrome P450 aromatase which is involved in oestrogen production from testosterone, and showed it is associated with increased ovarian cancer risk when compared with the CC genotype [37].

What is certain, is that the risk of developing ovarian cancer increases with age [38]. Additionally, two of the most commonly agreed upon risk factors is parity and the use of oral contraceptives as protective factors [39-43]. However, some studies showed decreased risk with the number of births as well as a younger age at first conception [19, 44], whilst others indicate that the age at first birth is not associated independently with risk [15, 45]. The protective effect of the oral contraceptive pill was apparent for as long as 15–19 years after cessation of use [42]. Additional births were protective in carriers and non-carriers of the *BRCA*1 and *BRCA2* mutations, but oral-contraceptive use appeared to reduce the risk only in non-carriers [19]. Risk of ovarian cancer has also been stated to increase with the duration of unprotected intercourse, especially in nulligravidae women [44].

Obesity has also been associated with increased ovarian cancer incidence [15, 46] particularly in post-menopausal women [47] and was positively associated with serous borderline tumours and serous peritoneal tumours [48]. Larger endometrial lesions in endometriosis patients were also an independent risk factor for ovarian cancer [49]. Neither age at menarche nor age at menopause was reported to be significantly associated with ovarian cancer risk by Harkinson et al. [45] however, Booth et al. documented that ovarian cancer risk increased with later age of natural menopause. Hysterectomy, breast feeding, vegetarian diet, and a diet high in fish were associated with decreased risk of ovarian cancer [44, 50], whilst hormone replacement therapy [51], smoking [52], the use of talcum powder in the genital area [15, 44], and aspirin use [53] were associated with increased risk.

Despite all of the studies which have been undertaken, the role of many of these risk factors is still mostly unknown as many of the studies had small samples sizes, poor selection criteria for the control groups, or did not have their results confirmed by independent studies. Greater collaborations between groups across the world are clearly needed to further validate the relationship between the various risk factors and ovarian cancer.

1.2. DIAGNOSIS AND TREATMENT OF OVARIAN CANCER

1.2.1. Diagnostic and prognostic markers for ovarian cancer

Cancer antigen 125 (CA125), the only clinically used ovarian cancer detection marker, is only detected in 50% of early stage ovarian cancer [54] but it is also detected in benign and non-malignant ovarian tissue [55], ruling it out as a potential early screening test. However, CA125 is still the only test used clinically to monitor the progress of ovarian cancer patients [56]. There is a lot of interest in combining CA125 with other markers in a detection test to increase the percentage of early stage ovarian cancers which can be detected by regular blood screening tests. BH-74 is one such potential marker [57, 58] and many others have also been studied. Early stage and borderline ovarian tumours expressed higher levels of prostate derived Ets transcription factor mRNA and protein and lower levels of survivin when compared with late stage ovarian tumours, whilst normal ovarian tissue expressed even higher levels Ets transcription factor [59]. High preoperative serum vascular endothelial growth factor (VEGF) was positively correlated with postoperative recurrence and survival in epithelial ovarian cancer [60] whilst the risk of relapse decreased with higher serum follicle stimulating hormone concentrations [61]. Topoisomerase IIα was observed in 73% of ovarian cancer tumour tissues. A statistically significant direct association between the percentages of positively immunostained topoisomerase IIα tumour cells and the relative risk of death was observed and was linked to poor prognosis in platinum resistant patients. [62].

Thus, there are many potential single biomarkers which have been identified over the years, however, few predict survival or diagnose the disease in the majority of cases. Thus, approaches combining multiple markers may be more likely to be effective.

So few proteins identified to have altered expression in ovarian cancer are found to be altered in the majority of all ovarian cancers, most likely due to the heterogeneity of the ovarian cancers. Thus, it has been difficult to successfully develop any screening tests for ovarian cancer, even for those with a strong familial history of the disease.

Many proteins including various enzymes have been assessed as prognostic markers for ovarian cancer patient outcome i.e. response to chemotherapy, progression free survival, and relapse occurrence. Human epidermal growth factor (EGF) receptors HER-3 and HER-4 but not HER-2 were significantly increased in ovarian cancer tissues compared with benign and normal ovaries [63, 64]. The protein levels of HER-1 was significantly lower in ovarian cancer compared with borderline tumours, benign ovarian tumours, and normal ovaries [63]. Increased HER-3 levels have been associated with decreased survival [64]. Tumours of serous histology express a higher level of HER-4 than endometrioid tumours, and long term survival for stage III serous tumours was associated with moderate to high expression of HER-4 [65].

The steroid receptors have been of great interest as potential breast and prostate cancer markers and therapeutic drug targets. The oestrogen receptor (ER), and PR were found in less than 50% of ovarian tumours, whilst androgen receptor (AR) was detected in greater than 80% of ovarian tumours [39-41, 66, 67]. Other reports show that serous tumours are frequently ER positive [68] and that ER level is associated with stage,

survival, and lymph node status [69]. Likewise, PR status was found to be of significant prognostic value in advanced epithelial ovarian cancer [70].

Predicting the response of a patient to treatment could be just as valuable as detecting the disease earlier. Several new studies have revealed proteins which predict response to treatment. Kallikrein-related peptidase 8 belongs to a subgroup of the serine protease enzyme family and was associated with grade, clinical response to chemotherapy, and progression-free survival of ovarian cancer patients [71]. Furthermore, kallikreins 4, 5, 6, 7, and 13 were upregulated in ovarian cancers compared with normal ovarian tissue and were associated with poor survival [72-75]. Trophonin, a homophilic adhesion molecule involved in blastocyst implantation had higher expression in cisplatin-sensitive ovarian cancer cell lines [76]. Eukaryotic elongation factor 1 alpha 2 had high expression levels in approximately 30% of all primary ovarian tumours and was associated with increased 20-year survival [77], making it a potential marker for patients who will respond well to treatment. The overall survival time in epithelial ovarian cancer patients with overexpression of matrix protein YKL-40 was significantly shorter than that in patients with normal expression of YKL-40 [78]. Thus there are a range of proteins that could potentially serve as markers of response to treatment and prognosis.

An *in vitro* assay designed to test for extreme drug resistance to taxanes and platinums, which are used in common chemotherapy regimes, was tested on tumours removed from surgery and proved successful in predicting poorer outcome and survival in a significant portion of patients [79]. This is a step towards developing a way to determine

which patients will respond to specific treatments before treatment is begun, allowing more patients to start with an effective treatment to improve their chance of survival.

1.2.2. Ovarian cancer metastasis

Most cancer types metastasize by way of the blood stream, and thus via the endothelial cells lining the blood vessels. However, metastasis from epithelial ovarian cancer can occur by three routes; the transcoelomic, haematogenous, and the lymphatics which differs from those of most other epithelial malignant diseases. The transcoelomic metastasis mechanism is the most prevalent for the spread of ovarian cancer and occurs by the direct extension of the tumour and the shedding of single cells from the primary tumour into the peritoneal cavity (Figure 1.3) [80]. Ovarian epithelial cancer cells initially spread by direct extension into adjacent organs, especially the uterus, fallopian tubes, contralateral adnexa, and occasionally invasion into the bladder, rectum, and pelvic sidewall, ultimately leading to the death of the patient. At the time of initial laparotomy, 70% of patients already have peritoneal metastases [81]. The three most commonly involved sites at the point of laparotomy are the greater omentum, right subphrenic region, and the Pouch of Douglas which is an extension of the peritoneal cavity behind the uterus [82]. A study which recorded the distribution and volume of peritoneal metastases in a group of 129 patients with various tumours, including epithelial ovarian cancer, showed that the omentum had a high incidence of implants [83]. Within the peritoneal cavity the flow of intraperitoneal fluid is directed by gravity to its most dependent sites, and then drawn towards the diaphragm by the generation

of negative intra-abdominal pressure in the upper abdomen during respiration [84]. Therefore, a natural flow of peritoneal fluid exists within the abdominal cavity providing a route for transcoelomic dissemination of detached tumour cells. Another theory to explain ovarian cancer metastasis to the peritoneum is that the omentum and ovarian epithelium share a common lineage, so omental lesions might not be true metastases but instead, an example of synchronous malignant transformation at multiple foci throughout the peritoneum [85]. However, despite these theories very little is still understood about the mechanism of ovarian cancer metastasis and why there appears to be a preference for implantation and invasion of the omentum over other sites within the peritoneal cavity. Potential mechanisms for the attachment to peritoneal mesothelium include binding to ECM proteins such as collagen type I [86], and IV, laminin, and fibronectin via integrins [87], and to polysaccharide hyaluronan (HA) on the surface of the peritoneal cells via its receptor, CD44 [88].

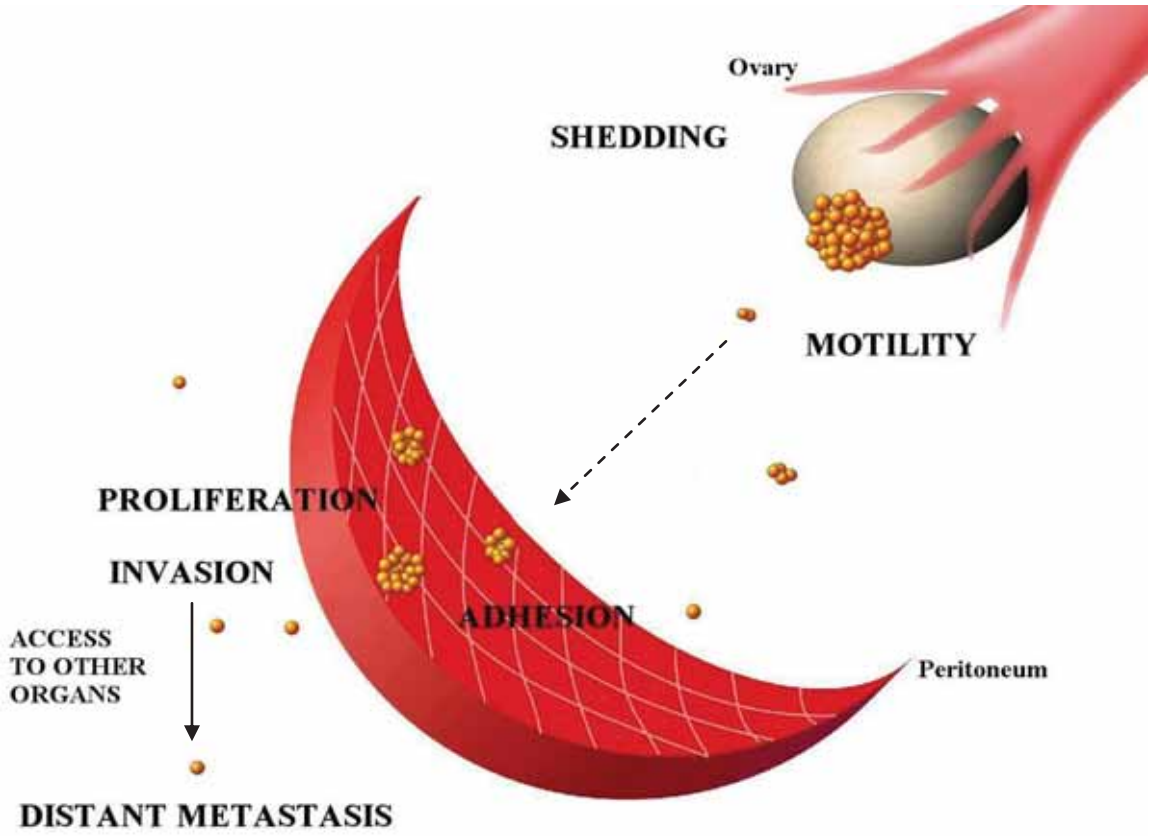

Figure 1.3. *Model of ovarian cancer metastasis.*

Step 1: Epithelial ovarian cancer cells detach from the ovary. Step 2: Cancer cells move towards the peritoneal mesothelium. Step 3: Cancer cells adhere to the peritoneum Step 4: Cancer cells invade through the peritoneal layer Step 5: Formation of metastases

1.2.3. Treatment strategies

Patients diagnosed with ovarian cancer at any stage undergo debulking surgery and treatment with either platinum or taxane containing chemotherapy regimes. Whilst most patients respond initially, the majority relapse with drug-resistant disease within 5 years and only approximately 25% of ovarian cancer patients survive 10 years [89, 90]. Drugs such as Tamoxifen which targets ER and Herceptin which targets HER-2, and have a high response rate in breast cancer patients, have little or no effect for ovarian cancer [91]. Thus finding more effective treatment strategies for ovarian cancer is one of the key goals for oncologists.

A phase II trial using Etoposide and Efosfamide combined therapy on recurrent epithelial ovarian cancer patients had a 19% response rate, i.e. complete response, or partial response [92, 93] whilst another phase II trial using topotecan combined with carbpolatin had a 26% response rate [94, 95]. Topotecan prevents DNA replication in cancer cells by inhibiting the enzyme topoisomerase I which is upregulated in ovarian cancer. Weekly treatments with topotecan had 40% demonstrated stable disease or better in 40% of patients [96], but there is some contradiction in the literature as to whether topotecan is more effective than paclitaxel with some studies showing no difference between paclitaxel and topotecan [97] whilst others show increased survival over paclitaxel [98]. It was found that intravenous topotecan improved survival time compared with oral delivery of the drug [99].

Another drug in clinical trials which has shown significant activity in platinum-resistant ovarian cancer is docetaxel [100]. A phase III trial demonstrated that

docetaxel/carboplatin had similar efficacy to paclitaxel/carboplatin in advanced ovarian cancer [101]. Combined docetaxel with oxaliplatin for treatment of recurrent epithelial ovarian cancer reported more than 8% and 47% of patients had complete and partial recovery respectively [102]. Treatment with Erlotinib, a highly potent, orally active inhibitor of the tyrosine kinase region of the EGF receptor, demonstrated a complete response in 21% of patients had a complete response and a partial response 30% of patients [103].

Sorafenib is an oral multi-kinase inhibitor which inhibits tumour growth by acting on the tumour cells and cells of the tumour vasculature in preclinical tumour models. It inhibits tumour cell proliferation by targeting the MAPK pathway at the level of Raf kinase and/or induces tumour cell apoptosis [104, 105]. Sorafenib's multiple targets including b-*raf* [104, 106] whose frequency of mutation is associated with ovarian cancer [107], enable it to act on the tumour and its vasculature to induce apoptosis and inhibit proliferation and angiogenesis in preclinical models [105, 108]. The combination of gemcitabine chemotherapy agent with sorafenib in a phase II trial reported few partial responses but a 26% stable disease rate [107, 109] and thus is being considered for second or third line treatment.

The humanized, monoclonal anti-VEGF antibody bevacizumab has also been used in trials in relapsed ovarian cancer patients and a partial, complete, or stable disease response was reported in up to 60% of patients [110-113]. Combination therapy with bevacizumab and cisplatin for 3 weeks was associated with the complete disappearance of all macroscopic evidence of disease. Additionally, maintenance treatment with bevacizumab after 3 weeks of induction combination therapy inhibited recurrence and

significantly prolonged survival [114], suggesting that this treatment could be used as a complementary treatment with traditional chemotherapy agents.

Mifepristone, also known as RU486 or the abortion pill, is a synthetic progesterone receptor inhibitor and is a relatively new player in the field of ovarian cancer treatment. Cisplatin resistant cell lines retain mifepristone sensitivity, making it a potential new first or second-line drug for ovarian cancer treatment [115]. Mifepristone, moreover, prevented cell growth between cisplatin cycles in ovarian cancer cell lines [116, 117]. However, a phase II trial using mifepristone in ovarian cancer treatment in a small group of patients saw no significant positive effects from the treatment [118].

Aromatase inhibitor therapy has been trialled in patients with recurrent ovarian cancer and it was shown to elicit clinical response rates of up to 35% and stable disease rates of up to 42% [119]. Given the limited treatment options for recurrent ovarian cancer and the safety and convenient use, aromatase inhibitor is a rational option for prolonging platinum-free interval in recurrent ovarian cancer.

Intravenous administration of chemotherapy drugs exposes the body to systemic toxicity, causing side effects such as nausea and headaches. Combined intravenous/intraperitoneal administration of the current drugs is currently being investigated as a more efficient method of targeted delivery, and is showing improved survival [120-124]. Unfortunately, intraperitoneal administration caused increased side effects, which fortunately did not persist beyond the duration of treatment. A new technique for delivering intraperitoneal chemotherapy drugs has emerged using tumour-penetrating microparticles made of two biocompatible and biodegradable polymeric components with different drug release rates. One component releases the

drug load rapidly to induce tumour priming, whereas the second component provides sustained drug release. This method showed lower toxicity to intestinal crypts and less body weight loss, greater therapeutic efficacy, and less frequent dosing. Thus, this technology has the potential to overcome the toxicities and compliance related problems that have limited the utility of intraperitoneal therapy in the past [125].

1.3. ROLE OF VERSICAN, HYALURONAN, AND CD44 IN CANCER

1.3.1. Hyaluronan

Hyaluronan (HA) is a large polymer which extrudes into the extracellular space and is made up of repeating disaccharides of n-acetyl glucosamine and glucuronic acid with a varying molecular weight and size depending on the tissue in which it is found [126] (Figure 1.4). Unlike proteoglycans, it does not have a core protein. HA is synthesised at the surface of cells by one of three HA synthases (HAS 1, 2, or 3). HA is involved in cell differentiation, proliferation, and migration [127] and thus influences tumour growth [128]. Many tumours appear to be selectively or preferentially enriched in HA, including human mesotheliomas, nephroblastomas, and breast carcinomas [129]. Yeo et al. showed HA levels increased daily in ovarian and breast cancer in correlation with the invasion and growth at the metastatic site [130].

There are a number of tumour cell surface receptors for HA, including RHAMM, LYVE-1, and CD44 [131]. Tumour cells express CD44, on the cell surface, at varying levels and exhibit the ability to stimulate their own synthesis of HA. HA often becomes deposited in the tissue spaces immediately surrounding invasive tumours [132, 133] and is thought to form a protective ECM matrix coat around the cancer cells [129]. In this ECM, HA is often bound by other matrix molecules, the most common of which is the hyalectin family, which includes the proteoglycans, versican, brevican, and aggrecan. It can also bind extracellular matrix protein 1 [134]. This ECM is visible around cancer cells as a unique matrix known as a pericellular sheath [135-137].

NOTE:
This figure is included on page 22
of the print copy of the thesis held in
the University of Adelaide Library.

Figure 1.4. *The structure of HA disaccharides.*

[138]

1.3.2. HA as a poor prognostic factor for cancer

HA has been investigated and associated with prognosis in many cancer types. The level of HA in tumour cells is predictive of malignancy and correlates with cancer aggressiveness in patients with breast cancers, ovarian carcinomas, non-small-cell lung cancers, and prostate cancer [133, 139-146]. Malignant gliomas have been shown to contain higher amounts of HA than normal brain tissue [147]. In these malignant tumour tissues, HA transmits signals into the cytoplasm and has been documented to increase tumour cell proliferation, motility, and invasion [148, 149]. Toole et al. showed that HA levels increased in aggressively invasive and metastatic rabbit carcinomas when compared with benign tumours [150]. HA levels can be increased within the tumour cells themselves or within the tumoural stroma [147]. Boregowda et al. reported that highly differentiated tumours such as lung, breast, colon, kidney, prostate, astrocytomas, and non-Hodgkin's lymphoma expressed increased amounts of HA in both the tumour epithelia and the intratumoural areas [133]. It has also been reported that a high proportion of HA-positive cancer cells and a high intensity of the HA-signal predicts a poor survival rate in colon carcinomas [144]. In addition, Auvinen et al. reported that both the stromal HA and tumour cell HA positivity were independent prognostic factors for overall survival in breast carcinoma patients [139]. A study by Afify et al. also reported increased levels of HA in the breast cancer stroma [145].

High HA levels have been strongly associated with the metastatic potential and invasive ability in ovarian tumour models [151]. Anttila et al. showed that the level of stromal HA staining was higher in intra- and peritumoural stroma than in normal ovarian stromal

tissue [140]. Higher levels of stromal HA were also observed in ovarian metastases when compared with primary ovarian tumours. A high level of stromal HA was found to be associated with poor prognosis, 5 year overall survival, and relapse free survival, particularly in the serous subtype of ovarian carcinoma [140].

HA synthesis has also been linked to tumour metastasis. Overexpression of HA synthases HAS2 and HAS3 were associated with enhanced tumourigenic ability of fibrosarcomas and melanoma cells [152, 153]. Furthermore, it has been shown that induced expression of HAS1 enhances the metastatic potential of mouse mammary carcinoma mutants previously shown to have low levels of HA synthesis and metastatic ability [154]. In breast cancer, HAS2 suppression inhibited the initiation and progression of primary and secondary tumour formation following subcutaneous and intracardiac inoculation into nude mice as well as increasing their survival [155]. In contrast, HAS 1 levels, but not HAS 2 and HAS 3 have been shown to be associated with reduced overall survival in ovarian cancer patients [156].

Full length HA has been found to have little effect on the metastatic behaviour of cancer cells [157, 158]. However, fragments ranging from 4 - 40-mers have been shown to increase angiogenesis, motility, adhesion, and invasion in cancer cells [159-162]. HA has been assessed as a diagnostic tool for cancer in the bodily fluids. HA degradation products of a specific size are known to induce an angiogenic response [163, 164]. Only intermediate-sized HA was found in the urine of normal and low-grade bladder tumour patients, whilst the urine of high-grade bladder cancer patients contained both high molecular mass HA and small HA fragments [165, 166]. Urinary HA measurement by the

ELISA-like assay shows a sensitivity of 91.9% and specificity of 92.8% to detect bladder cancer.

The level of urinary hyaluronidase (HAase), an enzyme which degrades HA into small fragments has also been reported to be elevated 3 to 8-fold in patients with bladder cancer (grade 2 or 3 tumours) compared with normal individuals [167]. The increase in urinary HAase levels is due to the secretion of a tumour-associated HAase. HA levels as determined by ELISA detected high-grade bladder tumours with a sensitivity of 100% and a specificity of 88.8%. A combined test of the levels of HA and HAase in the urine of patients had significantly higher sensitivity and specificity than that of the Immunocyt urine test which is currently used to detect bladder cancer [168, 169]. In addition, this combined test has also been shown to have high specificity and sensitivity in prostate cancer [142] and further testing may reveal it to be specific and sensitive for other cancer types including ovarian cancer.

HA levels are often increased in the sera of patients with a variety of different tumours [170-172]. In ovarian cancer patients (n = 45) serum HA was increased when compared with benign (n = 22) and healthy (n = 50) patient sera [173]. This increase was also observed specifically in the serous subtype. However, there was a large range across the serous ovarian cancer (357.9 ± 387.9 ng/ml).

1.3.3. CD44 – A key receptor for HA

The CD44 glycoprotein is an acidic molecule whose charge is largely determined by sialic acid. CD44 is a multi-structural cell surface receptor which binds HA with a particularly high affinity [174, 175] but also has a weak affinity for laminin [176], the shigella IpaB protein [177], and collagen types I, IV, VI, and XIV [178]. It belongs to a family of transmembrane glycoproteins which contain a variable extracellular domain, a 23-amino acid transmembrane domain, and a 70-amino acid cytoplasmic domain [179] (Figure 1.6). A stretch of 92 amino acid residues from position 12 to 103 at the N-terminus of CD44 has approx 35% homology with hyalectins including versican. The differential utilisation of the 10 variant exons shown in Figure 1.5 generates multiple CD44 variants (CD44v) using different combinations of exon splicing products (reviewed in [180, 181]). Theoretically, over 800 membrane-bound CD44 isoforms could be generated, although to date only ten different CD44 isoforms have been documented [180, 182]; the most common of which is standard CD44 (CD44s), in which exon 5 is spliced directly to exon 16, skipping the entire variant exon sequence (Figure 1.6) resulting in an approximately 85 kDa glycoprotein.

a

NOTE:
These figures are included on page 27 of the print copy of the thesis held in the University of Adelaide Library.

b

Figure 1.5. *The structure of CD44, the HA cell surface receptor.*

(*a*) Schematic of the domains of CD44 *(b)* Domains of CD44 showing the exons [183]

NOTE:
This figure is included on page 28
of the print copy of the thesis held in
the University of Adelaide Library.

Figure 1.6. *Structure of CD44 variants.*

Schematic showing the differences between CD44 standard and exon spliced variants (Adapted from [181]).

1.3.4. The role of CD44 and its interactions with HA in cancer

High CD44 levels have been associated with unfavourable prognosis in a variety of cancers including breast [184], gastric [185], head and neck [186], biliary tract [187], prostate [188], and ovarian [189, 190] cancer. Human ovarian cancers express variant isoforms of CD44 as well as the standard form [191] and can adhere strongly to peritoneal mesothelium which is enriched in HA [88, 130]. The binding of HA to CD44 triggers direct cross-signalling between two different tyrosine kinase-linked signalling pathways [190, 192] and it is this function that is thought to be involved in increased motility, adhesion, and invasion of cancer cells as well as tumour growth, especially in ovarian cancer [174, 193-196]. Furthermore, Afify et al. demonstrated that decreased expression of CD44s was accompanied by an increased expression of CD44v6 and accompanying increased stromal HA expression in breast cancer [145] whilst Bourguignon et al. showed that HA binding to CD44 induced chemoresistance in breast cancer cells [197].

Recently, Harrell et al. showed that CD44 is sparsely expressed in primary breast tumour cells but homogeneously over-expressed in the cancer cells transiting the lymphatics and also in those found populating the lymph nodes [198]. This suggests that acquisition of CD44 may aid migration through the lymphatics and formation of metastases. *In vivo* studies have suggested that the standard form of CD44 is required for human ovarian cancer cell adhesion to mesothelial cell surface HA [88, 199]. CD44 expression in ovarian cancer was shown to be higher in malignant tumour cases when compared with benign and borderline tumours [200]. However, some studies have shown that high CD44 levels

are associated with improved ovarian outcome [192, 201], whilst others found no association between CD44 expression and ovarian cancer survival outcome and metastasis [191, 202]. These contradictory results could be due to use of monoclonal versus polyclonal antibodies which have a variable efficacy in paraffin embedded tissues, variation in immunostaining methods and assessment, or the use of heterogeneous cohorts.

1.3.5. Versican – An interacting partner of HA

Proteoglycans are ubiquitous components of the ECM [203] and are thought to be a determinant of tumour growth as they bind and activate growth factors, chemokines, cytokines, and other signalling molecules. Versican is a large HA binding proteoglycan detected in increased quantities in tumour lesions. It is a member of the large aggregating chondroitin sulphate (CS) hyalectins family which includes aggrecan, neurocan, and brevican [204]. Versican consists of an N-terminal HA-binding, G1 domain, a glycosaminoglycan region, and a C-terminal, G3 domain (Figure 1.7). Alternative splicing produces five known isoforms of versican [205, 206] (Figure 1.7). The G1 and G3 domains bind specific proteins and have differing domains and motifs which bind to a wide range of molecules including fibronectin, and tenascin (Figure 1.8) [85].

An *in vivo* study in mice showed that versican is essential for matrix assembly involving HA and that diminished versican deposition increases free HA fragments which interact with CD44 and increase phosphorylation of ERK1/2, leading to cellular senescence

[207]. Furthermore, matrigel plug angiogenesis assays have suggested that versican-HA aggregates plays a role in HA-mediated angiogenesis by enhancing recruitment of host stromal cells [208]. This combined data supports a role for versican in a number of the steps needed for metastasis (Figure 1.9).

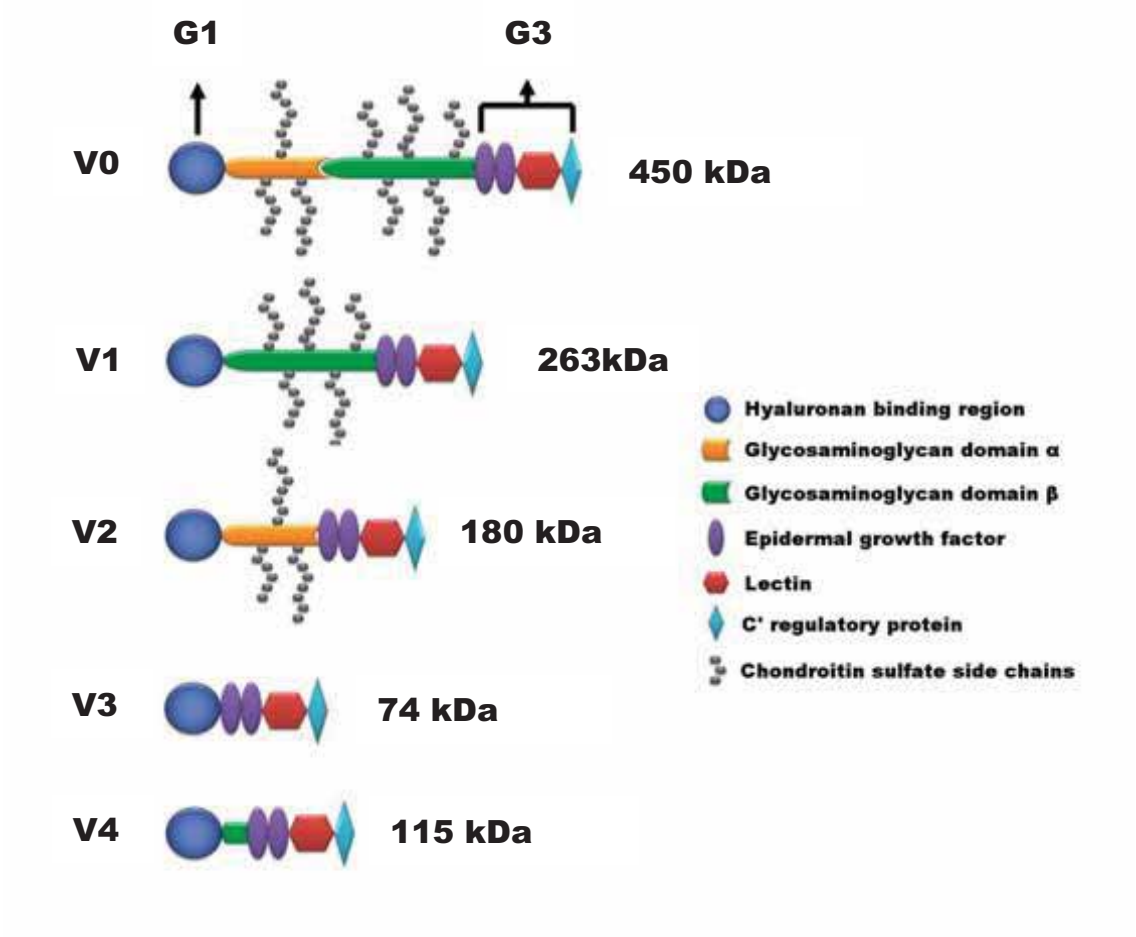

Figure 1.7. *Schematic of the structure of the versican isoforms.*

Shows the domains and structure of the four main isoforms that arise from alternative splicing [209].

NOTE:
This figure is included on page 33
of the print copy of the thesis held in
the University of Adelaide Library.

Figure 1.8. *Interaction of versican with other molecules.*

Versican interacts with a variety of molecules. Adapted from [210].

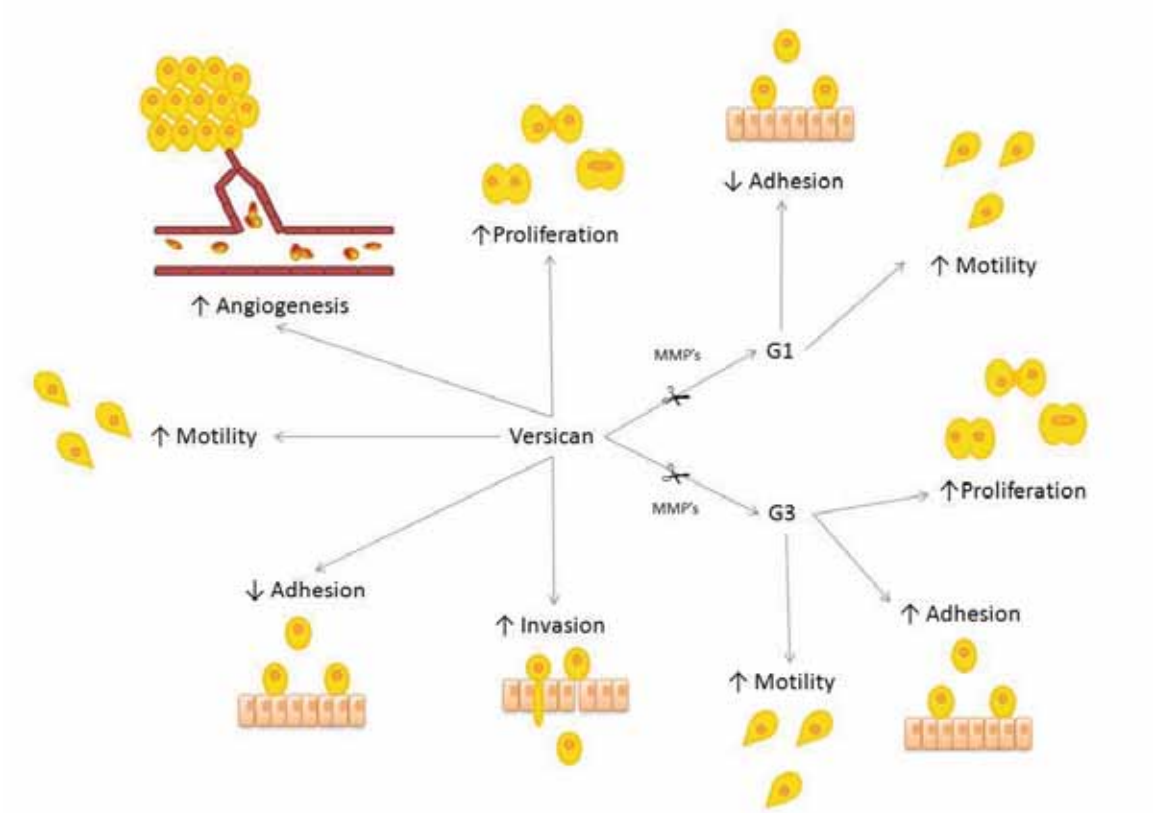

Figure 1.9. *Role of versican and its domains in cancer.*

Various isoforms of versican have been reported to play varying roles in the metastatic process.

1.3.6. The differing roles of the isoforms of versican

The five isoforms of versican are expressed by a diverse range of human tissues [211]. The V0 isoform is particularly prevalent during early embryonic development [212] but is less common in adult tissues [211]. Data is now emerging that the different isoforms may have distinct functions. V1 isoform may have a different function from the V2 isoform. V1 versican has been shown to enhance cell proliferation and protect fibroblasts from apoptosis [213]. By contrast, the V2 isoform exhibits opposing biological activities by inhibiting cell proliferation and lacking any association with apoptotic resistance [213]. Versican V1 and V2 isoforms may also have distinct functions in the brain [214, 215]. V0 and V1 are the predominant isoforms present in cancer tissues [216-219]. Versican isoforms V0 and V1 inhibited prostate and melanoma cell attachment to ECM components [220, 221].

The smallest splice variant, V3, consisting only of the amino- and carboxy-terminal (C-terminal domain) G1 and G3 domains and lacking CS chains, might be expected to have properties considerably different from the other isoforms. However, there have been no studies which have directly compared the biological activity of V3 with the other versican isoforms. The V3 isoform was found to be expressed in primary endothelial cell cultures only following activation by pro-inflammatory cytokines or growth factors [211]. The overexpression of V3 in arterial smooth muscle cells (SMCs) resulted in their increased adhesion to culture flasks but reduced proliferation and slower migration in scratch wound assays [222]. The overexpression of the V3 isoform in melanoma cancer cells which, although markedly reducing cell growth *in vitro* and *in vivo* [223], actually promoted metastasis to the lung [224]. These findings suggest that the V3 isoform may

have a dual role as an inhibitor of tumour growth and a stimulator of metastasis. The newly identified V4 isoform is upregulated in breast cancer and may also play a role in other cancers [206].

1.3.7. The role of G1 and G3 versican domains in cancer

Versican is a specific target for a number of proteases, specifically MMPs. MMPs are a family of calcium dependent endopeptidases which bind zinc ions at the catalytic site of their substrates. MMP-1, -2, −3, −7, and −9, have been shown to degrade versican [225-227]. Within this family of MMPs are the members of the ADAMTS (adamalysin with thrombospondin type 1 motifs) family. The ADAMTSs are a family of secreted proteases found in both mammals and invertebrates [228] which have the potential for the generation of multiple isoforms via alternative splicing. ADAMTS-1, −4, and −9 have also been shown to mediate versican cleavage [229, 230]. This versican cleavage by ADAMTS1 was demonstrated by in vivo studies by Russell et al. who have suggested that this may result in an alteration of versicans adhesive properties, matrix structure, and interactions [231].

The G1 domain of versican is composed of an immunoglobulin-like motif, followed by two proteoglycan tandem repeats which bind HA (Figure 1.8). The association of versican with HA is mediated by link protein, and both HA and isolated link protein have the ability to bind to the G1 domain of versican [232]. The G3 domain contains two epidermal growth factor-like repeats, a carbohydrate recognition domain (a lectin-like repeat) and complement binding protein-like subdomains with structural similarity to

the selectin family [233]. Several studies have focused on the function of the G1 and G3 domains of versican. Both the G1 and G3 domains have been shown to promote cell proliferation of fibroblasts and tumour cells [234-237]. The G1 domain of versican is thought to stimulate proliferation by destabilizing cell adhesion whilst the G3 induced proliferation is mediated, at least in part, by the action of EGF-like motifs in the G3 domain activating EGF receptors. Studies in astrocytoma cancer cell lines have demonstrated that the G1 domain, but not the G3 domain, of versican enhanced migration [238]. Overexpression of G3 versican in astrocytoma cells enhanced colony growth in soft agarose gel as well as tumour growth and blood vessel formation in nude mice [236]. Both G1 and G3 overexpressing osteosarcoma cells exhibited enhanced *in vitro* growth when cultured on ECM substrates or in the absence of ECM anchorage [237]. G1 overproducing sarcoma cells were more invasive than corresponding G3 transfectants and, upon inoculation into nude mice, the G1 transfectants formed larger tumour masses than vector transfected cells. In addition, G1 overexpressing sarcoma cells were resistant to apoptosis. Stable transfection of G1 versican into lung cancer cells did not alter tumour growth rate *in vivo*. Interestingly, clones expressing low or high levels of G1 versican had opposing effects on cancer cell motility *in vitro* and the incidence of metastasis in nude mice [239]. Only the cells expressing low levels of G1 versican demonstrated increased motility and metastasis to the lung [239]. These findings suggest that G1 versican can act both as a suppressor or a promoter of metastatic spread. Interestingly, in breast cancer cells, overexpression of G3 versican resulted in larger tumours and the promotion of metastasis to bones and soft tissues [240]. The effects of versican and its domains are summarized in Figure 1.9 and Table 1.2.

The accumulative data suggests that the G1 and G3 domains of versican may differentially control tumour growth rate and have interactive roles to promote tumour development and metastasis. However the mechanisms that regulate catabolism of versican and the levels of G1 and G3 versican are poorly understood.

Table 1.2. *Summary of versican's effects on cancer cells.*

Function	Effect	References
Cell proliferation	Knockdown of versican by siRNA in lung cancer cells significantly inhibited tumour growth *in vivo*	[241]
	V1 enhanced proliferation of NIH-3T3 cells whilst V2 inhibited proliferation	[213]
	Overexpression of G1 in leiomyosarcoma cells lead to larger tumour masses	[237]
	Overexpression of G3 versican in breast cancer cells resulted in larger tumours in vivo	[240]
	G1 and G3 induced NIH-3T3 cell proliferation *in vitro*	[234, 235]
	G3 versican domain promoted proliferation of astrocytoma cells *in vivo*	[236]
	Overexpression of V3 versican in human melanoma cell lines markedly reduced cell growth *in vitro* and *in vivo*	[224]
Apoptosis	V1 induced apoptotic resistance in NIH-3T3 cells	[213, 242]
Adhesion	V0 & V1 versican inhibited prostate and melanoma cell attachment to ECM components	[220, 221]
	G1 but not G3 reduced glioma cell adhesion	[238]
Motility	G1 versican domain promoted motility of glioma cells and lung cancer cells	[238, 239]
	V0 & V1 and recombinant V1 increased motility of prostate cancer cells	[135]
Invasion	G1-overexpressing sarcoma cells were more invasive than overexpressing G3 mutants	[237]

Pericellular matrix formation	V0 & V1 and recombinant V1 induced formation of pericellular matrix by prostate cancer cells	[135]
Angiogenesis	G3 enhanced endothelial cell adhesion, proliferation, and migration *in vitro* and blood vessel formation in nude mouse tumours *in vivo*	[236]
Metastasis	G1 versican promoted metastasis of lung cancer cells Overexpression of V3 versican in melanoma cells induced lung metastasis in nude mice Overexpression of G3 versican in breast cancer cells promoted metastasis to bones and soft tissues	[239] [224] [240]

1.3.8. Versican is associated with poor cancer patient outcome

Immunohistochemistry studies have demonstrated high levels of versican in the stroma surrounding malignant breast cancer cells, whilst low levels were present in non-malignant stroma [146, 243]. Cultured mammary and prostate fibroblasts produced significant amounts of versican [216, 217]. Furthermore, it was demonstrated that breast and prostate cancer cells could increase versican production by stromal cells by up to 3 fold [216, 217]. Suwiwat et al. showed that patients with small tumours and low versican expression levels experienced fewer relapses than patients with large tumours and low versican, whilst patients with high versican gave rise to a high rate of relapse, regardless of the tumour size [146]. This study demonstrated that versican concentration and tumour size were independent prognostic factors for relapse rate. It was determined that elevated expression of versican was solely a prognostic factor of relapse, and not death. Patients with endometrial cancer had higher stromal versican levels in the primary tumour and also in the matching ovarian metastases [244]. Likewise, epithelial versican expression was significantly higher in cervical cancer patients with non-squamous cell carcinoma, lymph-vascular space invasion, and lymph node and ovarian metastases, and proved to be a poor prognostic factor for disease-free survival [245].

In ovarian cancer, versican has been shown to be present in both cancer cells and the peritumoural stroma [246]. High versican stroma staining was associated with high FIGO stage, large residual tumour, serous histologic type, and reduced 5 year survival [246]. Increased expression of versican has recently been identified as a key protein involved

in ovarian cancer metastasis [247]. Elevated levels of versican have been observed in primary ovarian tumours and secondary metastases when compared with normal ovaries [248]. Although versican is enriched in the malignant stroma surrounding cancer cells and associates with unfavourable prognosis, neither stromal nor cancer cell-associated versican was an independent indicator of patient survival in multivariate analyses when conventional prognostic factors were included [246]. These contradictory findings may be due to the heterogeneity of the ovarian cancer cohort used.

1.3.9. Involvement of HA, CD44, and versican in the adhesion of ovarian cancer cells to peritoneal cells

Ovarian cancer cell adhesion to mesothelial cell monolayers is partially due to the interaction between HA and CD44 [249]. It has also been suggested that ovarian cancer cell interactions with mesothelial cell HA could mediate secondary tumour growth [250]. However, treatment with HA at 1-2 mg/ml inhibited ovarian cancer cell invasion [199, 250]. However Gardner et al. reported that HA increased four out of six ovarian cancer cell lines' adhesion to HA-coated wells [251] suggesting differing roles for high and low HA levels in adhesion to the peritoneal lining. Addition of anti-CD44 antibodies has been reported to significantly decrease adhesion of ovarian cancer cells to HA [251]. Surprisingly, HAase pre-treatment, which degrades HA and thus its interactions with other ECM proteins, had no effect [251]. Furthermore, HAase pre-treatment also had no effect on ovarian cancer cell migration towards ECM proteins [250].

1.3.10. Pericellular sheath formation is associated with cell migration

HA often becomes deposited in the tissue spaces immediately surrounding invasive tumours and is thought to combine with other ECM components to form a protective pericellular coat around the cells [252]. Evanko et al. first reported HA-versican pericellular sheath formation as a rapid and dynamic process in mitotic and migrating aortic SMCs [136]. Smooth muscle cells with a motile morphology showed a prominent sheath, whilst flat non-dividing cells did not produce sheaths. After wounding, 90% of cells which had migrated possessed a sheath compared with the 40% of controls [136]. HA oligosaccharide (oligos) addition prevented HA binding to the cell surface and thus prevented sheath formation and also reduced cell proliferation and migration [136]. By binding to proteoglycans such as versican in the pericellular environment, HA can stimulate smooth muscle cell migration [136] and modify the ECM [253]. This HA-versican interaction and alteration of the ECM has been shown to increase prostate cancer cell motility and increase formation of a polar pericellular sheath around the cells [135]. Prostate cancer cells with polar sheath were more motile than their counterparts which had not formed any sheath [135]. This data suggests that HA levels are correlated with the motility of cancer cells, via the formation of pericellular sheath around the cells. Thus we propose that versican from the stroma binds with HA during formation of the extracellular matrix, which in turn binds to CD44 on the peritoneal surface, enabling adhesion, and inevitably invasion and metastasis to other abdominal organs or beyond.

1.4. THERAPIES TARGETING HA, CD44, AND VERSICAN

1.4.1. Cancer therapies targeting the actions of HA

Because of the ability to bind cell surface CD44 which is upregulated in many cancer types, HA has been conjugated to traditional chemotherapy drugs in the hope of increasing the direct targeting of the drug to the cancer cells. When HA was conjugated to paclitaxel, the drug exhibited more pronounced cytotoxic effects on CD44 overexpressing breast cancer cells than for CD44 deficient cells, suggesting that HA conjugation can be potentially utilized as tumour-targeted therapies [254]. In ovarian cancer cells, paclitaxel-HA conjugate interacted with CD44, entered the cells through a receptor-mediated mechanism, and exerted a concentration-dependent inhibitory effect on tumour cell growth. Furthermore, after intraperitoneal administration in mice, HA bioconjugate distributed uniformly within the peritoneal cavity and was well tolerated, and was not associated with local histologic toxicity [255]. Blood levels of the paclitaxel-HA were also much higher and persisted longer than those obtained with the unconjugated paclitaxel. There was a 2.5-fold increase in therapeutic activity with paclitaxel-HA compared with paclitaxel alone [255] and decreased tumour burden in ovarian cancer xenograft mice [256]. HA with entrained irinotecan provided increased progression free survival over irinotecan alone although it also induced increased mild side-effects in a recent phase II trial for colon cancer treatment [257]. Additionally, HA coated poly butyl cyanoacrylate (PBCA) nanoparticles encapsulating paclitaxel had a 9.5-fold higher uptake in sarcoma cells than PBCA nanoparticles without the HA coating and

had a more potent tumour growth suppression activity in sarcoma tumour bearing mice [258].

Conjugated HA-cisplatin targeted breast cancer cells after subcutaneous peritumoural injection and showed improved efficacy over intravenous administration. This method delivered the drugs to the areas in which tumour burden is greatest, reducing systemic toxicity which often causes the patients great discomfort [259]. Prostate cancer patients receiving transperineal injection of HA in the anterior perirectal fat and low dose rate brachytherapy experienced decreased rectal toxicity from radiation when compared with those patients who did not receive the HA transperineal injection [260]. Breast cancer drugs trastuzumab and herceptin also showed increased efficacy against breast cancer cells when combined with HA [261].

HA has also been investigated as a potential conjugate to other cancer therapies besides chemotherapy drugs. Polyethylenimine (PEI) DNA particles used in gene treatment conjugated with HA were shown to specifically target malignant breast cancer cells with high CD44 levels [262]. A siRNA/PEI-HA complex exhibited higher gene silencing efficiency in melanoma cells with CD44 than siRNA/PEI complex alone. Intratumoural injection of anti-VEGF siRNA/PEI-HA complex resulted in an effective inhibition of tumour growth by receptor mediated endocytosis by tumour cells in mice [263]. Similarly, liposomes-protamine-HA nanoparticles used for systemic delivery of siRNA into melanoma cells had a broader effective therapeutic dose range than nanoparticles without HA [264].

Thus, HA presents a novel and likely candidate for increasing efficacy of cancer therapeutics, reducing systemic toxicity and discomfort of cancer patients and possibly

reducing the efficacious dose of the drugs which was previously thought to be too toxic for use. HA conjugates also have a potential role in the development of more effective intraperitoneal treatment regimes in ovarian cancer.

1.4.2. Cancer therapies targeting CD44

CD44 has increasingly become of interest in the development of novel cancer therapies. It has been showing promise using a number of techniques which target cancer cells, particularly as it has been documented that cancer cells expressing higher levels of CD44 are more likely to become metastatic. CD44 is therefore an ideal target for treatment of early stage tumours to prevent progression, which is the most common cause of death in cancer patients. Silibinin, a natural drug extracted from common thistles, which inhibits CD44 promoter activity and expression, is known to have anti-tumour properties in breast cancer [265], non small cell lung cancer [266], and colorectal carcinoma [267]. It has also been shown to decrease motility and invasion in prostate cancer cells. Furthermore, silibinin decreased adhesion of prostate cancer cells to HA and fibronectin [268].

Due to successful development of vaccines against cervical cancer, there is a desire to create vaccines against other, non viral associated, cancers. CD44 cDNA vaccination was shown to decrease tumour mass and metastatic potential in experimental mammary tumours in mice [269]. In addition, transfection of CD44 antisense into a highly metastatic mammary tumour cell line disrupted expression of CD44 in the tumour cells and reduced their ability to establish local tumours as well as metastatic colonies in the

lung [269]. Another method to block the action of CD44 is to use siRNA. Gemcitabine-resistant pancreatic cancer cells are more tumourigenic *in vitro* and *in vivo* than gemcitabine-sensitive cells [270]. After high-dose gemcitabine treatment, resistant cells were noted to be CD44 positive and proliferated and reconstituted the cancer cell population with resistant cells. Treatment of these CD44 positive cells with siRNA inhibited the proliferative activity of gemcitabine resistant cells [270]. Furthermore, in colon cancer and leukaemia xenografts, *In vivo* targeting of CD44 by siRNA resulted in anti-tumour activity [271, 272]. In hepatocellular carcinoma, CD44 antisense oligonucleotide significantly down-regulated CD44 expression, induced apoptosis, decreased tumourigenesis and invasion, and increased the cancer cells sensitivity to chemotherapy drugs [273]. *In vitro* adhesion, invasion, and resistance to apoptosis of ovarian cancer cells were also inhibited by siRNA downregulation of CD44 expression, as well as suppressing tumour growth and peritoneal dissemination of human ovarian cancer xenografts in nude mice [274].

Another very promising therapeutic is the use of anti-CD44 antibodies such as IM7 which resulted in a greater than 50% decrease of HA production in glioma cells, and was associated with changes in cell size and apoptosis [275]. Treatment of chondrosarcoma cells with IM7 resulted in a significant decrease in cell viability but did not reduce cell viability in normal human chondrocytes [276]. Another antibody against CD44, called P245, inhibited growth of breast cancer xenograft in mice [277]. Affify et al. showed that anti-CD44s could inhibit breast cancer cell adhesion, motility and invasion, whilst anti-CD44v6 inhibited cell motility [278]. Furthermore, Guo et al. showed that treatment with an anti-CD44 mAb inhibited the formation of melanoma metastases

[279]. Treatment of prostate cancer cells with a neutralising CD44 antibody, decreased cancer cell adhesion to human bone endothelial cells, a primary site for prostate cancer cell metastasis [280]. The biotech company AIRUS have thus recently taken out a patent on an anti-CD44 antibody for treatment of breast, prostate and liver cancer [281] after their research showed that their antibody would only induce apoptosis in cancer cells expressing CD44, leaving normal cells unharmed. Other groups have done work with different anti-CD44 antibodies. These CD44 antibodies disrupted the CD44-HA interaction and decreased the invasive ability of breast cancer cells [282]. Casey et al. showed that their CD44 mAb did not inhibit ovarian cancer cell invasion but inhibited motility [250], whilst Strobel et al. showed a decrease in the number of total peritoneal ovarian cancer metastases in mice when treated with their anti-CD44 antibody [194]. However, despite promising in vitro studies, clinical trials showed that antibodies against CD44v6 caused unacceptable levels of toxicity [283-285].

With so many studies finding that disruption of the HA-CD44 interaction decreases the proliferative and metastatic behaviour of tumour cells, there are likely to be many more CD44-HA targeted therapeutic drugs developed and trialled over the next several years.

1.4.3. Versican as a target for cancer therapies

Inhibiting versican synthesis may be a potential mechanism for reducing versican levels in cancer tissues. Treatment with the tyrosine kinase inhibitor, genistein, has been shown to inhibit versican synthesis induced by growth factors in malignant mesothelioma cell lines and vascular SMCs [286, 287]. Genistein can reversibly inhibit

PDGF-stimulated versican expression in vascular SMCs in a dose-dependent manner, without affecting the expression of other proteoglycans including decorin and biglycan [286]. No studies to date have investigated whether these inhibitors are effective in inhibiting versicans effects in cancer cell models.

More recent studies have demonstrated that asthma drugs including budesonide, a glucocorticoid steroid, and formoterol, a long acting β_2-adrenergic agonist, could decrease protein levels of a number of proteoglycans including decorin, biglycan, perlecan, and versican in human lung fibroblasts and airway SMCs [288, 289]. Combination treatment with budesonide and formoterol reduced versican levels to a significantly greater extent than either drug alone [289]. Versican synthesis could also be inhibited by the leukotriene receptor antagonist, montelukast, in both bronchial and arterial SMCs [290]. These studies suggest that the changes in versican deposition which occur in cancer tissues, as well as the asthmatic airway and atherosclerotic lesions, could be inhibited by a number of asthma drugs. The ability of asthma drugs including budesonide and formoterol to inhibit versican synthesis need to be evaluated in cancer cell models.

There is increasing evidence that ADAMTS proteases play an important role in the cleavage of versican, and the local accumulation of versican fragments generated by ADAMTS digestion may also promote cancer cell motility and invasion. The broad spectrum MMP inhibitor, GM6001 (Galardin) which inhibits the activity of MMPs and ADAMTS proteases has been shown to inhibit cancer cell invasion and metastasis in several model systems [219, 250, 291, 292]. One of the more interesting MMP inhibitors is present in the increasingly popular beverage, green tea, which is made from the

leaves of *Camellia sinensis* and contains catechin gallate esters. Catechin gallate esters have been shown to selectively inhibit ADAMTS-1,-4, and -5 and inhibit aggrecan processing in cartilage tissue [293]. The ability of GM6001 and catechin gallate esters to inhibit versican cleavage and versican-induced motility and metastasis has not been investigated. Manipulation of the versican catabolic pathways may provide novel therapeutic targets for cancer invasion and metastasis.

The formation of a pericellular matrix rich in HA and versican by vascular SMCs and tumour cells can be inhibited following treatment with HA oligos [136, 294]. Disruption of the HA-CD44 interaction with HA oligos has been shown to markedly inhibit the growth of melanoma cells [295]. Additionally, both link-TSG6 and G1 domain of aggrecan were shown to bind to polymeric HA and these interactions could be competed with HA (8) and HA (10) oligos, respectively [296], making it likely that HA oligos will also block the interaction of versican with HA. Treatment with HA (8) oligos inhibited the formation of pericellular matrix by osteosarcoma cells and reduced HA accumulation in local tumours, tumour growth, and the formation of distant lung metastases. Furthermore, in osteosarcoma cell lines, both motility and invasiveness were inhibited by the use of HA oligos [297]. Additionally, colorectal carcinoma growth was reduced both *in vitro* and *in vivo* after treatment with HA oligos [298].

HA oligos have also been shown to reverse chemotherapy resistance in some cancer cell lines. Adriamycin resistance of leukemic cells was effectively reversed by HA (4) oligos by increasing the intracellular accumulation of adriamycin [299], whilst in malignant peripheral nerve sheath tumours (MPNST), HA oligos disassembly of CD44-transporter complexes and induced internalization of CD44. Consequently, the oligos suppressed

drug transporter activity and increased chemotherapy sensitivity. Furthermore, *in vivo* systemic administration of HA oligos inhibited the growth of MPNST xenografts [300].

These findings suggest that the potent anti-tumour effects of HA oligos are due in part to the blocking of the formation of HA-rich cell-associated matrices. The use of HA oligos is a potentially attractive reagent to block versican HA interactions as well as local tumour invasion in ovarian cancer but needs further investigation.

STATEMENT OF AIMS

This study will assess the protein profile produced during interaction between human peritoneal cells and ovarian cancer cells in *in vitro* co-culture systems designed to mimic the early and late stages of *in vivo* cancer progression. The early steps of ovarian cancer progression involves no physical contact between peritoneal cells and ovarian cancer cells but they are both exposed to peritoneal fluid. Thus we have developed an indirect co-culture system where the cells share CM but have no physical contact. The late stages of ovarian cancer progression involves adherence of ovarian cancer cells to peritoneal cells and invasion through the peritoneal lining. Thus we have developed a direct co-culture system where a monolayer of peritoneal cells are exposed to and binds to a suspension of ovarian cancer cells allowing direct physical interaction between the two cell types. We will assess changes to the protein profiles of the cells during these interactions with the use of proteomic screening.

This study will also investigate the effects of versican and its interacting partners, HA and CD44 on ovarian cancer cell motility, invasion, and their adhesion to peritoneal cells. One way that cancer cells are thought to become motile is by formation of a pericellular matrix sheath [135]. SKOV-3 and OVCAR-5 mimic the progression of ovarian cancer when injected into *in vivo* mouse models [301]. Both have been shown to adhere to mesothelial cells in *in vitro* models [199, 251]. OVCAR-5 cells have also been shown to make a HA rich pericellular matrix, which is removable by HAase treatment [195].

SKOV-3 and OVCAR-5 as well as LP-9 human peritoneal cells have high expression of CD44 [195, 302] and both OVCAR-5 and SKOV-3 cells have high metastatic potential.

OVCAR-3 cells, which do not express CD44, and have low metastatic potential [302], will be used as a negative control cell line. Various doses of versican have been used on both OVCAR-5 and OVCAR-3 cell lines, whilst optimal concentrations of the experimental reagents have been used on SKOV-3 cells. Invasiveness of the ovarian cancer cell lines will be assessed by modified chemotaxis assays, where cells must migrate through the ECM components found in Geltrex, which is composed of ECM extracted from mouse Engelbreth-Holm-Swarm (EHS) sarcoma cells [303].

Hypotheses:

1. Proteins whose expression are regulated when ovarian cancer cells interact with peritoneal cells assist them in their adhesion, motility, and invasion.
2. BigH3 which is expressed by peritoneal cells is involved in ovarian cancer metastasis
3. HA, CD44, and versican are involved in ovarian cancer metastasis

Aims:

1. Explore the proteomic profile of peritoneal-ovarian cancer cell interactions and identify proteins which show an altered expression during peritoneal-ovarian cancer cell interaction.
2. Determine the functional role of one of the novel proteins identified to be regulated during peritoneal-ovarian cancer cell interaction in ovarian cancer.

3. Determine whether levels of versican and interacting partners HA and CD44 are increased in serous ovarian cancers and matching metastases.

4. Determine whether versican treatment promotes pericellular matrix formation and aids the motility and invasion of serous ovarian cancer cells and their adhesion to peritoneal cells.

5. Evaluate whether HA oligosaccharides can inhibit versican effects on pericellular sheath formation, motility, invasion, and adhesion.

Research Plan:

Peritoneal-ovarian cancer cell interaction will be studied using *in vitro* co-culture systems where the cells can communicate via soluble factors or by direct contact. Proteins modulated by co-cultured ovarian cancer and peritoneal cells will be analysed and identified by MS. The functional importance of one of the identified proteins will be assessed in cell adhesion, motility, and invasion assays.

We will determine whether serous ovarian cancer cells (OVCAR-3, OVCAR-5, and SKOV-3) have the ability to form HA-versican pericellular sheath following treatment with recombinant versican and HA using an established particle exclusion assay [8]. Using modified chemotaxis assays and wound migration assays, we will determine whether the formation of pericellular matrices promotes motility and invasion of ovarian cancer cells. Adhesion assays will be used to determine whether the assembly of a pericellular matrix aids ovarian cancer cell adhesion to peritoneal cells. HA oligos will be evaluated as an inhibitor of versican function.

We will identify whether the expression of the ECM protein versican and interacting molecules HA and CD44s are increased in serous ovarian carcinoma or matching metastases. We will additionally investigate the levels of HA in the serum of ovarian cancer patients undergoing chemotherapy to assess whether it can be used as a marker for patient response to treatment.

This study will determine whether versican aids the motility and invasion of serous ovarian carcinoma cells and promotes their specific adhesion to peritoneal cells via interactions with HA and CD44. We will determine whether HA oligos can interfere with HA-versican pericellular sheath formation and thus inhibit motility, invasion, and adhesion of ovarian cancer cells to peritoneal cells and whether these compounds should be evaluated as a therapeutic agent in *in vivo* models of ovarian carcinoma. A greater understanding of the molecular mechanisms whereby ovarian cancer cells interact with ECM components may lead to the identification of novel therapeutic approaches to inhibit metastasis of ovarian cancer cells.

CHAPTER 2 - IDENTIFICATION OF PROTEINS MODULATED IN OVARIAN CANCER – PERITONEAL CELL CO-CULTURE BY PROTEOMICS

2.1. INTRODUCTION

One of the most important developments in protein identification has been the development of mass spectrometry (MS) technology [304]. In the last decade, the sensitivity of analysis and accuracy of results for protein identification by MS has increased by several orders of magnitude down to identification of proteins from gels in the high fentomolar range [305]. Because of this we can now identify individual protein sequences in a mixture of other proteins and since MS has high throughput, it has essentially become the protein identification tool of choice.

Proteomics is defined as the large-scale characterization of the entire protein complement of a cell line, tissue, or an organism [306, 307] and its main purpose is to obtain a more global and integrated view of biology by studying sets of proteins produced together rather than each one individually. There are several types of proteomics which can be used in a diverse range of studies (Figure 2.1). These include protein-protein interaction studies, protein modifications, protein function, and protein localization studies as well as many others, which are constantly evolving as newer technologies develop and the scientific research community embrace them.

Proteomics and MS are currently being utilised in the development of new cancer diagnostics. It has been used to identify potential breast cancer diagnostic markers in nipple aspirate [308] as well as potential diagnostic markers in the serum for colorectal cancer [309], gastric cancer [310], and liver metastasis [311].

To date, many proteomic studies have investigated various aspects of ovarian cancer proteomics including; analysis of ovarian cancer produced effusions [312, 313], the difference between chemotherapy resistant cells and non-resistant ovarian cancers [314, 315], effects of potential therapies on ovarian cancer [316], and analysis of the serum from ovarian cancer patients [317, 318]. This has been undertaken with the purpose of finding novel biomarkers for early detection of ovarian cancer or to predict response to treatment. Most studies work with the tumours or cancer cells themselves, the serum of the patients, or effusions which are exposed to multiple cell types.

Proteomics has been successfully used to identify 6 proteins differentially expressed between benign and malignant epithelial ovarian tumours [319]. Kuk et al. also used a proteomic screen to identify 25 previously reported biomarkers and 52 proteins in ovarian cancer ascites fluid which were also identified in 4 ovarian cancer cell lines, warranting further validation [320]. Fibrinogen and collagen fragments were found in a proteomic screen of the urine of epithelial ovarian cancer patients which were not found in benign ovarian tumour patients [321]. Afamin has also been identified in a serum proteomic screen and was further validated by western blot and ELISA to be complementary to CA125 testing [322].

Bengsten et al. identified 217 protein spots on 2D gels which distinguished between normal, benign, borderline, and malignant ovarian tissue which require further

validation [323]. Three protein peaks identified as upregulated in the serum of ovarian cancer patients were able to be used to discriminate 33 out of 35 controls and 29 out of 30 cancers with 97% sensitivity and 94% specificity but the proteins have not been further investigated in independent studies [324]. Apolipoprotein A-I, transthyretin, and transferrin were identified in a proteomic screen of serum of ovarian cancer patients [325]. When combined with CA125 detection in serum, they distinguished normal samples from borderline samples with 91% sensitivity and 92% specificity, and normal samples from early stage ovarian cancer with a sensitivity of 89% and a specificity of 92% [325]. Furthermore, these three proteins were used to distinguish normal samples from mucinous borderline tumours with 90% sensitivity, and further distinguished normal samples from early stage mucinous ovarian cancer with a sensitivity of 95% whilst CA125 alone was only able to distinguish normal samples from borderline tumours and early stage ovarian cancer with a sensitivity of only 46% and 47%, respectively [325]. As proteomic screening in serum, tissue, and urine of ovarian cancer patients is still new to the scientific community, its efficacy is yet to be fully determined, and recently identified proteins need to be validated in independent studies.

Unfortunately, clinicians cannot identify which ovarian cancer patients are more to likely respond well to treatment as the clinical outcome varies considerably from patient to patient, even though many of their tumours share common clinical and histopathologic features. Thus, there is a need to identify new biomarkers to identify which patients will respond to chemotherapy and which would benefit from aggressive chemotherapy earlier, and which would be suited for enrolment in clinical trials. Development of individualised treatment plans are important and may be assisted using

proteomics to assess and screen biomarkers for each patient and assist in determining the likelihood of relapse and response to current first-line treatments [326].

There has been no proteomic study so far which has assessed the direct and indirect interactions between the cancer cells and their target cells, the peritoneal cells. This interaction could be vital to further understanding the metastatic steps of motility, adhesion, and invasion. It is already documented that ovarian cancer and mesothelial cells show expression of a number of adhesion molecules [327-329] which may play a role in adhesion to the peritoneum. Cancer cells also express proteases which are required to invade through the peritoneal layer [330-333]. What is still unknown is how the proteomic profile of peritoneal and ovarian cancer cells is modified when the cells interact. A greater understanding of this process could hold the key to developing novel treatment strategies or biomarker of ovarian cancer or.

In this study, we focused on functional proteomics using protein expression profiling to assess the changes in protein profiles which occur when human peritoneal cells interact with human ovarian cancer cells. We utilised an *in vitro* model designed to mimic ovarian cancer metastasis. We utilised 2-D electrophoresis for analysis and Matrix-assisted laser desorption/ionization time of flight/time of flight (MALDI-TOF/TOF) and liquid chromatography-electrospray ionisation (LC-ESI) MS for protein identification.

NOTE:
This figure is included on page 60
of the print copy of the thesis held in
the University of Adelaide Library.

Figure 2.1. *Types of proteomics and their applications.*

Proteomics includes a range of techniques to investigate unlimited possible protein profiles [334].

2.2. MATERIALS AND METHODS

2.2.1. Co-culture of ovarian cancer and peritoneal cells

The human ovarian tumour cell lines OVCAR-3 and SKOV-3 were kindly donated by Judith Clements (Queensland University of Technology, Brisbane) and OVCAR-5 cells were kindly donated by Dr. Stephen Williams (Fox Chase Cancer Centre Philadelphia, USA). All cancer cell lines (available for purchase from American Type Culture Collection, ATCC) were maintained in RPMI 1640 medium (Sigma Aldrich) supplemented with 4mM L-glutamine, 100 µg/ml penicillin, 100 µg/ml streptomycin, 20 µg/ml fungizone, 2 µg/ml amphotericin B. OVCAR-3 and SKOV-3 were additionally supplemented with 10% foetal bovine serum (FBS) whilst OVCAR-5 was additionally supplemented with 7.5 µg/ml insulin and 5% FBS. LP-9 peritoneal cells isolated from human omentum were purchased from Coriell Cell Repository (Camden, USA) and maintained in a 1:1 mixture of M199 medium (Sigma Aldrich) and Ham's F-12 nutrient medium (Sigma Aldrich) supplemented with 10% FBS, EGF (10 ng/ml, Sigma Aldrich), hydrocortisone (0.5 µg/ml, Sigma Aldrich), and antibiotics.

LP-9 peritoneal cells were cultured in 6-well plates in growth medium until they reached confluency. LP-9 cell monolayers were washed twice with LP-9 growth medium without FBS (serum-free LP-9 growth medium) and incubated with serum-free LP-9 growth medium for 1 hr at 37°C. LP-9 cell monolayers were then washed twice with serum-free LP-9 growth medium to remove remaining serum proteins. Ovarian cancer cells (OVCAR-5 and SKOV-3) were washed as per the LP-9 monolayers, trypsinized, centrifuged for 5 min at 1800 rpm, washed, and resuspended in serum-free LP-9 media

and added to the washed monolayers of LP-9 cells (2 x 10^5 cells/well). Cells were co-cultured directly for up to 96 hr at 37°C/5% CO_2 before collection of the CM.

LP-9 and OVCAR-5 were also cultured in an indirect two-way co-culture system using the Opticell-system (Nunc, Thermo Fisher Scientific, Roskide, Denmark) which allows cells to share the same culture media without being in direct physical contact with each other. CM was also collected from one way cultures where LP-9 cells were treated with serum-free CM collected from OVCAR-5 or SKOV-3 cells or where ovarian cancer cells (OVCAR-5 and SKOV-3) were cultured with serum-free CM collected from LP-9 cells.

2.2.2. 1D and 2D analysis

Collected CM was precipitated with 4 volumes of 100% cold acetone at -20°C overnight. The samples were centrifuged at 6000g for 5 min and the protein pellet washed with 100% cold acetone and dissolved in sodium dodecyl sulphate (SDS) sample buffer (NuPAGE, Invitrogen, Carlsbad, USA). For 1D analysis, an equal volume of each CM sample (10 µl) was mixed with 2.5 µl 4x LDS buffer (NuPAGE LDS, Invitrogen) and 0.5 M dithiothreitol (DTT, 1.6 µl) then heated at 70°C for 10 min before loading onto a polyacrylamide gradient gel (NuPAGE 4-12% Bis-Tris, Invitrogen). Molecular weight markers were run alongside the samples for reference, either Kaleidoscope prestained markers (Bio-Rad) or Novex sharp prestained markers (Invitrogen) were utilized as indicated. Otherwise, proteins were quantitated using an EZQ protein quantitation kit (Invitrogen) following the manufacturers' protocols. Protein samples were separated by electrophoresis at 200 V for 50 min. Following electrophoresis, gels were fixed and

stained with colloidal Coomassie G-250 or proteins were transferred to PVDF membranes (GE Healthcare, Little Chalfont, England) for western blotting.

For 2D gels electrophoresis analysis, immobilized pH gradient (IPG) strips (11cm, GE Healthcare) were rehydrated overnight in 200 µl rehydration buffer (1.2% (v/v) DeStreak, 0.5% pH 3-11 IPG buffer, 7 M urea, 2 M thiourea, 4% CHAPS, 30 mM Tris and a trace amount of bromophenol blue). Protein samples (50 µg) from the precipitated CM of LP-9, OVCAR-5, a mix of LP-9 and OVCAR-5 single cultures, and co-cultured LP-9 and OVCAR-5 were dissolved in lysis buffer containing 7 M urea, 2 M thiourea, 4% CHAPS, 0.8% IPG buffer, 65 mM DTT, 1 mM PMSF, and 30 mM Tris were loaded onto the rehydrated IPG strips. Isoelectric focusing was carried out and proteins were separated at room temperature using a step-wise gradient until 46,000 Vhrs was achieved using the Ettan IPGphor II system (GE Healthcare). Following equilibration, the IPG strips were applied to the Criterion XT precast gels 4- 12% Bis-Tris (Bio-Rad, Hercules, USA). SDS polyacrylamide gel electrophoresis (SDS-PAGE) was performed at 50 V for 0.5 hr and then 150 V until the dye-front reached the bottom. Gels containing protein from LP-9, OVCAR-5, a mix of LP-9 and OVCAR-5 (60:40), and LP-9 + OVCAR-5 co-culture were stained with silver stain (Biorad) scanned, and analysed using PDQuest advanced 2-D analysis software (v 7.0, Biorad). Gels were warped using identified landmark spots present in every gel as anchor points. Warped gels were overlaid in pairs and viewed in darkview in the multichannel viewer to determine which spots were differentially expressed in the LP-9 + OVCAR-5 co-culture media when compared with LP-9 alone, OVCAR-5 alone, and the mix of LP-9 and OVCAR-5. All experiments were

performed in duplicate and only spots identified as differentially expressed in both experiments were selected for MS identification.

2.2.3. Mass spectrometry

Selected spots of differentially expressed proteins were excised from the gels, destained, and digested with 50 or 100 ng of trypsin per sample. A control gel piece was cut from a blank portion of a gel as a negative control. The samples (5 μl from ~10 μl) were chromatographed using an Agilent Protein ID Chip column assembly (40 nl trap column with 0·075 x 43 mm C-18 analytical column) housed in an Agilent HPLC-Chip Cube Interface connected to an HCT ultra 3D-Ion-Trap mass spectrometer (Bruker Daltonik GmbH, Bremen Germany). The column was equilibrated with 4% acetonitrile (ACN) / 0.1% FA at 0.5 μL/min and the samples eluted with an ACN gradient (4%-31% in 32 min). Ionizable species (300 < m/z < 1,200) were trapped and two of the most intense ions eluting at the time were fragmented by collision-induced dissociation. MS and MS/MS spectra were subjected to peak detection using DataAnalysis (version 3.4, Bruker Daltonik GmbH) then imported into BioTools (version 3.1, Bruker Daltonik GmbH). The MS/MS spectra were submitted to the in-house MASCOT database-searching engine (version 2.2, Matrix Science). Using the following specifications: Taxonomy: mammals, Database: Swissprot 56.7, Enzyme: Trypsin, Fixed modifications: Carbamidomethyl (C), Variable modifications: Oxidation (M), Mass tol MS: 0.3 Da, MS/MS tol: 0.4 Da, Peptide charge: 1+, 2+ and 3+, Missed cleavages: 1.

2.3. RESULTS

2.3.1. Direct co-culture of peritoneal cells and ovarian cancer cells produces an altered protein profile

When peritoneal cells and ovarian cancer cells were grown in direct co-culture, we observed a change in the morphology of the LP-9 and OVCAR-5 cells. Cellular aggregates were observed protruding from the monolayer after 96 hr (Figure 2.2). There was also clear difference in the protein profiles of the CM collected from ovarian cancer cells and the peritoneal cells cultured alone when compared with LP-9 and ovarian cancer cells directly co-cultured together (Figure 2.3a). We observed a visible loss of a number of bands from the LP-9 alone profile when compared with the direct co-culture protein profile including; several high molecular weight proteins visible greater than 150 kDa, a group of proteins between 66 and 97 kDa, and a very strong band at approximately 45 kDa (Figure 2.3b). There were also bands which appeared to be upregulated proteins in the co-culture at approximately 34 and 64 kDa. These were selected for identification by MS.

In addition to identifying differentially expressed proteins by 1D electrophoresis, we also subjected the CM from co-cultured OVCAR-5 cells and LP-9 to 2D electrophoresis. We compared the protein profile of CM from co-cultured LP-9 peritoneal cells and OVCAR-5 cells with the CM from individually cultured LP-9 and OVCAR-5 cells which were mixed together. We observed marked changes in the protein profile, evident by additional spots present, spots now absent, and spot trains which appeared to have shifted in either molecular weight, pI, or both (Figure 2.4). Spots upregulated in the co-

culture were visible in red in the multichannel viewer in PDQuest, including a spot train at 50 kDa which appeared to have shifted from 55 kDa in the mix gel and also appeared to have become more basic. The proteins which were downregulated when the cells were in direct co-culture are shown in green.

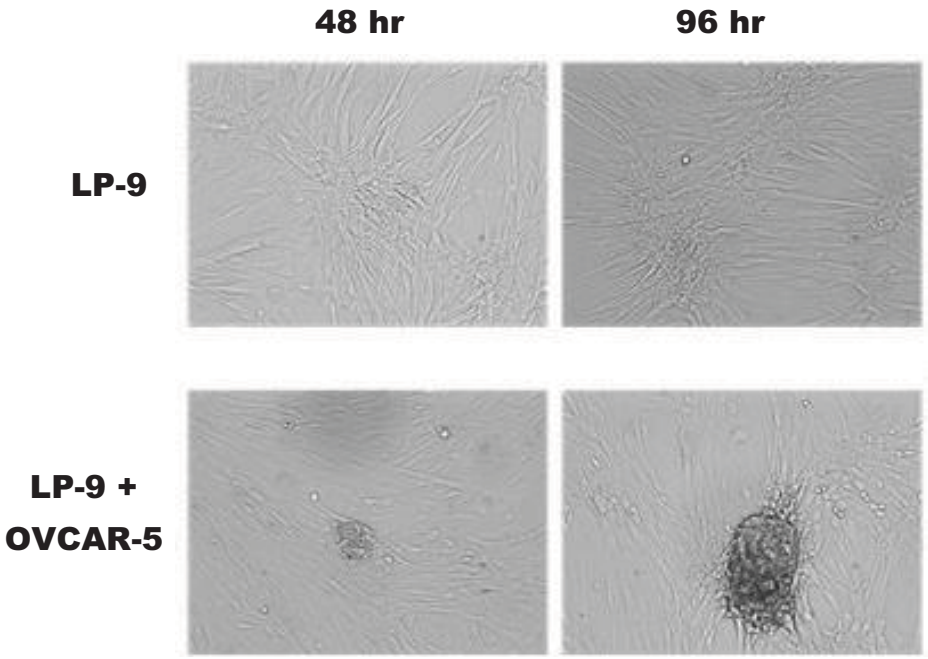

Figure 2.2. *Co-culture of LP-9 cells with OVCAR-5 cells induces a morphological change in the cells.*

A monolayer of LP-9 cells was directly co-cultured with a suspension of OVCAR-5 cells for 48 hr to mimic the *in vivo* situation of ovarian cancer metastasis.

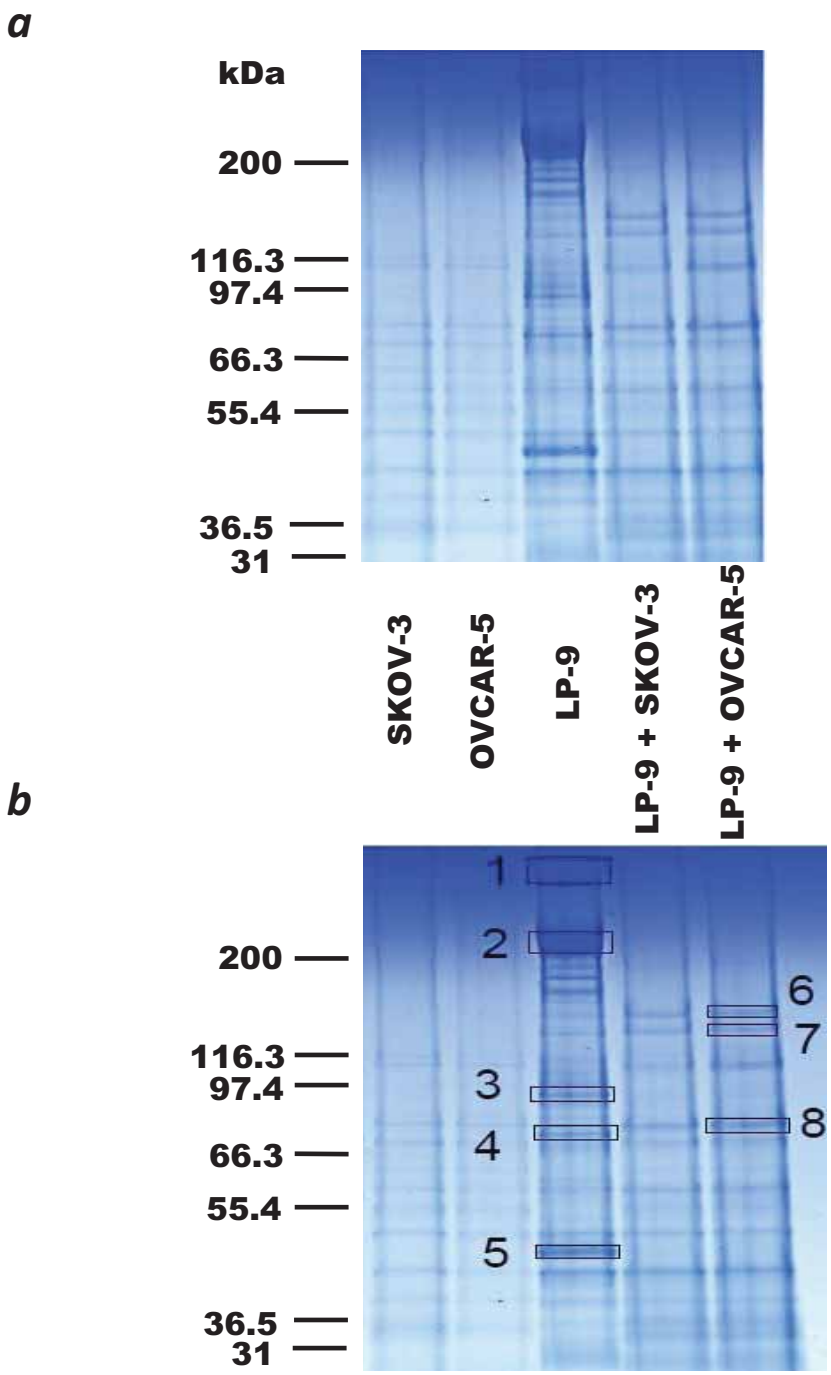

Figure 2.3. *Co-culture of LP-9 cells with OVCAR-5 cells produces an altered protein profile.*

(*a*) A monolayer of LP-9 cells was exposed to a suspension of OVCAR-5 or SKOV-3 cells for 48 hr to mimic the *in vivo* situation of ovarian cancer metastasis and the CM collected, precipitated in acetone, and run on an SDS gel and stained with coomassie. (*b*) Bands were selected for excision and mass spectrometry identification if they were apparent in either the single cell culture or the co-culture only.

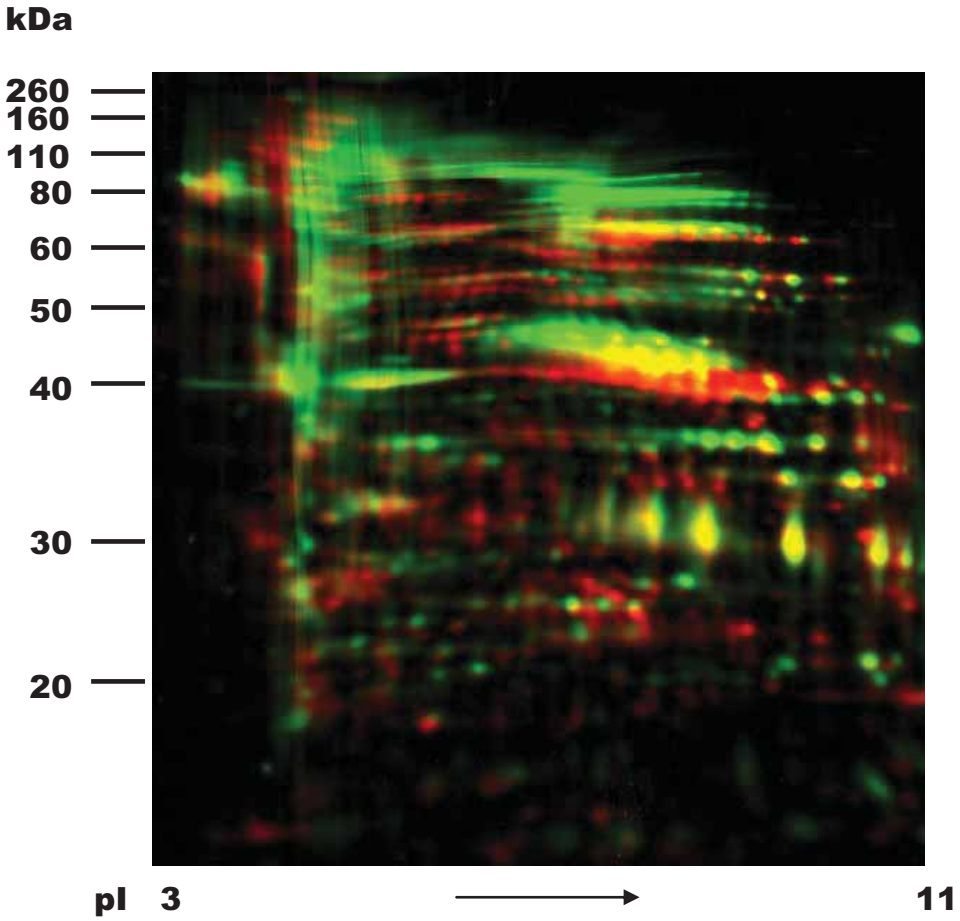

Figure 2.4. *PDQuest analysis of the proteomic profile of a mix of CM collected from LP-9 and OVCAR-5 cells and from LP-9 + OVCAR-5 direct co-culture.*

After the gels were warped and matched using PDQuest, the gel of the mix of LP-9 and OVCAR-5 protein was viewed overlaid with the LP-9 + OVCAR-5 co-culture gel in a multichannel viewer using the dark view setting. Red spots indicate proteins present in the co-culture gel but not in the mix gel suggesting upregulation of the proteins. Green spots indicate proteins present in the mix CM but not in co-culture, indicating downregulation of the proteins. Yellow spots indicate proteins present in both the mix and co-culture CM samples.

2.3.2. Identification of proteins altered in direct peritoneal-ovarian cancer cell co-culture

Protein bands identified as being either upregulated in direct co-culture or downregulated in single cell culture from Figure 2.3 were excised from the coomassie stained gel and digested with trypsin. Identification spectra were obtained using the MALDI-TOF/TOF mass spectrometer (Table 2.1). The majority of proteins had a MASCOT score of approximately two-fold or higher than the probability cut-off score of 55, indicating very high probability of success in the identification of the proteins. Fibronectin, periostin, transforming growth factor β inducible protein (TGFBIp), and plasminogen activator inhibitor-1 (PAI-1) were identified as bands 1-5 respectively in the LP-9 culture which were not visible in the protein profile of LP-9 cells directly co-cultured with OVCAR-5 cells in a coomassie stained gel. Bands 6-8 were identified in the direct co-culture CM as keratin type II skeletal I (CK-1), and two forms of cleaved fibronectin respectively in the direct co-culture which were not visibly present in the single cell culture protein profiles.

The ten spots in the 2D gel determined to be upregulated in the direct co-culture (Figure 2.5a) when compared with the 2D gel of the mix of protein from the single cell cultures were excised and digested with trypsin. These samples were then run through ion trap mass spectrometry and the spectra identified by peak detection. The majority of spots were identified as various forms of cytokeratins, but spots 4, 7, and 8 were identified as PAI-1, and two different sizes of annexin A2 respectively (Table 2.2). Similarly, spots which were determined to be downregulated in the LP-9 peritoneal cell culture or in the OVCAR-5 ovarian cancer cell culture compared with the direct co-

culture in duplicate experiments, as shown in Figure 2.5b and Figure 2.5c respectively. However, the down-regulated spots were not further identified in this study due to time restrictions.

a

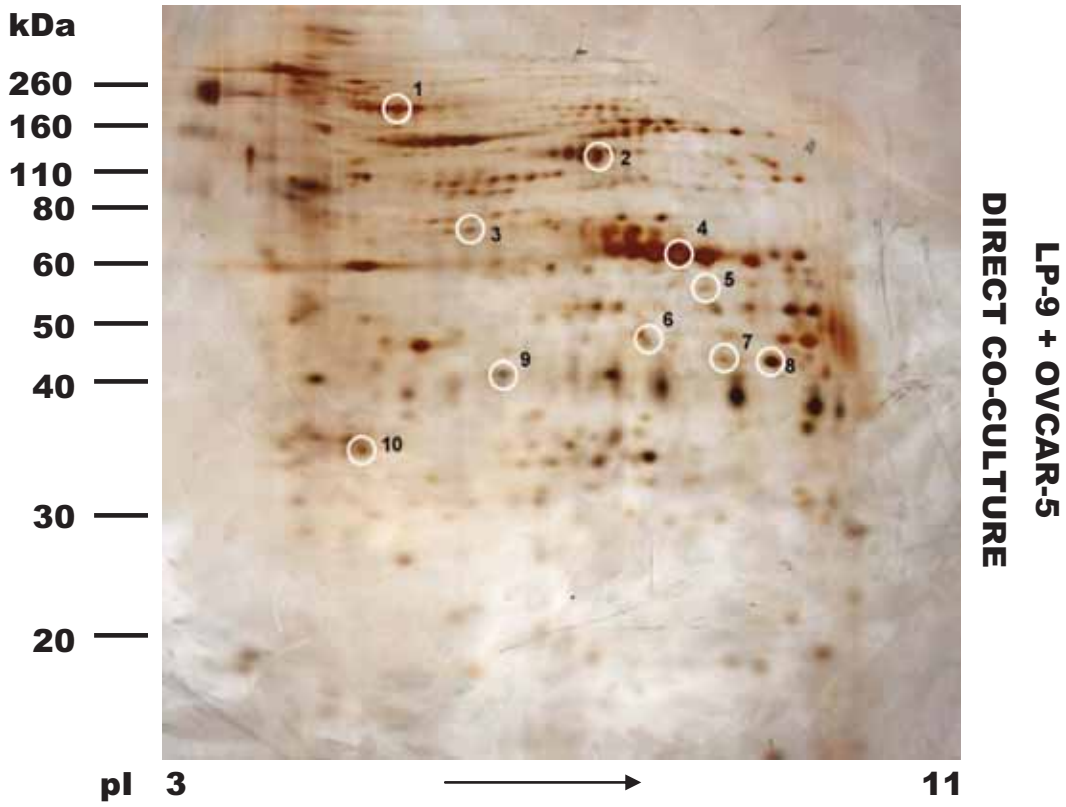
kDa
260
160
110
80
60
50
40
30
20
1
2
3
4
5
6
7
8
9
10
pI 3
11
LP-9 + OVCAR-5
DIRECT CO-CULTURE

b

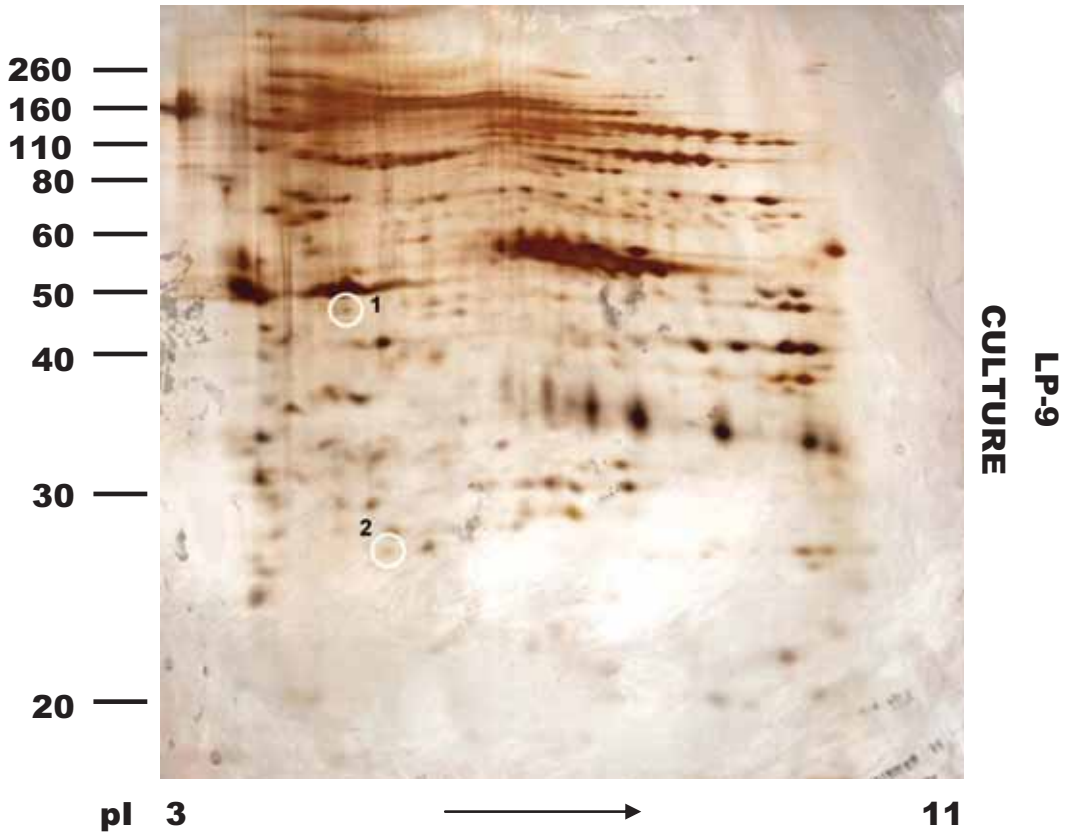
260
160
110
80
60
50
40
30
20
1
2
pI 3
11
LP-9
CULTURE

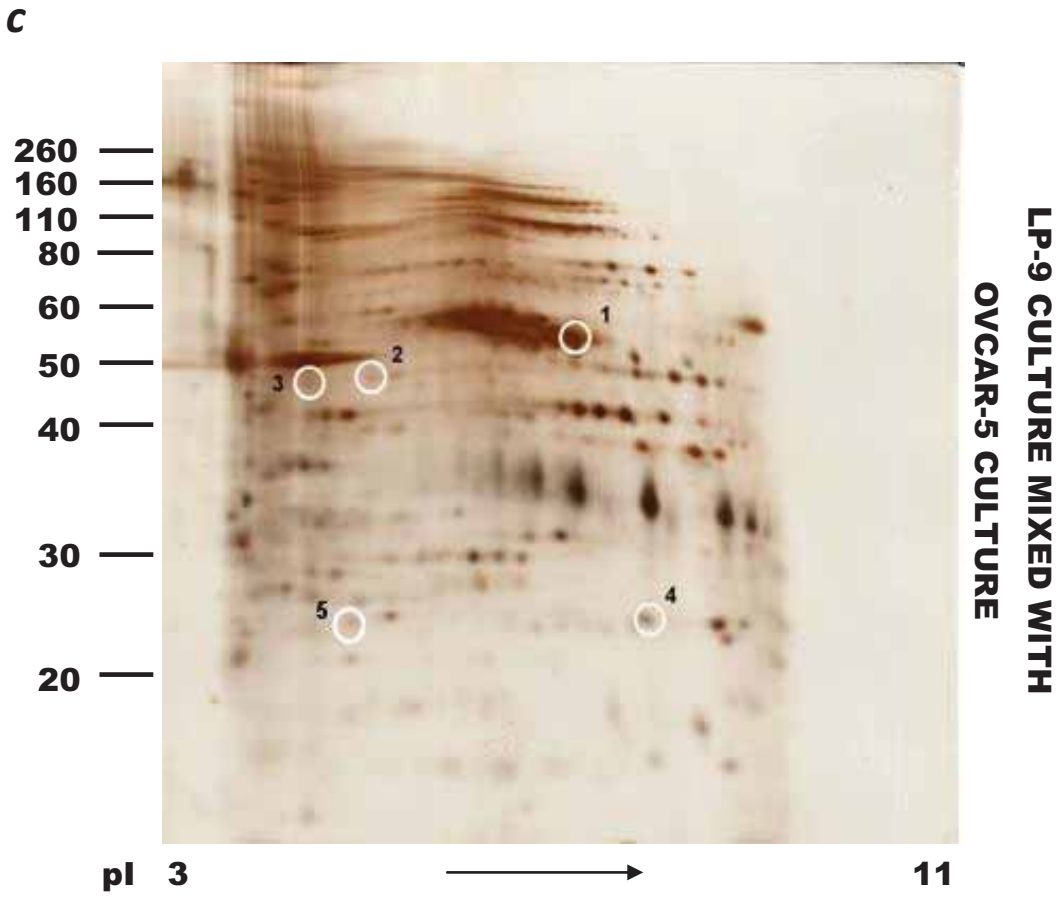

Figure 2.5. *Identification of upregulated and downregulated proteins during ovarian cancer direct interaction with peritoneal cells.*

Red and green spots identified in Figure 2.4 were identified in the original silver stained gel images in duplicate experiments. *(a)* Upregulated proteins in the peritoneal-ovarian cancer cell co-culture *(b)* Downregulated proteins in the peritoneal -OVCAR-5 co-cell culture *(c)* Proteins downregulated in the peritoneal-ovarian cancer cell co-culture shown on the gel containing a mix of protein from LP-9 and from OVCAR-5 cells cultured individually.

Table 2.1. *Identification of proteins up or down regulated in peritoneal-ovarian cancer cell direct co-culture.*

Bands from Figure 2.3 were excised, destained, and digested with trypsin. The tryptic peptides were extracted and applied to an AnchorChip. Spectra were acquired using a MALDI TOF/TOF mass spectrometer, and proteins identified by running the data through the MASCOT database with cut off score set to 55. Biotools analysis of the peptide matches can be found in the Appendix.

Sample	Protein identification	Regulation in co-culture	No. Unique Peptides	Predicted MW (kDa)	Observed MW (kDa)	Match Strength	Peptide Sequence.
A1	Fibronectin	↓	29	266 kDa	> 250	Strong	Figure A.1a
A2	Fibronectin	↓	18	266 kDa	~220	Strong	Figure A.1b
A3	Periostin	↓	8	93.9 kDa	~90	Strong	Figure A.2
A4	Transforming growth factor-beta-induced protein ig-h3 (TGFBIp)	↓	22	75.3 kDa	~65	Strong	Figure A.3
A5	Plasminogen activator inhibitor- 1 (PAI-1)	↓	16	45.1 kDa	~44	Strong	Figure A.4a
A6	Keratin, type II skeletal 1 (CK-1)	↑	8	66.1 kDa	~140	Strong	Figure A.5a
A7	Fibronectin	↑	18	266 kDa	~120	Strong	Figure A.1c
A8	Fibronectin precursor	↑	17	266 kDa	~70	Strong	Figure A.1d

Table 2.2. *Identification of upregulated proteins during peritoneal-ovarian cancer cell direct co-culture by LC-ESI mass spectrometry*

Spots identified in Figure 2.5a were excised, destained, and digested with trypsin. The samples were then chromatographed and ionisable species were eluted from an ion trap column and fragmented by collision induced dissociation. MS and MS/MS spectra were subjected to peak detection using DataAnalysis and data was imported in the MASCOT search database to identify the proteins. Biotools analysis of the peptide matches for moderate and strong matches can be found in the Appendix.

Sample	Protein identification	No. Unique peptides	Predicted MW (kDa)	Predicted pI	Observed MW (kDa)	Observed pI	Match strength	Peptide Sequence
B1	CK-1	2	66.1	8.37	80	5.5	Weak	
B2	CK-1	2	66.1	5.14	65	7.0	Weak	
B3	CK-1	3	66.1	8.37	50	6.0	Mod	Figure A.5b
	Keratin, type II skeletal 10 (CK-10)	3	59.7	5.14				Figure A.6a
B4	PAI-1	21	45.1	6.73	44	7.4	Strong	Figure A.4b
B5	CK-1	1	66.1	8.37	40	7.5	Weak	
B6	CK-10	1	59.7	5.14	36	7.3	Weak	
B7	Annexin A2 (Anx A2)	3	38.8	7.86	34	7.6	Mod	Figure A.7a
B8	Anx A2	11	38.8	7.86	34	7.8	Strong	Figure A.7b
	CK-1	10	66.1	8.37				Figure A.5c
	Keratin, type I skeletal 9 (CK-9)	6	62.3	5.19			Mod	Figure A.8a
B9	CK-1	7	66.1	8.37	33	6.2	Mod	Figure A.5d
B10	CK-9	3	62.3	5.19	28	5.3	Mod	Figure A.8b

2.3.3. One way co-culture of peritoneal cells and ovarian cancer cells

We investigated the protein profile from one way cultures where LP-9 cells were treated with serum-free CM collected from OVCAR-5 or SKOV-3 cells over a time course or where ovarian cancer cells (OVCAR-5 and SKOV-3) were cultured with serum-free CM collected from LP-9 cells over a time course. We observed no obvious change in the protein profile from the single cell line culture CM when OVCAR-5 or SKOV-3 cells were incubated in LP-9 CM over a 48 hr period in a 1D coomassie blue stained gel (Figure 2.6). Likewise, there was no obvious change in the protein profile from the single cell line CM when LP-9 cells were incubated in OVCAR-3, OVCAR-5, or SKOV-3 CM over a 48 hr period (Figure 2.7).

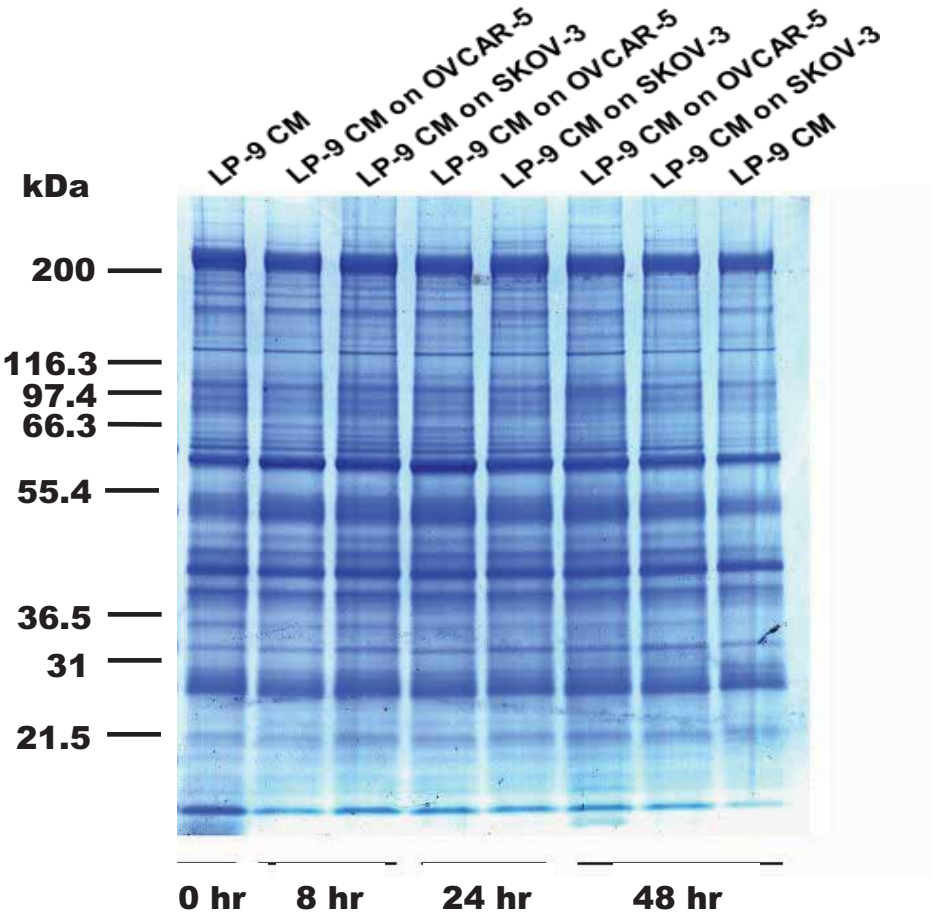

Figure 2.6. *Protein profile of OVCAR-5 and SKOV-3 cells following treatment with LP-9 CM.*

Ovarian cancer cells OVCAR-5 and SKOV-3 were incubated in serum free CM collected from LP-9 cells for 48 hr.

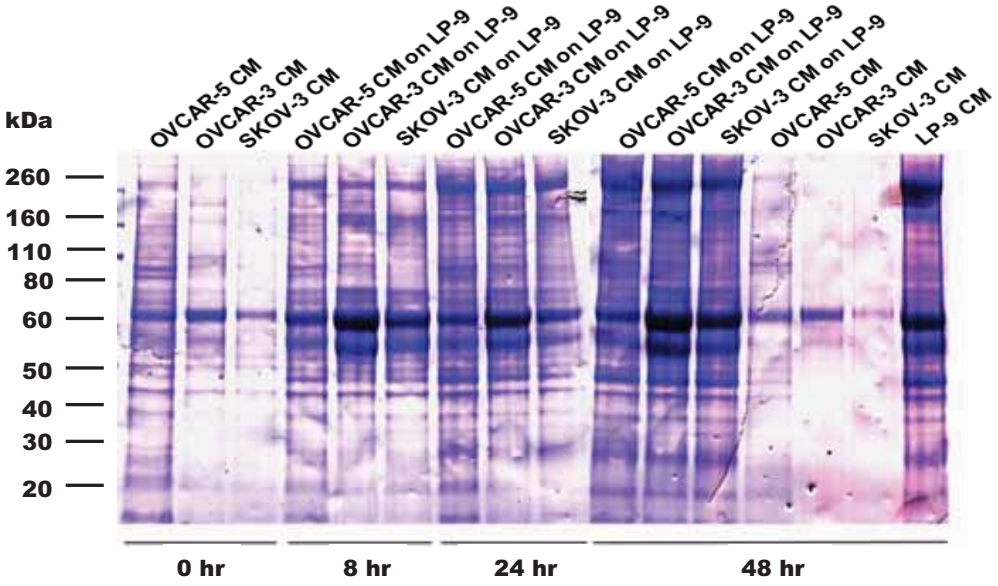

Figure 2.7. *Protein profile of LP-9 peritoneal cells following treatment with OVCAR-5 or SKOV-3 CM.*

LP-9 cells were incubated in serum free CM collected from OVCAR-3, OVCAR-5, and SKOV-3 cells for 48 hr.

2.3.4. Indirect co-culture of peritoneal and ovarian cancer cells produces and altered protein profile

When peritoneal cells and ovarian cancer cells were grown in Opticell indirect co-culture, where the ovarian cancer cells were sharing CM with the peritoneal monolayer, there was a visible loss of a number of bands when compared with the profiles of LP-9 and OVCAR-5 culture alone including high molecular weight proteins visible on a coomassie blue stained gel at approximately 260 kDa, medium molecular weight proteins at 80 kDa, and a band at about 48 kDa (Figure 2.8) which was similar to that seen in the direct co-culture coomassie (Figure 2.3). There were also bands which appeared to be upregulated proteins in the co-culture at approximately 100, 60, 35, 28, and 12 kDa. This was even more evident when the proteins were run on a 2D gel and stained with silver with very different protein profiles apparent between peritoneal cells and ovarian cancer cells. When a mix of peritoneal Opticell culture protein and ovarian cancer Opticell culture protein were mixed and compared with the Opticell indirect co-culture protein on silver stained gels, there was clearly a change in the proteomic profile, evident by additional spots present, spots now absent, and spot trains which appeared to have shifted in either molecular weight, pI, or both. By warping and aligning the spots using the PD Quest software, the mix and co-culture gels were able to be overlaid (Figure 2.9) and spots upregulated in the co-culture were visible in red, including a spot train at 50 kDa which appeared to have shifted from 55 kDa in the mix gel and also appeared to become more basic. There were also spot trains at approximately 80 kDa and at 60 kDa which do not appear to be a shift in size or pI from

the mix gel. Proteins which are downregulated when the cells were in direct co-culture are shown in green and any upregulated are shown in red.

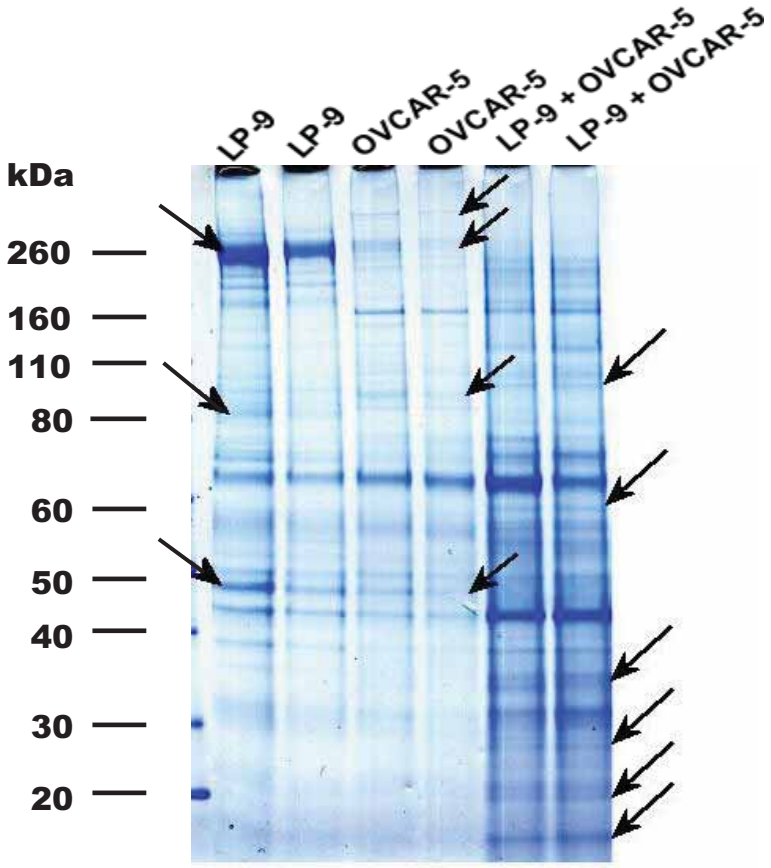

Figure 2.8. *Opticell co-culture of LP-9 cells with OVCAR-5 cells produces an altered protein profile.*

A monolayer of LP-9 cells were grown on one membrane in the Opticell. The Opticell was then flipped over, and OVCAR-5 cells added in suspension to attach to the second membrane for 48 hr to mimic the *in vivo* situation of ovarian cancer metastasis where both cell types share their secreted proteins in the peritoneal cavity. The CM was collected, precipitated in acetone, and run on an SDS gel and stained with Coomassie. Arrows indicate protein bands which are up or downregulated during co-culture.

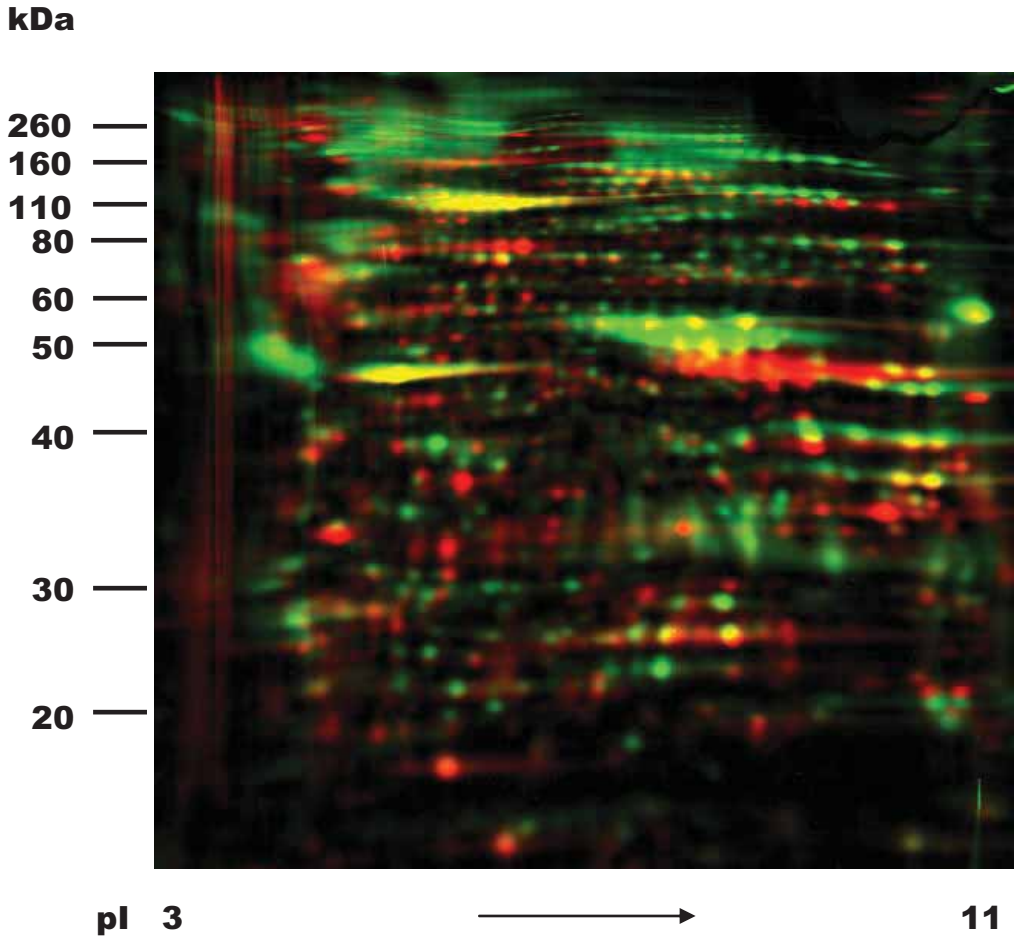

Figure 2.9. *PDQuest analysis of the proteomic profile of a mix of CM collected from LP-9 and OVCAR-5 cells and from LP-9 + OVCAR-5 Opticell indirect co-culture.*

After the gels were warped and matched using PDQuest, the gel of the mix of LP-9 and OVCAR-5 protein was viewed overlaid with the LP-9 + OVCAR-5 Opticell co-culture gel in a multichannel viewer using the dark view setting. Red spots indicate proteins present in the Opticell co-culture gel but not in the mix CM suggesting upregulation of the proteins. Green spots indicate proteins present in the mix CM but not in Opticell co-culture, indicating downregulation of the proteins. Yellow spots indicate proteins present in both the mix and co-culture CM samples.

2.3.5. Identification of proteins altered in Opticell indirect peritoneal-ovarian cancer cell co-culture

The thirteen spots determined to be upregulated in the Opticell indirect co-culture (Figure 2.10a) when compared with the mix of protein from the single cell cultures in duplicate experiments were excised and digested with trypsin. These samples were then passed through ion trap mass spectrometry and the spectra identified by peak detection. Many of spots were identified as varying types of cytokeratins, but spots 1, 4, 6, 7, 8, 9, and 11 were identified as transketolase (TKT), PAI-1, a TKT fragment, annexin A6, annexin A2, and elongation factor 2 (EEF-2) respectively (Table 2.3). Spots which were determined to be downregulated in the LP-9 peritoneal cell culture or in the OVCAR-5 ovarian cancer cell culture compared with the Opticell indirect co-culture in duplicate experiments, as shown in Figure 2.10b and Figure 2.10c respectively. However, these spots were not further identified in this study.

a

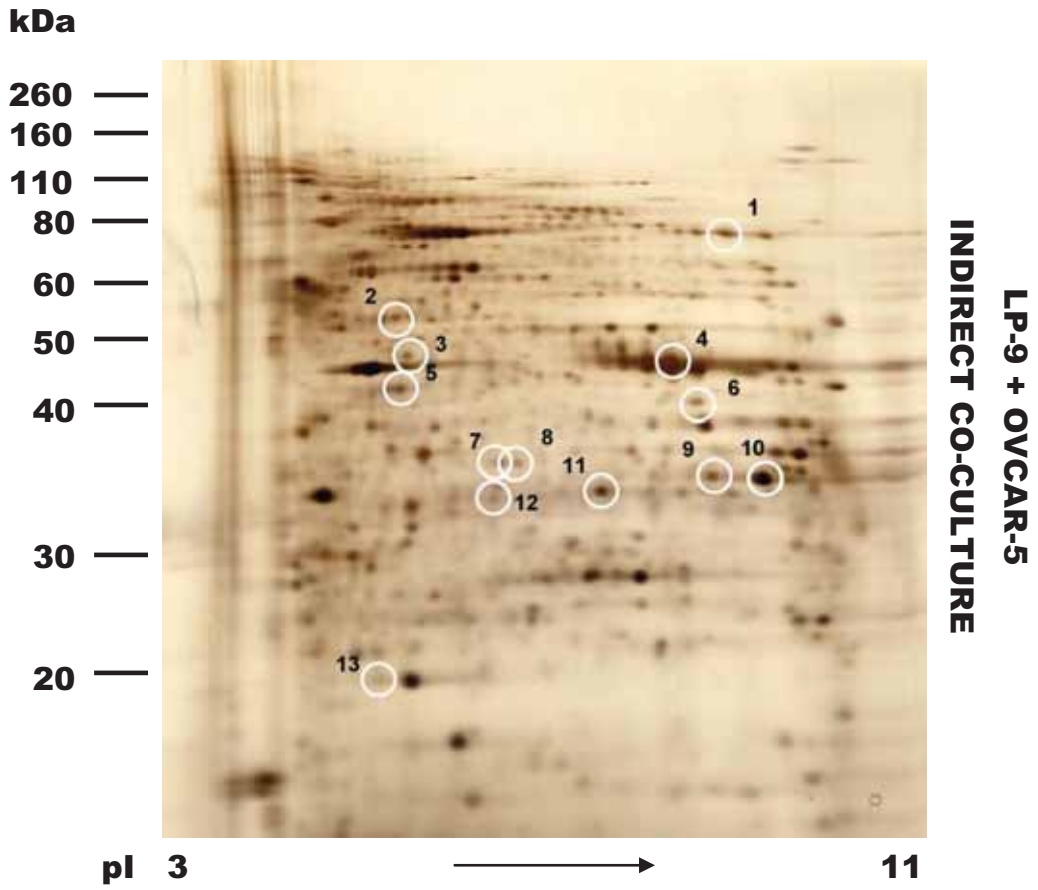
kDa
260
160
110
80
60
50
40
30
20
1
2
3
4
5
6
7
8
9
10
11
12
13
pI 3
11
LP-9 + OVCAR-5
INDIRECT CO-CULTURE

b

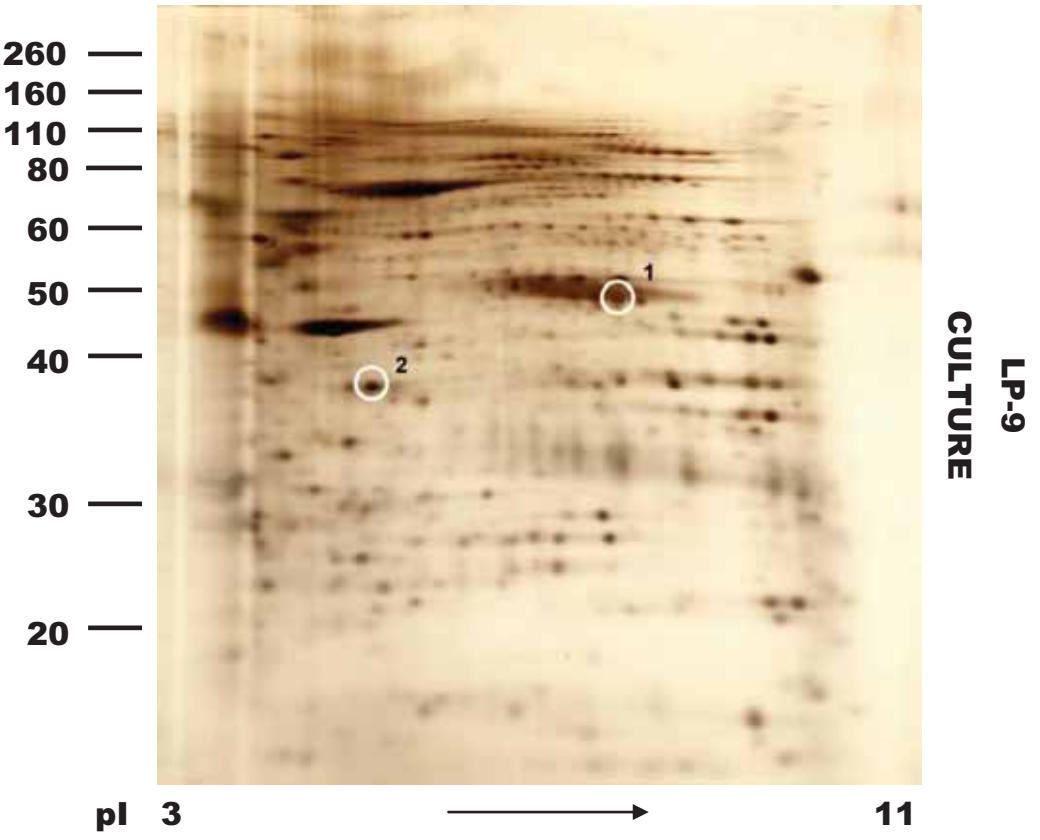
260
160
110
80
60
50
40
30
20
1
2
pI 3
11
LP-9
CULTURE

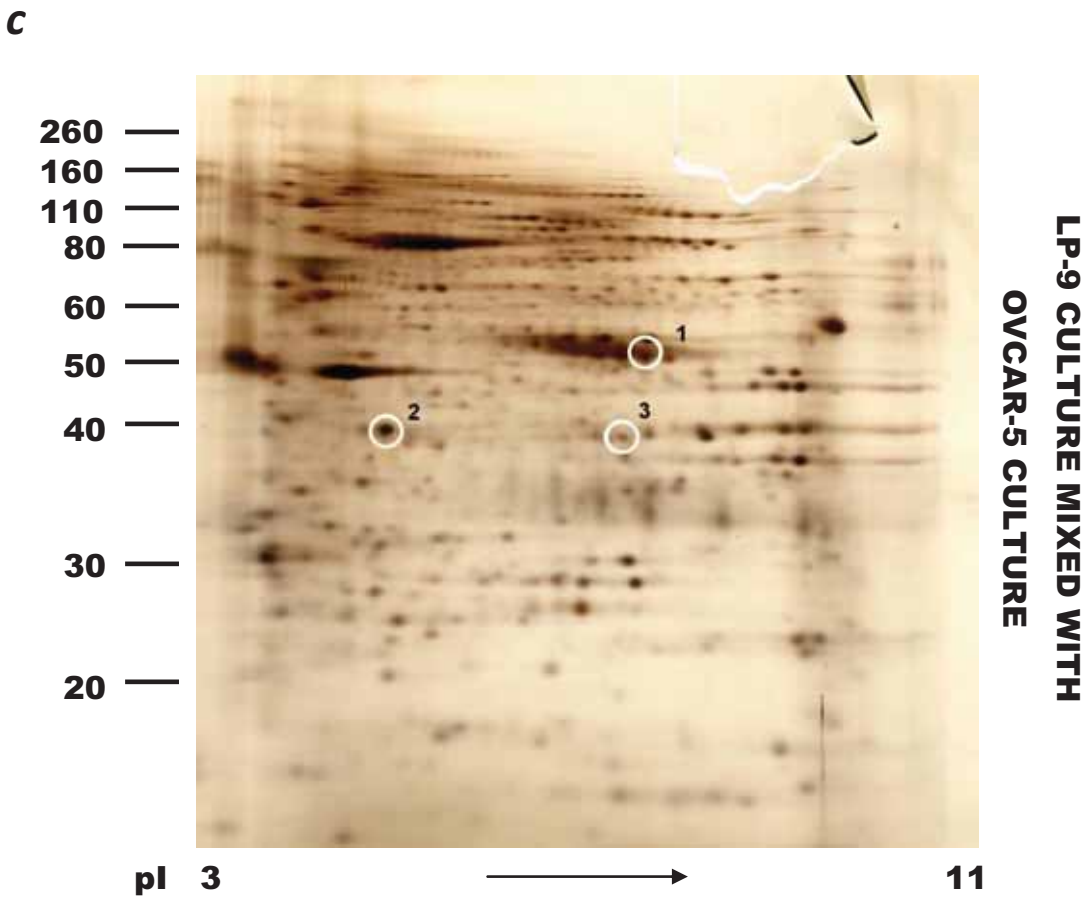

Figure 2.10. *Identification of upregulated and downregulated proteins during ovarian cancer interaction with peritoneal cells through shared media in the Opticell system.*

Red and green spots identified in Figure 2.9 were identified in the original silver stained gel images by eye in duplicate experiments. Spots identified in both experiments are shown here *(a)* Upregulated proteins in the peritoneal-ovarian cancer cell Opticell co-culture *(b)* Downregulated proteins in the peritoneal cell culture *(c)* Proteins downregulated in the peritoneal-ovarian cancer cell co-culture shown on the gel containing a mix of protein from LP-9 and from OVCAR-5 cells.

Table 2.3. *Identification of upregulated proteins during peritoneal-ovarian cancer cell Opticell indirect co-culture by LC-ESI mass spectrometry*

Spots identified in Figure 2.10a were excised, destained, and digested with trypsin. The samples were then chromatographed and ionisable species were eluted from an ion trap column and fragmented by collision induced dissociation. MS and MS/MS spectra were subjected to peak detection using DataAnalysis and data was imported in the MASCOT search database to identify the proteins. Biotools analysis of the peptide matches for moderate and strong matches can be found in the Appendix.

Sample	Protein identification	No. Unique peptides	Predicted MW (kDa)	Predicted pI	Observed MW (kDa)	Observed pI	Match Strength	Peptide Sequence
C1	Transketolase (TKT)	10	68.5	7.92	80	5.5	Strong	Figure A.9a
C2	CK-1	8	66.1	8.37	55	5.4	Strong	Figure A.5e
	CK-10	4	59.7	5.14			Mod	Figure A.6b
C3	CK-9	3	62.3	5.19	50	5.5	Weak	
C4	PAI-1	21	45.1	6.73	48	7.2	Strong	Figure A.4c
	CK-1	11	66.1	8.37				Figure A.5f
	CK-9	10	62.3	5.19				Figure A.8c
	Cytokeratin-6C (CK-6C)	7	60.3	8.39				Figure A.
	Cytokeratin-16 (CK-16)	9	51.6	4.99				Figure A.
	Cytokeratin-14 (CK-14)	9	51.9	5.09				Figure A.
	Cytokeratin-5 (CK-5)	8	62.6	7.89				Figure A.

Sample	Protein identification	No. Unique peptides	Predicted MW (kDa)	Predicted pI	Observed MW (kDa)	Observed pI	Match Strength	Peptide Sequence
C5	CK-1	7	66.1	8.37	44	5.4	Strong	Figure A.5g
	CK-10	3	59.7	5.14			Mod	Figure A.6c
C6	TKT	7	68.5	7.92	43	7.4	Strong	Figure A.9b
C7	Carboxypeptidase B	1	47.8	5.24	36	6.2	Very Weak	
C8	Annexin A6 (Anx A6)	5	76.2	5.42	36	6.3	Mod	Figure A.10
C9	Anx A2	14	38.8	8.15	34	7.6	Strong	Figure A.7b
	CK-1	6	66.1	8.37			Mod	Figure A.5h
C10	Anx A2	26	38.8	7.86	34	7.8	Strong	Figure A.7c
	CK-1	6	66.1	8.37			Mod	Figure A.5i
	CK-9	5	62.3	5.19				Figure A.8d
C11	Elongation factor 2 (eEF-2)	6	96.2	6.44	34	7.0	Mod	Figure A.11
	CK-1	4	66.1	8.37				Figure A.5j
	CK-10	3	59.7	5.14				Figure A.6d
C12	CK-1	3	66.1	8.37	33	6.2	Weak	
C13	CK-1	4	66.1	8.37	20	5.2	Weak	

2.3.6. Annexin A2 and A6 are cleaved during peritoneal-ovarian cancer cell co-culture

Table 2.4 provides a summary of protein modulation during ovarian cancer-peritoneal cell interaction. Further investigation of the annexin A2 fragments identified in Table 2.3 by Ms Noor Lokman in our laboratory confirmed by 2D western immunoblotting that annexin A2 is cleaved during direct co-culture of OVCAR-5 and LP-9 cells (Figure 2.10). Annexin A2 was detected at 37 kDa in the CM of both LP-9 and OVCAR-5 alone across a range of pI values. In the co-culture, two smaller forms of annexin A2 were observed (Figure 2.11). Likewise, we observed that LP-9 cells produced an approximately 42 kDa cleaved form of annexin A6, and that annexin A6 is cleaved to a smaller approximately 37 kDa form in the direct co-culture (Figure 2.12).

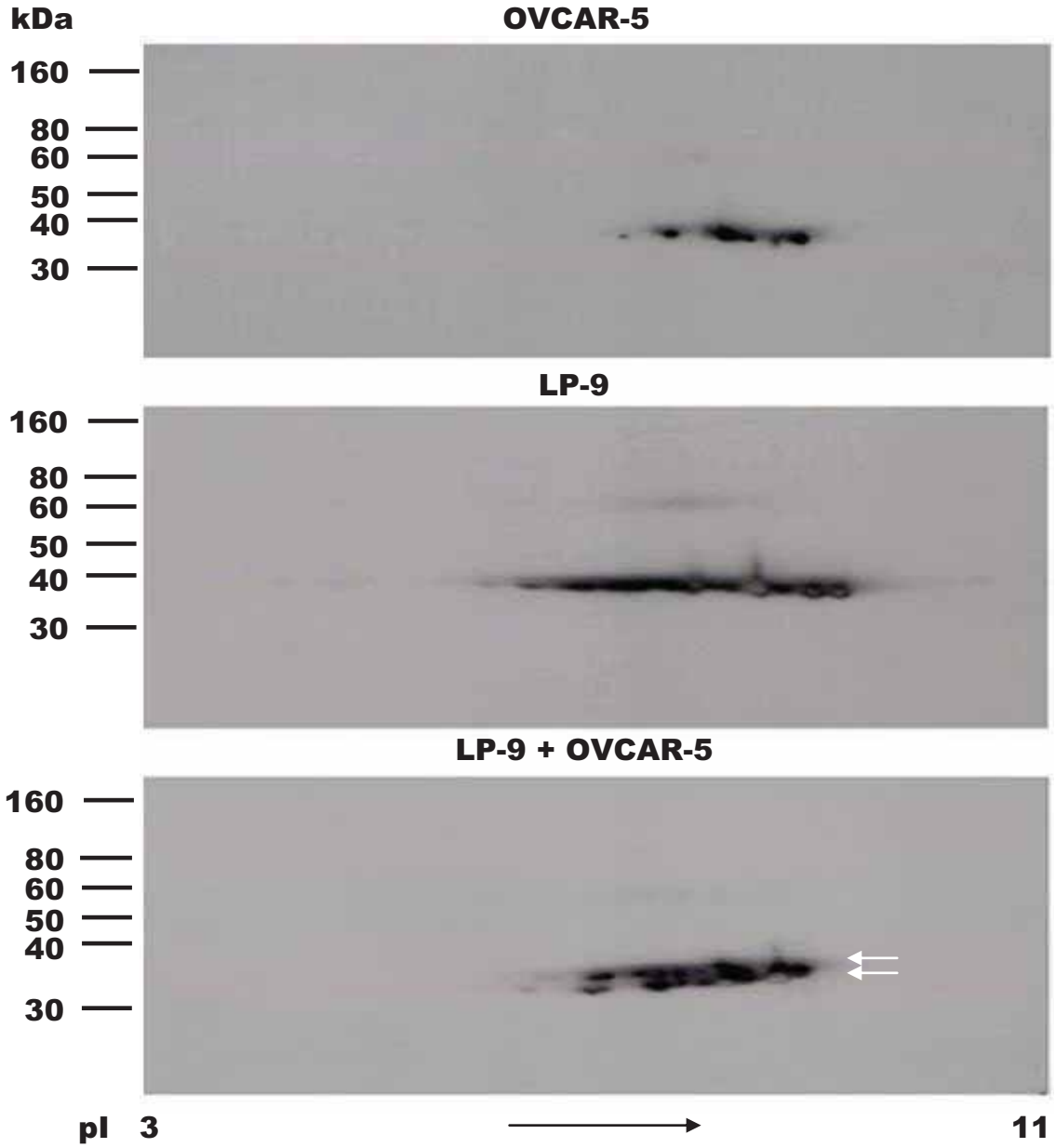

Figure 2.11. *Annexin A2 is cleaved during OVCAR-5/LP-9 direct co-culture.*

2D western blot against annexin A2 monoclonal antibody (amino acid residues 123-328, 1/2000, #610069, BD Sciences) in CM of OVCAR-5 and LP-9 cells alone and direct co-culture CM of OVCAR-5 and LP-9 cells. Multiple spots of annexin A2 were identified at approximately 36 kDa for OVCAR-5 and LP-9 over a pI range of 6 to 8. In the CM from co-cultured of LP-9 and OVCAR-5 cells, annexin A2 spots were observed at approximately 36 and 35 kDa.

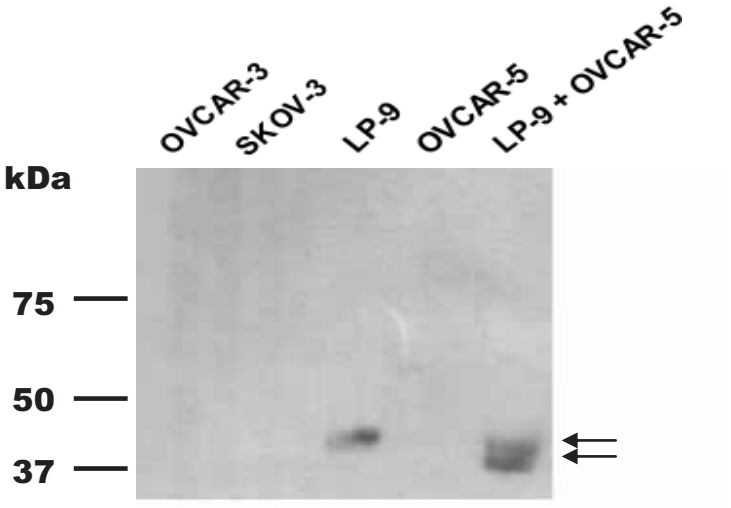

Figure 2.12. *Annexin A6 is cleaved during OVCAR-5 and LP-9 direct co-culture.*

CM was collected from direct co-culture after culture for 48 hours and precipitated with acetone. An equal volume was run on a Tris-HCl SDS-PAGE gel, transferred to PVDF membrane and immunoblotted with anti-annexin A6 (amino acids 497-610, Santa Cruz Biotechnology)

Table 2.4. *Summary of protein expression and processing during peritoneal-ovarian cancer cell co-culture.*

Protein	Indirect Co-culture	Direct Co-culture	Full Length Expressed by Peritoneal Cells	Full Length Size	Cleaved Sizes
CK-1	Cleaved	Full length upregulated/Cleaved	Unknown	66 kDa	55, 50, 48, 44, 40, 34, 33, 28, 20 kDa
CK-5	Cleaved	Unknown	Unknown	62 kDa	48 kDa
CK-6C	Cleaved	Unknown	Unknown	60 kDa	48 kDa
CK-9	Cleaved	Cleaved	Unknown	62 kDa	50, 48, 34 kDa
CK-10	Cleaved	Cleaved	Unknown	60 kDa	55, 50, 44, 36, 34 kDa
CK-14	Cleaved	Unknown	Unknown	52 kDa	48 kDa
CK-16	Cleaved	Unknown	Unknown	52 kDa	48 kDa
PAI-1	Cleaved	Cleaved	Yes	45 kDa	44 kDa
TKT	Full length upregulated/Cleaved	Unknown	Unknown	69 kDa	43 kDa
Annexin A2	Cleaved	Cleaved	Yes	39 kDa	34 kDa
Annexin A6	Cleaved	Cleaved	Yes	76 kDa	34 kDa
EEF-2	Cleaved	Unknown	Unknown	96 kDa	34 kDa
TGFßIp	Unknown	Full length lost	Yes	75 kDa	N/A
Periostin	Unknown	Full length lost	Yes	94 kDa	N/A
Fibronectin	Unknown	Cleaved	Yes	266 kDa	120, 70 kDa

2.4. DISCUSSION

2.4.1. Fibronectin is cleaved in the direct co-culture of peritoneal ovarian cancer cells

In our study, the fibronectin band observed at approx 120 kDa in direct co-culture contained detectable peptides only between amino acids 831 and 1539 (Figure A.1c) whilst the 70 kDa band contained detectable peptides only between amino acids 939 and 1540 (Figure A.1d) suggesting N terminal domain processing. Fibronectin is a 440 kDa, 2390 amino acid long prototypic ECM comprised of three different types of homologous repeating units or modules arranged into protease-resistant domains which are separated by more flexible, protease susceptible regions [335].

Although fibronectin has many biological activities, its role in cancer is well documented to promote cell adhesion and migration, key steps in the metastatic process [336, 337]. Fibronectin contains at least two distinct regions which can interact independently with distinct cell surface receptors [337-340]. The first fibronectin cell-adhesive site to be identified was isolated in the form of protease-resistant fragments of 110-120 kDa, 75 kDa, and 37 kDa [337-340] derived from the internal section of the protein. The fragments detected in our study could be the same observed in these studies which were shown to retain similar cell adhesive activities as those of intact fibronectin [339, 341]. The cell adhesive activity attributed to these fragments is contributed to the RGD sequence motif known for binding integrins [342, 343].

There are many proteases which are capable of cleaving fibronectin. Plasmin has been observed to cleave fibronectin to similar sized fragments as those observed in our study [344-346].

MMP-2 also mediates cleavage of fibronectin into fragments including 120 and 70 kDa fragments [336, 347]. Kenny et al. showed that ovarian cancer cells, which express α5β1 and αVβ3 integrins, demonstrated preferential binding to these fibronectin fragments, and also vitronectin fragments, which could be blocked by use of siRNA knock down of α5β1 and αVβ3 integrins or an anti-MMP-2 antibody [336]. This indicates that fibronectin processing may occur to increase ovarian cancer cell adhesion to the peritoneum via integrin receptors. The 120 kDa fibronectin fragment has also been demonstrated to increase oral squamous carcinoma cell migration [347]. Whilst MMP-3 [348], MMP-19 [349], MT1-MMP [350], and MMP-7 [351] also cleave fibronectin, as well as kallikrein-7 which is upregulated in ovarian cancer cells [73, 352]. Fibronectin cleavage observed in the peritoneal ovarian cancer cell co-culture may be mediated by plasmin or MMPs.

2.4.2. The role of periostin in cancer

Our study identified a downregulation of full length periostin produced by LP-9 cells in the CM of peritoneal-ovarian cancer cell co-culture due to the cell-cell interactions. Periostin is a member of the fasciclin (FAS) family and a unique ECM protein in collagen-rich connective tissues, such as periodontal ligament, periosteum, fascia of skeletal muscles, and cardiac valve [353-357]. Periostins expression is up-regulated by

transforming growth factor β (TGFβ) signalling [354] and is in the same family of proteins as TGFBIp whose expression was also observed to be modulated in the peritoneal-ovarian cancer co-culture (see Chapter 3).

Periostin has been detected by immunohistochemistry and in situ hybridisation at the invasive front of colon and lung cancer in associated fibroblasts [358, 359]. Periostin was also found to have decreased expression in bladder cancers with increasing tumour grade when compared with the high expression in normal bladder tissues [360]. Periostin mRNA was not detected in cell lines involved in cervical, endometrial, colon, bladder, gastric, melanoma, pancreatic, non-small cell lung cancer cell lines or in fibrosarcoma, neuroblastoma, and Wilms' tumour cell lines. However, when periostin was over-expressed in low or non-expressing cancer cell lines, periostin increased tumour growth and angiogenesis in mice xenografts [361]. A conflicting study reported that viral transfection of bladder cancer and osteosarcoma cells with periostin inhibited their anchorage-dependent growth on soft agar [362] indicating a potential tumour-suppressing role for periostin.

However, there are conflicting reports reviewed by Ruan et al, that many of these same cancer types had been found to have high expression of periostin, and/or is associated with poor outcome [363]. Increased periostin has been documented in papillary thyroid cancers [364], breast cancer [365], gastric cancer [366], oral squamous-cell carcinoma [367], and metastatic melanoma [368]. Periostin was increased in colorectal cancer and liver metastases, and it increased colorectal cancer cell proliferation [369]. Pancreatic cancer cells secreted periostin into the surrounding ECM and made the cells resistant to hypoxia induced death and increased their motility [370]. Periostin was also found to be elevated in the serum of colorectal cancer patients [371], breast cancer patients with

bone metastasis but not lung cancer patients with bone metastases [372], and stage IV thyoma patients [367].

Periostin has been detected in epithelial ovarian cancer cells but not in normal ovarian epithelial cells and was shown to increase motility of the cancer cells and their adhesion to the peritoneum [373]. Furthermore, periostin has been detected in the ascites of ovarian cancer patients [373]. As our study showed that periostin was produced by LP-9 peritoneal cells and no matching band appeared in the OVCAR-5 or SKOV-3 ovarian cancer CM, it is more plausible to deduce that the periostin originates from the peritoneal cells exposed to the ascites fluid. This combined data indicates that periostin may have a pro or anti tumorigenic role depending on the cancer type, and might be an effective biomarker or therapeutic target for ovarian cancer.

2.4.3. PAI-1 is inactivated in peritoneal-ovarian cancer cell co-culture

In this study, we found that full length PAI-1 was present in LP-9 culture but was cleaved during peritoneal-ovarian cancer cell direct and indirect interactions.

Plasminogen activators are serine proteases which catalyse the conversion of the plasminogen to the active enzyme, plasmin [374]. Two types of plasminogen activators have been characterized extensively: the urokinase type (uPA) and the tissue type (tPA) activators [375-378] (Figure 2.14). The plasminogen activators play a key role in the regulation of extracellular proteolysis during normal and malignant conditions [374-376]. uPA [379] has been shown to be elevated in primary ovarian tumours [380] and omental metastases [381] and can be used as a prognostic marker for patient response to chemotherapy and survival [382].. A study by Keski-Oja et al. showed that lung cancer

cells responded to TGFβ1 by producing more uPA and tPA than PAI-1, whilst the associated lung fibroblasts responded by producing more PAI-1 and less uPA and tPA [383]. Likewise, TGFβ1 has been shown to affect both the secretion of plasminogen activators and PAI-1 in HRA ovarian cancer cells [384]. Ovarian cancer CM was able to stimulate PAI-1 production in peritoneal cells but did not affect uPA levels [384].

Analysis of the MS peptide fingerprinting for PAI-1 revealed that LP-9 cells produce intact PAI-1 but during co-culture PAI-1 is cleaved. This cleavage occurs between amino acids 379-412 at the C-terminal domain, which includes a known cleavage site for prostate specific kallikrein 2 (Figure 2.13). We observed that PAI-1 was most likely cleaved at the Arg^{346}-Met^{347} position in both the direct and Opticell indirect ovarian cancer-peritoneal cell co-cultures. Cleavage at this site by the prostatic serine protease human kallikrein 2 has been shown to inactivate PAI-1 and prevent its inactivation of uPA and tPA [385]. Ovarian cancer cells also produce a range of kallikreins which are known to stimulate the plasminogen conversion to plasmin [386]. It is possible that a kallikrein is responsible for the processing and inactivation of PAI-1. The interactions between kallikreins, PAI-1, and uPA needs further elucidation in ovarian cancer to fully understand their roles in tumourigenesis.

Figure 2.13. *PAI-1 is cleaved during OVCAR-5 and LP-9 direct co-culture.*

Yellow amino acids sequences indicate those detected by MS/MS peptide mass fingerprinting. The black box indicates the known kallikrein 2 cleavage site whilst the red dotted box indicates the most C-terminal peptide detected in the LP-9 produced full length PAI-1

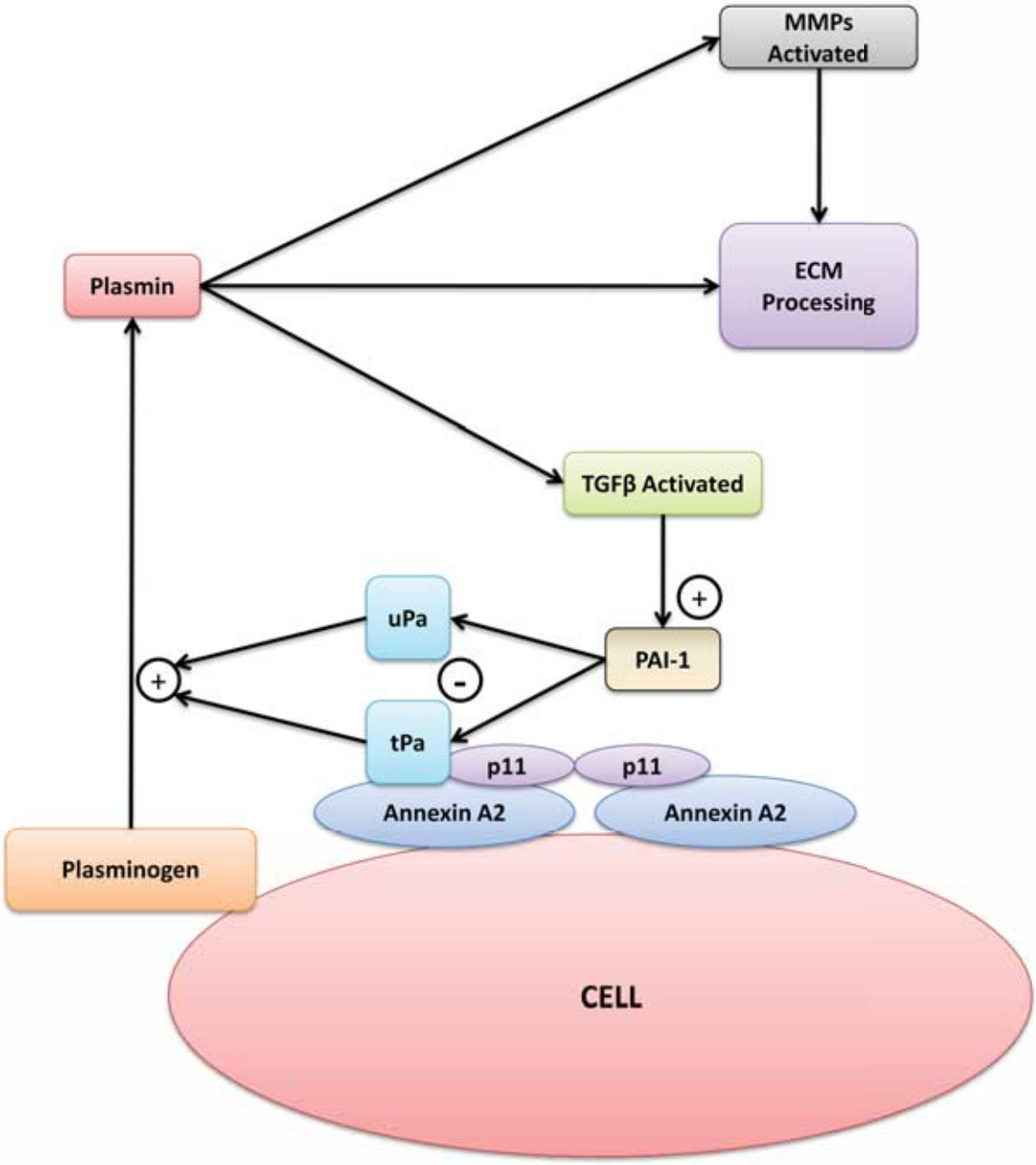

Figure 2.14. *The plasmin production pathway in healthy humans.*

Plasminogen bound to cells is converted to plasmin in the presence of the plasmin activators, uPa or tPA. Plasmin activity results in MMP activation and ECM protein processing. Plasmin also activates TGFβ, which acts as a negative feedback loop, increasing production of PAI-1 to inactivate uPa and tPa resulting in decreased plasmin production.

2.4.4. The role of keratins in cancer

Whilst keratin detection in our study could easily be assumed to be due to contamination from skin cells, it is unlikely due the large number of unique keratins detected by MS. It must also be remembered that keratins are expressed by epithelial cells, which are the precursors to epithelial ovarian cancer cells. Full length 66 kDa CK-1 as well as a range of fragments between 20 and 55 kDa were identified in the CM of peritoneal-ovarian cancer co-culture but not in the CM of either cell line alone. CK-1 is part of a large family of related cytoskeletal proteins most commonly found in the skin above the basal membrane layer in cells that are migrating [387, 388]. Very little is known about the specific role of full length CK-1 in cancer. It is known to be present in the membranes of adherent neuroblastoma cells and binds to β1 integrins, indicating a possible role for CK-1 in tumourigenesis [389]. Full length CK-1 was found in papillary thyroid cancer as well as 45 and 49 kDa bands similar to the fragment sizes of CK-1 we detected in the peritoneal-ovarian cancer co-culture [390]. An additional study identified 37 and 50 kDa CK-1 fragments in bladder cancer but not normal tissue adjacent to the tumour or healthy tissue [391]. Apart from these two studies, there is no other documentation of cleaved CK-1 in other cancers. Thus, our findings support the investigation of CK-1 fragments in ovarian cancer diagnostics in future studies.

CK-1 is also involved in the plasmin pathway. It is known to bind to high molecular weight kininogen (HK), a bradykinin (BK) precursor [392]. Pre-kallikreins also bind to HK which form a multi-component receptor which incorporates CK-1 [393] and the uPA receptor (uPAR) [394] on endothelial cells. This results in the activation of uPA and

kallikreins [395] and liberate BK [396], which can liberate tPA [389]. These findings also suggest a role for CK-1 in the changes to the plasmin pathway observed during peritoneal-ovarian cancer cell interaction.

A 48 kDa fragment of CK-5 was also identified in the CM of indirect peritoneal-ovarian cancer cell co-culture. CK-5 is expressed in squamous, stratified epithelium, which is found mainly in the basal cell layers and is associated with cell proliferation [397, 398]. CK-5, which is usually detected using a CK-5/6 combination antibody as it is closely related to CK-6 and expressed by the same cells [399]. Co-expression has been reported in a number of different types of tumours including basal cell carcinoma [400], prostate cancer [401, 402], ductal breast carcinoma [403, 404], liver mesothelioma [405], peritoneal mesothelioma [406], pleural mesothelioma [407], lung carcinomas [408], melanoma, basal cell carcinoma, thyoma, and salivary gland tumour [409]. CK-5/6 expression is most frequent in ER/PR/HER-2 negative breast tumours [410, 411] and is correlated with breast tumour grade [412], poor outcome [413] and brain metastasis [414].

CK5/6 as a biomarker has superior sensitivity and reliability at differentiating between benign and malignant prostate gland when compared with that of the currently used marker, K903 (high molecular weight cytokeratins) [401]. CK-5 expression is increased after androgen deprivation in prostate cancer cell lines which suggests it may be useful as a treatment response or outcome marker [415]. CK-5/6 has been used successfully in a five antibody panel (which also targets TRIM29, CEACAM5, SLC7A5, MUC1) to better classify the subtypes of lung carcinoma than the currently used two antibody

panel [416]. The expression of CK-5/6 together with p63 has been used to differentiate between adenosquamous carcinoma and adenocarcinoma in pleural effusion samples [417-421]. High CK-5/6 levels in pleural effusions is also associated with longer survival in non-small cell lung cancer patients [422].

Up to 25% of ovarian adenocarcinomas express CK-5 [409], whilst ovarian sex chord stromal tumours have been shown to be negative for CK5/6 [423]. There have been three studies which document fragments of CK-5 in carcinoma; a 56 kDa CK-5 fragment in rat liver carcinoma [424], a 54 kDa fragment in bladder cancer [391], and a 50 kDa CK-5 fragment in bladder cancer [425].

We identified a 48 kDa fragment of CK-6C produced during indirect co-culture of peritoneal cells with ovarian cancer cells. CK-6 is expressed in hair follicle keratinocytes undergoing proliferation and in inter-follicular keratinocytes that are hyper-proliferative due to wounding, irritation or neoplastic growth [426]. The expression of the CK- 6C isoform has yet to be characterised in human tissue besides one report of its upregulation in the conjunctival epithelium of patients with Sjögren's syndrome [427]. However, a 49 kDa CK-6 fragment was identified in bladder cancer [425]. The lack of studies investigating associations between CK-5 and CK-6 and patient outcome in cancer highlights the need to investigate their potential as a biomarker or therapeutic target, particularly in ovarian cancer.

A range of 28-50 kDa fragments of CK-9 were identified in the CM of peritoneal-ovarian cancer direct and indirect co-culture, but not in the CM of either cell line

cultured alone. CK-9 is found specifically in palmar and plantar epidermis [428, 429]. CK-9 is downregulated 4-fold in colorectal cancer cell lines after chemotherapy and is part of a hetero-polymer with CK-6 found in invasive breast tumour tissue [430]. CK-9 has also been found to be increased 2-fold in metastatic hepatocellular carcinoma compared with non metastatic disease [431] and was found to be present in a single case of bile duct carcinoma [432]. There have been no studies to date which have identified the presence of cleaved CK-9 in human tissues. Further studies are required to assess the role of CK-9 and its fragment in ovarian cancer and its potential as a biomarker or therapeutic target.

In the CM of peritoneal cells co-cultured directly or indirectly with ovarian cancer cells analysed in this study, a range of 34-55 kDa fragments of CK-10 were identified by mass spectrometry. Little is known about CK-10, which is a marker of normal epithelial differentiation [433]. A currently used cervical cancer diagnostic test relies on possible cancerous cervical cells turning white after exposure to acetic acid. These white cells have far greater levels of CK-10 than their normal counterparts which do not turn white. CK-10 has thus been considered as a potential marker for cervical cancer [434]. Full length CK-10 has been reported in papillary thyroid cancer [390] and oral squamous cell cancers but not lung cancers [435]. There have been no studies to date which describe cleaved CK-10 fragments such as those seen in our study. The examination of biological fluid samples from ovarian cancer patients for CK-10 fragments is warranted to determine whether CK-10 can be used as a novel ovarian cancer biomarker.

We also identified a 48 kDa fragment of CK-14 in the CM of indirect peritoneal-ovarian cancer cell co-culture. CK-14 is found on basal cells and is lost upon keratinocyte differentiation [436]. CK-14 is greatly increased in suprabasal layers in venous eczema and lipodermatosclerosis suggesting prolonged proliferation of the basal cells [437]. CK-14 has been well documented as a biomarker for various cancers including squamous lung carcinoma [438], epithelial tumours [400], subungual squamous cell carcinoma [439], malignant eyelid tumours [440], and squamous carcinoma of the cervix [441]. CK-14 is found in squamous cell carcinoma regardless of origin and degree of differentiation [442]. It also is used as a marker to distinguish between epithelial hyperplasia and DCIS involving papillomas in breast [443]. CK-14 has also been associated with stage and lymphatic invasion in squamous cell carcinoma of the oesophagus [444, 445]. CK-14 has been associated with growth in salivary gland carcinoma [446], hepatocellular carcinoma [447], and metastatic potential of squamous cell carcinoma of the lung [448]. RT-PCR for CK-14 has been shown to be very sensitive at detecting micrometastasis in lymph nodes that are negative by routine pathological examination in head and neck carcinoma [449, 450].

CK-14 fragments have been reported in the literature in two studies. A 50 kDa fragment has been documented to be produced by HMEC breast cancer cells [451] and a 44 kDa fragment of a similar size to that seen in our study was observed in differentiated bladder cancer but not in normal bladder tissue [425]. Thus further investigation assessing CK-14 levels and fragments as novel biomarkers in ovarian cancer is warranted.

We also identified a 48 kDa fragment of CK-16 in the CM of peritoneal-ovarian cancer cell indirect co-culture. CK-16 is characteristically expressed in hyperproliferative epithelium and is associated with fast cell turnover [452, 453]. CK-16 has been found to be elevated in prostate cancer [454], head and neck cancer [455], nonfollicular epithelial tumours [456], subungual squamous cell carcinoma [439], and pancreatic cancer [457]. CK-16 increases with lesion severity in cervical neoplasia [458] and is correlated with breast tumour grade [412]. CK-16 is a useful marker for identification of the squamous subtype of lung carcinoma [438]. A search of the literature only found one reference to a cleaved form of CK-16. Ostergaard et al. ran 2D gels and identified CK-16 in differentiated keratinocytes in bladder cancer but not in healthy tissue. The CK-16 that they identified by mass spectrometry was a 44 kDa fragment [425] which matches the CK-16 fragment seen in our study. It is possible that the unknown protease responsible for cleaving CK-16 in bladder cancer is also responsible for the cleavage seen in our co-culture system. Thus further investigation into the role of CK-16 fragments in ovarian cancer and its potential as a biomarker or therapeutic target is also warranted.

The role of keratins in cancer in general is rarely investigated, most likely because they are often considered to be contaminants in proteomic screens. Cytokeratins and their fragments may yet prove to be important prognostic markers of ovarian cancer or detection biomarkers. In fact, a cytokeratin-19 fragment has been used to detect lung cancer with 57.3% sensitivity and a specificity of 94.9% [459], giving weight to the idea that cytokeratin fragments can be used diagnostically. Further investigations are

required to further elucidate the role of cytokeratins and their fragments in ovarian cancer.

2.4.5. The role of TKT in cancer

Increased levels of full length TKT and a 43 kDa fragment were identified in the CM of indirect peritoneal-ovarian cancer co-culture. TKT is a non-receptor tyrosine kinase which connects the pentose phosphate pathway to glycolysis in mammals, feeding excess sugar phosphates into the main carbohydrate metabolic pathways [460]. Its presence is necessary for tissues actively engaged in biosyntheses, such as fatty acid synthesis by the liver and mammary glands, and for steroid synthesis by the liver and adrenal glands [461].

Clinical observations indicate an important role of the non-oxidative TKT reactions in cancer cell proliferation in patients with breast and bronchial carcinoma. These patients have the tendency to develop a depleted state of TKT co-factor thiamine [462, 463]. TKT was highly expressed in prostate cancer xenografts [464] and had increased TKT activity in colon cancer cells [465] and in the blood of stomach and mammary gland cancer patients [466]. TKT was shown to be expressed in lung cancer cells but not normal lung cells [467] and TKT levels were additionally found to be upregulated in metastatic lung cancer cells when compared with non metastatic cells [468, 469]. TKT was also found to be upregulated in hepatocellular carcinoma compared with normal liver tissue [470] and was furthermore shown to be upregulated in metastatic hepatocarcinoma [471].

TKT has been used as anti-tumourigenic agent in some studies. Treatment of tumour cells with specific TKT inhibitors led to a reduction in tumour cell proliferation [472]. In a pharmacodynamic study where nude mice with xenografted colon cancer tumours were dosed with an inactive analog of thiamine, TKT activity was almost completely suppressed in blood, spleen, and tumour cells and tumour growth was significantly inhibited [473].

Little is known about TKT processing. A single study demonstrated that a cysteine proteinase was able to cleave TKT in the brains of alzheimer patients to produce a similar size fragment to that detected in our study [474]. Further studies are required to determine whether cleaved TKT can be used as an ovarian cancer biomarker or therapeutic target.

2.4.6. The role of annexin A2 in cancer

Full length annexin A2 was found to be produced by ovarian cancer and peritoneal cells. However, two forms of cleaved annexin were observed in direct and indirect peritoneal-ovarian cancer cell co-culture. Annexin A2 is a phospholipid calcium-binding protein which is found in a range of cells such as endothelial cells, epithelial cells, and tumour cells [475]. Annexin A2 is a 36 kDa monomer found in the cytoplasm and 94 kDa protein heterotetramer which consists of two annexin A2 monomers and two 11 kDa molecules known as annexin 2 light chains or p11 proteins which are found at the membrane surface of various cells [476]. It is a multifunctional protein which is involved in actin and cytoskeleton regulation [477] and serves as a receptor for ECM

proteins such as collagen I, cathepsin B, tPA, and plasminogen [475]. Since annexin A2 lacks a signal peptide and it is not secreted via endoplasmic reticulum pathways, the mechanism which regulates annexin A2 secretion is unknown.

The annexin A2 hetero-tetramer plays an important role in the plasminogen activation system and annexin A2 acts as a tPA receptor on the surface of endothelial and cancer cells which activates the conversion of plasminogen into plasmin [478, 479] (Figure 2.14) which facilitates ECM degradation leading to enhanced cell migration [480], invasion [481], angiogenesis [482] and metastasis [475]. Plasminogen serves as a binding site for annexin A2 at lysine 307 in endothelial cells [478] and p11 proteins at lysine residues at the carboxyl terminal in epithelial cells [483] which results in plasmin production. Annexin A2 dependent plasmin generation has been demonstrated to be essential for the invasion and migration of invasive breast cancer cells [484].

Over-expression of annexin A2 has been demonstrated in several cancer types such as; breast, pancreas, colorectal, and prostate cancer [481, 484-486]. A recent study found that annexin A2 mRNA is upregulated 3-fold in metastatic ovarian cancer when compared with normal ovarian tissue [487]. A proteomic study reported that annexin A2 was upregulated in ovarian cancer cell lines with high invasive capacity compared with those with low invasive capacity [488], suggesting it could be used as a biomarker or therapeutic target for ovarian cancer.

Annexin A2 neutralizing antibodies have been shown to regulate prostate cancer cell adhesion to osteoblasts and endothelial cells [489] and inhibit cell migration, invasion, and block plasminogen conversion in breast cancer cells [484], Lewis lung carcinoma [490], and monocytes [491]. Knockdown of annexin A2 expression has been shown to

decrease cell migration of human glioma [492] and pancreatic cancer cell lines [493], reduce cell invasion through Matrigel for multiple myeloma [494] and pancreatic cancer cells [493], as well as decrease adhesion of prostate cancer cells to osteoblasts [489]. Diaz et al. showed that annexin A2 interactions with tPA are essential for invasiveness of the pancreatic cancer cells [481]. The presence of 6-aminocaproic acid (ε-ACA), a lysine analogue, affects the interaction between plasminogen and annexin A2 which blocks plasmin generation inhibited cell migration and invasion in breast cancer cells [484]. Furthermore, the importance of annexin A2 in tumour development has been confirmed *in vivo* studies where annexin A2 knockout (KO) mice did not develop tumours [482].

Peptide analysis of the four annexin A2 protein spots identified in the co-culture CM samples failed to identify any annexin A2 peptides in the N-terminal domain (amino acid residues 1-35, Figure A.7). These findings suggest that there is cleavage of annexin A2 in the N-terminal domain as a result of the co-culture interactions. The N-terminal domain of annexin A2 consists of multiple phosphorylation sites including a tyrosine at position 23 by $pp60^{c\text{-}src}$ [495] and Ser^{25} by protein kinase C [496]. Cleavage of annexin A2 at the N-terminal domain by plasmin has been reported in monocytes [497] and endothelial cells [483] resulting in loss of the first 27 amino acid residues and a band at approximately 33-34 kDa similar to that seen in this study. Matrilysin (MMP-7) cleaves annexin A2 at the N-terminal domain which results in a truncated form of annexin A2 which may assist tumour invasion and metastasis of colorectal and breast cancer cell lines [498]. MMP-7 cleaves annexin A2 at Lys^{10} in the N-terminal to produce a 35 kDa form. Annexin A2 was observed in a proteomic study investigating Morris hepatoma

[499] at a similar size but different pI value to that identified in our study. They also did not detect any peptides in the first 35 amino acids, indicating cleavage in the N terminal domain, similar to the annexin A2 identified in our study. However, they also did not detect peptides at the end of the C terminal domain, which all 4 of our annexin A2 fragments retained. This is likely due to the annexin A2 found in the Morris' hepatoma being further processed at the C terminal domain which would result in a different pI value to ours. The first 12 amino acids of annexin A2 have also recently been shown to block stem cell adhesion to osteoblasts [500]. Binding sites to the p11 proteins and tPA have been identified in the N-terminal domain of annexin A2 at the amino acids residues 1-14 and 8-13 respectively [478, 501]. Tsunezumi et al. reported that the first 9 amino acids of annexin A2 bound to the tPA molecule more efficiently than intact annexin A2 [498]. Thus it is likely that cleaved annexin A2 acts to promote increased activation of the plasmin pathway to produce increased levels of plasmin.

The research to date provides solid support for further examination of the role of annexin A2 in ovarian cancer as a biomarker or a therapeutic target.

2.4.7. The role of annexin A6 in cancer

A 36 kDa annexin A6 fragment was identified in the indirect co-culture of peritoneal cells and ovarian cancer cells. Annexin A6 (previously annexin VI) is a 67 kDa member of the annexin family of calcium and phospholipid binding proteins [502]. Early studies identified annexin A6 as a major calcium-dependent component of lymphocyte plasma membranes [503-505] and intestinal epithelial cell cytoskeletons [506]. It is found

abundantly in the heart [507, 508] and is involved in lipid formation [509, 510] as well as affecting the renin angiotensin aldosterone system (RAAS) [421, 511].

Little is known about the role of annexin A6 in cancer, besides its effects on the RAAS. Annexin A6 has been identified in breast cancer cells predominantly in membranous structures [512] and was found to be downregulated during metastatic development in mouse melanoma [513]. Similarly, annexin A6 was significantly reduced in 20 cancer microarrays [511]. In a prostate cancer model, annexin A6 is downregulated during progression from a benign to a malignant state [511]. Ectopic expression of annexin A6 in epithelial carcinoma cells which do not express annexin A6 [511] reduces cell proliferation and tumour growth in nude mice [514]. Furthermore, annexin A6 was upregulated in Morris hepatoma when compared with normal liver in rats [499]. Despite this, annexin A6 KO-mice appear normal and do not develop spontaneous tumours and furthermore have increased annexin A2 levels [515], indicating a potential redundancy for annexin A6 in cancer development.

A single study identified a 15 kDa annexin A6 fragment in a proteomic screen of injured hepatocytes [516], but there is no literature describing cleaved annexin A6 in cancer. Thus, further studies are justified to evaluate the role of cleaved annexin A6 as a diagnostic marker for ovarian cancer.

2.4.8. The role of eEF-2 in cancer

A 34 kDa fragment of eEF-2 was upregulated and identified in the indirect co-culture of peritoneal cells and ovarian cancer cells but not in the single cell cultures. eEF-2 is a 100 kDa protein that catalyses the ribosomal translocation reaction, resulting in the movement of ribosomes along mRNA, activation of GTPase, and protein synthesis. Phosphorylation of eEF-2 makes it inactive in translation [517]. eEF-2 has proved to be surprisingly sensitive to inhibition via phosphorylation or ADP-ribosylation, both of which lead to an immediate translational arrest [517, 518]. Phosphorylation of eEF-2 is accompanied by a decrease in short half-life of anti-apoptotic proteins [519].

eEF-2 is expressed in over 90% of colorectal and gastric cancers. Knockdown with short-hairpin RNA arrested G2/M growth in colon and gastric cancer cell lines whilst overexpression increased cell proliferation [520]. It is also a marker for the TC2 class of multiple myeloma [521]. eEF-2 was upregulated in cervical cancer causing human papilloma virus 16 oncogene E6 transfected lung cancer cells when compared with wild type cells suggesting a role for eEF-2 in cervical cancer [522].

eEF-2 was found to be upregulated in metastatic breast cancer compared with non metastatic breast cancer [523]. Similarly, eEF-2 auto-antibodies were found in the serum of patients with DCIS breast cancer but not in the serum of healthy or benign patients [524]. Likewise, eEF-2 was detected in 11/15 breast cancers by serological proteome analysis when compared with normal tissue [525]. In other proteomic studies, eEF-2 was identified in melanoma tumours probed with cancer patient serum but not in tissue probed with healthy serum by 2D electrophoresis analysis [526].

Likewise, full length eEF-2 was identified as an auto-antigen in 93/118 hepatocellular carcinomas by serological proteome analysis when compared with normal tissue but not lung cancer, oesophageal cancer, and gastric cancer [525]. Only one very recent study documents a role for eEF-2 in ovarian cancer. It was found that eEF-2 was upregulated 4-fold in cisplatin resistant ovarian cancer cells when compared with the non resistant parent cell line [527].

Furthermore, there is little evidence of cleaved forms of eEF-2 in the literature apart from a single study that showed that trypsin cleaves eEF-2 at Arg^{66} and Lys^{571}/Lys^{572}. eEF-2 cleaved at Arg^{66} was unable to form a high-affinity complex with ribosomes whilst retaining its ability to form a low-affinity complex and to hydrolyse GTP. The second cleavage at Lys^{571}/Lys^{572} was accompanied by a loss of both this low-affinity binding and also the GTPase activity [528]. The limited literature regarding the role of eEF-2 in cancer, and more importantly documentation of eEF-2 fragments gives strong support for further studies into the role of eEF-2 in ovarian cancer as a biomarker or therapeutic target.

2.4.9. The role of TGFBIp in cancer

In this study, peritoneal cell expressed full length TGFBIp was observed to be downregulated during peritoneal ovarian cancer co-culture. TGFBIp was originally named Big-h3 derived from its initial identification and cloning as a major TGFβ-responsive gene in the A549 lung adenocarcinoma cell line: TGFβ-induced gene human clone 3, abbreviated to Big-h3 [529]. TGFBIp has also been referred to other names

over the years including; MP78/70 [530], collagen fibre associated protein (RGD-CAP) [531], and keratoepithelin [532] but *TGFBI* is now the accepted terminology for the gene name and TGFBIp for the protein. Human TGFBIp consists of 683 amino acids with a molecular weight of 68 kDa in its secreted form. To date, only two isoforms of TGFBIp at 78 and 68 kDa have been reported [533], both of which are encoded by a single gene [534]. It includes a signal peptide in the first 24 amino acid residues at the N-terminus, a cysteine rich EMI domain, four highly conserved FAS domains, and a C-terminal Arg-Gly-Asp (RGD) motif which serves as a ligand recognition site for several integrins including α1β1 [535], α3β1 [536, 537], αvβ3 [538-540], αvβ5 [541, 542], α6β4 [543], and α7β1 [544] integrins, indicating a role in cell adhesion.

TGFBIp is regulated not only by TGFβ signalling, but also by retinoid [545], IL-4 [546], IL-1, and TNF-α [539] in various cell types. However, a number of cells, both cancerous and non-cancerous, produce TGFBIp in response to TGFβ stimuli, including; prostate cancer cells [529], lung carcinomas cells [529], melanoma cells [547], astrocytoma cells [548], and pancreatic cells [549].

There have been few studies which have investigated the effects of TGFBIp on tumour cell function and the knowledge about the role of TGFBIp in ovarian cancer is limited. Recent studies have shown that the level of TGFBIp in ovarian cancer tissue is predictive of the disease response to the treatment with the aromatase inhibitor letrozole [550] or the chemotherapeutic drug paclitaxel [551]. We have further examined the role of TGFBIp in ovarian cancer in chapter 3.

2.4.10. Protein regulation in peritoneal-ovarian cancer co-culture

When we cultured peritoneal cells with ovarian cancer cells, whether in direct contact, or indirect co-culture where both cell types shared the same media, we observed that a number of proteins were degraded or processed. Some of these proteins such as fibronectin have been discussed in the literature as being beneficial to various cancer types when cleaved [336]. Others, such as the various cleaved cytokeratins we identified in peritoneal-ovarian cancer cell co-culture, have not been documented in the literature, making these findings very novel. Those proteins which have been reported to be cleaved have very little literature regarding the subject, and no documentation in relation to the role of the cleaved proteins in ovarian cancer. Cleaved CK-1 PAI-1, and annexin A2 were present in both the direct co-culture and Opticell indirect co-culture, indicating that these cleavage events occur early in the metastatic process, and are either involved in the earliest interactions between peritoneal and ovarian cancer cells as the proteins were also detected in the direct co-culture, or the processing can occur through paracrine effects and can also be triggered by direct contact.

Full length CK-1, annexin A2, and TKT were also identified to be upregulated in peritoneal-ovarian cancer cell co-culture. These proteins and their fragments need to be evaluated as potential biomarkers or therapeutic targets for ovarian cancer.

Ultimately, we can conclude from these experiments, that when peritoneal cells are exposed to ovarian cancer cells, whether by direct contact, or by shared peritoneal fluid, that a proteolytic response is triggered. This results in numerous proteins being

processed or degraded by proteases. This proteolytic pathway needs further investigation, as inhibiting the proteolytic response triggered by peritoneal-ovarian cancer cell interaction could be a potential therapy target. Further investigation of the various cleaved proteins produced as a result of this proteolytic response may lead to development of novel ovarian cancer biomarkers for diagnosis, prognosis, or response to therapy.

CHAPTER 3 – TGFBIp INCREASES OVARIAN CANCER CELL MOTILITY, INVASIVENESS, AND ADHESION TO PERITONEAL CELLS

3.1. INTRODUCTION

A greater understanding of the interaction which occurs between ovarian cancer cells and the peritoneum would potentially lead to the identification of novel molecular targets to block this critical step during ovarian cancer metastasis. Our study has therefore analyzed the protein expression of ovarian cancer cells (OVCAR-3, OVCAR-5, and SKOV-3) and peritoneal (LP-9) cells in co-culture in chapter 2. One of the proteins identified by MS to be differentially expressed in the co-culture secretome was the ECM protein TGFBIp.

TGFBIp comprises 683 amino acids with a predicted molecular mass of 68 kDa. Expression of TGFBIp is induced by TGFβ in several cancer cell types [528, 531, 537, 539, 547, 552-559], including lung carcinoma [529], prostate cancer [529], melanoma [547] astrocytoma [548], and pancreatic cancer [549] cells. In many cell types TGFBIp functions as a linker protein that connects various matrix molecules to each other as well as to cells [530, 554, 560, 561]. TGFBIp contains four internal FAS1 domains and a carboxy terminal RGD motif which serves as a ligand recognition site for several integrins (Figure 3.1) [535-544] in several cell types [536, 562-565]. TGFBIp can bind to types I, II and IV collagens. Proteoglycans such as small leucine-rich biglycan and decorin are another group of ECM proteins which can bind directly to TGFBIp [561].

Immunohistochemical studies show TGFBIp to be a protein distributed in the ECM of a wide range of developing and mature tissues including endothelial cells of human vascular tissues [566], papillary dermis [559], primary spongiosa, periosteum, and perichondrium [567]. It has also been linked with bone formation [540, 568]. TGFBIp expression is induced in endothelium and stroma-derived cells in healing cornea [569] and reactive astrocytes in rat cerebral cortex at stab wound sites [548].

TGFBIp has also been associated with a range of other diseases including; cyclosporine nephropathy [570], atherosclerosis [566], and rheumatoid arthritis [539, 546]. It also has a role in reproduction [571, 572] and wound healing [546, 548]. Mutations in the *TGFBI* gene are well characterised in a number of corneal dystrophies [573-576]. In addition to playing a role in corneal dystrophies, TGFBIp has been found to be increased in the urine of diabetics [553, 577] and it has been suggested that combined monitoring of albumin excretion rate and urinary TGFBIp can predict the severity of diabetic nephropathy [562].

There is conflicting data in the literature reporting that TGFBIp can have either a tumour suppressive or tumour promoting role. High TGFBIp expression has been reported for various tumour tissues [549, 578-586] but low expression has also been observed in other tumour types [587-589]. TGFBIp overexpression has been shown to markedly reduce tumourigenicity of CHO cells and lung cancer cells *in vivo* [547, 590]. Likewise, a recent observation by Becker et al. suggested that increased expression of TGFBIp suppresses neuroblastoma cell adhesion to various extracellular matrix proteins, thus inhibiting their proliferation and invasiveness [591].

TGFBIp plays a role in the adhesion and migration of keratinocytes/fibroblasts mediated through α3β1 integrin at wound sites where they are synthesizing new ECM [592]. This is supported by *in vitro* studies demonstrating adhesion and migration of dermal fibroblasts, monocytes, keratinocytes, chondrocytes, peritoneal fibroblasts, and lung fibroblasts to TGFBIp [535, 557, 559, 565].

There has been some interest in the integrin binding peptides in the C terminus of TGFBIp. RGD peptide released from the C-terminal of TGFBIp was shown to mediate TGFβ induced apoptosis in lung carcinoma cells [593] and osteosarcoma cells [594]. The structural analysis of the NKDIL and EPDIM sequence motifs showed that they can adopt a β-turn structure similar to the RGD peptide and could interact with integrins during adhesion [595]. Another adhesion motif identified is the highly conserved tyrosine and histidine residues (YH motif) flanked by several leucine/isoleucine residues in the FAS1 domain which supports αvβ5 integrin mediated adhesion of lung fibroblast MRC-5 cells [542] providing multiple mechanisms by which TGFBIp may mediate adhesion in normal, and malignant physiology.

Many reports suggest TGFBIp is a negative player in tumourigenesis. However, TGFBIp was able to support adhesion of osteoblasts *in vitro* by recruiting αvβ3/αvβ5 integrins [540] as well as adhering to dermal fibroblasts, chondrocytes, peritoneal fibroblasts and human MRC-5 fibroblasts [535, 559]. Additionally, TGFBIp has also been shown to mediate invasion and metastasis [543, 592, 596-598].

Knowledge about the role of TGFBIp in ovarian cancer is limited. It has been shown that the level of TGFBIp in ovarian cancer tissue is predictive of the disease response to the treatment with the aromatase inhibitor letrazole [550] or the chemotherapeutic

drug paclitaxel [551]. Thus the role of TGFBIp in ovarian cancer needs to be further elucidated. In this study, we have therefore investigated TGFBIp expression in tissue and ascites of ovarian cancer patients and have performed functional *in vitro* studies with ovarian cancer and peritoneal cells to study its potential effects on ovarian cancer metastasis.

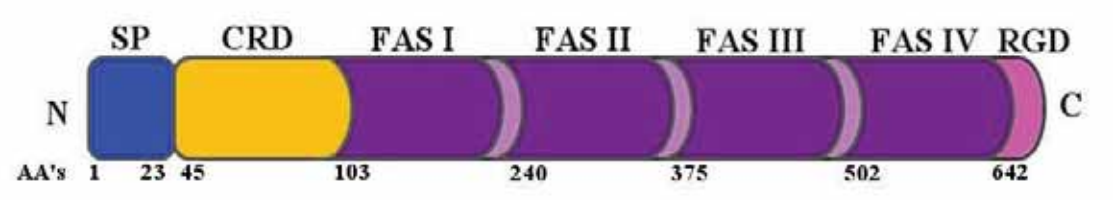

Figure 3.1. *The structure of TGFBIp.*

TGFBIp consists of a signal peptide and a cysteine rich domain in the N terminus, four fasciclin domains, and several motifs in the C terminal domain, including the Arg-Gly-Asp motif.

3.2. MATERIALS AND METHODS

3.2.1. Co-culture of peritoneal and ovarian cancer cells

Cells were maintained as described in section 2.2.1. LP-9 peritoneal cells and OVCAR-5, OVCAR-3, and SKOV-3 cells were co-cultured and the CM was collected and prepared as described in section 2.2.1. Additional co-cultures were incubated in the presence of broad spectrum MMP inhibitor GM6001 (20 µM, #M5939, Sigma Aldrich, St. Louis, USA) [599], broad spectrum protease inhibitor for serine, cysteine, and aspartic aminopeptidases which has been reported to be non toxic to mammalian cells (PI, 1/800, #P1860, Sigma Aldrich), or plasminogen conversion inhibitor, ε-ACA (150 mM, #A2504, Sigma Aldrich).

3.2.2. MALDI-TOF/TOF and LC-ESI-IT mass spectrometry

Designated bands were excised from Coomassie-G-250 stained gels for mass spectrometry as described in section 2.2.3. The MOWSE and probability scores calculated by MASCOT were used as the criterion for protein identification. Data was also matched to the predicted sequence of TGFBIp.

3.2.3. Western immunoblotting

CM samples were precipitated with acetone as described in section 2.2.2 above, and re-dissolved in 4X LDS sample buffer (Invitrogen). Equal volumes of each CM sample were diluted in 5X loading buffer containing 0.05% v/v β-mercaptoethanol were heated at 96°C for 5 min before loading onto a SDS-PAGE gel (10% bis-Tris, Biorad). Protein samples were electrophoresed at 100 V and transferred to PVDF membranes (GE Healthcare). Recombinant TGFBIp (rTGFBIp, 0.5 µg, R&D Systems, Minneapolis, USA) was loaded as a positive control for the western blot. For plasmin digestion of TGFBIp, TGFBIp was incubated with 0.3 U/mL plasmin from human serum (#P1867, Sigma Aldrich) in 1 mM $CaCl_2$ for 3 hr at 37°C in the presence or absence of broad spectrum protease inhibitor cocktail at 1/200. Non specific binding to PDVF membranes was blocked with 3% skim milk in Tris-buffered saline containing 0.1% Tween 20 for 1 hr before incubation with rabbit polyclonal TGFBIp antibody (1/200, sc-28660, Santa Cruz Biotechnology, CA) for 2 hr at room temperature (RT). TGFBIp protein was visualized with anti-rabbit IgG peroxidase-conjugated secondary antibodies (Millipore Australia, Sydney, Australia), followed by enhanced chemiluminescence and autoradiography (ECL Hyperfilm, GE Healthcare) for 1-10 min.

Ascites samples (n = 3) from ovarian cancer patients were collected prospectively during surgery at the Department of Gynaecological Oncology, Royal Adelaide Hospital (RAH) from January 2007 to January 2010 with approval from the RAH Human Ethics Committee. Ascites samples were centrifuged at 3000 rpm for 10 min to remove debris and stored at -70°C. Ascites fluid (200 µl) was passed through an 8cm Sephacryl

S400 column (GE Healthcare) in PBS and 150 µl fractions collected. Fractions containing TGFBIp, as determined by a dot blot with rabbit polyclonal TGFBIp antibody (1/200, sc-28660, Santa Cruz), were pooled and total protein estimated using a Bradford's protein assay as per the manufacturer's instructions (Biorad) and immunoblotted for TGFBIp as above. 2D gels were ran as described in section 2.2.2 then transferred to PVDF membrane and immunoblotted using the same protocol as for 1D westerns.

3.2.4. Immunohistochemistry

Archived formalin fixed paraffin tissue blocks of normal ovaries (n = 7), benign serous tumours (n = 8), serous ovarian carcinomas (n = 20), matching omental metastatic implants (n = 20), and serous borderline tumours (n = 10) were obtained from the Institute of Medical & Veterinary Science (IMVS), Adelaide, Australia with approval from the Royal Adelaide Hospital (RAH) and University of Adelaide human ethics committees. Borderline tumours, serous ovarian carcinomas and matching omental metastatic implants were assembled into tissue microarrays. Three representative cores (1.0 mm) identified by a pathologist were mounted on multi-tissue block microarrays using a tissue arrayer (Millipore). Immunostaining was measured by image analysis using a high throughput image analysis system. Normal and benign tissue sections (4 µm) were likewise mounted onto positively charged slides (SuperFrost®Plus, Menzel-Glaser, Braunschweig, Germany) and all were heated at 60°C for 1.5 hr. Sections were dewaxed in xylene, washed in ethanol and PBS, and

endogenous peroxidase activity quenched with 0.3% H_2O_2, followed by microwave antigen retrieval using 0.1 M citrate buffer, pH 6.0, as described previously [600]. To eliminate non-specific binding, tissues were blocked in 5% goat or rabbit serum (Sigma Aldrich) for 20 min and then incubated overnight at 4°C with rabbit polyclonal TGFBIp antibody (1/200, sc-28660, Santa Cruz Biotechnology). The tissues were subsequently incubated with biotinylated goat anti-rabbit (1/400, Dako Australia, Sydney, Australia) for 1 hr at room temperature (RT) followed by streptavidin-horseradish peroxidase conjugate (1/500, Dako Australia). Immunoreactivity was detected using diaminobenzidine/H_2O_2 substrate. Sections were counterstained with 10% haematoxylin, dehydrated, and mounted in pertex (HD Scientific, Sydney, NSW, Australia). Each tissue sample had a matching negative control without the primary antibody incubation step. The immunostaining intensity of TGFBIp in the ovarian and omental tissues was assessed using a manual scoring method: strong (3+), moderate (2+), weak (1+), or negative (0). We defined a score of 0 or 1+ as low immunostaining and a score or 2+ or 3+ as high immunostaining.

3.2.5. Motility and invasion assays

Ovarian cancer cell lines (OVCAR-5, OVCAR-3, and SKOV-3) were trypsinized, washed, resuspended at a concentration of 1 x 10^6 cells/ml in RPMI media containing 0.1% BSA and antibiotics and labelled with calcein-AM (1 µg/ml) for 30 min at RT by mixing on an oscillating platform (Nutator, Clay Adams, Becton Dickinson, Sparks, MD). Cells were pelleted and washed three times with 0.1% BSA RPMI and subsequently mixed at a

concentration of 1 x 10^6 cells/ml with control (PBS) or rTGFBIp (0.5-10 µg/ml, R&D systems) for 2-3 hr at RT on the Nutator in the dark. To assess the role of the RGD peptide motif in promoting motility and invasion, ovarian cancer cells were also pre-treated with TGFBIp peptide ERGDEL (50 µg/ml, Mimotopes, Clayton, Victoria, Australia) or ERGEEL control peptide (50 µg/ml). The cell suspension (40,000 cells/well in 50 µl) was added to the top of uncoated 12 µm filter 96 well chemotaxis assay plates (Neuroprobe Inc, Gaithersburg, USA) or 12 µm filter chemotaxis plates coated with Geltrex (0.6ul/well of 9mg/ml, Invitrogen) containing 30 µl of 10% FBS RPMI as a chemoattractant in the lower chamber. Cells were allowed to migrate for 6 hr at 37°C in an environment of 5% CO_2. Non-migratory cells on the top side of the filter were gently removed with a moistened cloth and the fluorescence was measured at 485-520 nm using a Fluostar Galaxy fluorescent plate reader (BMG Labtech, Offenburg, Germany).

3.2.6. Adhesion assays

LP-9 mesothelial cells were plated at 16,000 cells/well in 96-well plates for 48 hr. Confluent monolayers were washed with RPMI media containing 0.1% BSA and antibiotics for 30 min prior to the adhesion assay at 37°C. Ovarian cancer cell lines (OVCAR-5) were trypsinized, washed, and resuspended in RPMI media containing 0.1% BSA and antibiotics and were labelled with calcein-AM as per motility and invasion assays. Ovarian cancer cells were mixed at a concentration of 100,000 cells/ml with PBS or rTGFBIp (0.5-10 µg/ml) for 3 hr at RT on a Nutator. Additional experiments

were performed in the presence or absence of neutralizing TGFBIp mouse monoclonal antibody (5 µg/ml, 60007-1-Ig, Proteintech Group Inc [601]), mouse IgG immunoglobulins (5 µg/ml, Sigma Aldrich), or PI (1/800). To assess the role of the RGD peptide motif in promoting adhesion, ovarian cancer cells were pre-treated with TGFBIp peptide ERGDEL (50 µg/ml) or ERGEEL control peptide (50 µg/ml). The cell suspension (80 µl) was added to each well of LP-9 cell monolayers, and cells allowed to adhere for 8 min. LP-9 cell monolayers were subsequently washed three times with 100 µl/well of RPMI media containing 0.1% BSA and antibiotics. The cells were solubilised with 0.2 M NaOH containing 1% SDS (100 µl/well) in the dark for 10 min. An aliquot of 85 µl for each well was transferred to a white 96-well plate, and the fluorescence was measured at 485-520 nm on a Fluostar Galaxy fluorescent plate reader.

3.2.7. Plasmin activity assay

Plasmin activity levels in CM were measured using the chromozym PL substrate (Roche Diagnostics Inc, Mannhein, Germany) according to the manufacturer's instructions. CM was collected from OVCAR-5 and LP-9 cells either cultured alone or directly co-cultured in a time course experiment over 72 hr using culture conditions described in section 2.2.1. Plasmin activity levels were assayed in duplicate in a total reaction volume of 100 µl in 96-well plates containing 15 µl Tris buffer (50 mM, pH 8.2), 10 µl 0.9% NaCl, 15 µl chromozyme PL substrate (3 mM in 100 mM glycine) and 60 µl of CM. The 96-well plates were incubated for 1 hr at 37°C and absorbance was measured at

405 nm using an automated 96-well plate reader (Bio-Rad). The colorimetric change resulting in the formation of yellow p-nitroaniline is a direct measure of the plasmin activity level present in the CM samples. Negative controls included parallel wells containing no chromozym PL substrate and growth media alone which served as the reagent blank. Increasing concentrations of human plasmin (0.1 - 0.8 U/ml, Sigma-Aldrich) were incubated with chromozym PL in order to generate a standard curve to calculate plasmin levels in the CM samples (data not shown).

3.2.8. Statistical analysis

All analyses were performed using SPSS 15.0 for Windows Software (SPSS Inc., Chicago, IL). The Student's t-test, one way ANOVA with Dunnett C or Dunnett T post-hoc tests, Chi squared test with Fisher's Exact test, and Pearson's correlation test were used to determine statistical significance between control and treatment groups. Statistical significance was accepted at $p < 0.05$.

3.3. RESULTS

3.3.1. Expression of TGFBIp in ovarian cancer and peritoneal cells

The level of TGFBIp identified by 1D-gel electrophoresis and mass spectrometry was reduced in the CM of co-cultured ovarian cancer cells (OVCAR-5 and SKOV3) and LP-9 peritoneal cells when compared with CM from LP-9 cells alone (Figure 3.2a). Western blotting was employed to further investigate TGFBIp expression in ovarian cancer cell lines and LP-9 peritoneal cells. We found that TGFBIp was abundantly secreted by LP-9 cells (Figure 3.2b). Low levels of TGFBIp were present in the CM of OVCAR-5, whilst TGFBIp was undetectable in the CM of OVCAR-3 and SKOV-3 cells (Figure 3.2b).

Immunohistochemistry showed that normal surface ovarian epithelial cells (OSE) (Figure 3.3a, Table 3.1) and peritoneal cells of normal omentum (Figure 3.3b, Table 3.2) had high levels of TGFBIp (2+ or 3+). TGFBIp was also abundant in the epithelium of 6/8 benign serous ovarian tumours (Figure 3.3c, Table 3.1). In contrast, all serous borderline tumours (Figure 3.3d, Table 3.1), primary serous carcinomas (Figure 3.3e, Table 3.1, Table 3.2), and matching metastatic tumours (Figure 3.3f, Table 3.2) exhibited low TGFBIp immunoreactivity (defined as 0 or 1+) ($p < 0.0001$, Pearson Chi-Square test). No difference in the level of TGFBIp immunostaining was observed between primary and metastatic serous ovarian cancer cells ($p = 0.150$, Pearson Chi-Square test). High TGFBIp levels were also observed in omental peritoneal cells adjacent to metastatic cancer cells in implants whilst the metastatic cells in the implant had low levels of TGFBIp (Figure 3.3g, Table 3.2).

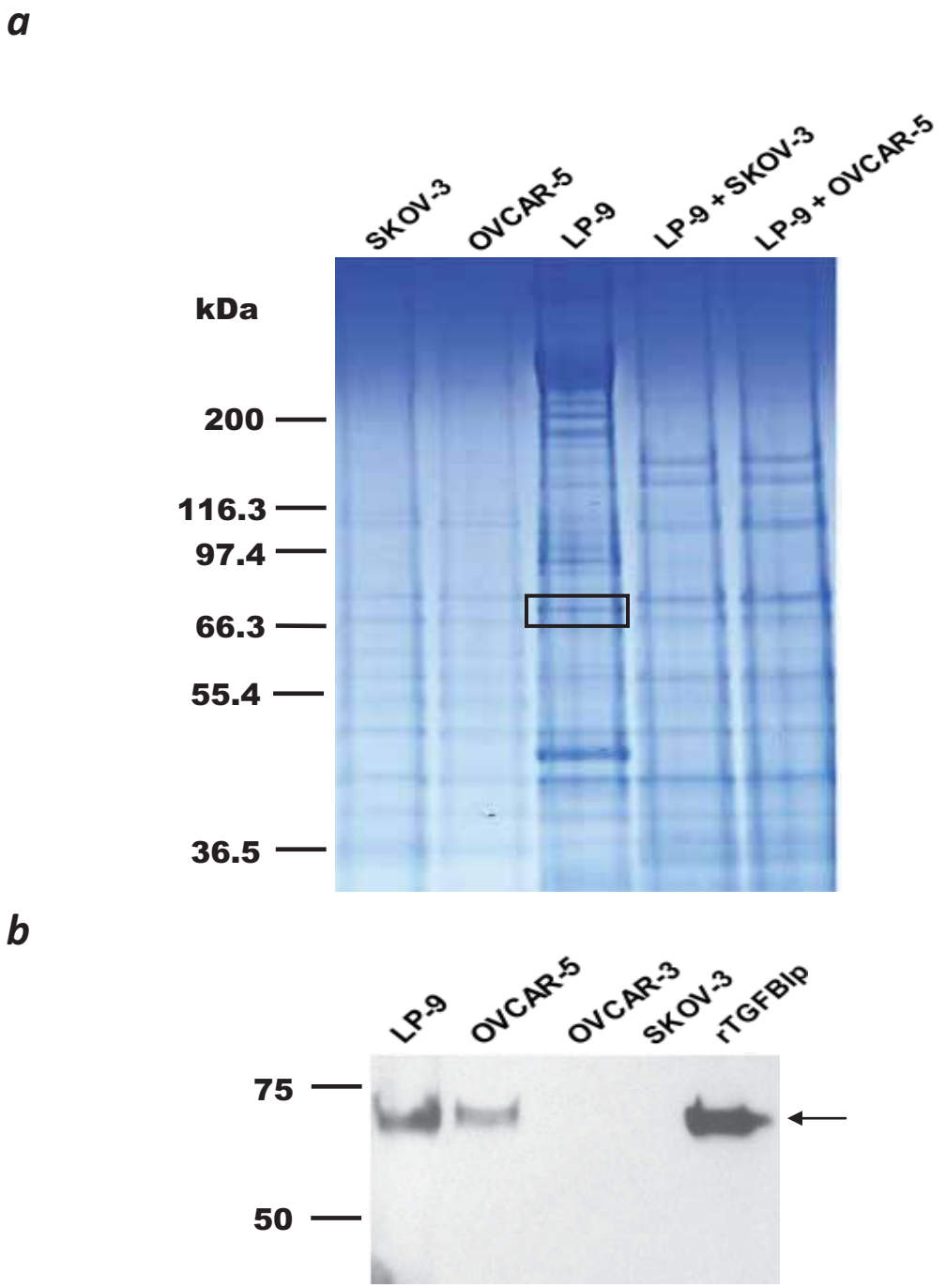

Figure 3.2. *Expression of TGFBIp in ovarian cancer cells and LP-9 peritoneal cells.*

(*a*) CM from OVCAR-5, LP-9, and OVCAR-5 co-cultured with LP-9 cells was collected and precipitated with acetone. Protein band in boxed area was identified to be TGFBIp by MALDI-TOF/TOF mass spectrometry. (*b*) Western blot of TGFBIp in CM from OVCAR-3, OVCAR-5, SKOV3 and LP-9 cells cultured for 48 hr in serum free LP-9 medium. Proteins were transferred to PVDF membrane and immunoblotted with polyclonal rabbit TGFBIp antibody (amino acids 626-683, Santa Cruz Biotechnology).

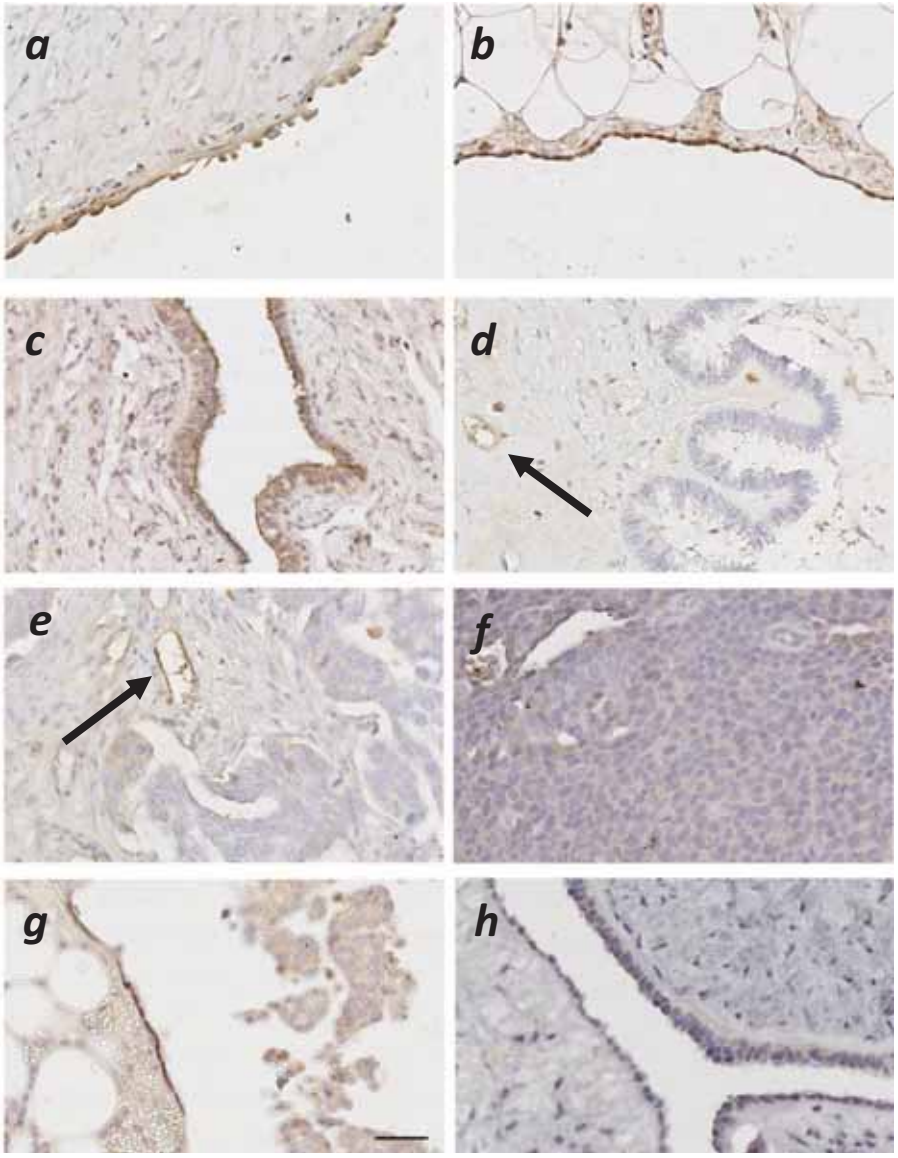

Figure 3.3. *TGFBIp immunostaining of ovarian and omental tissues.*

High (2+) TGFBIp immunoreactivity is present in (*a*) normal surface ovarian epithelial cells, (*b*) peritoneal cells from normal omentum, and (*c*) epithelial cells from benign serous cystadenomas and peritoneal cells adjacent to metastatic serous ovarian carcinomas. TGFBIp levels are low (0 or 1+) in (*d*) serous borderline tumours, (e) primary serous carcinomas, (*f*) matching metastatic lesions, and (*g*) serous ovarian cancer cells adjacent to omental peritoneal cells. *(h)* Is a section from a benign ovarian tumour of the no primary antibody negative control, included for reference. Arrows in *d)* and *e*) illustrate blood vessels with high TGFBIp immunostaining in the stroma which was used as an internal positive control. Magnification bar = 50 µm. All images are at the same magnification.

Table 3.1. *Summary of TGFBIp immunostaining of ovarian tissues.*

Levels of TGFBIp in ovarian tissues were assessed using a manual scoring method. The immunostaining intensity in the ovarian cancer was scored as strong (3+), moderate (2+), weak (1+), or negative.

	Median age (Range)	**Epithelial Intensity**	
		Low (0/1+)	**High (2+/3+)**
Normal	50 (48-58)	0/7 (0%)	7/7 (100%)
Benign	51 (35-62)	2/8 (25%)	6/8 (75%)
Borderline	52 (32-81)	10/10 (100%)	0/10 (0%)
Carcinoma	69 (49-87)	26/27 (96.3%)	1/27 (3.7%)
Chi Squared Test		$p < 0.0001$	

Table 3.2. *Summary of TGFBIp immunostaining of ovarian and omental tissues.*

Levels of TGFBIp in ovarian tissues were assessed using a manual scoring method. The immunostaining intensity was scored as strong (3+), moderate (2+), weak (1+), or negative.

	Median age (Range)	**Epithelial Intensity**	
		Low (0/1+)	**High (2+/3+)**
Carcinoma (Stage III)	68 (49-87)		
Primary tumour		20/20 (100%)	0/20 (0%)
Matching metastasis		17/20 (85%)	3/20 (15%)
Chi Squared Test		p = 0.150	
Omentum	57 (40-80)		
Normal peritoneal cells		2/8 (25%)	6/8 (75%)
Peritoneal cells adjacent to implants		1/5 (20%)	4/5 (80%)
Carcinoma cells adjacent to peritoneal cells		5/5 (100%)	0/5 (0%)

3.3.2. TGFBIp promotes ovarian cancer cell motility and invasion

We investigated the effects of TGFBIp on ovarian cancer motility and invasion. rTGFBIp significantly increased the motility of OVCAR-5 ovarian cancer cells (Figure 3.4a, $p < 0.0001$). Maximal effects on OVCAR-5 motility (150% of PBS control) were observed at a concentration of 5 µg/ml rTGFBIp whilst higher concentrations of rTGFBIp were less effective. Treatment with 5 µg/ml rTGFBIp also increased the motility of OVCAR-5 and SKOV-3 cells (Figure 3.4b) and significantly increased invasion of OVCAR-5 and SKOV-3 cells through basement membrane proteins (Geltrex) by up to 20% (Figure 3.4c, $p < 0.0001$). rTGFBIp did not affect either the motility or invasion of OVCAR-3 cells.

To further explore the decrease in cancer cell motility at higher rTGFBIp concentrations, we investigated the effects of rTGFBIp on OVCAR-5 cell viability using a trypan blue exclusion cell viability assay. We found that when cells were exposed to concentrations ≥ 5 µg/ml rTGFBIp for the same duration as both the mixing time (2 hr exposure) and additional time in the chemotaxis plate (8 hr exposure) in the motility assays, the proportion of non-viable OVCAR-5 cells increased significantly (Figure 3.5).

a

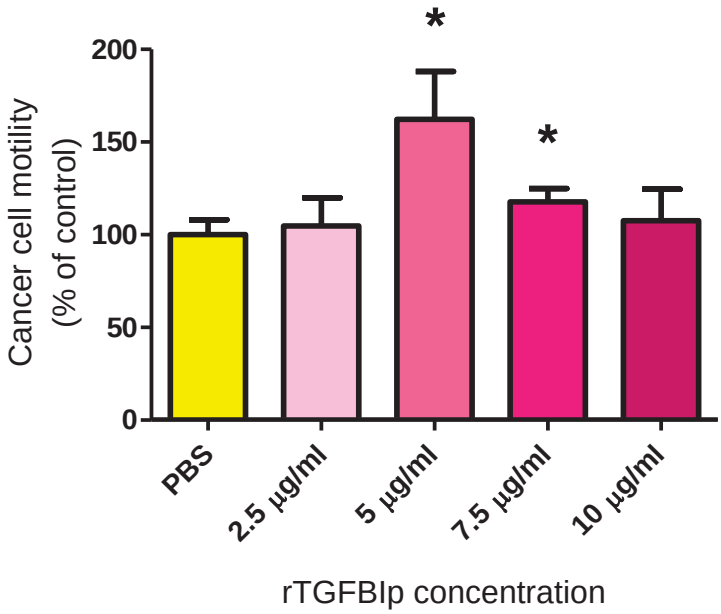
Cancer cell motility
(% of control)
200
150
100
50
0
*
*
PBS
2.5 µg/ml
5 µg/ml
7.5 µg/ml
10 µg/ml
rTGFBIp concentration

b

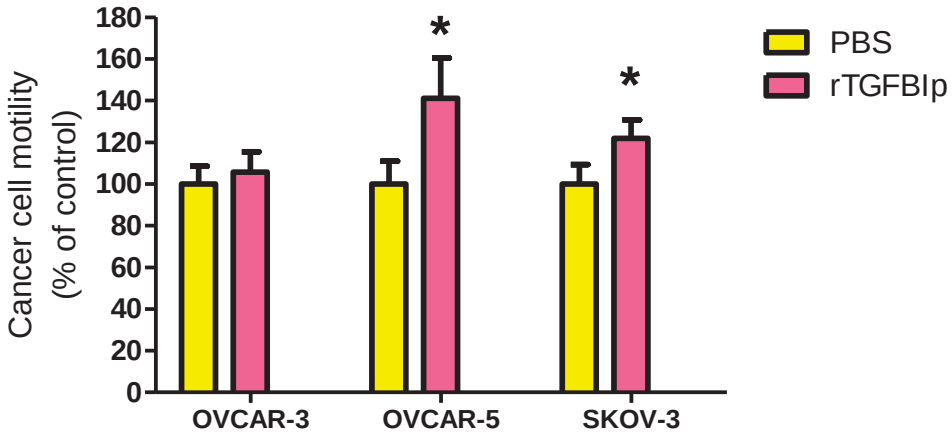
Cancer cell motility
(% of control)
180
160
140
120
100
80
60
40
20
0
*
*
OVCAR-3
OVCAR-5
SKOV-3
PBS
rTGFBIp

c

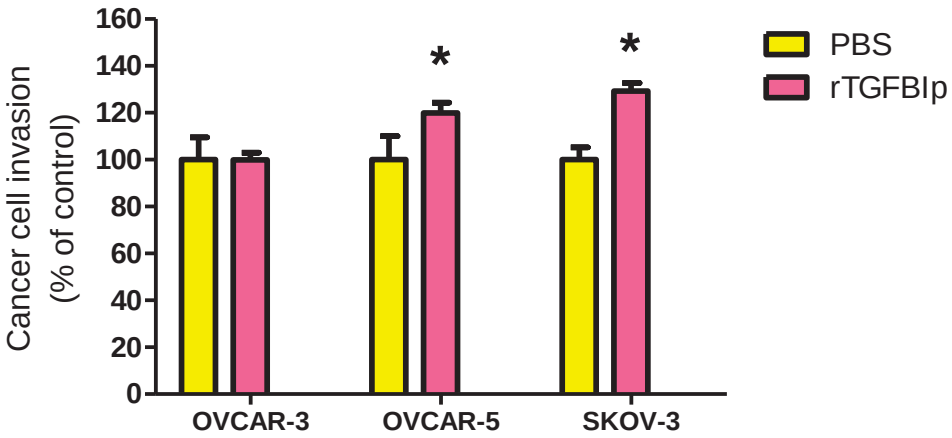
Cancer cell invasion
(% of control)
160
140
120
100
80
60
40
20
0
*
*
OVCAR-3
OVCAR-5
SKOV-3
PBS
rTGFBIp

Figure 3.4. *TGFBIp promotes motility and invasion of ovarian cancer cells*.

(*a*) Ovarian cancer cells (OVCAR-5) were treated with a range of rTGFBIp concentrations (2.5-10 μg/ml) or PBS for 3 hr in control RPMI media containing 0.1% BSA. Cells were placed on top of uncoated 12 μm pore filter inserts using 10% FBS as a chemoattractant and allowed to migrate through the filter for 6 hr. Numbers of migrating cells were counted and expressed as percentage of PBS control, mean ± SD from at least three independent experiments performed in triplicate. * denotes significant difference from PBS control, $p < 0.0001$, one-way ANOVA. Calcein labelled OVCAR-3, OVCAR-5, and SKOV-3 cells were incubated with 5 μg/ml rTGFBIp for 3 hr and then allowed to (*b*) migrate through uncoated filters or (*c*) invade through a layer of Geltrex matrix for 6 hr. Fluorescence was assessed and data is expressed as percentage of control media, mean ± SD from at least four independent experiments performed in triplicate. * denotes significant difference from PBS, $p < 0.05$, Student's t test.

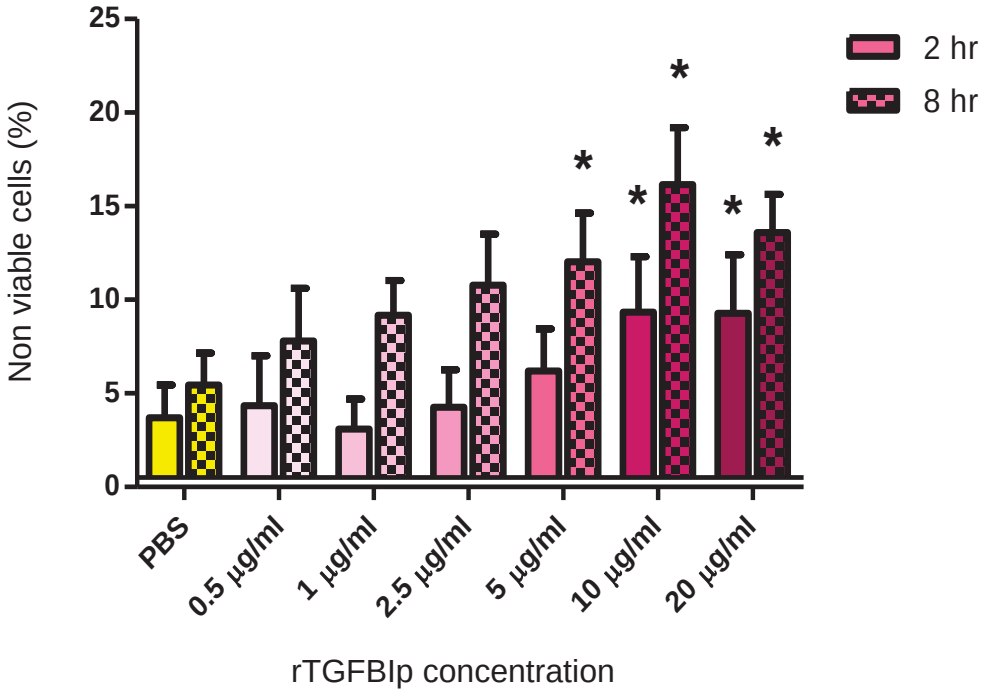

Figure 3.5. *TGFBIp decreases ovarian cancer cell viability.*

An aliquot of OVCAR-5 cells mixed with rTGFBIp for 2 hr at RT or for an additional 6 hr at 37°C to mimic motility assays. An aliquot of cells were mixed with trypan blue to assess cell viability. Data is expressed as mean ± SD from at least three independent experiments performed in triplicate. * denotes significant difference from control media, $p < 0.05$ one-way ANOVA.

3.3.3. TGFBIp promotes ovarian cancer adhesion to peritoneal cells

Cell adhesion experiments were conducted to determine whether TGFBIp could modulate ovarian cancer cell adhesion to LP-9 cells. rTGFBIp significantly increased adhesion of OVCAR-5 cells to LP-9 cells at concentrations ≥ 1 µg/ml (Figure 3.6a). Maximum effect on peritoneal cell adhesion was observed following treatment with 7.5 µg/ml rTGFBIp (Figure 3.6a, $p < 0.0001$). rTGFBIp at 5 µg/ml also significantly increased adhesion of OVCAR-3 and SKOV-3 cells to LP-9 cells (Figure 3.6b). Treatment with neutralizing TGFBIp antibody (5 µg/ml) was able to significantly reduce OVCAR-5 cell adhesion to LP-9 cells to 79% of the control (Figure 3.6c, $p < 0.0001$). However, a higher concentration of TGFBIp neutralizing antibody (20 µg/ml), was required to block the effect of 2 µg/ml exogenous rTGFBIp on OVCAR-5 cell adhesion to LP-9 cells (Figure 3.6c).

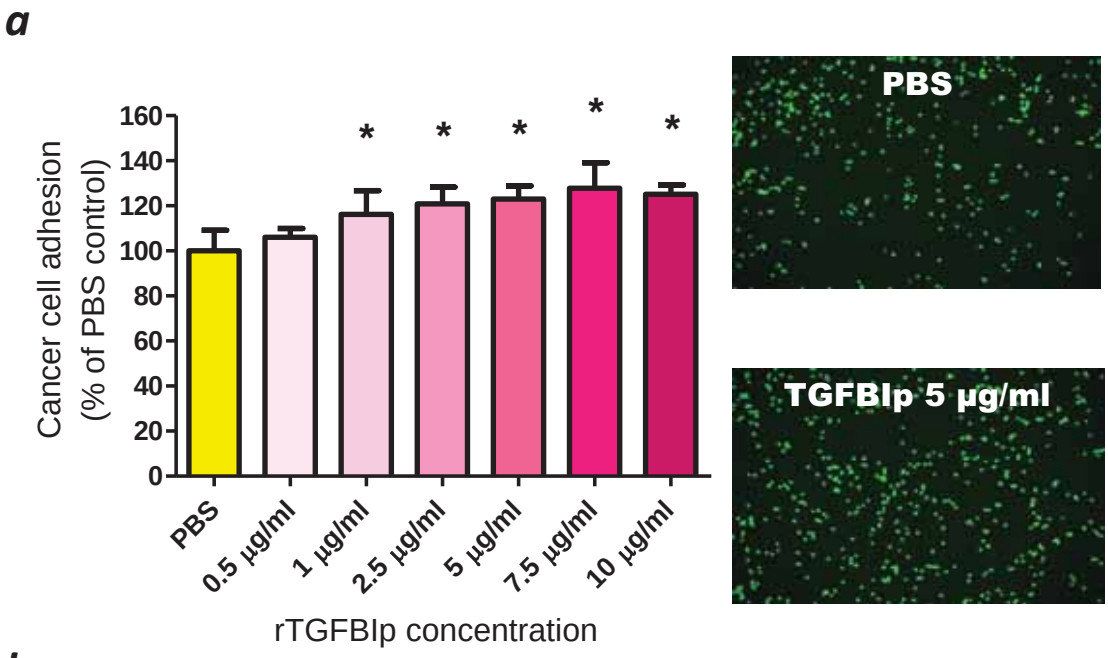
a
Cancer cell adhesion
(% of PBS control)
160
140
120
100
80
60
40
20
0
*
*
*
*
*
PBS
0.5 µg/ml
1 µg/ml
2.5 µg/ml
5 µg/ml
7.5 µg/ml
10 µg/ml
rTGFBIp concentration
PBS
TGFBIp 5 µg/ml

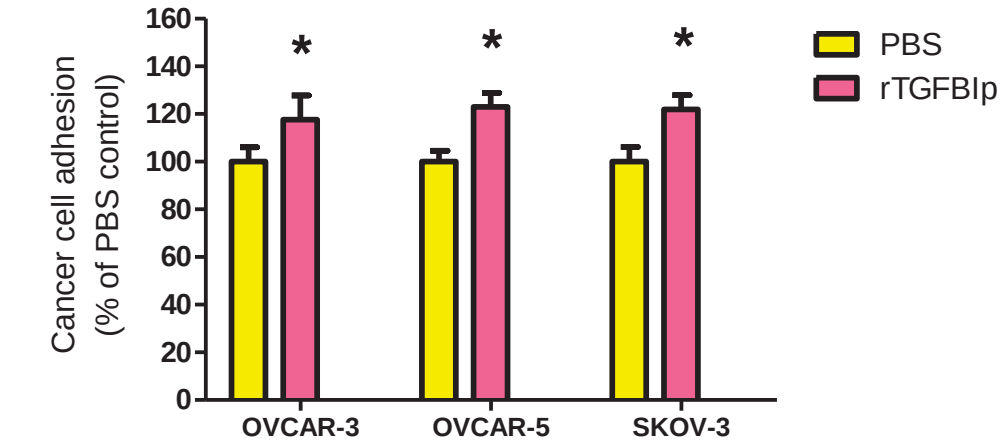
b
Cancer cell adhesion
(% of PBS control)
160
140
120
100
80
60
40
20
0
*
*
*
OVCAR-3
OVCAR-5
SKOV-3
PBS
rTGFBIp

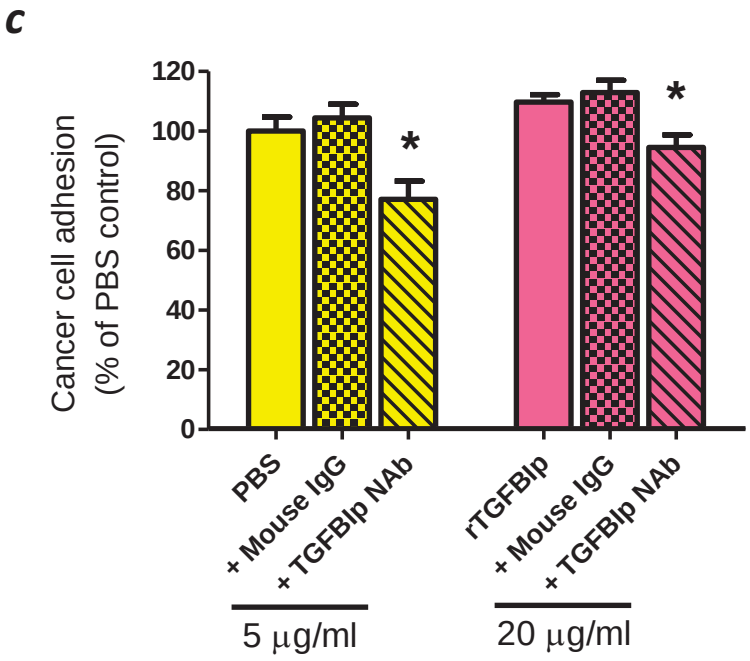
c
Cancer cell adhesion
(% of PBS control)
120
100
80
60
40
20
0
*
*
PBS
+ Mouse IgG
+ TGFBIp NAb
rTGFBIp
+ Mouse IgG
+ TGFBIp NAb
5 µg/ml
20 µg/ml

Figure 3.6. *TGFBIp promotes adhesion of ovarian cancer cells to LP-9 peritoneal cells*.

(*a*) Ovarian cancer cells (OVCAR-5) were incubated with rTGFBI (0.5-10 μg/ml) or PBS in control media (0.1% BSA RPMI) for 3 hr and then allowed to adhere to a monolayer of peritoneal cells (LP-9) for 8 min. Data are expressed as a percentage of fluorescence compared with PBS control, mean ± SD from at least three independent experiments performed in triplicate. * indicates significant difference from PBS control, $p<0.005$, one-way ANOVA. Images demonstrate fluorescently labelled OVCAR-5 cells bound to LP-9 cells in the absence or presence of 5 μg/ml TGFBIp (*b*) Ovarian cancer cells (OVCAR-3, OVCAR-5, or SKOV-3) were treated with TGFBIp (5 μg/ml) or PBS for 3 hr. Data is expressed as percentage of fluorescence compared with PBS control, mean ± SD from at least three independent experiments performed in triplicate. * $p < 0.0001$ denotes significant difference from control media, Student's t test. (*c*) OVCAR-5 cells were treated with mouse IgG (5 μg/ml) or neutralizing TGFBIp antibody (5 μg/ml) or in the absence of TGFBIp. Additional experiments included treatment with mouse IgG (20 μg/ml) or neutralizing TGFBIp antibody in the presence of 2 μg/ml TGFBIp. Fluorescence was assessed and data is expressed as percentage of control media, mean ± SD from at least three independent experiments performed in triplicate. * denotes significant difference from PBS control, $p < 0.05$, one-way ANOVA.

3.3.4. TGFBIp is processed in the ovarian cancer and peritoneal cell co-culture and in ascites of ovarian cancer patients

Western blotting of CM revealed that TGFBIp produced by LP-9 cells was processed into smaller forms when LP-9 cells were direct co-cultured with ovarian cancer cells (Figure 3.7a). The TGFBIp processing also occurred when LP-9 cells were co-cultured in Opticell chambers in which LP-9 cells and ovarian cancer cells share the same growth media but don't physically touch (Figure 3.7b). TGFBIp was not processed when CM from ovarian cancer cells (SKOV-3 and OVCAR-5) was added to LP-9 cells (Figure 3.7d) or when CM from LP-9 cells was added to ovarian cancer cell lines (SKOV-3 and OVCAR-5) (Figure 3.7c).

The TGFBIp bands from the western blot in Figure 3.8a were excised from a corresponding gel stained with Coomassie blue and analyzed by LC-ESI-IT mass spectrometry. The sequencing data revealed two TGFBIp forms: A 65 kDa TGFBIp form (band 3) with a truncated C-terminal domain and a 60 kDa TGFBIp form (band 4) with both truncated C-terminal and N-terminal domains (Table 3.3). C-terminal peptide processing was confirmed using an antibody to the C-terminal TGFBIp peptide residues 671-683, which was only able to detect the full length TGFBIp in LP-9 cells but not the truncated forms of TGFBIp in the co-culture CM (Figure 3.8b). The MS data indicates that C-terminal cleavage of TGFBIp must therefore occur between amino acid residue 626 and amino acid residue 657 since the rabbit polyclonal TGFBIp antibody used in the western blot in Figure 3.7 (amino acid residues 626-683) detected the processed forms of TGFBIp (Figure 3.8c). 2D western blotting also confirmed that TGFBIp was processed to smaller, more acidic forms in the secretome of co-cultured ovarian

cancer and LP-9 cells (Figure 3.9a). Furthermore, abundant cleaved TGFBIp was also demonstrated in the ascites fluid of patients with ovarian cancer (Figure 3.9b).

Table 3.3. *LC-ESI-IT mass spectrometry analysis of TGFBIp protein processing in direct co-culture system.*

TGFBIp band	No. Unique peptides	% seq MS/MS	Combined Mascot score (threshold score/cut)	Predicted MW	Observed MW	N terminal peptide	C terminal peptide
Recombinant protein band (1)	27	39	1444/34	72.4	72	SPYQLVLQHSR (AA27-37)	GDELADSALEIFK (AA 643-655)
LP-9 band (2)	21	33	1236/34	72.4	72	SPYQLVLQHSR (AA27-37)	GDELADSALEIFK (AA 643-655)
Co-culture band (3)	15	24	773/34	72.4	65	SPYQLVLQHSR (AA27-37)	SLQGDKLEEVSLK (AA591-602)
Co-culture band (4)	12	19	431/34	72.4	60	STVISYECCPGYEK (AA 77-90)	YHIGDEILVSGGIGALVR (AA 571-588)

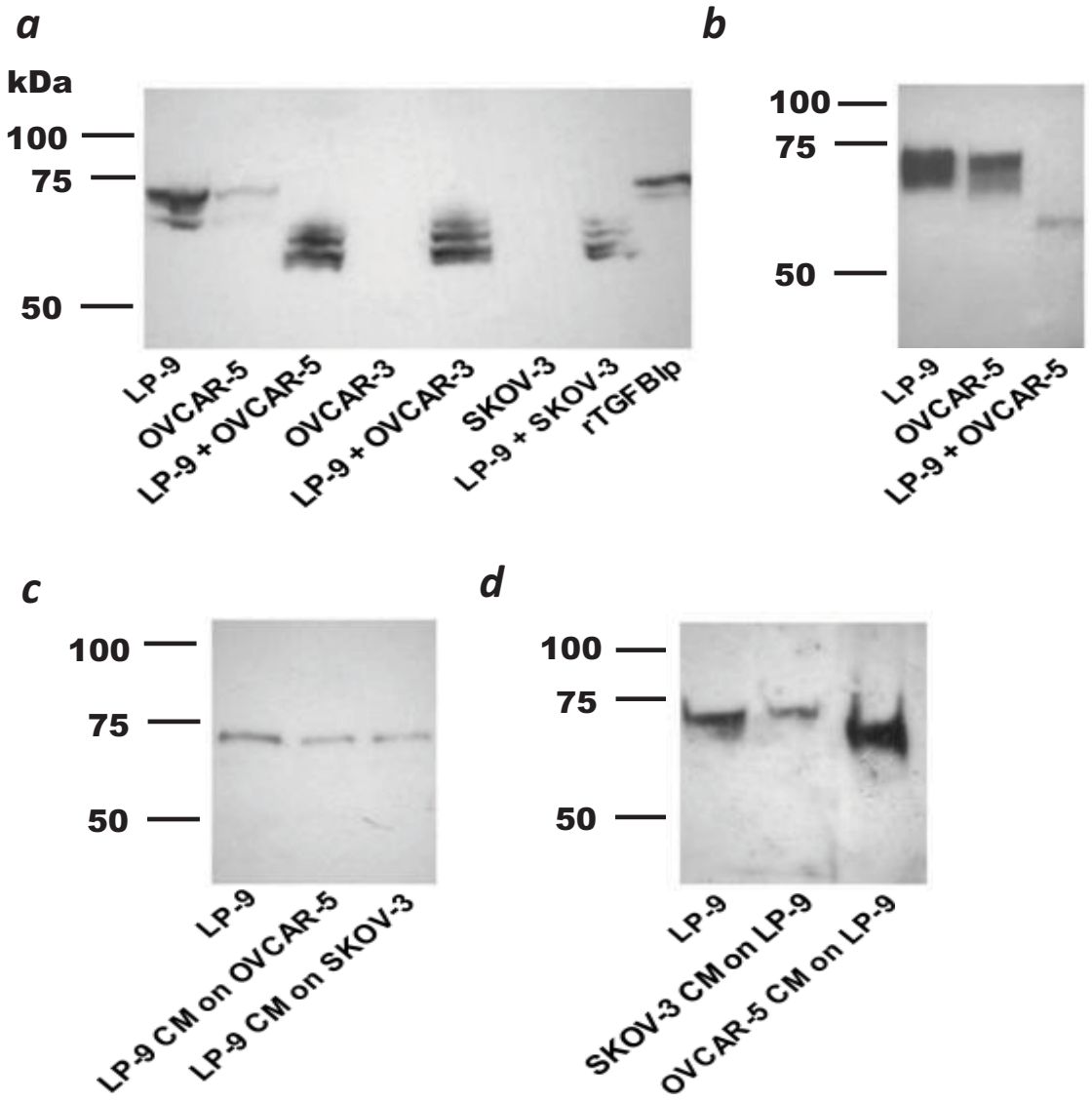

Figure 3.7. *Regulation of TGFBIp secretion by LP-9 peritoneal and ovarian cancer cells.*

CM was collected from co-culture after 48 hr and precipitated with acetone. An equal volume was loaded onto a Tris-HCl SDS-PAGE gel, transferred to PVDF membrane and immunoblotted with rabbit polyclonal TGFBIp antibody (amino acids 626-683, Santa Cruz Biotechnology). (*a*) Two-way direct co-culture where the ovarian cancer cells (OVCAR-3, OVCAR-5 and SKOV-3) and LP-9 cell lines interact whilst in direct contact with each other (equal volume). (*b*) Two-way indirect co-culture using the Opticell system where cell lines (OVCAR-5 and LP-9) interact by shared media (equal protein). (*c)* One-way co-culture where LP-9 cells are treated with ovarian cancer cell (SKOV-3 and OVCAR-5) CM (equal volume). (*d*) One-way co-culture where ovarian cancer cells (SKOV-3 and OVCAR-5) are treated with LP-9 cell CM (equal volume).

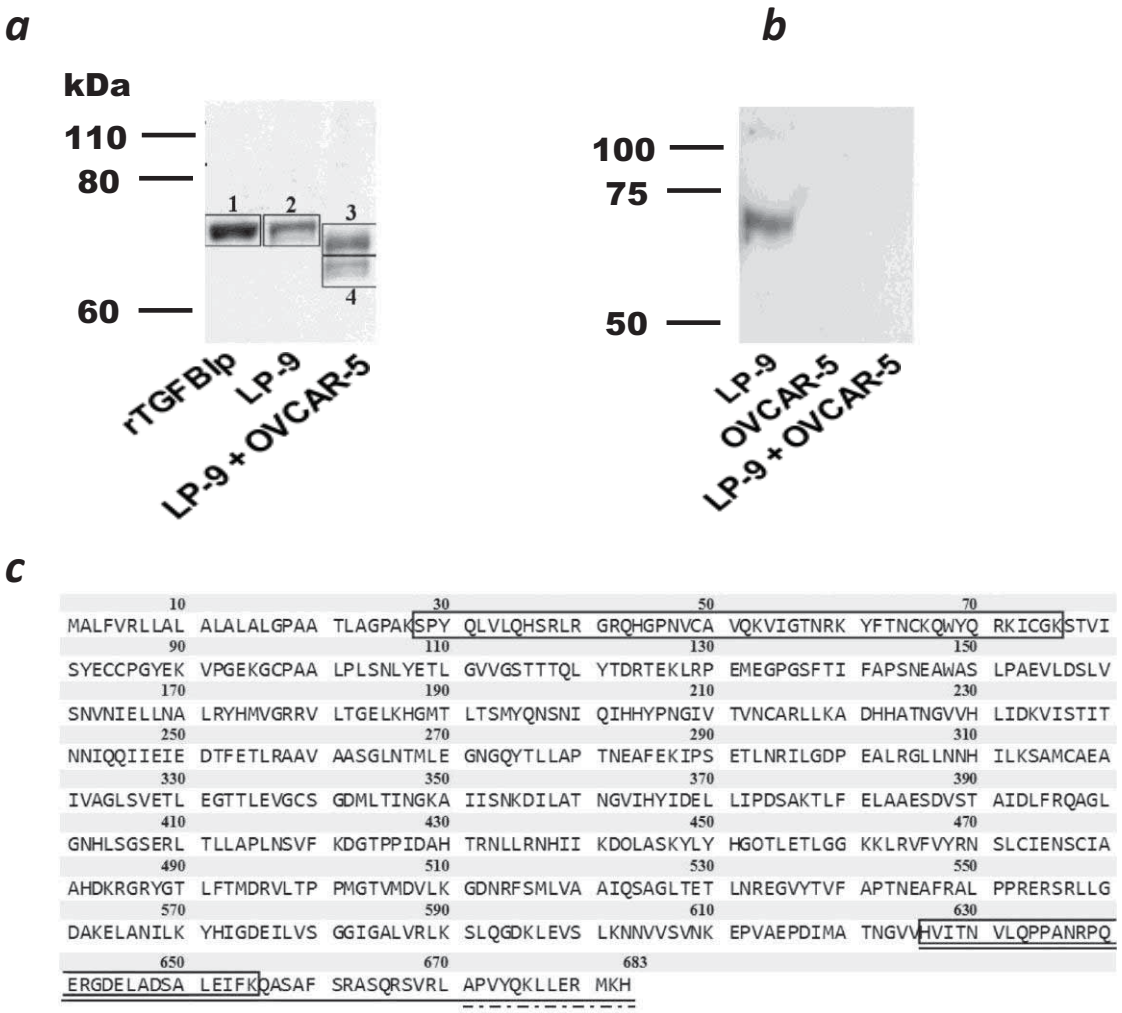

Figure 3.8. *TGFBIp amino acid cleavage sites in the ovarian cancer co-culture and following plasmin treatment.*

Equal protein from CM samples were run on a SDS-PAGE gel and immunoblotted with *(a)* polyclonal rabbit TGFBIp antibody (Santa Cruz Biotechnology) or (*b*) TGFBIp polyclonal rabbit antibody raised to amino acids 671-683 (obtained from by Dr. J.J. Enghild, Aarhus University, Denmark). (*c*) Bands 1-4 from *(a)* were excised from a corresponding coomassie blue stained gel, digested and analyzed by mass spectrometry. The boxed areas in the N-terminus and C-terminus indicate the TGFBIp amino acid cleavage sites identifed by LC-ESI-IT mass spectrometry from ovarian cancer-peritoneal co-culture and following plasmin digestion. The black line and dotted lines indicate the amino acid sequences that the rabbit polyclonal TGFBIp antibody (Santa Cruz Biotechnology) and TGFBIp C-terminal antibody obtained from by Dr. J.J. Enghild were raised to, respectively.

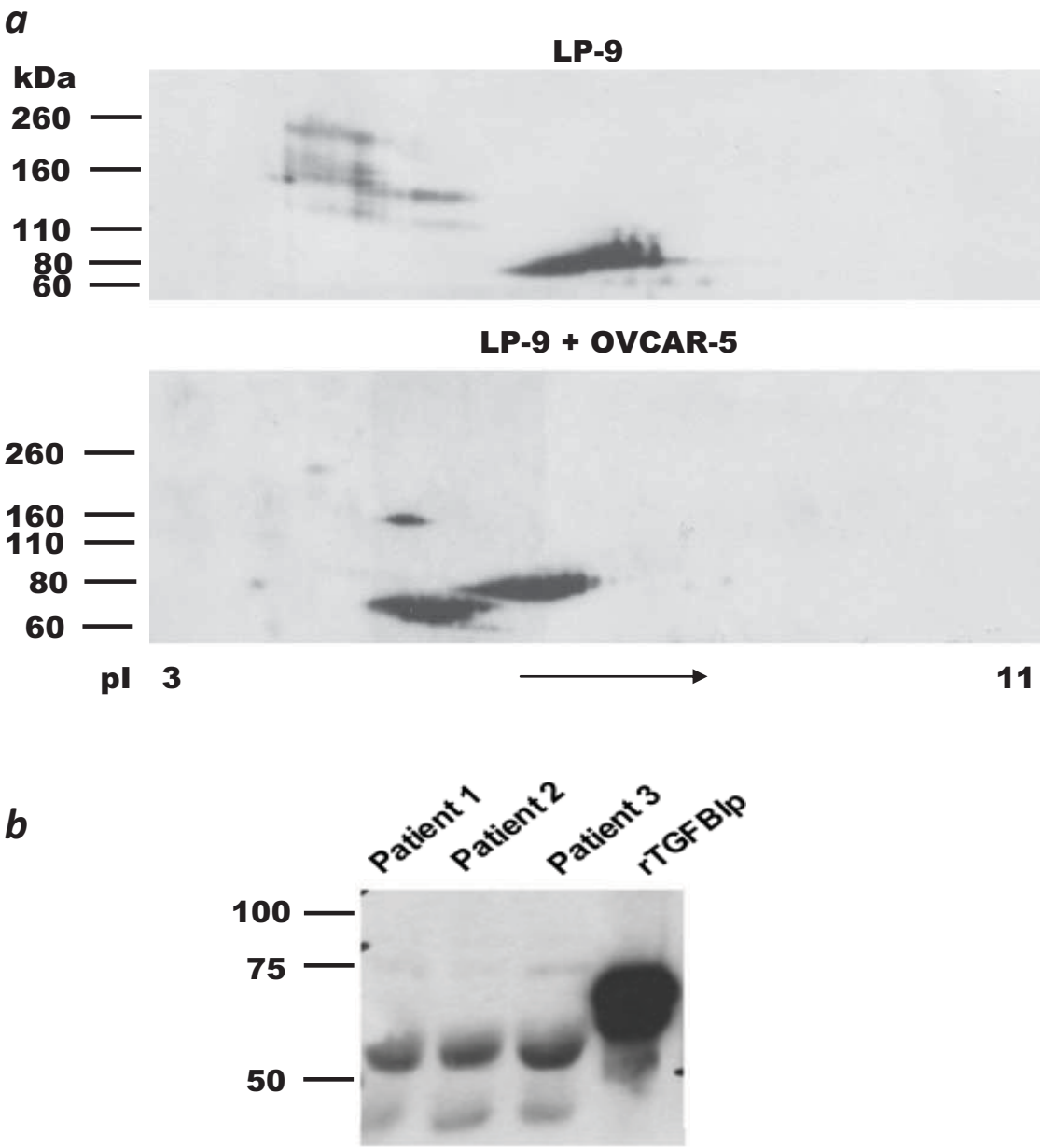

Figure 3.9. *Expression of TGFBIp in peritoneal cells, co-culture, and ovarian cancer patient ascites*

(*a*) 2D TGFBIp western. CMs from LP-9 cells alone and co-culture of OVCAR-5 and LP-9 cells (50 µg protein) was applied to an IPG strip. Isoelectric focussing was carried out and the IPG strip applied to SDS-PAGE gradient gels and electrophoresed followed by transfer to PVDF membrane. Western blotting was performed with rabbit polyclonal TGFBIp antibody (amino acids 626-683, Santa Cruz Biotechnology). (*b*) TGFBIp protein immunoblotting of ascites of ovarian cancer patients. Pooled fractions of ascites (5 µg protein) were run on a gel, transferred to PVDF membrane, and immunoblotted with polyclonal rabbit TGFBIp antibody (amino acids 626-683, Santa Cruz Biotechnology).

3.3.5. TGFBIp processing is mediated by plasmin

To evaluate whether TGFBIp processing was mediated by proteases, co-cultured OVCAR-5 cells and LP-9 cells were treated with the broad spectrum PI cocktail or the MMP inhibitor GM6001. Western blotting revealed that TGFBIp processing to smaller forms was inhibited by PI but not by GM6001 (Figure 3.10a). Furthermore, PI was able to significantly reduce OVCAR-5 cell adhesion to LP-9 cells (Figure 3.10b, $p = 0.002$), but had no effect on OVCAR-5 cell viability (data not shown).

The protease plasmin cleaved TGFBIp and this effect could be inhibited by the PI cocktail (Figure 3.10c). LC-ESI-IT mass spectrometry analysis confirmed that the TGFBIp cleavage by plasmin occured in the same region as observed in the peritoneal-ovarian cancer cell co-culture (Figure 3.8c). Furthermore, cleavage of TGFBIp could be partially blocked when OVCAR-5 and LP-9 were co-cultured in the presence of 150 mM of the plasmin inhibitor ε-ACA (Figure 3.10d). Additionally, plasmin levels were found to be almost immediately increased in the CM of co-cultured OVCAR-5 and LP-9 cells (Figure 3.10e). The plasmin levels were highest after 1 hr of co-culture which was equivalent to 0.4 U/ml of human plasmin. The level of plasmin progressively decreased following 8 to 72 hr of co-culture. No plasmin activity was detected in the CM collected from OVCAR-5 or LP-9 cells alone after 1 hr (Figure 3.10e) or after 48 hr culture (not shown). Parallel western blot analysis of the CM samples demonstrated that cleaved TGFBIp could be detected as early as 12 hr after OVCAR-5 and LP-9 co-culture (Figure 3.10f).

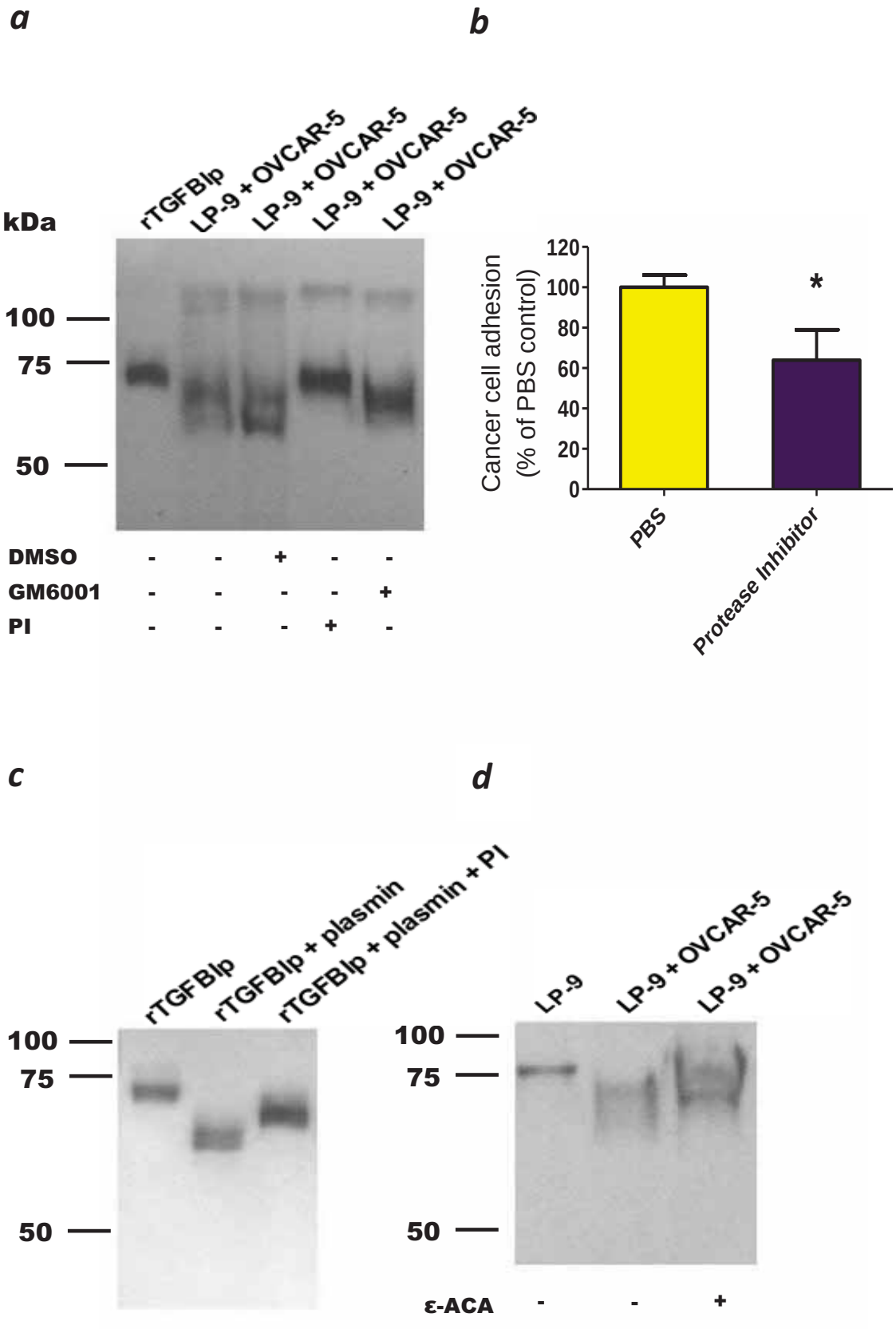
a
b
rTGFBIp
LP-9 + OVCAR-5
LP-9 + OVCAR-5
LP-9 + OVCAR-5
LP-9 + OVCAR-5
kDa
100
75
50
DMSO - - + - -
GM6001 - - - - +
PI - - - + -
Cancer cell adhesion (% of PBS control)
120
100
80
60
40
20
0
*
PBS
Protease Inhibitor
c
d
rTGFBIp
rTGFBIp + plasmin
rTGFBIp + plasmin + PI
100
75
50
LP-9
LP-9 + OVCAR-5
LP-9 + OVCAR-5
100
75
50
ε-ACA - - +

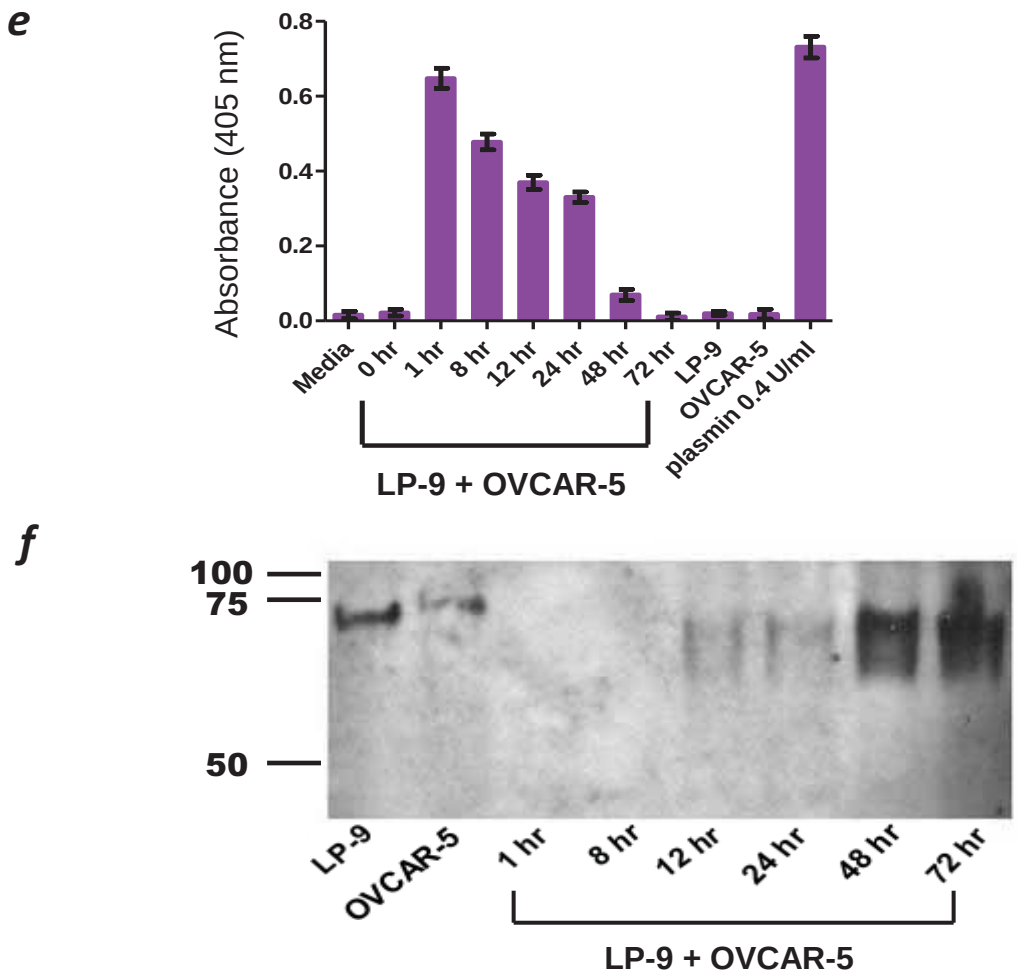

Figure 3.10. *TGFBIp processing during ovarian cancer and peritoneal cell co-culture is mediated by plasmin.*

Equal volumes of protein samples were immunoblotted with TGFBIp antibody (Santa Cruz Biotechnology) (*a, c, d, f*) (*a*) LP-9 peritoneal cells were directly co-cultured with OVCAR-5 ovarian cancer cells in the presence or absence of a broad spectrum PI (1/800) or the MMP inhibitor GM6001 (20 µM). (*b*) OVCAR-5 cells were incubated with PI (1/800) and allowed to attach to a monolayer of LP-9 cells. Data is expressed as percentage of fluorescence compared with control media, mean ± SD from at least three independent experiments performed in triplicate. * denotes significant difference from DMSO vehicle control, p = 0.002, Student's t test. (*c*) rTGFBIp (0.5 µg/ml) was treated with 0.3 U/ml human plasmin in the absence or presence of PI. (*d*) LP-9 peritoneal cells were directly co-cultured with OVCAR-5 ovarian cancer cells in the presence or absence of 150 mM ε-ACA. (*e*) Plasmin levels in co-cultured OVCAR-5 and LP-9 cells over 72 hr. (*f*) CM samples collected from co-cultured cells in (e) were assessed for TGFBIp cleavage.

3.3.6. TGFBIp RGD peptide motif is not required to promote OVCAR-5 invasive properties

Previous studies have demonstrated that C-terminal processing of TGFBIp at Ala^{647} after the RGD domain (amino acids 642-644) occurs *in vivo* in human cornea [602]. To assess the role of the RGD peptide motif in promoting adhesion, motility, or invasion, ovarian cancer cells were pre-treated with TGFBIp and peptide ERGDEL or control peptide ERGEEL. Treatment with either the ERGDEL peptide or control ERGEEL peptide did not affect OVCAR-5 motility and the ability of TGFBIp to promote ovarian cancer cell motility (Figure 3.11a), invasion (Figure 3.11b), or adhesion to LP-9 cells (Figure 3.11c). This suggests that the effects of TGFBIp on OVCAR-5 cell motility, invasion, and adhesion to peritoneal cells are independent of the RGD peptide motif.

a

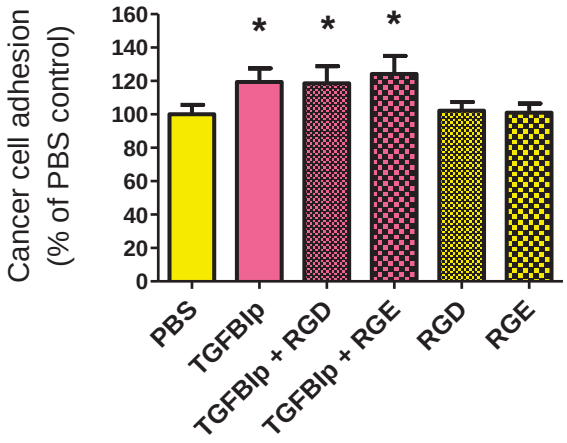
Cancer cell adhesion
(% of PBS control)
160
140
120
100
80
60
40
20
0
*
*
*
PBS
TGFBIp
TGFBIp + RGD
TGFBIp + RGE
RGD
RGE

b

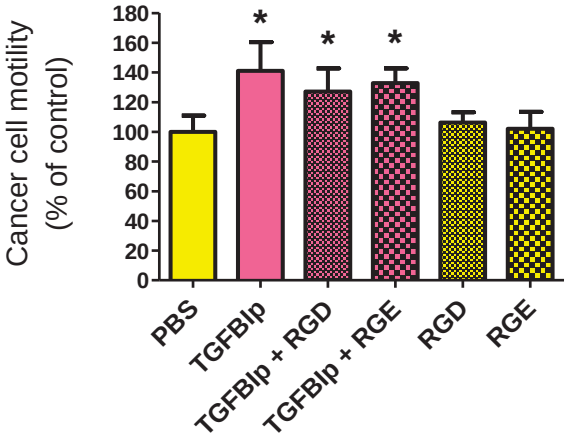
Cancer cell motility
(% of control)
180
160
140
120
100
80
60
40
20
0
*
*
*
PBS
TGFBIp
TGFBIp + RGD
TGFBIp + RGE
RGD
RGE

c

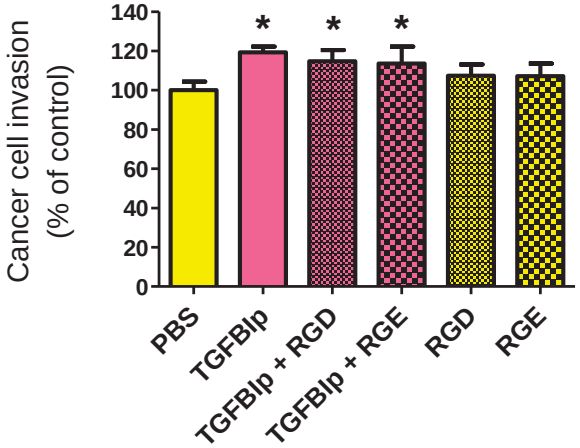
Cancer cell invasion
(% of control)
140
120
100
80
60
40
20
0
*
*
*
PBS
TGFBIp
TGFBIp + RGD
TGFBIp + RGE
RGD
RGE

Figure 3.11. *The effects of TGFBIp on ovarian cancer cell motility, invasion, and adhesion is independent of the integrin binding RGD motif*.

Calcein labelled OVCAR-5 cells were treated with PBS or rTGFBIp (5 μg/ml) in the presence of TGFBIp peptide ERGDEL (50 μg/ml) or ERGEEL control peptide (50 μg/ml) in motility (*a*), invasion (*b*) and adhesion assays (*c*) as described in the methods section. Data is expressed as percentage of fluorescence compared with PBS control, mean ± SD from at least three independent experiments performed in triplicate. * indicates significant difference from control treatment group, $p < 0.05$, one-way ANOVA.

3.4. DISCUSSION

One of the crucial steps in ovarian cancer metastasis involves the implantation of ovarian cancer cells onto the peritoneal lining. As the underlying molecular mechanisms have not been well characterized we have studied the interaction between ovarian cancer and peritoneal cells *in vitro*. The ECM protein TGFBIp was found to be differentially regulated in the secretome of peritoneal-ovarian cancer cell co-culture. In this study we have demonstrated that TGFBIp is abundantly expressed by peritoneal mesothelial cells and can promote ovarian cancer cell motility, invasion and adhesion to LP-9 peritoneal cells. Furthermore, we found that TGFBIp undergoes processing in the ovarian cancer–peritoneal cell co-culture via the protease plasmin.

The low level of TGFBIp observed in ovarian cancer cell lines and ovarian cancer tissue in this study is consistent with previous studies which have shown TGFBIp expression to be down-regulated in many cancer cell lines and human cancers [578, 587-589]. Our data shows high levels of TGFBIp in normal ovarian surface epithelial cells and benign serous ovarian tumours but low TGFBIp expression in human serous ovarian cancer cells also suggests that TGFBIp may be down-regulated during the process of ovarian cancer tumourigenesis. Furthermore, the presence of low levels of TGFBIp in borderline serous ovarian tumours suggests that the down-regulation of TGFBIp may be any early event in the neoplastic process. Interestingly, TGFBIp over-expression has been shown to markedly reduce tumourigenicity of lung cancer cells in nude mouse xenograft models [547, 590] and mediate apoptosis through the RGD motif in CHO cells [593]. More recent studies demonstrating that the loss of TGFBIp predisposes

mice to spontaneous tumour development [603] has provided strong evidence that TGFBIp functions as a tumour suppressor. Our finding that high concentrations of TGFBIp (≥ 5µg/ml) induce OVCAR-5 cell death also supports an anti-tumourigenic role for TGFBIp.

Although these studies indicate that TGFBIp has an anti-tumourigenic role, a large number of studies have also found that TGFBIp is over-expressed in other cancer cell lines and human tumours including colorectal, renal, lung, oesophageal, and pancreatic cancers [549, 579-582, 586]. Furthermore, several reports indicate that TGFBIp can mediate cancer cell invasion and metastasis as well as enhance cancer cell extravasation [543, 596-598]. In our study, we have demonstrated that rTGFBIp induces both motility and invasion of OVCAR-5 and SKOV-3 cells but did not affect motility or invasion of OVCAR-3 ovarian cancer cells which are known to be less metastatic. We have also shown that rTGFBIp promotes attachment of OVCAR-5, SKOV-3, and OVCAR-3 to LP-9 peritoneal cells. These findings suggest that TGFBIp may function in multiple ways to promote ovarian cancer metastasis and that the effects on motility may be independent of those on adhesion. A related protein, periostin has also been shown to increase motility of ovarian cancer cells and promote their adhesion to the peritoneum [373].

Recently, TGFBIp has been shown to mediate lymphatic endothelial migration and adhesion to ECM under low oxygen conditions [601]. These observations suggest that during hypoxia, which commonly occurs in tumours, TGFBIp may aid the metastatic process by promoting the adhesion to lymphatic endothelial cells. These findings indicate that TGFBIp expression and function may be cell type specific and dependent

on the tumour microenvironment. Our study has presented evidence that TGFBIp can act as both a tumour suppressor and tumour promoter. Whilst our findings demonstrating that rTGFBIp can enhance ovarian cancer adhesion, motility and invasion support a pro-metastatic role, we have also demonstrated that TGFBIp is down-regulated in the tumorigenic process and that high levels of TGFBIp can induce ovarian cancer cell death. Consequently, TGFBIp is likely to act as a "double edged sword" where the loss of TGFBIp has a pro-tumourigenic role and the high expression of TGFBIp by peritoneal cells aids the metastatic process.

TGFBIp has been reported to support adhesion of many cell types by recruiting different integrins, the only cell surface receptors that have been identified for TGFBIp to date (reviewed in [564]). In our study, the effects of TGFBIp on OVCAR-5 cells were independent of the TGFBIp RGD integrin binding motif (amino acids 642-644) since treatment with ERGDEL peptide did not block the ability of TGFBIp to promote ovarian cancer cell motility, invasion, or adhesion to peritoneal cells. Our findings are inconsistent with the observation that a TGFBIp peptide encompassing the 4^{th} FAS1 domain, also known as fastatin, could inhibit endothelial cell adhesion and migration in an RGD dependent manner [604]. However, it is in agreement with the study by Cannistra et al. which demonstrated ovarian cancer binding to peritoneal cells was independent of the RGD motif [191]. TGFBIp mediated adhesion has also been shown to be independent of the RGD motif in cultured epithelial cells of the cornea [536]. However, peptides to the NKDIL motif (amino acids 354-358) in the second FAS-1 domain, EPDIM motif (amino acids 617-621) and YH18 motif (amino acids 563-580) in the fourth FAS-1 domain of TGFBIp have been shown to inhibit TGFBIp mediated

adhesion and migration of fibroblasts, keratinocytes, endothelial cells, synoviocytes, and vascular smooth muscle cells [536, 557, 563, 604, 605]. Our data suggests that TGFBIp activity on OVCAR-5 cells is mediated by other sites in the TGFBIp molecule other than the RGD motif which may include the EPDIM and NKDIL motifs as well as the sequence spanning the YH18 motif.

We have shown that TGFBIp cleavage in the ovarian cancer-peritoneal cell co-culture occurs between amino acid residues 27-76 in the N-terminus and amino acid residues 626-657 in the C-terminal domain. Although the functional role of the N-terminal TGFBIp domain has not been well studied, the C-terminus has several integrin binding motifs including the RGD and EPDIM sequences. TGFBIp fragments containing the final 69 amino acids of TGFBIp, including the RGD and EPDIM domains have recently been shown to promote apoptosis of osteosarcoma cancer cells [594]. In contrast, a truncated TGFBIp lacking these integrin-binding sequences failed to induce apoptosis in osteosarcoma cells [594].

Whilst it is not known whether the C-terminal processed TGFBIp in the secretome of the ovarian cancer-peritoneal co-culture retains its RGD sequence at amino acid 642-644, the EPDIM motif at amino acid 617-621 is maintained in the C-terminal processed TGFBIp. Crystal structure of fascilin 1 (*Drosphilia* TGFBIp homologue) has identified a novel fold domain consisting of a seven-stranded beta wedge and a number of alpha helices in the 3rd and 4th FAS1 domains [606]. The EPDIM motif maps to a conserved kink in the β6 strand of the fourth TGFBIp FAS1 domain and is predicted to be buried within the domain protein core [606]. TGFBIp processing by proteases, including plasmin, in this region may liberate this site for integrin interactions and promote the

integrin binding activity on the surface of the peritoneum [328, 607, 608] with ovarian cancer cells [87, 191] and enhance ovarian cancer metastatic behavior. TGFBIp has been shown to trigger phosphorylation and to activate several intracellular pathways including AKT, extracellular signal-regulated kinase, FAK, and paxillin, thus mediating adhesion and migration of vascular smooth muscle cells through interactions with αvβ5 integrins [563]. It is possible that cleaved TGFBIp may augment these signaling pathways in ovarian cancer cells via enhanced integrin binding.

Interestingly, TGFBIp processing was only observed when ovarian cancer cells and peritoneal cells were in direct physical contact in culture or when the cells shared the same growth media in the Opticell system. TGFBIp processing did not occur when CM from LP-9 cells was added to cultured ovarian cancer cell lines or when CM from ovarian cancer cells was added to the cultured LP-9 cells. This indicates that TGFBIp processing is not mediated by a simple up-regulation of ovarian cancer cell derived proteases but requires multiple levels of cross-talk between both ovarian cancer and peritoneal cells. A similar paracrine effect was previously reported for endometrial cancer epithelium–stroma cell co-cultures, where hepatic growth factor secreted by the stromal cells acted on the endometrial cancer cells by inducing the cleavage of MMPs pro-forms to mature active forms [609]. Our findings suggest, however, that cleavage of TGFBIp in the ovarian cancer and peritoneal cell co-culture is not MMP mediated as the broad spectrum MMP inhibitor, GM6001, failed to inhibit TGFBIp processing. Instead we found that the protease plasmin cleaved TGFBIp in the same region as observed in the ovarian cancer-peritoneal cell co-culture and that this could be inhibited by the PI cocktail.

It is likely that increased production or activation of proteases like u-PA [610], as a result of the ovarian cancer-peritoneal cell interaction, catalyzes the conversion of the proenzyme plasminogen to the active enzyme plasmin leading to C-terminal TGFBIp processing. This hypothesis is further strengthened by our experiments demonstrating that the plasmin inhibitor ε-ACA, which inhibits plasminogen conversion into plasmin, could at least partially inhibit TGFBIp processing. Furthermore, we demonstrated that plasmin activity was increased in the CM of co-cultured OVCAR-5 + LP-9 whilst no plasmin activity could be detected in the CM collected from OVCAR-5 or LP-9 cells alone. Our study demonstrated that plasmin activity was maximal after 1 hr of co-culture and decreased progressively over 72 hr when cleaved TGFBIp was detected. Although plasmin activity was markedly reduced after 48 hr of co-culture, plasmin activity was still 2-3 fold higher than the basal level present in CM collected from LP-9 or OVCAR-5 cells cultured alone. Our data suggest that low plasmin activity is sufficient to maintain TGFBIp in the cleaved form. These findings add to our understanding of the interaction between ovarian cancer and peritoneal cells and suggest that increased plasmin production and TGFBIp cleavage may be early events in the process of ovarian cancer metastasis.

We detected abundant cleaved TGFBIp in ascites fluid collected from ovarian cancer patients at the time of surgery. Ascites has also been shown to induce an up-regulation of uPA by ovarian cancer cells [610]. It is likely that increased production or activation of proteases like uPA as a result of the ovarian cancer-peritoneal cell interaction catalyze the conversion of the pro-enzyme plasminogen to the active enzyme, plasmin, and leads to C-terminal TGFBIp processing. From the western blots using rTGFBIp for comparison, we estimated levels of TGFBIp in the ascites to range

between 5-25 μg/ml TGFBIp whilst LP-9 cells produced approximately 3-5 μg/10^6 cells (data not shown). These concentrations are effective at promoting ovarian cancer cell adhesion to peritoneal cells. However as we have shown that concentration ≥ 5μg/ml can also have apoptotic effects on OVCAR-5 cells, further studies are required to determine whether cleaved TGFBI present in ascites can play a tumour promoting or a pro-apoptotic role.

A recent study by Kenny and colleagues using 3D co-culture of ovarian cancer and peritoneal cells demonstrated that MMP-2 mediated cleavage of ECM proteins fibronectin and vitronectin into small fragments increased binding of ovarian cancer cells to the fibronectin (α5β1 integrin) and vitronectin (αVβ3 integrin) receptors on peritoneal cells [336]. Ovarian cancer cells adhere more efficiently to the smaller fibronectin and vitronectin cleavage products than their full-length forms, and the increased adhesion was abrogated when $\alpha_5\beta_1$ and $\alpha_V\beta_3$ integrins were knocked down by siRNA or blocked by treatment with an MMP-2 inhibitor. Consistent with these findings, we also observed increased levels of cleaved fibronectin in the secretome of co-culture ovarian cancer cells and peritoneal cells.

Our study has shown that TGFBIp is expressed by peritoneal mesothelial cells and increases motility, invasion, and adhesion of ovarian cancer cells to peritoneal cells. We therefore conclude that TGFBIp promotes ovarian cancer metastasis to the peritoneum as part of a tumour-host signal pathway or cascade and is therefore a potential novel therapeutic target against ovarian cancer.

CHAPTER 4 - THE ROLE OF VERSICAN, HA, AND CD44, IN OVARIAN CANCER

4.1. INTRODUCTION

There is increasing evidence to suggest that ECM components play an active role in tumour progression and are an important determinant for the growth and progression of solid tumours [611, 612]. Tumour cells interfere with the normal programming of ECM biosynthesis and can extensively modify the structure and composition of the matrix [613]. Alterations in the extracellular environment may be critical for tumour initiation and progression and intra-peritoneal dissemination.

HA is a large polymer which is a component of the ECM and is capable of binding several proteoglycans including versican. [126]. Many tumours appear to be selectively or preferentially enriched in HA [129]. HA has been investigated and associated with prognosis in many cancer types including breast, lung, colon, and prostate [133, 139, 144, 145, 147, 150] and also associated with metastasis [130, 146, 150]. It has also been correlated with cancer aggressiveness in patients with breast cancers, prostate cancer, gliomas, and ovarian carcinomas [139-143, 147]. HA levels have been strongly associated with the metastatic potential and invasive ability in ovarian tumour models [151] as well as prognosis and survival [140]. Furthermore, HA has been shown to increase tumour cell proliferation, motility, and invasion of tumour cells [148, 149].

There are a number of cell surface receptors for HA, which includes CD44 [131]. CD44 has been associated with unfavourable prognosis in a variety of cancers [184-186, 188]

including ovarian cancers [189, 190]. Human ovarian cancers have higher levels of CD44 in malignant tumours compared with benign and borderline tumours [200]. CD44 expression on ovarian cancer cells causes a strong adhesion to HA-enriched peritoneal mesothelium [88, 130, 199]. It is this interaction between CD44 and HA which is thought to be involved in increased motility, adhesion, and invasion of cancer cells as well as tumour growth in many tumours, especially in ovarian cancer [174, 193-195]. Blocking the CD44-HA interaction using various methods has been shown to inhibit tumour growth, motility, invasion, and cell adhesion in breast cancer [277, 278] and cell adhesion in prostate cancer [280]. Anti-CD44 antibodies inhibited peritoneal ovarian cancer metastases [194] whilst siRNA down-regulation of CD44 expression reduced adhesion, invasion, and resistance to apoptosis as well as suppressing tumour growth and peritoneal dissemination of human ovarian cancer xenografts in nude mice [274].

HA levels are often increased in the serum of patients with a variety of different tumours [170-172]. It has also been shown that HA is significantly elevated in the serum of patients with metastatic disease compared with the sera of patients without metastatic disease [170]. Combined ELISA tests for urinary HA and HAase levels to detect high-grade bladder tumours had significantly higher sensitivity and specificity than that of the currently used Immunocyt test [168, 169], and is now used as a non-invasive bladder cancer detection test. In addition, this test has high specificity and sensitivity in prostate cancer [142] and may yet be found to detect other cancer types, including ovarian cancer. Serum and urine HA levels were found to be elevated in

small cohorts of ovarian cancer patients in comparison with controls [614] and serum HA levels were shown to increase with stage [173].

Elevated levels of the HA binding proteoglycan, versican, are associated with cancer relapse and poor patient outcome in breast, prostate, and many other cancer types including ovarian cancer [146, 217, 244-246, 615-619]. Elevated levels of versican have been observed in primary ovarian tumours and secondary metastases when compared with normal ovaries [248, 249] and increased by 3-fold in ovarian cancer tissues when compared with normal ovarian surface epithelial cells [620]. In ovarian cancer, high versican stromal staining was associated with high FIGO stage, large residual tumour, serous histologic type, and reduced survival [246]. Increased expression of versican, has been identified as a candidate marker for the early detection of ovarian cancer [621] and increased gene expression has been associated with ovarian cancer metastases [247, 622].

HA often becomes deposited in the tissue spaces immediately surrounding invasive tumours [132, 133] and is thought to form a protective matrix coat around the cancer cells themselves [129] by binding other matrix molecules including versican, brevican, and aggrecan [134]. This ECM is visible around cancer cells as a unique matrix known as a pericellular sheath. By providing a pericellular environment, HA can stimulate cell migration indirectly, partly dependent on this ability to bind versican [136], and modifying the properties of the ECM [253]. This HA-versican interaction and alteration of the ECM to form a polar sheath has been shown to increase prostate cancer cell motility [135]. These studies give strong evidence linking complexes formed between versican, HA, and CD44, aid the motility of cancer cells.

Treatment with HA oligos blocked sheath formation in both vascular SMCs and tumour cells [136, 294, 297]. Furthermore, disruption of the HA CD44 interaction using HA oligos has been shown to markedly inhibit the growth of melanoma cells [295], colorectal carcinoma [298], and lung metastases formation, as well as motility and invasiveness [297]. These findings suggest that the potent anti-tumour effects of HA oligos are mediated in part by the blocking of the formation of HA-rich cell-associated matrix. The use of HA oligos is a potentially effective reagent to block versican HA interactions as well as local tumour invasion.

In this study, we will assess whether HA, versican, and CD44 in ovarian tumours are associated with ovarian cancer stage or metastasis. Additionally, we will also investigate whether the levels of HA in the serum of ovarian cancer patients is increased and/or associated with chemotherapy treatment. We will assess whether treatment with recombinant versican can induce the formation of a pericellular sheath around ovarian cancer cells (OVCAR-3, OVCAR-5, and SKOV-3 cell lines) and promote their motility and invasion. Furthermore, we will investigate whether small HA oligos, previously shown to inhibit pericellular matrix formation by smooth muscle cells, can be used to inhibit ovarian cancer sheath formation and thus their motility and invasion.

4.2. MATERIALS AND METHODS

4.2.1. Cell lines

OVCAR-5, OVCAR-3, SKOV-3, and LP-9 cell lines were maintained as described in section 2.2.1. Chinese hamster ovary (CHO) cells overexpressing versican isoform V1 were obtained from Dr Richard Le Baron (University of Texas at San Antonio, Texas, USA) and parental CHO K1 cells were purchased from the ATCC and maintained in α-MEM medium (Sigma Aldrich) supplemented with 4 mM L-glutamine, 100 µg/ml penicillin, 100 µg/ml streptomycin, 20 µg/ml fungizone, 2 µg/ml amphotericin B, and 10 % FBS. Cell CM was collected from the flasks and centrifuged at 2000 rpms for 5 min to remove any cell debris.

4.2.2. Immunohistochemistry

Archived formalin-fixed paraffin tissue blocks of normal ovaries (n = 11), benign serous tumours (n = 8), serous ovarian carcinomas (n = 26), matching omental metastatic implants (n = 26), borderline tumours (n = 10), stage I (n = 11), stage II (n = 11), stage III (n = 12), and stage IV (n = 10) serous ovarian carcinomas were obtained and mounted as described in section 3.2.4 and then incubated overnight at 4°C with rabbit antibody to recombinant human versican (Vc) (1/500, kindly provided by Professor Richard LeBaron), mouse anti-CD44 (1/800 Clone 156-3C11, Neomarkers, Fremont, USA), biotinylated HA-Binding protein (HABP, 1/500, Seigaku Corporation, Tokyo, Japan). The tissues were subsequently incubated with biotinylated goat anti-

rabbit/mouse (1/400, Dako Australia) for 1 hr at RT followed by streptavidin-horseradish peroxidise conjugate (1/500, Dako Australia). Immunoreactivity was detected using diaminobenzidine/H_2O_2 substrate. Sections were counterstained with 10% haematoxylin, dehydrated, and mounted in Pertex. Each tissue had a matching negative control which lacked the primary antibody incubation step.

4.2.3. Purification of versican

Versican was isolated from freshly collected CHO V1 CM using a combination of anion exchange and gel filtration chromatography. Initially CM was batch-adsorbed to Q-Sepharose (10 ml, GE Healthcare) at 4°C for 48 hr in the presence of protease inhibitors (1 tablet/25 ml, Roche Australia), batch eluted with 2 M NaCl and separated by gel chromatography on a sephacryl S400 column (15 x 650mm, GE Healthcare) as described previously [221]. Versican-containing fractions determined by dot blot using the 12C5 mouse monoclonal versican antibody (Developmental Studies Hybridoma Bank, University of Iowa, USA) were then pooled and concentrated 10-30 fold to 100-200 U/mL using Centriprep centrifugal filters (Amicon Bioseparations, Bedford, USA) and Nanosep micro-concentrators (Pall Gelman Laboratory, Ann Arbor, USA) with M_r 50 and 300 kDa cut-offs respectively. The molecular integrity of the purified versican samples was determined by immunoblotting with 12C5 antibody at 1/250 (Figure 4.1a). Visualization was achieved by anti-mouse IgG peroxidase-conjugated secondary antibodies (Dako Australia) with enhanced chemiluminescence. A matching gel was stained with silver to detect any contaminating proteins in the pooled samples (Figure 4.1b).

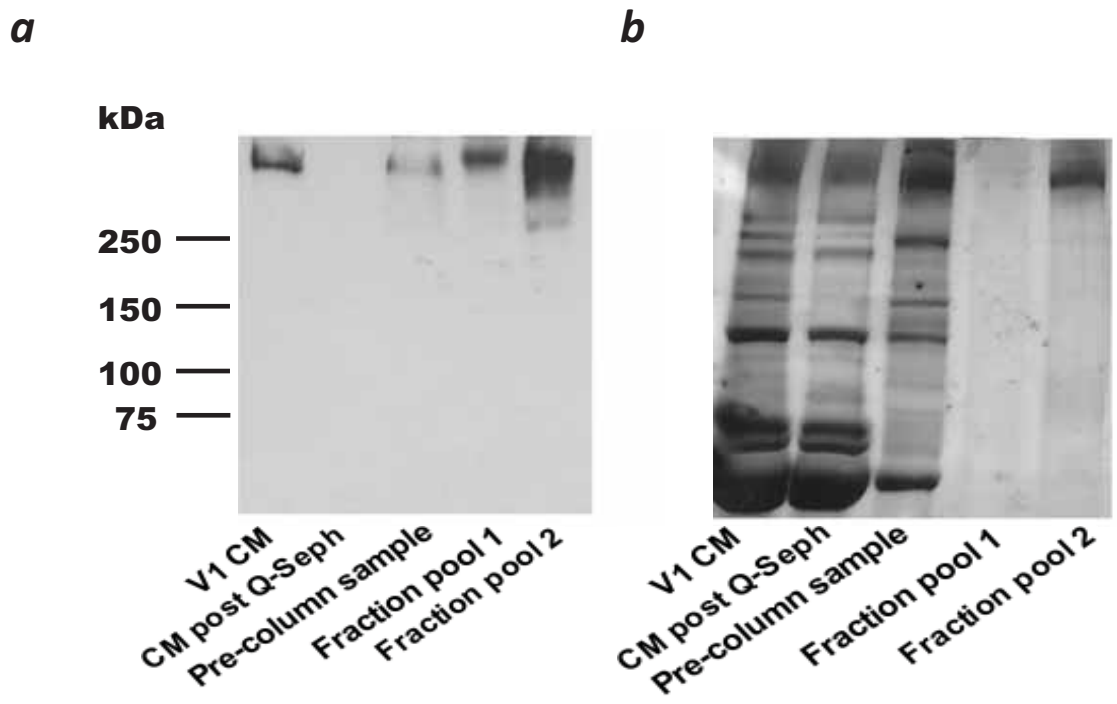

Figure 4.1 *Purification of versican isoform V1*.

(a) Fractions separated with Sephacryl 400 immunoblotted with 12C5 mouse antibody to human versican. Unconcentrated CM from CHO V1 cells cultured in MEM + 10% FBS (20µl), CM after Q-sepharose absorption (20µl), 2M NaCl elute (5µl) which was then loaded onto the Sephacryl column and pooled fractions (10µl of 25x concentrate). *(b)* Corresponding silver stained gel. No contaminating proteins were detected in fraction pools 1 or 2.

4.2.4. Versican quantitation

Tissue culture (Nunc) 96 well plates were coated overnight with 100 µl 25 µg/ml HA (#H1504, Sigma Aldrich) in PBS at RT and then washed three times with PBS + 0.1% BSA (dilution buffer, DB). Wells were blocked for 90 min with 100 µl PBS + 1% BSA at 37°C and washed three times with PBS + 0.05% Tween (PBS-T). Wells were then treated with 50 µl of control or versican sample (in DB) for 2 hr at RT, washed three times with PBS-T, and coated with 100 µl primary 12C5 monoclonal antibody (1/250 in DB) overnight at 4°C. Wells were washed three times with PBS-T and then coated with 100 µl biotinylated anti mouse antibody (Dako Australia) (1/2000 in DB) for 90 min at RT. Wells were subsequently washed three times with PBS-T before coating with 100 µl of streptavidin (Dako Australia) per well for 90 min. 100 µl Sigmafast OPD solution (Sigma Aldrich) was added to each well. After incubation at RT for 15 min, the reaction was stopped by addition of 25 µl 2.5 M H_2SO_4 to each well, and absorbance was read at 450 nm using a spectrophotometer (BioRad). Purified and concentrated rV1 samples typically ranged between 100-200 U/ml in comparison with CHO V1 CM which ranged between 4-6 U/ml. (Coefficient of variability = 10.1%, R^2 = 0.98).

Furthermore we assessed the levels of serum versican by ELISA, but found that the commercial kit (#CSB-E11884H, Cusabio, China) was unable to detect versican in either CHO V1 CM or purified V1. Serum levels of versican were below the current sensitivity range of our in house ELISA.

4.2.5. Quantitation of HA

Serum was collected from control (ovaries inspected and found to be normal at time of surgery n = 14 and asymptomatic women n = 6), serous benign (n = 14), and serous malignant ovarian tumour (n = 24) patients at the time of surgery, 2 weeks after surgery, or after a chemotherapy cycle (6 patients, 6 cycles, approx 2 weeks between each) at the Department of Gynaecological Oncology, RAH with approval from the RAH Human Ethics Committee. Venous blood samples were collected into vacutainer plain tubes from the patients. The blood was allowed to clot, centrifuged at 3000 rpms for 10 min at RT and serum was stored at -80°C until assayed. An HA ELISA kit (DY3614, R & D Systems) was used to determine the concentration of HA in serum samples and CM from cells treated with carboplatin at their IC_{50} (OVCAR-5 = 80uM , SKOV-3 = 198uM, OVCAR-3 = 145uM) as per the manufacturer's instructions (detection limit 100 pg/ml, coefficient of variability = 9.21%, $R^2 = 0.985$).

4.2.6. Motility and invasion assays

Ovarian cancer cell lines were prepared as described in section 3.2.5 and treated with control (PBS) or rV1 versican (0.1 U/ml – 10 U/ml) with HA (20 µg/ml). Sheath forming OVCAR-5 cells were also prepared in the presence or absence of HA oligos (HYA-OLIGO 6-10, 250 µg/ml, North Star Bioproducts, Associates of Cape Cod, Inc, East Falmouth, USA) for 2 hr at RT on the Nutator in the dark. The assay was subsequently carried out as described in section 3.2.5.

4.2.7. Red blood cell exclusion assay

A 10 µl aliquot of OVCAR-3, OVCAR-5, or SKOV-3 cells taken after treatment described in section 4.2.6 were plated into 48 well plates for an hour in a red blood cell solution (10^7/ml). Pericellular sheath formation was visualised using an inverted microscope with Hoffman interference optics. The proportion of cells with a surrounding zone excluded by red blood cells were counted in 10 random fields. To demonstrate the dependence on HA for the formation of the pericellular sheath, cells were additionally treated with HAase (from *Streptomyces hyalurolyticus,* 10 U/ml, Sigma-Aldrich) for 20 min at RT.

4.2.8. Wound migration assays and time lapse photography

Wound migration assays were performed using OVCAR-5 and SKOV-3 cells (2×10^4 cells/well) cultured in 8 well chamber slides (Nuclon Lab-Tek II Chamber slide, RS Glass Slide) in 500 µl of 5% FBS RPMI for 3-4 days. The resulting confluent cell monolayers were scratch-wounded and washed to remove floating cells then treated with CHO K1 CM or CHO V1 CM (5 U/ml versican) for 18 hr. Cell migration was monitored using an IX 81 microscope (Olympus) equipped with a 37°C incubator and aerated with 5% CO_2 in oxygen. Directional movement and pericellular sheath formation were assessed by time-lapse and particle exclusion assays. Cells migrating into the wounded area were imaged over a 3 hr period in the presence of red blood cells (10^7/ml) using Analysis software (Soft Imaging System, Johann-Krane-Weg Munster, Germany). The

percentage of CD44 positive OVCAR-5 and SKOV-3 cells was assessed as described previously [135].

4.2.9. Adhesion assays

Adhesion assays were set up and performed as described in section 3.2.6. Ovarian cancer cells were mixed at a concentration of 100,000 cells/ml with PBS, HA (20 µg/ml), CHO K1 CM, or CHO V1 CM (5 U/ml) in the presence or absence of HA oligos (10-250 µg/ml) for 2 hr at room temperature on the Nutator. Additional experiments involved exposure of the cancer cells to HAase (10 U/ml) during the 2 hr mixing period, or exposure of the peritoneal monolayer to HAase (10 U/ml) for 8 minutes prior to adhesion of the ovarian cancer cells.

4.2.10. Statistical analysis

All analyses were performed as described in section 3.2.8. Statistical significance was accepted at $p < 0.05$.

4.3. RESULTS

4.3.1. Expression of HA, CD44, and versican in ovarian tissue

Tissue microarrays of borderline and malignant ovarian tumours from stage I to IV as well as primary ovarian tumours and matching metastases and tissue from normal ovaries and benign ovarian tumours were immunostained with antibodies against versican, CD44, and HA. We observed that versican, HA, and CD44 were present in the stroma of ovarian carcinoma, predominantly adjacent to epithelial cells, and CD44 was additionally present in the epithelial cells. The immunostaining levels of versican, HA, and CD44 in normal, benign, borderline, and malignant ovarian tissue is summarised in Table 4.1.

We observed a significantly higher proportion of ovarian cancers with high stromal versican (56.8%) compared with normal ovaries (0%) and benign tumours (37.5%, $p < 0.0001$ Table 4.1, Figure 4.2). There was also a significantly higher proportion of ovarian cancers with high stromal CD44 (54.5%, Figure 4.2) compared with normal ovaries (10%,), benign (11.2%,), or borderline ovarian tumours (0%, $p = 0.001$ Table 4.1, Figure 4.2). However, there was no significant difference in the levels of CD44 immuno-positive epithelial cells. There was also no association between stromal HA, stromal versican, stromal CD44, or epithelial CD44 and tumour stage (Table 4.2). We observed a significant positive correlation between high stromal versican and high stromal HA between the tissue cores (Pearson's correlation test, $R = 0.422$ $p < 0.002$). However, we didn't observe any significant difference in the HA levels between the different ovarian tissues examined ($p = 0.364$). There was a significant positive

correlation between high stromal and high epithelial CD44 staining between the different stages and primary tumours and matching metastases ($R = 0.483$ $p < 0.0001$, Table 4.3).

Table 4.1. *Intensity of CD44, HA, and versican staining in ovarian tumours.*

Levels of versican, HA, and CD44 in ovarian tissues were assessed using a manual scoring method (0, 1+, 2+, 3+). The immunostaining intensity was classified as low = 0/1+ (a) or high = 2+/3+ (b)

	Median age (Range)	Versican		HA		CD44		CD44	
		Stroma Intensity		Stroma Intensity		Stroma Intensity		Epithelial Intensity	
		Low[a]	High[b]	Low[a]	High[b]	Low[a]	High[b]	Low[a]	High[b]
Normal	57 (48-83)	11/11 (100%)	0/11 0%	7/10 (70%)	3/10 (30%)	9/10 (90%)	1/10 (10%)	7/9 (77.8%)	2/9 (22.2%)
Benign	54 (35-62)	5/8 (62.5%)	3/8 (37.5%)	5/9 (55.6%)	4/9 (44.4%)	8/9 (88.9%)	1/9 (11.1%)	7/9 (77.8%)	2/9 (22.2%)
Borderline	50 (32-82	1/10 (10%)	9/10 (90%)	2/7 (28.6%)	5/7 (71.4%)	8/8 (100%)	0/8 (0%)	6/8 (75%)	2/8 (25%)
Cancer	69 (48-87)	19/44 (43.2%)	25/44 (56.8%)	21/46 (45.7%)	25/46 (54.3%)	20/44 (45.5%)	24/44 (54.5%)	31/44 (70.5%)	13/44 (29.5%)
Chi-Squared Test		**p < 0.0001**		p = 0.364		**p = 0.001**		p = 0.959	

Table 4.2. *Intensity of CD44, HA, and versican staining in ovarian tumours by stage.*

Levels of versican, HA, and CD44 in ovarian tissues were assessed using a manual scoring method (0, 1+, 2+, 3+). The immunostaining intensity was classified as low = 0/1+ (a) or high = 2+/3+ (b)

	Median age (Range)	Versican		HA		CD44		CD44	
		Stroma Intensity		Stroma Intensity		Stroma Intensity		Epithelial Intensity	
		Low[a]	High[b]	Low[a]	High[b]	Low[a]	High[b]	Low[a]	High[b]
Stage I	59 (44-80)	3/11 (27.3%)	8/11 (82.7%)	7/11 (63.6%)	4/11 (35.4%)	4/11 (36.4%)	7/11 (63.6%)	7/11 (63.6%)	4/11 (36.4%)
Stage II	62 (45-83)	5/11 (45.5%)	6/11 (44.5%)	4/12 (33.3%)	8/12 (66.6%)	3/10 (30%)	7/10 (70%)	8/10 (80%)	2/10 (20%)
Stage III	66 (40-86)	7/12 (58.3%)	5/12 (41.7%)	3/12 (25%)	9/12 (75%)	6/13 (46.1%)	7/13 (43.9%)	8/13 (61.5%)	5/13 (38.5%)
Stage IV	64 (27-78)	4/10 (40%)	6/10 (60%)	7/11 (63.6%)	4/11 (35.4%)	7/10 (70%)	3/10 (30%)	8/10 (80%)	2/10 (20%)
Chi-squared Test		p = 0.508		p =0.153		p =0.372		p =0.592	

Table 4.3. *Intensity of CD44, HA, and versican staining in ovarian primary tumours and matching metastases.*

Levels of versican, HA, and CD44 in ovarian tissues were assessed using a manual scoring method (0, 1+, 2+, 3+). The immunostaining intensity was classified as low = 0/1+ (a) or high = 2+/3+ (b)

	Median age (Range)	Versican		HA		CD44		CD44		CD44
		Stroma Intensity		Stroma Intensity		Stroma Intensity		Epithelial Intensity		High Stromal and High Epithelial Intensity
		Low[a]	High[b]	Low[a]	High[b]	Low[a]	High[b]	High[b]	Low[a]	
Primary tumour	68 (49-87)	9/26 (34.6%)	17/26 (85.4%)	1/27 (37%)	26/27 (63%)	19/24 (79.1%)	5/24 (28.9%)	19/24 (79.15)	5/24 (28.9%)	3/24 (12.5%)
Omental metastasis		8/27 (29.6%)	19/27 (79.4%)	2/26 (7.7%)	24/26 (92.3%)	15/26 (57.7%)	11/26 (42.3%)	22/26 (84.6%)	4/26 (15.4%)	2/26 (7.7%)
Chi Squared Test		p =1.0		p =0.351		p =0.128		p =1.00		p = 0.42

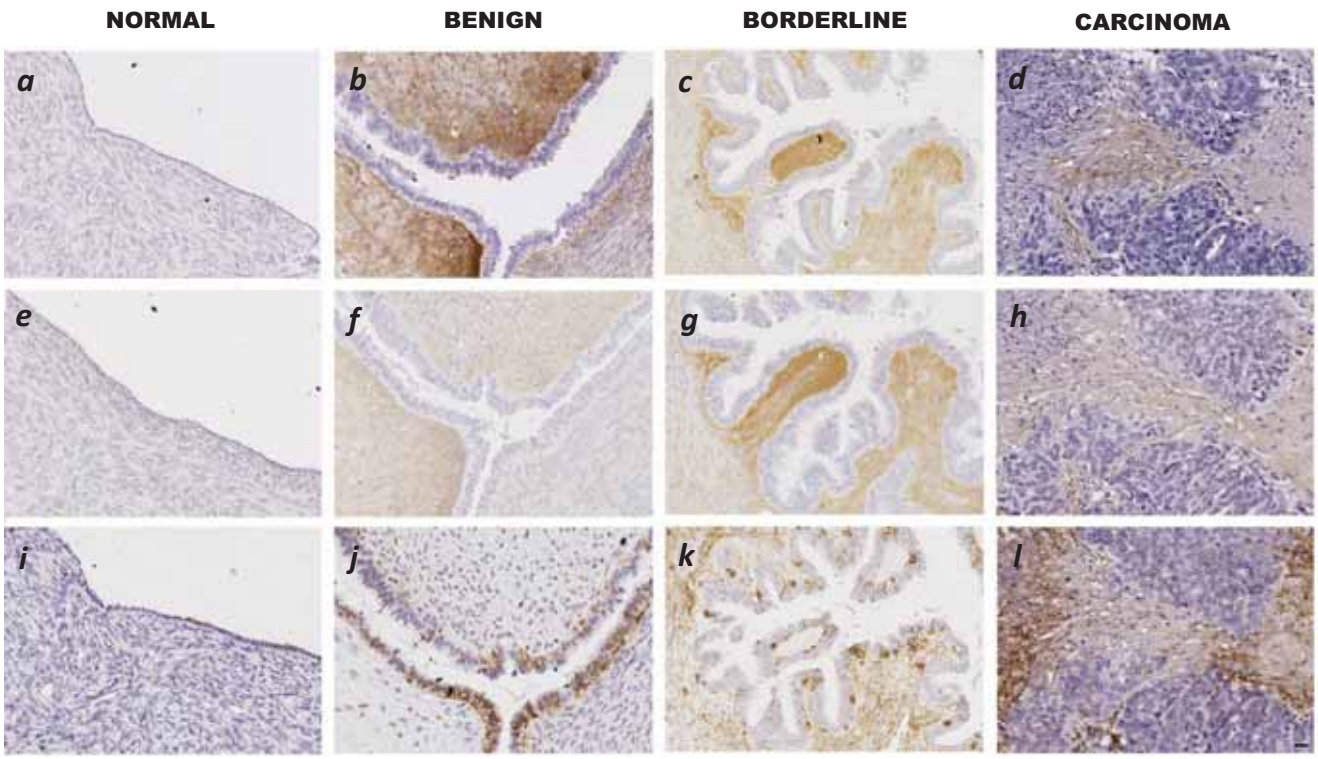
NORMAL
BENIGN
BORDERLINE
CARCINOMA
a
b
c
d
e
f
g
h
i
j
k
l

Figure 4.2. *Immunostaining of normal, serous benign, serous borderline, and serous malignant ovarian tissue.*

(*a*) Weak (1+) versican staining in the stroma adjacent to normal surface epithelial cells (*b*) Strong (3+) versican staining in the stroma adjacent to benign ovarian epithelial cells (*c*) Strong (3+) versican staining in the stroma adjacent to ovarian epithelial cells *(d*) Moderate (2+) versican staining in the stroma adjacent to malignant ovarian epithelial cells (*e*) Weak (1+) HA staining in the stroma adjacent to normal surface epithelial cells (*f*) Moderate (2+) HA staining in the stroma adjacent to benign ovarian epithelial cells (*g*) Strong (3+) HA staining in the stroma adjacent to ovarian epithelial cells (*h*) Moderate (2+) HA staining in the stroma adjacent to malignant ovarian epithelial cells (i) Weak (0) CD44 staining in the stroma adjacent to normal surface epithelial cells and weak (1+) CD44 staining in the normal surface epithelial cells (j) Weak (1+) CD44 staining in the stroma adjacent to benign ovarian epithelial cells and strong (3+) CD44 staining in the benign epithelial cells (k) Moderate (2+) CD44 staining in the stroma adjacent to ovarian epithelial cells and weak (1+) CD44 staining in the epithelial cells (l) Strong (3+) CD44 staining in the stroma adjacent to malignant ovarian epithelial cells and weak (1+) CD44 staining in the malignant epithelial cells. Magnification bar = 20 µm. All images are at the same magnification.

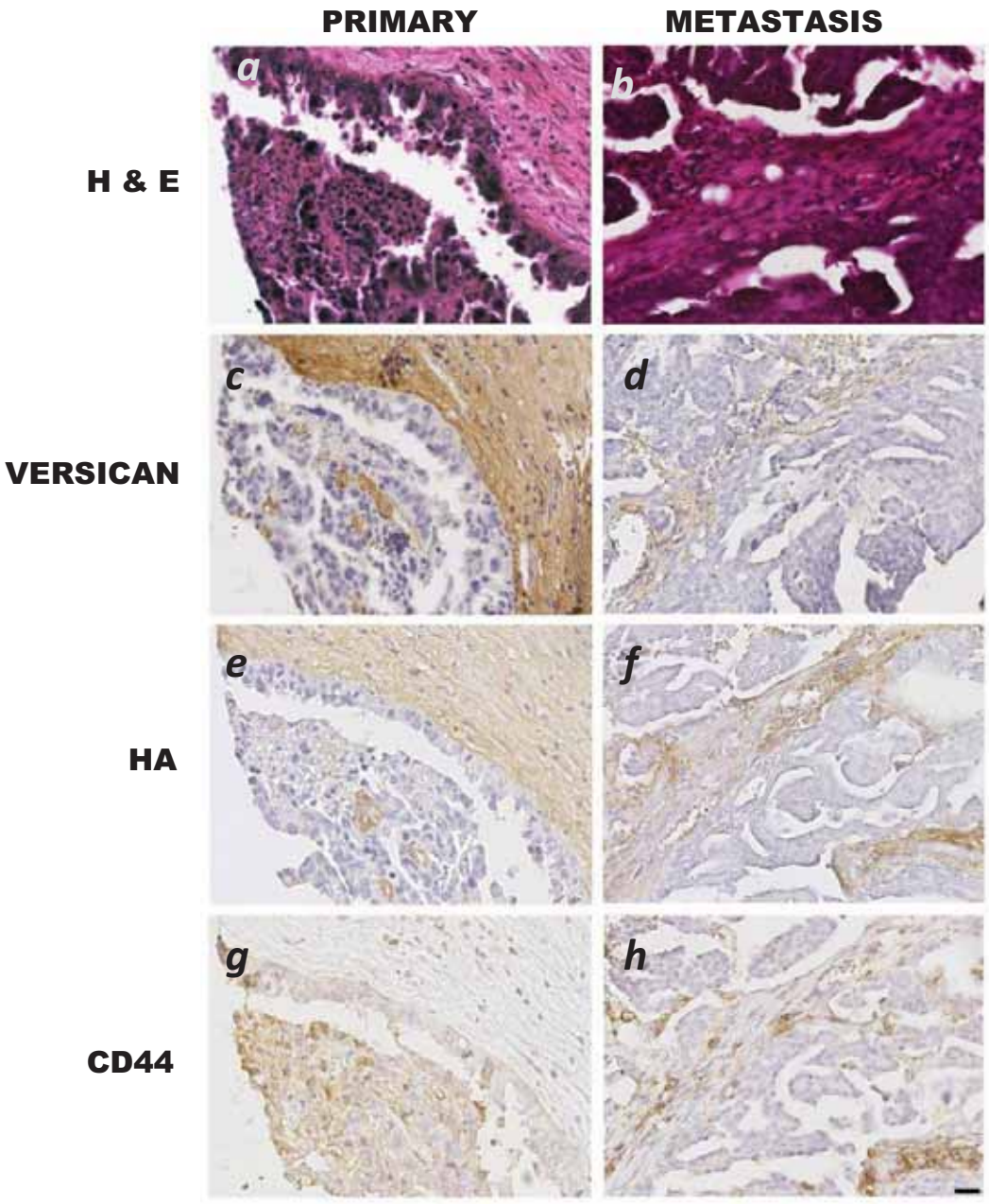

Figure 4.3. Immunostaining of primary ovarian tumour and matching metastases.

(*a*) H&E staining of a primary ovarian tumour (*b)* H&E staining of a matching metastasis (*c*) Strong (3+) versican staining in the stroma of a primary ovarian tumour (*d*) Weak (1+) versican staining in the stroma of a matching metastasis *(e)* Moderate (2+) HA staining in the stroma of a primary ovarian tumour (*f*) Moderate (2+) HA staining in the stroma of a matching metastasis *(g)* Weak (0) CD44 staining in the stroma and strong (3+) CD44 staining in the epithelial cells of a primary ovarian tumour (*h*) Moderate (2+) CD44 staining in the stroma and weak (1+) CD44 staining in the epithelial cells of a matching metastasis. Magnification bar = 20 µm. All images are at the same magnification.

4.3.2. Serum HA levels in patients undergoing chemotherapy

We investigated the levels of HA in the serum of patients with benign serous ovarian disease and serous malignant ovarian disease when compared with controls. We observed no significant difference in the median serum level of HA between normal control (6.94 ng/ml), benign (19.11 ng/ml), and serous ovarian cancer (21.94 ng/ml, Table 4.4, Figure 4.4a). However, when we tracked HA serum levels in 6 patients during the course of their chemotherapy regime, we observed 4 out of 4 patients with data collected after their first cycle of chemotherapy showed an average 224% increase in HA serum levels compared with their pre surgical levels (Figure 4.4b, c). Interestingly, all 6 patients showed an increase in HA serum levels from pre-surgical levels after at least one of the chemotherapy cycles (112.4-2669.3%, Figure 4.4c). In addition, when OVCAR-5, OVCAR-3, and SKOV-3 cells were treated with carboplatin for 72 hr, it was found that they produced increased levels of HA (1.4 - 5.2 fold) when compared with non treated cells.

Table 4.4. *Characteristics of patients and serum HA levels.*

	Number	Median age (Range)	Median HA (ng/ml) (range)
Controls		45 (36 - 76)	6.94 (1.42 - 58.91)
Surgical	14		
Asymptomatic	6		
Benign	14	56 (41 - 77)	19.11 (11.42 -111.63)
Malignant		62.5 (42 - 84)	21.94 (0.26 – 82.36)
Stage			
I	5		
II	1		
III	16		
IV	1		

a

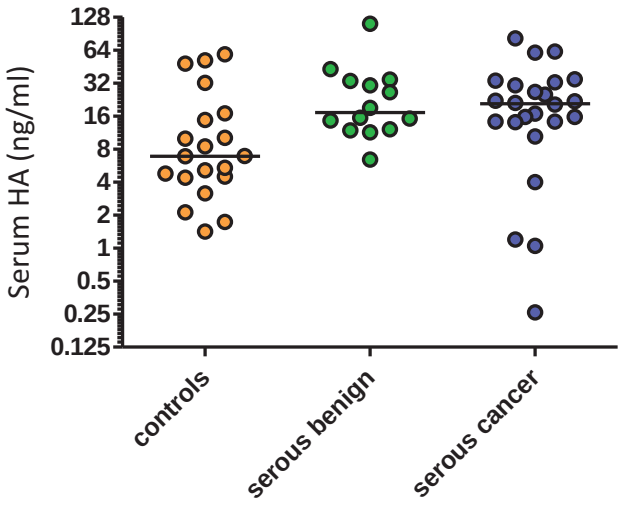
Serum HA (ng/ml)
128
64
32
16
8
4
2
1
0.5
0.25
0.125
controls
serous benign
serous cancer

b

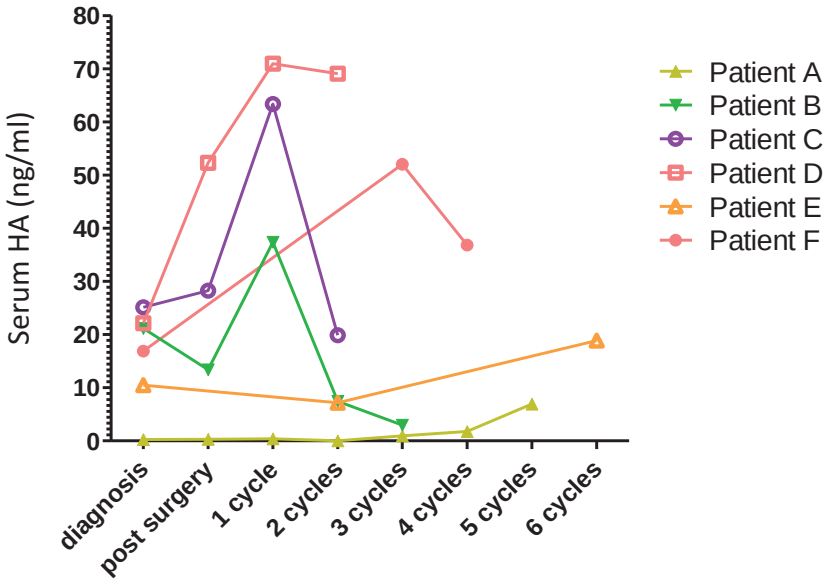
Serum HA (ng/ml)
80
70
60
50
40
30
20
10
0
diagnosis
post surgery
1 cycle
2 cycles
3 cycles
4 cycles
5 cycles
6 cycles
Patient A
Patient B
Patient C
Patient D
Patient E
Patient F

c

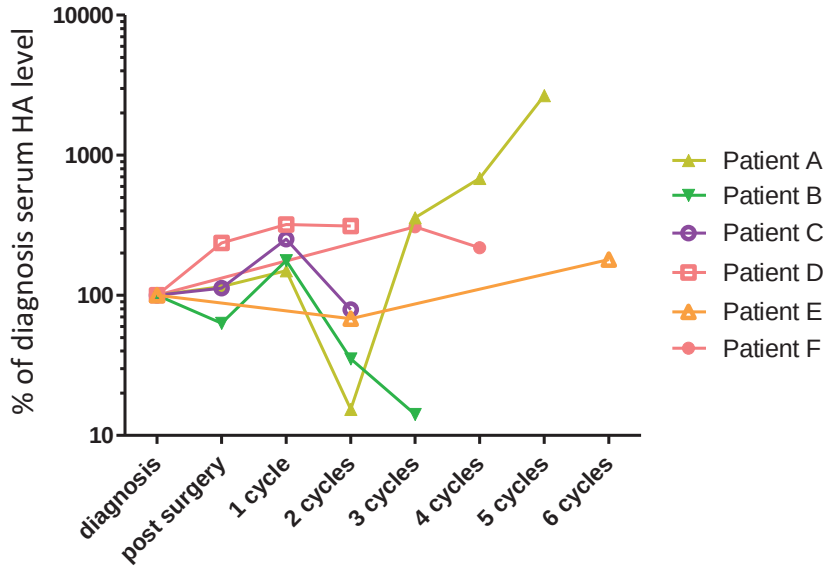
% of diagnosis serum HA level
10000
1000
100
10
diagnosis
post surgery
1 cycle
2 cycles
3 cycles
4 cycles
5 cycles
6 cycles
Patient A
Patient B
Patient C
Patient D
Patient E
Patient F

Figure 4.4. *Serum HA levels decrease in response to chemotherapy treatment.*

(a) Serum HA levels were established using an ELISA kit (R&D Systems) for patients undergoing surgery with normal ovaries, benign ovarian conditions, serous ovarian cancer, or patients who had undergone 3 or more chemotherapy cycles *(b)* Serum HA levels were established for serous ovarian cancer patients undergoing multiple chemotherapy cycle regimes. (*c*) Serum HA levels shown as a percentage of serum HA levels at time of diagnosis

4.3.4. Versican induces pericellular matrix formation by ovarian cancer cells

Treatment with either conditioned medium containing versican (Figure 4.5a, b) or purified recombinant versican (Figure 4.6a) in the presence of exogenous HA resulted in increased pericellular sheath formation by OVCAR-5 and SKOV-3 cells, but not OVCAR-3 cells. Negligible pericellular sheath formation was detected around ovarian cancer cells (OVCAR-3, OVCAR-5, and SKOV-3) following treatment with control CHO K1 CM lacking versican, in the presence of HA (Figure 4.5a, b). Treatment with increasing concentrations of purified rV1 versican in the presence of exogenous HA resulted in pericellular sheath formation by OVCAR-5 in a dose-dependent manner (Figure 4.6a). Maximal pericellular sheath formation was observed (18% of OVCAR-5 cells) following treatment with 5 U/ml rV1 versican. Likewise, treatment with 5 U/ml rV1 versican resulted in maximal pericellular sheath formation in 17% of SKOV-3 ovarian cancer cells (Figure 4.6a). We demonstrated that pericellular sheath formation was dependent on the presence of HA, as treatment with HAase (10 U/ml) almost completely destroyed the pericellular sheath around OVCAR-5 and SKOV-3 cells (Figure 4.5b, c). The capacity of ovarian cancer cells to form a pericellular sheath correlated with the level of the HA receptor, CD44. CD44 was detected in the membrane of 1.3 % of OVCAR-3, 27 % of OVCAR-5, and 13.4 % of SKOV-3 cells respectively. All LP-9 cells were immuno-positive for CD44 (Figure 4.6b).

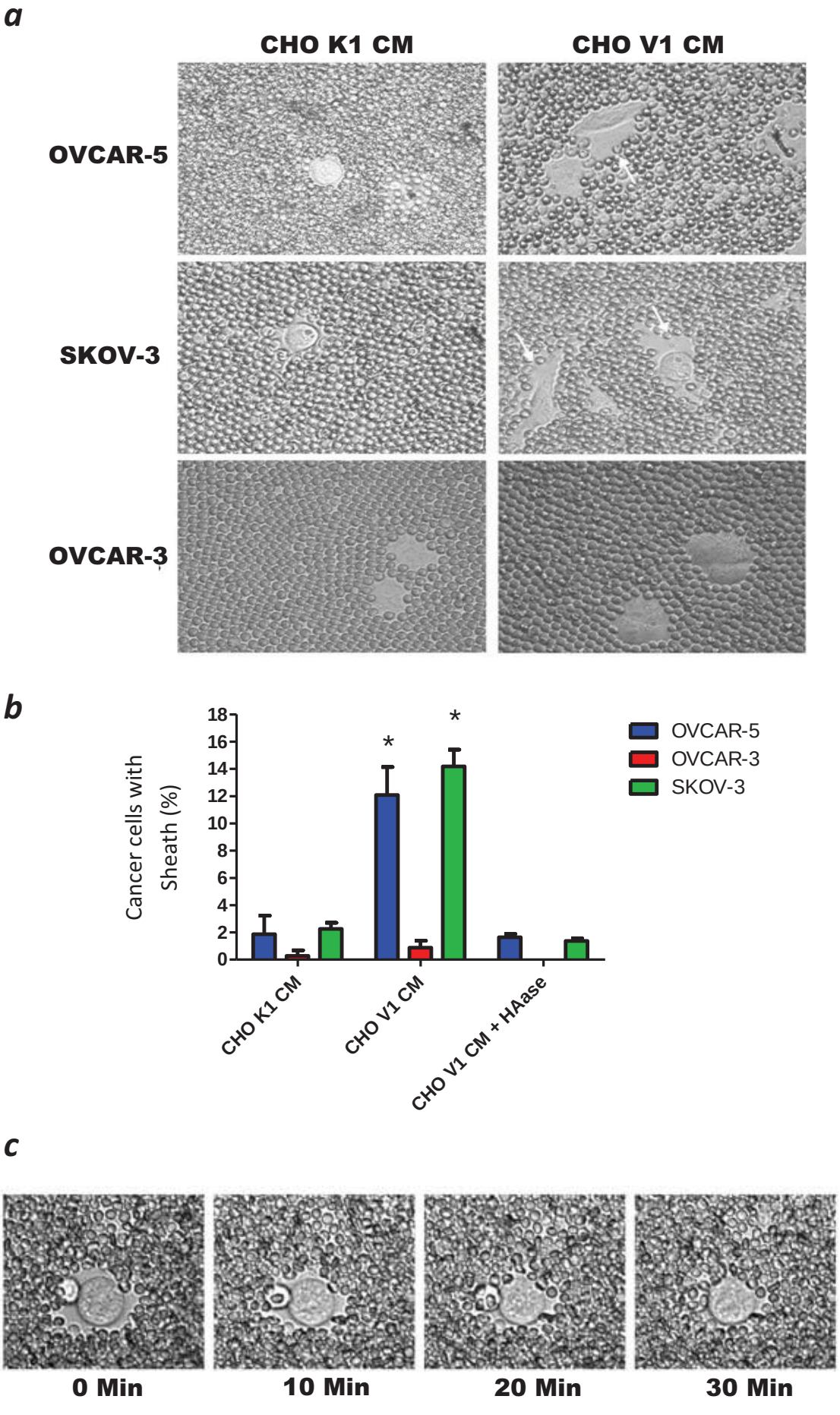
a
CHO K1 CM
CHO V1 CM
OVCAR-5
SKOV-3
OVCAR-3
b
Cancer cells with Sheath (%)
18
16
14
12
10
8
6
4
2
0
*
*
OVCAR-5
OVCAR-3
SKOV-3
CHO K1 CM
CHO V1 CM
CHO V1 CM + HAase
c
0 Min
10 Min
20 Min
30 Min

Figure 4.5. *Versican promotes the formation of a pericellular matrix by ovarian cancer cells.*

(a) Pericellular sheath formation by ovarian cancer cells following 24 hr treatment with versican was assessed using a red blood cell exclusion assay. Ovarian cancer cells (3 x 10^3) were plated in 48-well tissue culture plates and treated with versican containing CHO V1 conditioned medium (~5 U/ml) or CHO K1 from parental cells expressing no versican. Red blood cell diameter = 7 µm. The white arrows illustrate OVCAR-5 cells and SKOV-3 cells with a prominent polar pericellular sheath. *(b)* Pericellular sheath formation by ovarian cancer cells following treatment with CHO V1 and CHO K1 CM is dependent on HA. Structural necessity for HA within the pericellular sheath was confirmed by treatment with hyaluronidase (30 min at room temperature, 10 U/ml). Data represents percentage (mean $\pm$ SD) of cells (n $\approx$ 100) with pericellular sheath from at least 6 determinations in 3 separate experiments. * denotes significant difference from control $p < 0.05$ one-way ANOVA. *(c)* Visualisation of the destruction of versican-HA pericellular sheath in OVCAR-5 cells by exposure to hyaluronidase (10 U/ml) over 30 min.

a

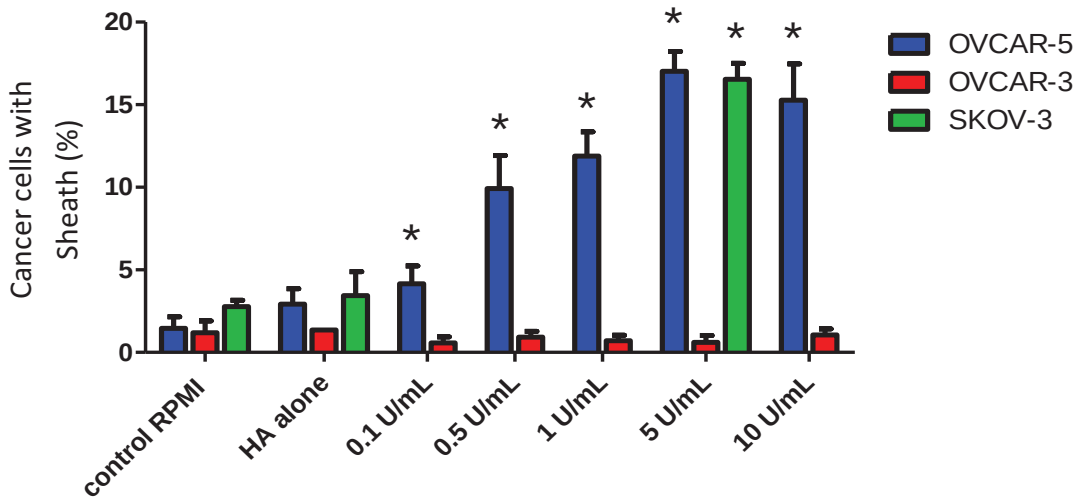
Cancer cells with Sheath (%)
20
15
10
5
0
control RPMI
HA alone
0.1 U/mL
0.5 U/mL
1 U/mL
5 U/mL
10 U/mL
OVCAR-5
OVCAR-3
SKOV-3

b

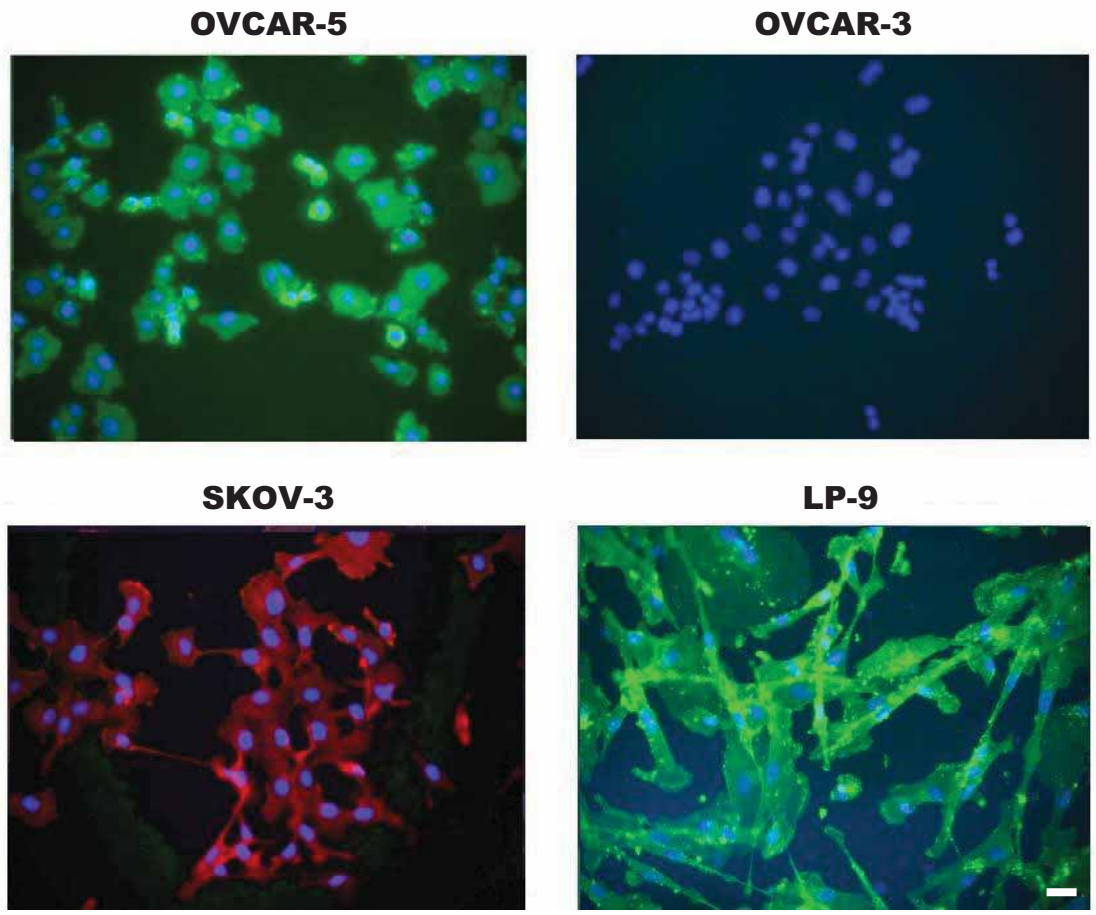
OVCAR-5
OVCAR-3
SKOV-3
LP-9

Figure 4.6. *Pericellular sheath formation by ovarian cancer cells is associated with CD44 expression.*

(a) Effect of purified rV1 versican on pericellular sheath formation by ovarian cancer cells. Ovarian cancer cells (5 x 10^5 cells/ml) were treated with purified versican (OVCAR-5 and OVCAR-3 - 0.1-10.0 U/ml, SKOV-3 5 U/ml) + HA (20 µg/ml) or PBS + HA (20 µg/ml) in 0.1% BSA RPMI on a rotating platform for 2 hr at RT and plated in 48-well plates (3 x 10^3 cells) for 2 hr prior to assessing pericellular sheath formation using red blood cell exclusion. Data represents percentage (mean $\pm$ SD) of cells (n ≈ 100) with pericellular sheath from at least 6 determinations in 3 separate experiments. *denotes significant difference from control $p < 0.01$, one-way ANOVA. *(b)* Ovarian cancer cells (OVCAR-3, OVCAR-5, and SKOV-3) and peritoneal LP-9 cells were plated at a low density in 8-well chamber slides. Cells were fixed with paraformaldehyde and incubated with CD44 monoclonal antibody. CD44 immunostaining was detected by immunofluoresence (green for OVCAR-5, OVCAR-3 and Lp-9 cells, red for SKOV-3 cells) and nuclei are counterstained with Hoescht dye. Magnification bar = 20µm. All images are at the same magnification.

4.3.5. Versican promotes ovarian cancer cell motility and invasion

We investigated the effects of rV1 versican on ovarian cancer motility and invasion using modified 96-well chemotaxis plates. rV1 versican treatment for 6 hr significantly increased the motility of ovarian cancer OVCAR-5 and SKOV-3 ovarian cancer cell lines but not of OVCAR-3 cells (Figure 4.7a, $p < 0.0001$). A maximal effect on OVCAR-5 and SKOV-3 cell motility (125% of PBS control) were observed following treatment with 1 U/ml rV1 versican. rV1 versican also significantly increased invasion of OVCAR-5 and SKOV-3 cells through Geltrex by up to 20% (Figure 4.7b, $p < 0.0001$). Maximal effects on OVCAR-5 and SKOV-3 cell invasion were observed with 5 U/ml rV1 versican. rV1 versican treatment did not, however, affect OVCAR-3 cell motility (Figure 4.7a) or invasion (Figure 4.7b).

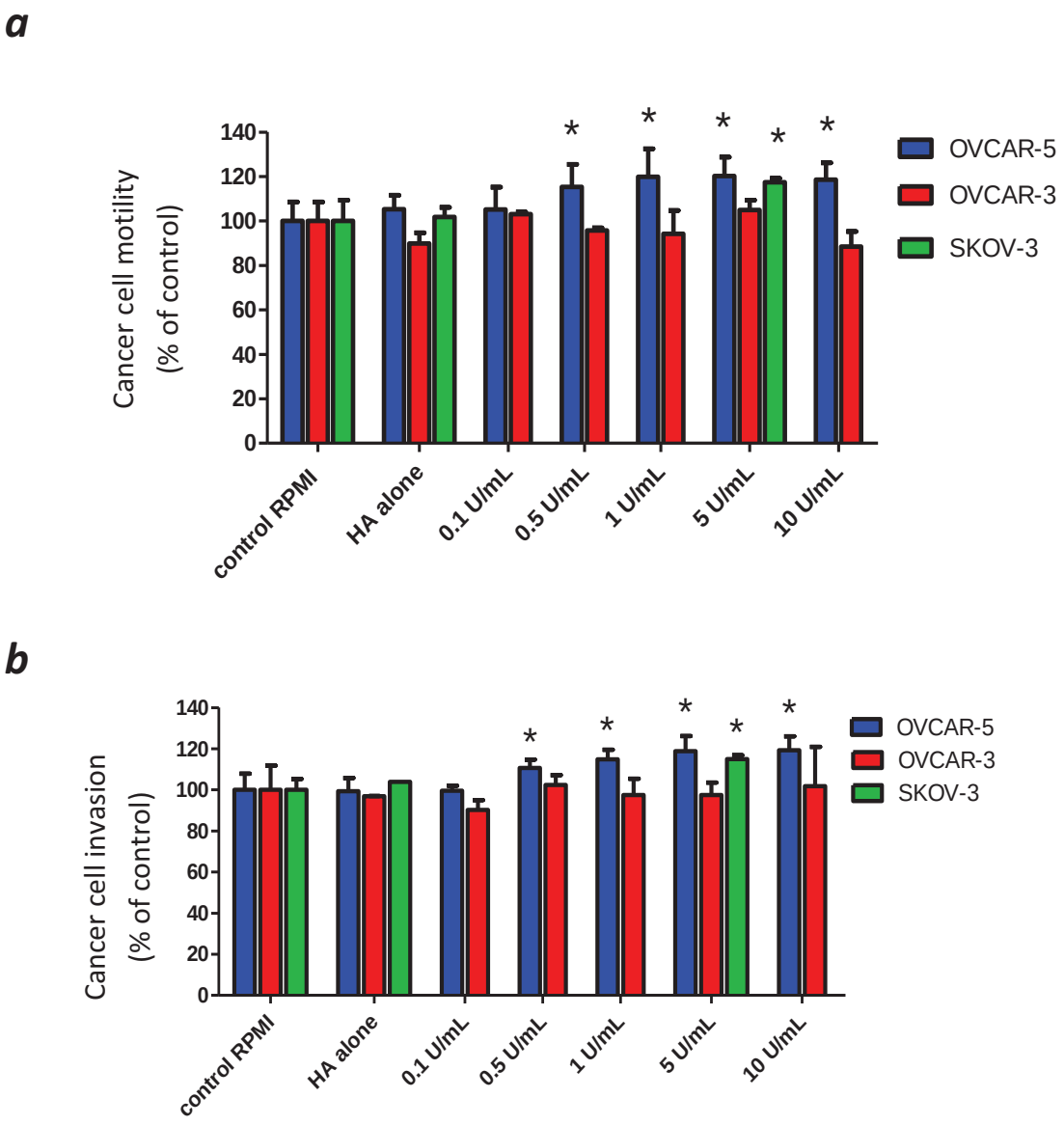

Figure 4.7. *Versican promotes ovarian cancer motility and invasion.*

Ovarian cancer cells (OVCAR-5, OVCAR-3 and SKOV-3) were treated as in Figure 4.10b. A calcein labelled cell suspension (50,000 cells/well in 50 µl) was added to the top of uncoated 12 µm filters inserts for motility assays *(a)* or to 12 µm filters coated with Geltrex for invasion assays *(b)* Cells were allowed to migrate for 6 hr at 37°C in an environment of 5% CO_2 using 10% FBS RPMI as a chemoattractant in the lower chamber. The fluorescence of migratory cells was measured at 485-520 nm. Data is expressed as mean percentage of control ± SD of 6 determinations from 3 separate experiments. * denotes significant difference from control, $p < 0.05$, one-way ANOVA.

4.3.6. Pericellular sheath formation in migrating ovarian cancer cells

A wound migration assay was used to examine effects on directional ovarian cancer cell motility following versican treatment. Treatment with CHO V1 CM (5 U/ml versican) significantly increased the number of SKOV-3 (Figure 4.8a) and OVCAR-5 (Figure 4.8b) cells entering the wounded area after 24 hr by 2-fold when compared with treatment with CHO K1 CM containing no versican. Time lapse photography combined with a particle exclusion assay enabled us to simultaneously observe directional cell movement and pericellular sheath formation. A polar pericellular sheath was consistently observed by motile SKOV-3 cells migrating into the scratch wound over a 2 hr treatment period (red arrow, Figure 4.9a and supplementary video). No pericellular sheath was observed in non-motile cells (Figure 4.9a, supplementary video). Interestingly, immunohistochemical localization of CD44 and HA demonstrated polar expression of both CD44 and HA in OVCAR-5 cell following treatment with versican containing media (Figure 4.9b). Polarized CD44/HA was not observed in non-motile cells (data not shown).

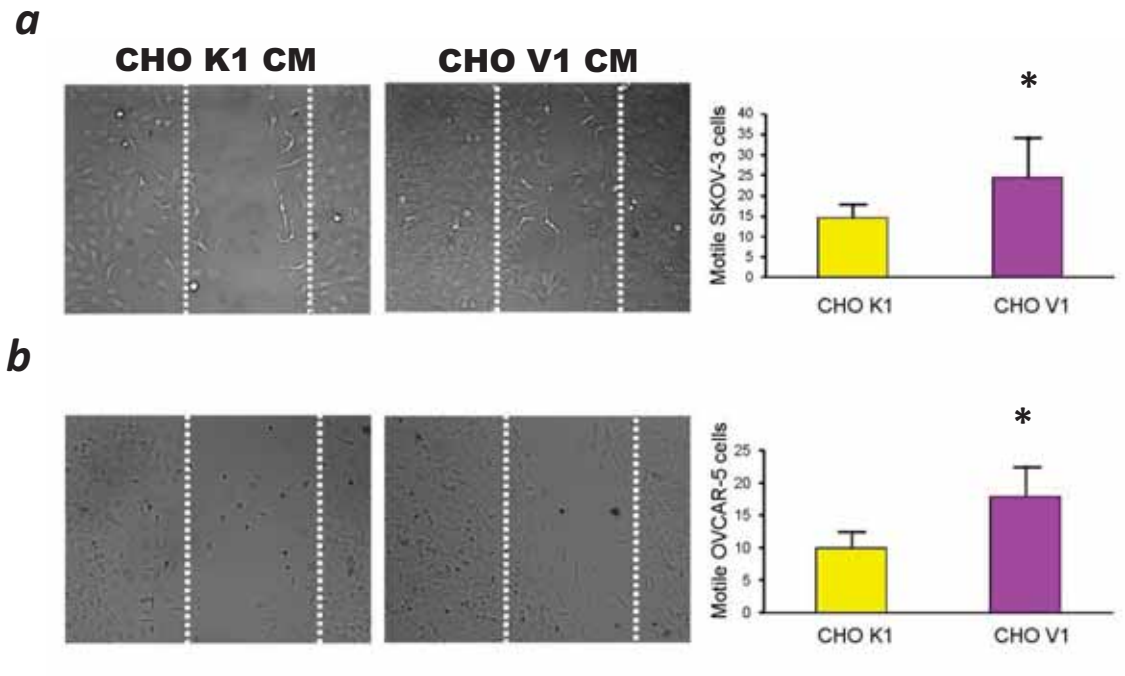

Figure 4.8. *Versican promotes ovarian cancer cell motility in a wound migration assay.*

Confluent monolayers of SKOV-3 cells *(a)* and OVCAR-5 *(b)* were wounded and treated with CHO K1 CM or CHO V1 CM for 24 hr. Data represent number of cells that migrated into the wounded area (mean $\pm$ SD, 8 determinations from 2 experiments). * denotes significant difference from CHO K1, $p < 0.05$, student t-test.

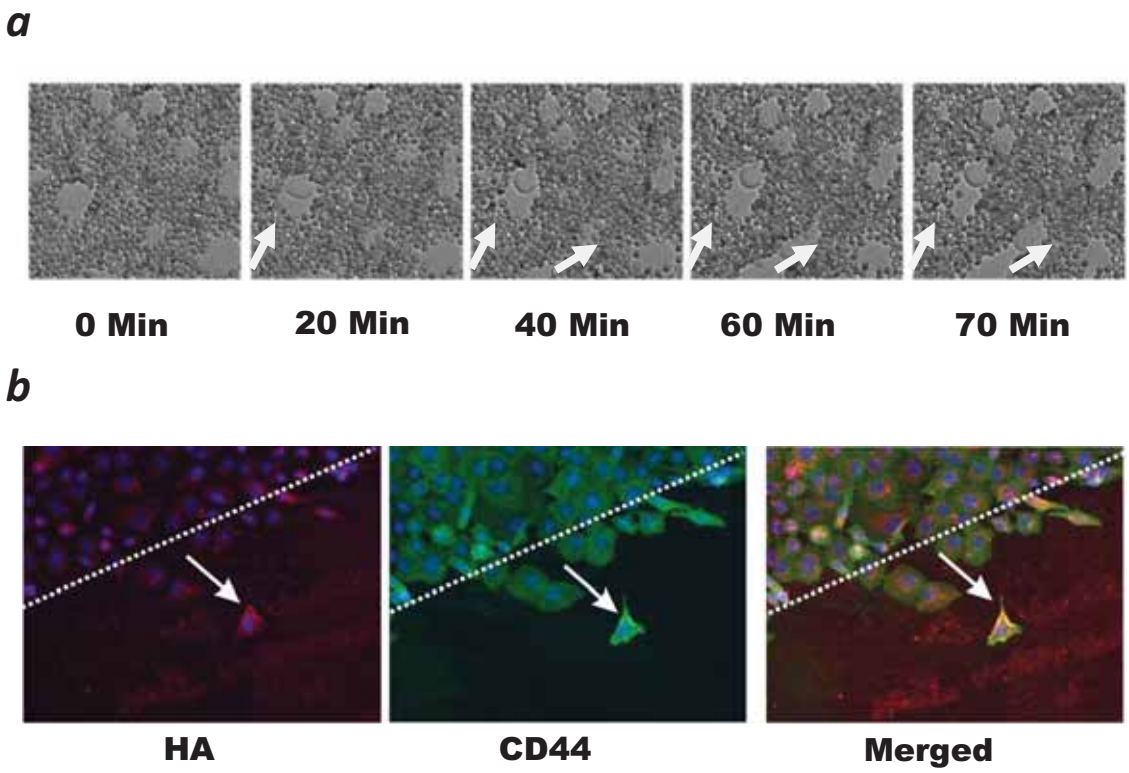

Figure 4.9. *Versican promotes formation of a polarized pericellular sheath by OVCAR-5 and SKOV-3 cells.*

(a) The confluent SKOV-3 monolayer was wounded and treated with CHO V1 CM (5 U/ml) for 8 hr. The white arrows indicate motile SKOV-3 cell with a polar pericellular sheath observed over a 2 hr time period. The red arrows indicate the direction of cell movement. Red blood cells diameter = 7 µm. *(b)* CD44 expression and HA staining in migratory OVCAR-5 cells following 24 hr treatment with CHO V1 CM. White arrows indicate polar CD44 expression and polar HA staining.

4.3.7. HA-oligos can block pericellular sheath formation and versican induced motility and invasion

It was investigated whether small HA oligos (6-10) previously shown to block pericellular matrix formation around chondrocytes [294, 623] could block pericellular sheath formation by OVCAR-5 cells and versican induced increase in motility and invasion. Treatment with HA oligos (250 µg/ml) significantly inhibited HA-versican pericellular sheath formation by OVCAR-5 cells (Figure 4.10a, $p < 0.0001$) and significantly reversed OVCAR-5 versican induced motility (Figure 4.10b, $p = 0.007$) and invasion (Figure 4.10c, $p = 0.013$). These effects on motility and invasion were not due to decreased cancer cell viability following HA oligo treatment as even the the highest HA oligo concentration, 250 µg/ml had no affect on OVCAR-5 cell viability using a trypan blue exclusion assay (data not shown).

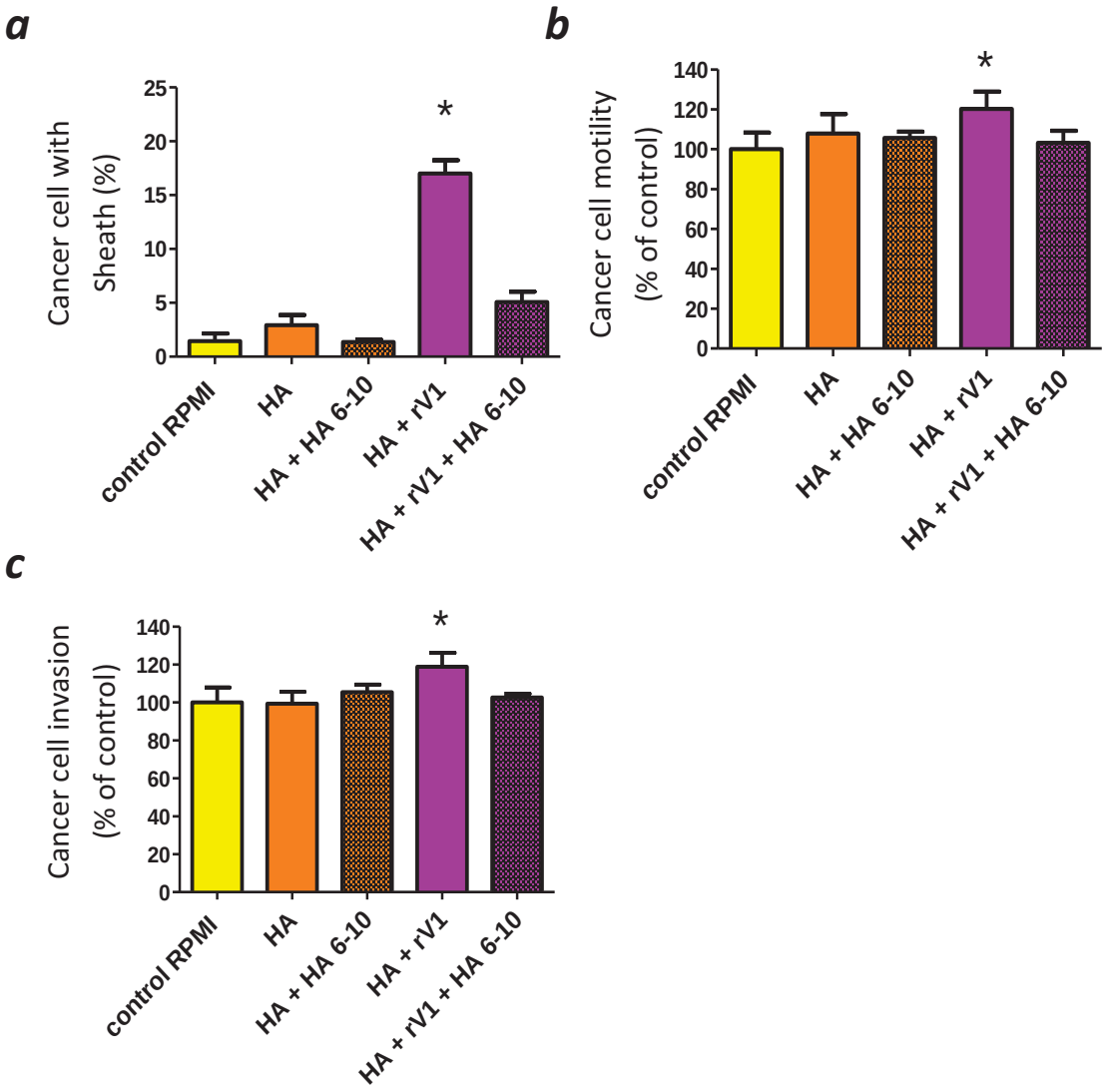

Figure 4.10. *HA oligosaccharides block ovarian cancer metastatic behaviour.*

OVCAR-5 cells were treated in the presence or absence of HA oligos (250 µg/ml) *(a)* Pericellular sheath formation was assessed as described in Figure 4.6. Data represents percentage (mean ± SD) of cells (n ≈ 100) with pericellular sheath from at least 6 determinations in 3 separate experiments. * denotes significant difference from control, $p < 0.05$, one-way ANOVA. Motility *(b)* and invasion *(c)* of OVCAR-5 were performed as described for Figure 4.7. The fluorescence of migratory/invasive cells was measured at 485-520 nm. Data is expressed as percentage of control ± SD of 6 determinations from 3 separate experiments. * denotes significant difference from control, $p < 0.05$, one-way ANOVA.

4.3.8. The role of versican and HA in ovarian cancer cell adhesion to peritoneal cells

We observed that metastatic ovarian cancer OVCAR-5 and SKOV-3 cells bound increasingly to LP-9 peritoneal cells over a 20 min time course. Maximal adhesion was observed after 10 minutes of adhesion to LP-9 cells (Figure 4.11a). Non-metastatic OVCAR-3 cells were observed to have minimal ability to adhere to peritoneal cells. Adding CHO V1 CM in the presence of HA to the cancer cell suspension didn't increase their adhesion to peritoneal cells when compared with either CHO K1 parent cell line CM or HA alone (Figure 4.11b). However, the addition of HA to the ovarian cancer cell suspension increased the number of ovarian cancer cells binding to peritoneal cells. Adding HAase to the HA treated cell suspension successfully blocked the effects of exogenous HA on adhesion, but also reduced the number of adhered cells below that of the PBS control. Additionally, treating the PBS control cancer cell suspension with HAase, decreased OVCAR-5 and SKOV-3 adhesion to LP-9 peritoneal cells by 28% and 25% respectively (Figure 4.11c). To determine whether this effect was observed due to the HAase digestion of HA produced by peritoneal cells during exposure of the monolayer to the HAase containing cell suspension, we treated the monolayer with HAase for 8 min prior to adhesion of PBS control treated cancer cells. We observed a 30% and 31% decrease in adhesion of OVCAR-5 and SKOV-3 cells to the monolayer respectively (Figure 4.11c). Furthermore, treatment with HA oligos successfully blocked the effects of exogenous HA on OVCAR-5 cell adhesion to peritoneal cells, and also at least partially blocked the adhesive properties of endogenous HA produced by either the OVCAR-5 or LP-9 cells (Figure 4.12).

a

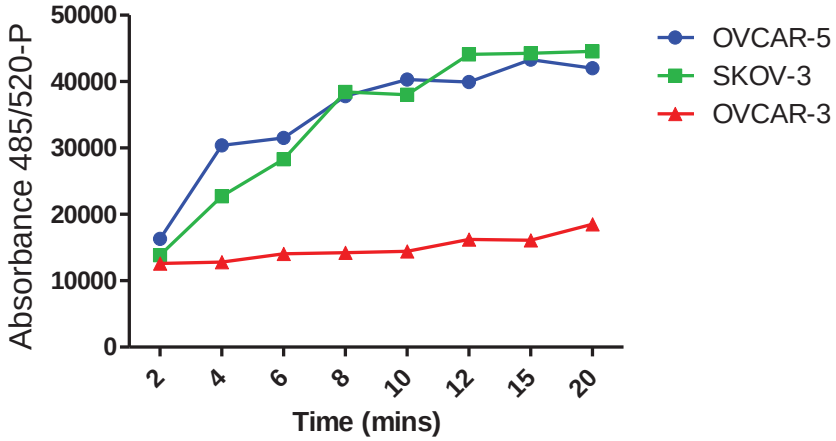
Absorbance 485/520-P
50000
40000
30000
20000
10000
0
2
4
6
8
10
12
15
20
Time (mins)
OVCAR-5
SKOV-3
OVCAR-3

b

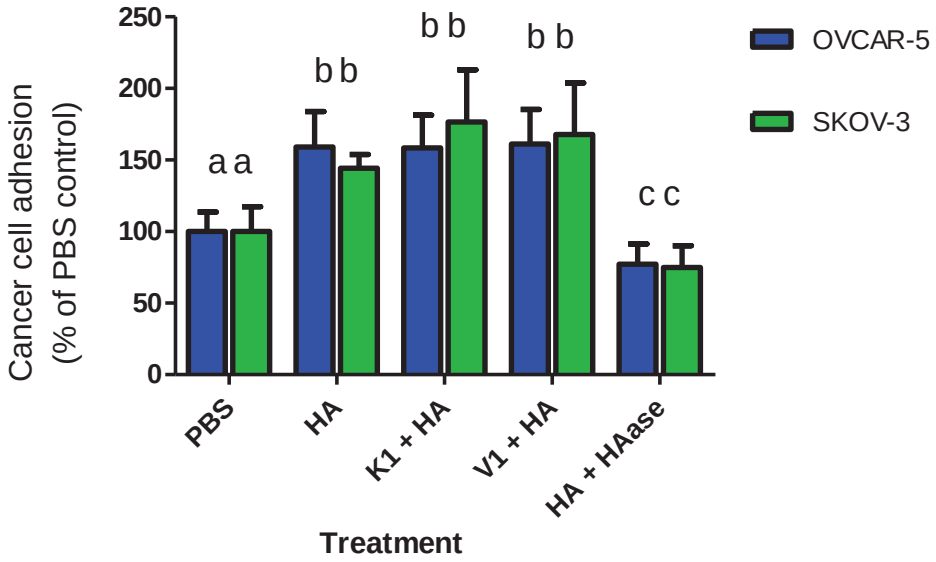
Cancer cell adhesion
(% of PBS control)
250
200
150
100
50
0
a a
b b
b b
b b
c c
PBS
HA
K1 + HA
V1 + HA
HA + HAase
Treatment
OVCAR-5
SKOV-3

c

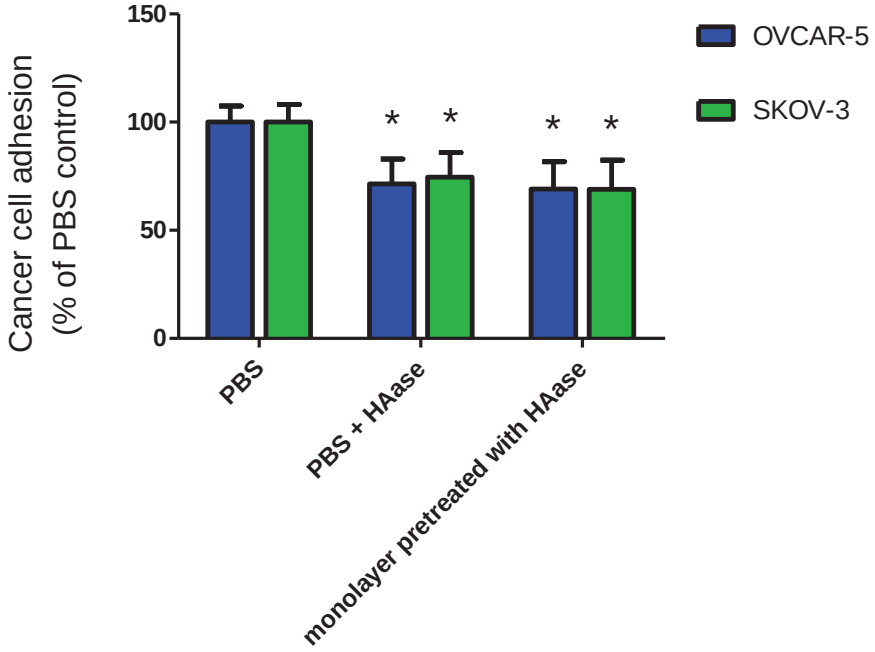
Cancer cell adhesion
(% of PBS control)
150
100
50
0
*
*
*
*
PBS
PBS + HAase
monolayer pretreated with HAase
OVCAR-5
SKOV-3

Figure 4.11. *Adhesion of ovarian cancer cells to LP-9 peritoneal cells*.

(a) The ability of metastatic and non metastatic human ovarian cancer cells to bind to human peritoneal cells was demonstrated by allowing a suspension of calcein labelled cancer cells to bind to a monolayer of peritoneal cells over 20 min. *(b)* Calcein labelled ovarian cancer cells were mixed with CM from CHO V1 cells or parent CHO K1 cells and HA for 2 hr to allow formation of pericellular sheath to occur, then allowed to adhere to the peritoneal monolayer for 8 min. Different letters denote significant difference $p < 0.01$, one-way ANOVA (*c*) In addition to PBS control, ovarian cancer cells were mixed with 10 U/ml HAase. As an additional experiment, peritoneal cell monolayers were pre-treated with 10 U/ml HAase for 8 min prior to 8 min exposure to PBS control ovarian cancer cells. * denotes significant difference from control, $p < 0.05$, one-way ANOVA.

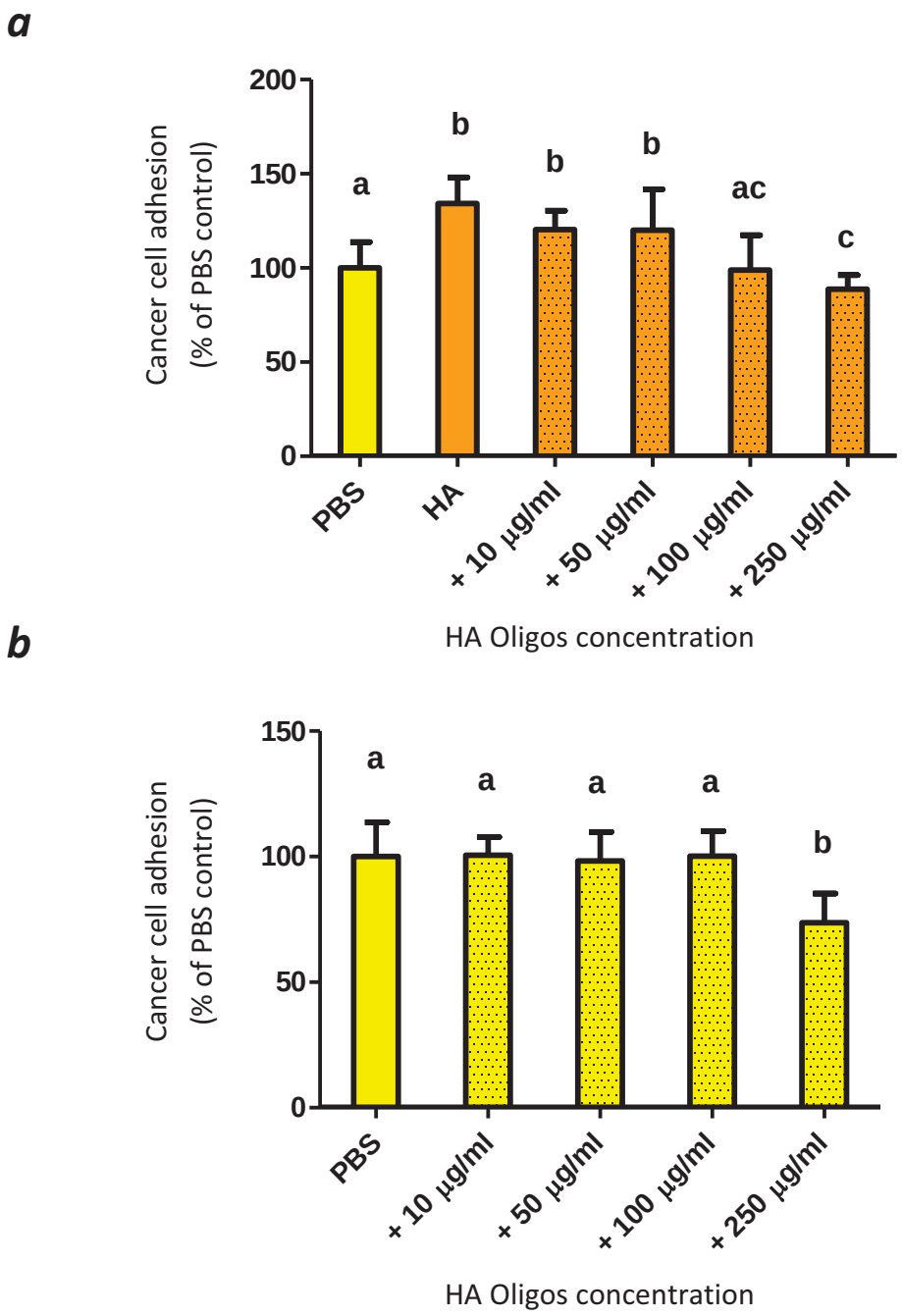

Figure 4.12. *HA oligos can block HA induced adhesion to LP-9 peritoneal cells.*

OVCAR-5 cells were incubated with (*a*) HA (20 µg/ml) or (*b*) PBS in control media in the presence or absence of HA oligomers 6-10 (10-250 µg/ml) for 3 hr and adhesion to LP-9 cells was assessed as described in Figure 4.8. Data is expressed as percentage of fluorescence compared with PBS, mean ± SD from at least three independent experiments performed in triplicate. * denotes significant difference from PBS control and different letters denote significant difference between groups, $p < 0.05$, one-way ANOVA.

4.3. DISCUSSION

This study found that versican levels were low in normal ovarian stroma and stroma surrounding OSE cells but elevated in borderline and malignant tumours. We also observed that there was no difference in versican stromal levels between primary tumours and matching metastases which supports the findings by Lu et al. and Casey et al. which found that both primary ovarian tumours and omental metastases showed increased levels of versican when compared with normal OSE cells [249, 620]. We saw no association of versican levels and ovarian cancer stage which is contradictory to the finding by Voutelainen et al. which reported low levels of stromal versican to be correlated with early stage ovarian cancer. They also reported higher levels were associated with the serous subtype which is the only subtype included in this study [246].

Our finding that there was no significant difference in stromal HA expression between normal, benign, and malignant tissue is in conflict with the findings by Jojovic et al. that high levels of HA in the stroma is associated with malignant tissue [140, 151]. The study by Anttila et al. also demonstrated that high stromal HA was more frequent in metastases than in primary tumours [140] which was not observed in this study. We did however, observe a significant positive correlation between high stromal versican and high stromal HA, suggesting an interaction between these molecules in ovarian cancer.

Interestingly, we also observed an increase in the stromal levels of CD44 in malignant tissue when compared with normal and benign ovarian tissue as well as an association

between stage and high stromal CD44, but no difference between primary tumours and matching metastases. Furthermore, we observed a significant positive correlation between high stromal CD44 and high epithelial CD44, indicating that CD44 on both the tumour cells and the surrounding stromal cells may play a role in ovarian cancer, particularly in its interaction with HA.

Our findings support the observations by Zagorianakou et al. that CD44 expression in ovarian cancer was shown to be higher in malignant tumour cases when compared with benign and borderline tumours [200]. However, epithelial CD44 expression was found to be unaltered in primary ovarian cancers when compared with normal tissue in our study. We observed no correlation between versican or HA and CD44 which is supported by the finding by Sillanpaa et al. [202].

We assessed whether HA is a useful biomarker in the serum of ovarian cancer patients. However, we observed that serum HA was not elevated in the serum of serous benign and serous malignant ovarian tumour patients when compared with controls. This was in contradiction with findings reported in the literature that a range of cancers were associated with increased HA in the serum [170-173, 624]. However, our serum data agrees with our tissue date that there is no significant difference in the stromal HA expression between normal, serous benign, and serous malignant ovarian tissues.

We observed that all of the patients with serum collected after the first cycle of first line chemotherapy showed an increase of serum HA levels compared with the levels at surgery, up to 320%. We also noted that all six patients with serum collected showed an increase in serum HA levels at some point during their chemotherapy regime. Four

patients undergoing chemotherapy subsequently showed a decrease in HA levels at a later chemotherapy cycle, with two of these patients having serum HA levels below that of samples collected at the time of surgery. In addition, we showed that all four cell lines had increased production of HA when exposed to carboplatin. Interestingly, the SKOV-3 cells which were most resistant to carboplatin treatment had the smallest increase of HA production in response to carboplatin. The work done by Delpech et al. showed similar decreases after chemotherapy but these did not correlate with patient outcome [624]. Likewise, the study by Obayashi et al. found that elevated HA in the serum was not linked with response, however the study analysed serum HA in a heterogeneous patient cohort. They assessed HA levels after the completion of a full chemotherapy regime (6 cycles) [173]. Thus, it seems possible that our finding that serum HA levels were not elevated in the cancer patients could be specific to the serous subtype of ovarian cancer.

Although our study into the serum HA levels during chemotherapy only had a small patient number, it is possible that that serum levels of HA may function as an indicator of patient response to chemotherapy when assessed after the first cycle of a chemotherapy regime, or tracked over several cycles. Serum HA measurement may provide a method for determining whether a patient should be moved onto more aggressive therapies earlier in their treatment and potentially lead to greater survival rates. This study should be expanded to include more patients in order to assess the relationship between serum HA levels during chemotherapy and outcome. Further investigation into the role of HA in chemoresistance is also warranted.

In this study, we show that ovarian cancer cells are able to bind strongly with human peritoneal cells within mere minutes, indicating the importance of this step in the metastatic process, and making it a potential key target for therapies for ovarian cancer patients. Furthermore, we have demonstrated that ovarian cancer cells *in vitro* can utilize the ECM components HA and versican to assemble a pericellular matrix.

Activation of the host stromal microenvironment is a critical step in tumour metastasis. Stromal cell activation or desmoplasia has been described for many adenocarcinomas including prostate, lung, colon and breast [625] and is characterized by extensive synthesis of ECM components such as collagen, fibronectin, versican, HA, tenascin C, periostin, and MMPs [146, 615, 626-628]. A reactive stroma is believed to play an important role in ovarian cancer progression and invasion [629, 630]. Thus it seems most likely that versican and HA located in the supporting tumour stroma, provides the necessary components for cancer cells to form a pericellular sheath. Our study also demonstrates that there is a relationship between versican concentration and the percentage of ovarian cancer cells able to form a pericellular sheath and increases in ovarian cancer cell motility and invasion. Our findings support the findings in the literature that lower levels of stromal versican or HA in ovarian cancer patients is associated with a better prognosis for recurrence free 5-year survival than those with higher levels. An *in vitro* study using embryonic fibroblasts from mice with versican lacking the G1 HA binding domain showed that versican is essential for matrix assembly involving HA. It also demonstrated that diminished versican deposition due to lack of HA binding in the ECM increased the level of free HA fragments which interact with CD44 and increase cellular senescence [207].

In this study, we have shown that increased pericellular sheath formation due to increased versican and HA is associated with increased motility. This HA-versican interaction and alteration of the ECM has been shown to form a polar pericellular sheath around the cells and increase their motility [135]. We have also demonstrated this polar sheath in motile ovarian cancer cells. Furthermore we have demonstrated in this study that increased versican and HA levels can induce ovarian cancer cell invasion through an ECM barrier, similar to that found coating human peritoneal cells. Previous studies demonstrating a strong association between the development of ovarian cancer metastasis and increased versican or HA in the peritumoural stroma in ovarian cancer tissues [140, 246] have implicated these molecules in ovarian cancer invasion and metastasis. The present study supports the role of both versican and HA in promoting ovarian cancer cell invasion.

We have also demonstrated that formation of a HA-versican pericellular sheath has no visible effect on ovarian cancer cell adhesion to peritoneal cells in the presence of exogenous HA. It is possible that the other factors present in the CM used may have prevented any effect from being observed, or that any effect versican had on adhesion was masked by the large effect of HA, as exogenous HA induced a significant increase in adhesion of OVCAR-5 and SKOV-3 cancer cells to LP-9 peritoneal cells, which has been documented previously [251, 631]. Addition of HAase or HA oligos successfully blocked the effect of exogenous HA on adhesion. Furthermore, pre-treatment of the LP-9 peritoneal layer with HAase for 45 min prior to addition of ovarian cancer cells resulted in decreased adhesion providing strong evidence that ovarian cancer cell

adhesion to peritoneal cell monolayers is due, at least partially, to the interactions between HA and CD44 [249].

To further understand the role of the versican-HA sheath in ovarian cancer cell adhesion to peritoneal cells, a study should be conducted using purified recombinant versican in the presence or absence of HA. We have shown that peritoneal cells express both CD44 and HA, and that metastatic, adherent ovarian cancer cells also express CD44. Thus we suggest that the adhesion of ovarian cancer cells to peritoneal cells is mediated by HA binding to CD44 found on both cell types which allows a strong anchoring and interaction between the two cell types. The binding of HA to CD44 is known to trigger direct cross-signalling between two different tyrosine kinase-linked signalling pathways [190, 192] and it is this function which is thought to be involved in increased motility, adhesion, and invasion of cancer cells as well as tumour growth, especially in ovarian cancer [174, 193-195]. Thus we propose that versican from the stroma binds with HA during formation of the extracellular matrix, which in turn binds to CD44 on the peritoneal surface, enabling adhesion, and inevitably metastasis to other abdominal organs.

It is known that small HA oligos can compete with larger HA polymers for receptors such as CD44 [632, 633]. HA oligos have also been shown to reverse chemotherapy resistance [299] and increase chemotherapy sensitivity in some cancer cell lines, by disassembling CD44-transporter complexes and induced internalization of CD44, acting as an effective adjuvant to chemotherapy treatment [300]. Highly invasive bladder cancers produce HA fragments in the 30-50 saccharide range which have been shown

to be angiogenic for endothelial cells [165]. By contrast, the HA fragments ranging from 6 to 24 saccharides inhibit melanoma cell proliferation as well as the formation of tumours in nude mice [295]. Small HA oligos in the 6-10 range appear to have unique biological properties and can also inhibit a variety of tumours *in vivo* and *in vitro* [295, 297, 298, 300, 633]. HA oligos have been shown to inhibit the formation of pericellular sheath around chondrocytes [294, 623]. HA oligos are thus a potential therapy to inhibit tumour growth and to counteract the effects of degradation fragments (< 50-mers) which can stimulate tumour cell motility, angiogenesis, and cancer progression.

In this study, we have demonstrated that small HA oligos (6-10) can block the HA-CD44 interaction which forms when ovarian cancer cells bind to peritoneal cells. The HA oligos inhibited the formation of HA-versican pericellular sheath around CD44 expressing ovarian cancer cells and the motility and invasion induced by versican treatment. Our results support further investigations of utilizing that HA oligos either alone or in conjunction with chemotherapeutic agents to block invasion and metastasis of CD44 positive ovarian cancers. The HA-versican pericellular sheath formation has been shown to be inhibited following treatment with HA oligos in bladder, fibrosarcoma, osteosarcoma, and melanoma tumour cells [136, 294, 297]. Treatment with the HA oligos inhibited the formation of pericellular matrix by osteosarcoma cells and reduced HA accumulation in local tumours, tumour growth, motility, invasion, and the formation of distant lung metastases [297]. These findings suggest that the potent anti-tumour effects of HA oligos are mediated in part by the blocking of the formation of HA-rich cell-associated matrices as well as blocking the

interaction between HA and CD44. The use of HA oligomers is a potentially attractive reagent to block versican-HA interactions as well as local tumour invasion and needs further investigation.

CHAPTER 5 - GENERAL DISCUSSION

Ovarian cancer is the 9th most common cancer in women, but has the 6th highest death rate [1]. This poor prognosis is due to more than 50% of ovarian tumours being detected at an advanced stage (III or IV) due to non specific symptoms, and lack of a regular early detection screening tests available to the public. Late stage ovarian cancer has a much lower 5-year survival rate of 12-30% compared with 50-90% for those with an earlier diagnosis [2]. Patients diagnosed with ovarian cancer at any stage undergo debulking surgery and treatment with either platinum or taxane containing chemotherapy regimes, however most patients relapse with drug-resistant disease within 5 years and only approximately 25% of ovarian cancer patients survive 10 years [89, 90]. Unfortunately, there are no effective treatment options currently available for drug resistant ovarian cancer.

Metastasis from epithelial ovarian cancer can occur by ovarian epithelial cancer cells shedding from the primary tumour on the ovary into the peritoneal cavity attaching to the omentum, and then by direct extension into adjacent organs [80]. Little is still understood about ovarian cancer metastasis and why there appears to be a preference for implantation and invasion of the omentum over other sites within the peritoneal cavity. Potential mechanisms for the attachment to peritoneal mesothelium include binding to ECM proteins such as collagen type I [86], and IV, laminin, and fibronectin via integrins [87], and to polysaccharide HA on the surface of the peritoneal cells via its receptor, CD44 [88].

Many proteins, enzymes, and genes have been assessed for potential as markers for ovarian cancer diagnosis and patient outcome. CA125, the only marker currently available for detection and prognosis in ovarian cancer [56], is only detected in the abnormal range in 50% of early stage ovarian cancers [54] but it is also detected in benign and non-malignant ovarian tissue [55]. There is a lot of interest in combining a CA125 test with other serum biomarkers to increase the percentage of early stage ovarian cancers which can be detected.

Utilising a proteomic screening approach to assess the changes in the protein profile when peritoneal cells interact with ovarian cancer cells, we identified a number of proteins which were modulated in peritoneal-ovarian cancer cell co-culture. We identified that TGFBIp, fibronectin, PAI-1, cytokeratins 1, 5, 6C, 9, 10, 14, and 16, TKT, annexin A2, annexin A6, and eEF-2 were processed as a result of the interaction between peritoneal cells in direct contact with ovarian cancer cells, or when both cells shared the same media. Very few of these proteins have been investigated in other ovarian cancer studies. Processed forms have only been detected in human tissue for a handful of these proteins.

We conclude from these experiments, that when peritoneal cells are exposed to ovarian cancer cells, whether by shared CM which represents the early stages of ovarian cancer or by direct contact which represents late stage ovarian cancer, a proteolytic response is triggered. This results in numerous proteins being cleaved or degraded by proteases. This will be an important response to investigate further, as inhibiting this proteolytic response could prove to be an effective novel ovarian cancer therapy. Our studies implicate a role for a disrupted PAI-1-regulation of the plasmin

pathway during the interaction between peritoneal and ovarian cancer cells ultimately leading to increased plasmin secretion and most likely also increased MMP activation, ultimately leading to the processing of a range of proteins, including those detected in this study (Figure 5.1).

We further investigated the role of the ECM protein TGFBIp in ovarian cancer. Further characterisation of this protein found that TGFBIp is abundantly expressed by peritoneal mesothelial cells and weakly expressed by ovarian cancer cells. In peritoneal-ovarian cancer cell co-culture only cleaved forms of TGFBIp were observed. The low level of TGFBIp observed in ovarian cancer cell lines and ovarian cancer tissue and the high levels of TGFBIp observed in normal ovarian tissue is consistent with previous studies which have shown TGFBIp expression to be downregulated in many cancer cell lines and human cancers [578, 587-589]. Recent studies have shown that a low level of TGFBIp in ovarian cancer tissue is predictive of disease progression following treatment [550, 551] whilst TGFBIp over-expression could markedly reduce tumourigenicity [547, 590].

More recent studies demonstrating that the loss of TGFBIp predisposes mice to spontaneous tumour development has provided strong *in vivo* evidence that TGFBIp functions as a tumour suppressor [603]. Although these studies indicate that TGFBIp has an anti-tumourigenic role, a large number of studies have also found that TGFBIp is over-expressed in other cancer cell lines and human tumours including colorectal, renal, lung, oesophageal, and pancreatic cancers [549, 579-582, 586]. Furthermore, several reports indicate that TGFBIp can mediate cancer cell invasion and metastasis as well as enhance cancer cell extravasation [543, 596-598]. Recently TGFBIp has been

shown to mediate lymphatic endothelial migration and adhesion to ECM under low oxygen conditions [601]. These observations suggest that during hypoxia, which commonly occurs in tumours, TGFBIp may aid the metastatic process by promoting the adhesion to lymphatic endothelial cells.

We investigated the cleavage of TGFBIp in the peritoneal-ovarian cancer cell co-culture and further demonstrated that it occurs between amino acid residue 27 and amino acid residue 76 in the N-terminal domain and between amino acid residue 626 and amino acid residue 657 in the C-terminal domain. Although the functional role of the N-terminal TGFBIp domain has not been well studied, the C terminus has several integrin binding motifs including the RGD and EPDIM sequences and the YH18 motif in the FAS IV domain. Whilst it is not known whether processed TGFBIp in the secretome of the peritoneal-ovarian cancer cell co-culture retains its RGD sequence, the EPDIM motif is maintained in the C-terminal processed TGFBIp. Surprisingly, TGFBIp processing was only observed when ovarian cancer cells and peritoneal cells were both present. These findings suggest that a two-way paracrine interaction involving multiple levels of cross-talk between the ovarian cancer cells and peritoneal cells is required for the TGFBIp processing to occur.

Our investigation into the protease responsible for cleaving TGFBIp indicate that cleavage of TGFBIp in the ovarian cancer and peritoneal cell co-culture is not MMP mediated as the broad spectrum MMP inhibitor, GM6001, failed to inhibit TGFBIp processing. We have shown that the protease plasmin, which was found to be almost immediately upregulated in peritoneal-ovarian cancer cell co-culture, cleaves TGFBIp

in the same region as that observed in the co-culture. Furthermore, this processing could be at least partially blocked by the addition of plasmin inhibitors.

Further investigation into the functional role of TGFBIp in ovarian cancer metastasis showed that rTGFBIp can promote ovarian cancer cell motility, invasion, and adhesion to peritoneal cells, the latter of which could be reversed by the addition of a neutralising TGFBIp antibody. Surprisingly, high levels of TGFBIp were also found to cause increases in ovarian cancer cell death.

In our study, the effects of TGFBIp on ovarian cancer cells were independent of the TGFBIp RGD integrin binding motif since treatment with an RGD peptide did not block the ability of TGFBIp to promote ovarian cancer cell motility, invasion, or adhesion to peritoneal cells. It is likely that TGFBIp activity on ovarian cancer cells is mediated by other sites in the TGFBIp molecule other than the RGD motif, which includes the EPDIM or NKDIL motifs and the sequence spanning the YH18 motif. A limitation of our study was to identify the exact position of the C terminal cleavage and thus which motif is most likely responsible for the effects we observed. We were also thus unable to determine the function of the cleaved form of TGFBIp in ovarian cancer.

Our findings indicate that in ovarian cancer, TGFBIp is likely to act as a “double edged sword” where the loss of TGFBIp has a pro-tumourigenic role and the expression of TGFBIp by peritoneal cells aids the metastatic process (Figure 5.2). TGFBIp is therefore a potential novel therapeutic target against ovarian cancer.

In addition to the ECM protein TGFBIp, we investigated the expression of ECM components versican, HA, and CD44 in ovarian cancer tissues. In this study, we found

that versican was significantly elevated in serous ovarian carcinoma when compared with normal and serous benign ovarian tissue. We also observed that CD44 in the stroma was also significantly elevated in serous ovarian carcinoma when compared with normal ovaries or benign serous tumours. These findings are in agreement with previous studies in ovarian cancer which showed that versican is up-regulated in primary tumours and omental metastases when compared with normal surface epithelial cells [244, 249, 620]. Versican has also been found to be associated with serous histological type [140].

Furthermore, we investigated the levels of HA in the serum of serous ovarian cancer patients, and found that the serum levels of HA were not elevated in either serous benign or serous carcinoma patients when compared with controls. This was consistent with our findings that there was no significant difference in the level of HA expression between normal, benign and malignant ovarian tissue, but contradicted the findings by Obayashi et al., that serum HA levels were elevated in a heterogeneous cohort of ovarian cancer patients [173]. It is likely that that the results that we observed in this study could be specific to the serous subtype of ovarian cancer.

As predicting the response of a patient to treatment could be just as valuable as detecting the disease earlier, we tracked HA serum levels in patients at various stages during the course of their chemotherapy regime, and observed that all patients with data collected after their first cycle of chemotherapy showed an increase in HA serum levels when compared with their pre-surgical levels. Additionally, all patients showed an increase in HA serum levels from pre-surgical levels during the course of the chemotherapy regime. One third of the patients completed their chemotherapy

regime with lower levels of serum HA than at diagnosis, which is supported by, the work done by Delpech et al., and Obayashi et al., which showed serum HA levels decreased after chemotherapy [173, 624]. Further investigation in a larger cohort of patients is required to determine whether the measurement of serum HA levels during chemotherapy can be used as an indicator of chemotherapy response or an earlier indication of chemoresistance.

In an additional study into the functional role of ECM components HA and versican, we demonstrated that ovarian cancer cells *in vitro* can utilize HA and versican to assemble a pericellular matrix. In this study, we have shown that pericellular sheath formation was observed in motile OVCAR-5 and SKOV-3 cells. Furthermore, we also demonstrated that versican and HA levels can enhance the motility of ovarian cancer cells and their invasion through an ECM barrier (Figure 5.3). This HA-versican interaction and alteration of the ECM has been shown to increase prostate cancer cell motility and increase formation of a polar pericellular sheath around the motile prostate cells [135]. Previous studies demonstrating a strong association between the development of ovarian cancer metastasis and increased versican or HA in the peritumoural stroma in ovarian cancer tissues [140, 246], have implicated these molecules in ovarian cancer invasion and metastasis. The present study supports the role of both versican and HA in promoting ovarian cancer cell motility and invasion. We propose that versican from the peritumoural stroma binds to HA to form pericellular sheaths around the cancer cells. This enhances the motility of the cancer cells and their ability to invade through the peritoneal lining, ultimately leading to distant metastases (Figure 5.4). Thus, it seems most likely that versican and HA located

in the supporting tumour stroma, provides the necessary components for cancer cells to form a pericellular sheath and become metastatic.

In agreement with previous studies, we have also demonstrated that exogenous HA alone could increase ovarian cancer adhesion to peritoneal cells. Our findings suggest that the adhesion of ovarian cancer cells to peritoneal cells is mediated by HA binding to CD44 found on both ovarian cancer cells and peritoneal cells by allowing a strong anchorage and interaction between the two cell types. In this study, we have demonstrated that small HA oligos (6-10) can block the HA-CD44 interaction which occurs when ovarian cancer cells bind to peritoneal cells.

Addition of HA oligos also inhibited the formation of HA-versican pericellular sheath around CD44 expressing ovarian cancer cells and the increases in motility and invasion following versican treatment (Figure 5.3). The HA-versican pericellular sheath formation has been shown to be inhibited following treatment with HA oligos in other cancer types including; urinary, fibrosarcoma, osteosarcoma, and melanoma tumour cells [136, 294, 297]. Treatment with the HA oligos inhibited the formation of pericellular matrix by the cells and reduced HA accumulation in local tumours, tumour growth, motility, invasion, and the formation of distant lung metastases by blocking the HA CD44 interaction [136]. Our results support further investigations of utilising HA oligos either alone or in conjunction with chemotherapeutic agents to block invasion and metastasis of CD44 positive ovarian cancer cells. The use of HA oligos is a potentially effective therapy to block HA-versican interactions as well as local tumour invasion and needs further investigation.

Overall the studies in this thesis indicate a very strong role for the tumour microenvironment and in particular highlights the proteolytic mechanisms triggered to create a modified tumour microenvironment. Further investigation of the proteolytic response will increase our understanding involved in the ovarian cancer metastatic process as well as the interactions between ECM components HA, versican, and CD44.

Many of the novel proteins and their cleaved products identified in this study hold the potential to be novel diagnostic biomarkers of ovarian cancer. Similarly, these proteins may prove to be novel therapeutic targets for ovarian cancer and further investigation is warranted.

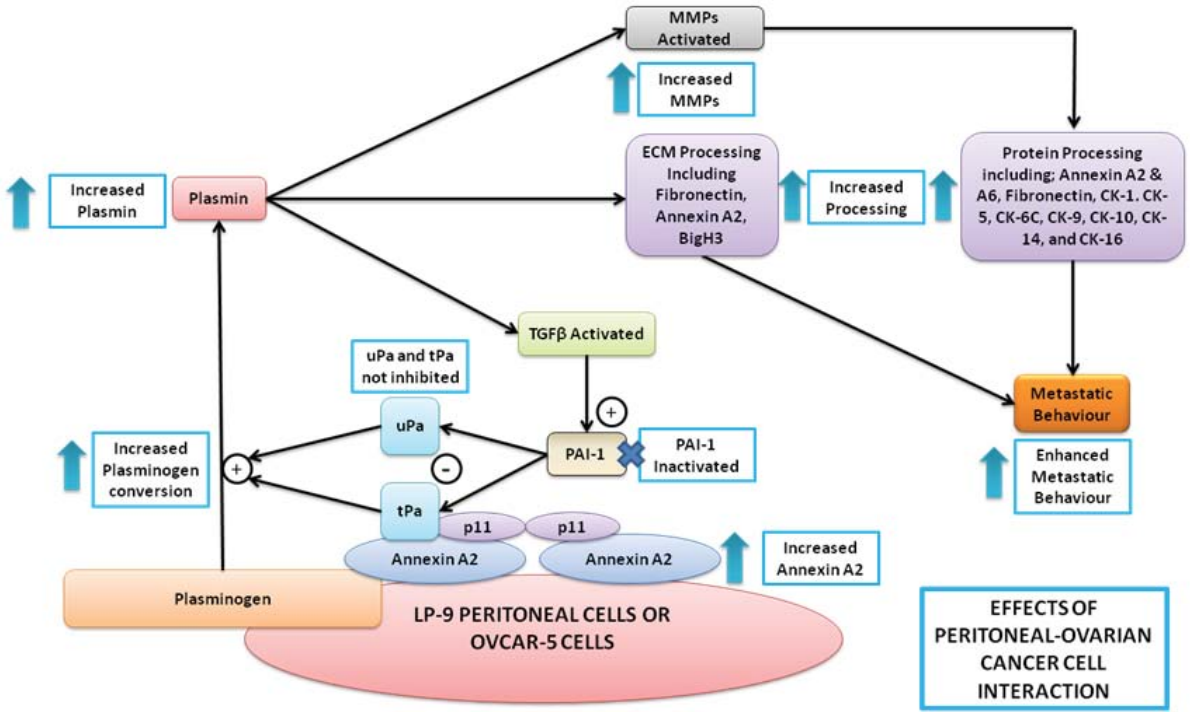

Figure 5.1. *The proposed role of the plasmin pathway in ovarian cancer metastasis*

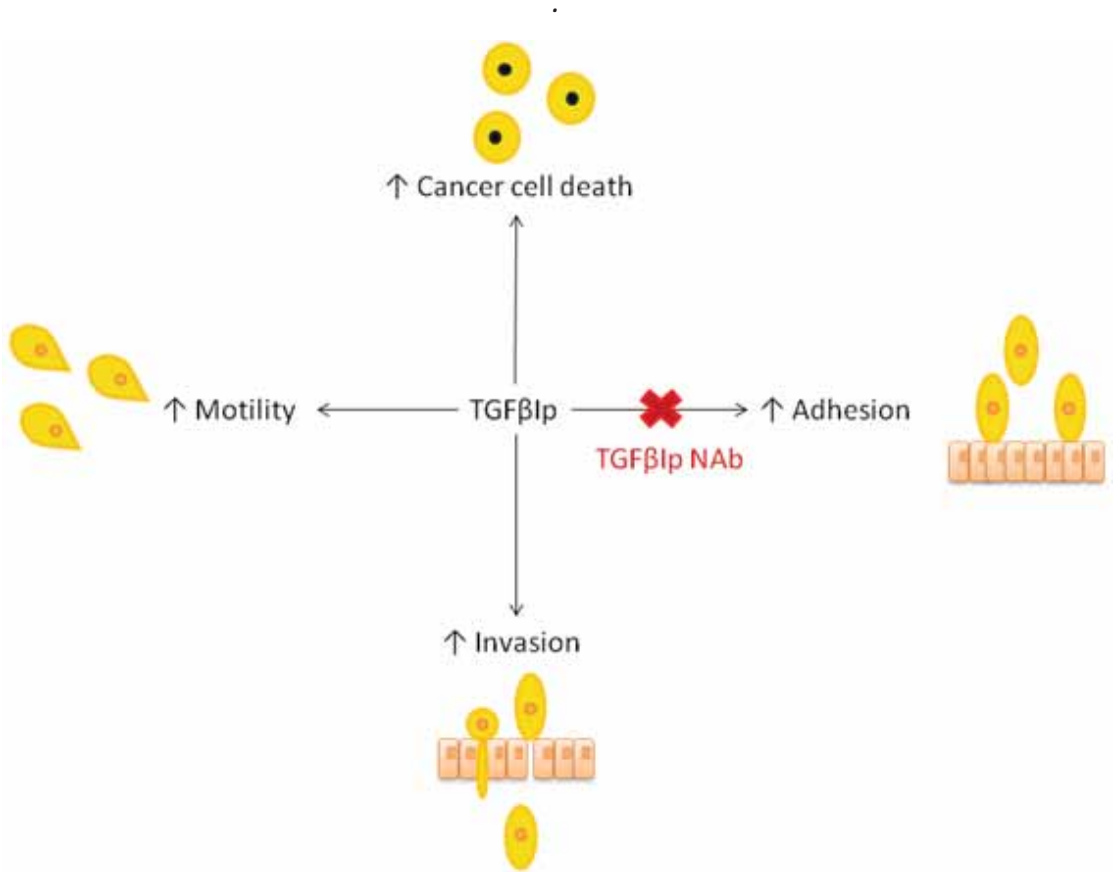

Figure 5.2. *The effects of TGFBIp on the metastatic steps involved in ovarian cancer and the inhibitory effects of a neutralising TGFBIp antibody.*

In this study, rTGFBIp increased ovarian cancer motility and invasion as well as their adhesion to peritoneal cells. A TGFBIp neutralising antibody was able to successfully block the effects of rTGFBIp on ovarian cancer cell adhesion to peritoneal cells.

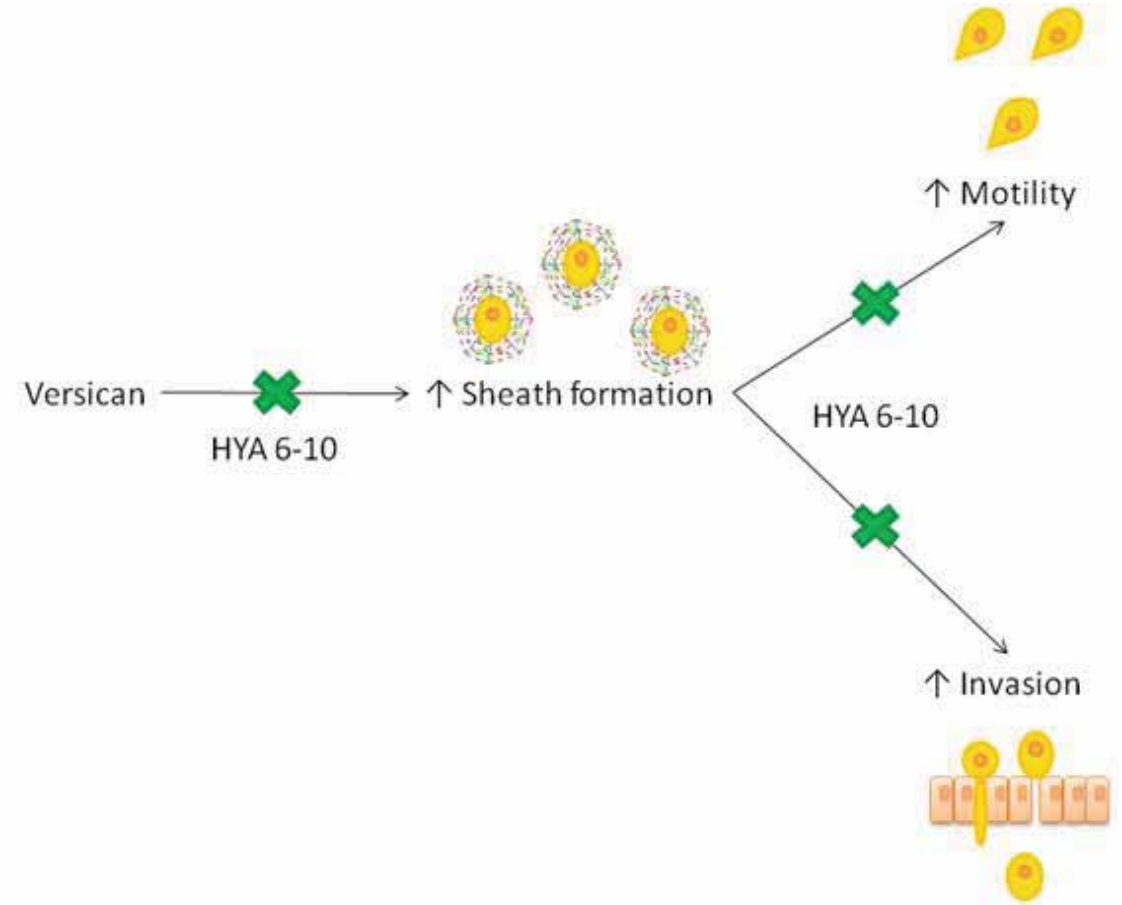

Figure 5.3. *The effects of versican on CD44 positive ovarian cancer cells and the inhibitory effect of HA oligos.*

Purified human versican V1 stimulated pericellular sheath formation around CD44 positive ovarian cancer cells which led to increased motility and invasiveness. Addition of HA oligos successfully blocked sheath formation and the increases in motility and invasion observed in the presence of versican.

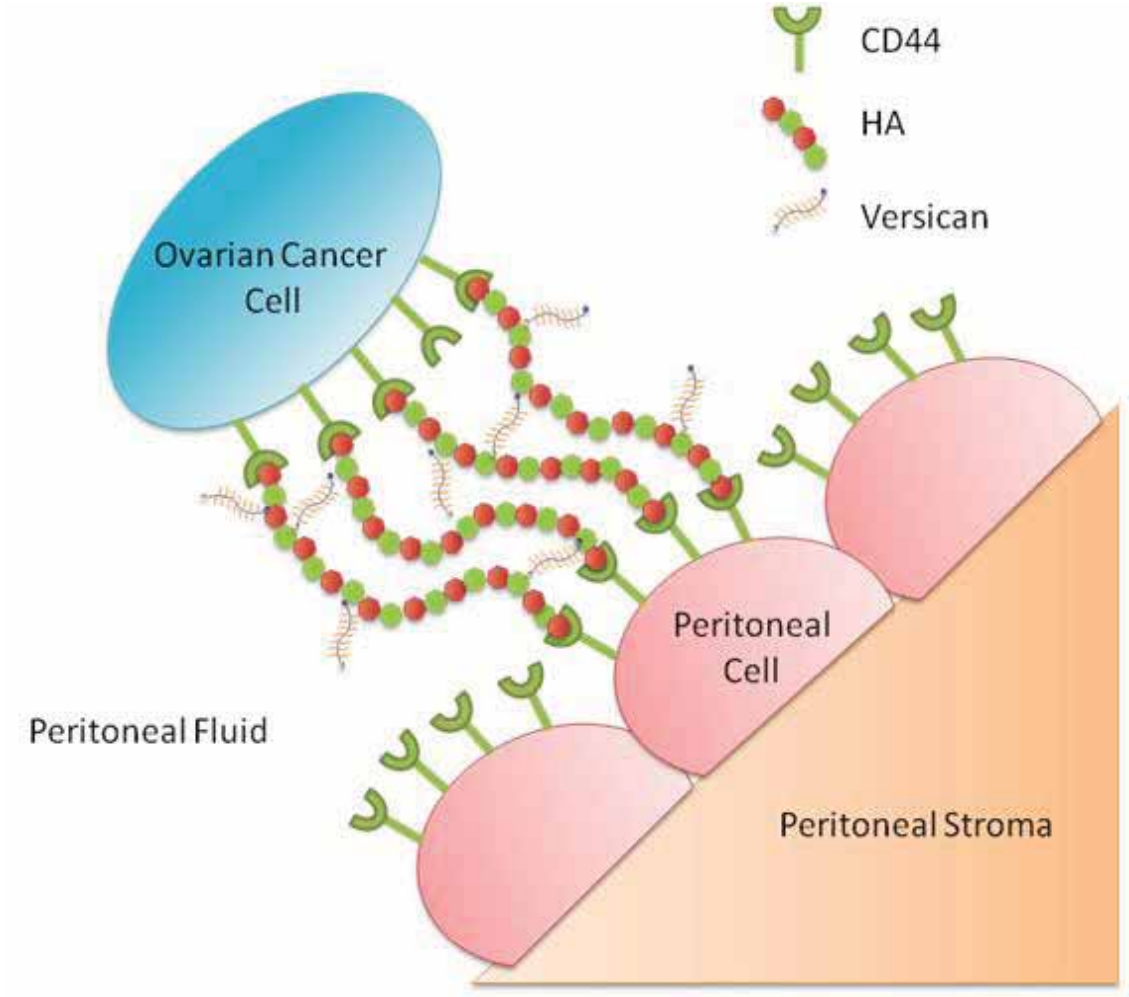

Figure 5.4. Proposed m*odel of HA, CD44, and versican interactions in ovarian cancer.*

Proposed model of HA, CD44 and versican interactions between ovarian cancer and peritoneal cells. The formation of a stabilized HA/versican pericellular matrix surrounding ovarian cancer cells increases motility and protects the ovarian cancer cells against the mechanical forces in the peritoneal cavity and enable ovarian cancer cells to strongly adhere to CD44 expressed on peritoneal cells. This allows subsequent ovarian cancer invasion and peritoneal dissemination.

APPENDIX

a

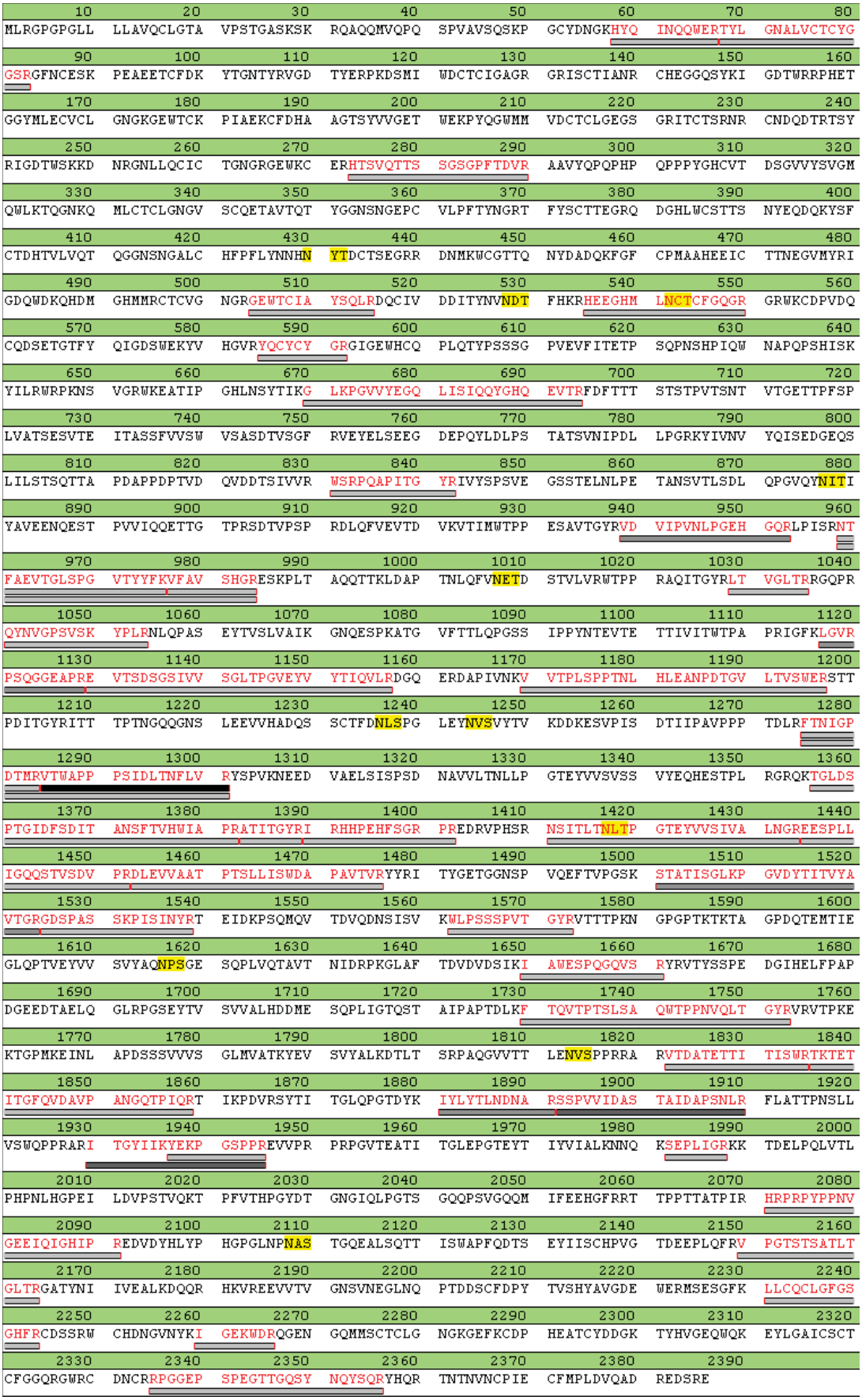
10 20 30 40 50 60 70 80
MLRGPGPGLL LLAVQCLGTA VPSTGASKSK RQAQQMVQPQ SPVAVSQSKP GCYDNGKHYQ INQQWERTYL GNALVCTCYG
90 100 110 120 130 140 150 160
GSRGFNCESK PEAEETCFDK YTGNTYRVGD TYERPKDSMI WDCTCIGAGR GRISCTIANR CHEGGQSYKI GDTWRRPHET
170 180 190 200 210 220 230 240
GGYMLECVCL GNGKGEWTCK PIAEKCFDHA AGTSYVVGET WEKPYQGWMM VDCTCLGEGS GRITCTSRNR CNDQDTRTSY
250 260 270 280 290 300 310 320
RIGDTWSKKD NRGNLLQCIC TGNGRGEWKC ERHTSVQTTS SGSGPFTDVR AAVYQPQPHP QPPPYGHCVT DSGVVYSVGM
330 340 350 360 370 380 390 400
QWLKTQGNKQ MLCTCLGNGV SCQETAVTQT YGGNSNGEPC VLPFTYNGRT FYSCTTEGRQ DGHLWCSTTS NYEQDQKYSF
410 420 430 440 450 460 470 480
CTDHTVLVQT QGGNSNGALC HFPFLYNNHN YTDCTSEGRR DNMKWCGTTQ NYDADQKFGF CPMAAHEEIC TTNEGVMYRI
490 500 510 520 530 540 550 560
GDQWDKQHDM GHMMRCTCVG NGRGEWTCIA YSQLRDQCIV DDITYNVNDT FHKRHEEGHM LNCTCFGQGR GRWKCDPVDQ
570 580 590 600 610 620 630 640
CQDSETGTFY QIGDSWEKYV HGVRYQCYCY GRGIGEWHCQ PLQTYPSSSG PVEVFITETP SQPNSHPIQW NAPQPSHISK
650 660 670 680 690 700 710 720
YILRWRPKNS VGRWKEATIP GHLNSYTIKG LKPGVVYEGQ LISIQQYGHQ EVTRFDFTTT STSTPVTSNT VTGETTPFSP
730 740 750 760 770 780 790 800
LVATSESVTE ITASSFVVSW VSASDTVSGF RVEYELSEEG DEPQYLDLPS TATSVNIPDL LPGRKYIVNV YQISEDGEQS
810 820 830 840 850 860 870 880
LILSTSQTTA PDAPPDPTVD QVDDTSIVVR WSRPQAPITG YRIVYSPSVE GSSTELNLPE TANSVTLSDL QPGVQYNITI
890 900 910 920 930 940 950 960
YAVEENQEST PVVIQQETTG TPRSDTVPSP RDLQFVEVTD VKVTIMWTPP ESAVTGYRVD VIPVNLPGEH GQRLPISRNT
970 980 990 1000 1010 1020 1030 1040
FAEVTGLSPG VTYYFKVFAV SHGRESKPLT AQQTTKLDAP TNLQFVNETD STVLVRWTPP RAQITGYRLT VGLTRRGQPR
1050 1060 1070 1080 1090 1100 1110 1120
QYNVGPSVSK YPLRNLQPAS EYTVSLVAIK GNQESPKATG VFTTLQPGSS IPPYNTEVTE TTIVITWTPA PRIGFKLGVR
1130 1140 1150 1160 1170 1180 1190 1200
PSQGGEAPRE VTSDSGSIVV SGLTPGVEYV YTIQVLRDGQ ERDAPIVNKV VTPLSPPTNL HLEANPDTGV LTVSWERSTT
1210 1220 1230 1240 1250 1260 1270 1280
PDITGYRITT TPTNGQQGNS LEEVVHADQS SCTFDNLSPG LEYNVSVYTV KDDKESVPIS DTIIPAVPPP TDLRFTNIGP
1290 1300 1310 1320 1330 1340 1350 1360
DTMRVTWAPP PSIDLTNFLV RYSPVKNEED VAELSISPSD NAVVLTNLLP GTEYVVSVSS VYEQHESTPL RGRQKTGLDS
1370 1380 1390 1400 1410 1420 1430 1440
PTGIDFSDIT ANSFTVHWIA PRATITGYRI RHHPEHFSGR PREDRVPHSR NSITLTNLTP GTEYVVSIVA LNGREESPLL
1450 1460 1470 1480 1490 1500 1510 1520
IGQQSTVSDV PRDLEVVAAT PTSLLISWDA PAVTVRYYRI TYGETGGNSP VQEFTVPGSK STATISGLKP GVDYTITVYA
1530 1540 1550 1560 1570 1580 1590 1600
VTGRGDSPAS SKPISINYRT EIDKPSQMQV TDVQDNSISV KWLPSSSPVT GYRVTTTPKN GPGPTKTKTA GPDQTEMTIE
1610 1620 1630 1640 1650 1660 1670 1680
GLQPTVEYVV SVYAQNPSGE SQPLVQTAVT NIDRPKGLAF TDVDVDSIKI AWESPQGQVS RYRVTYSSPE DGIHELFPAP
1690 1700 1710 1720 1730 1740 1750 1760
DGEEDTAELQ GLRPGSEYTV SVVALHDDME SQPLIGTQST AIPAPTDLKF TQVTPTSLSA QWTPPNVQLT GYRVRVTPKE
1770 1780 1790 1800 1810 1820 1830 1840
KTGPMKEINL APDSSSVVVS GLMVATKYEV SVYALKDTLT SRPAQGVVTT LENVSPPRRA RVTDATETTI TISWRTKTET
1850 1860 1870 1880 1890 1900 1910 1920
ITGFQVDAVP ANGQTPIQRT IKPDVRSYTI TGLQPGTDYK IYLYTLNDNA RSSPVVIDAS TAIDAPSNLR FLATTPNSLL
1930 1940 1950 1960 1970 1980 1990 2000
VSWQPPRARI TGYIIKYEKP GSPPREVVPR PRPGVTEATI TGLEPGTEYT IYVIALKNNQ KSEPLIGRKK TDELPQLVTL
2010 2020 2030 2040 2050 2060 2070 2080
PHPNLHGPEI LDVPSTVQKT PFVTHPGYDT GNGIQLPGTS GQQPSVGQQM IFEEHGFRRT TPPTTATPIR HRPRPYPPNV
2090 2100 2110 2120 2130 2140 2150 2160
GEEIQIGHIP REDVDYHLYP HGPGLNPNAS TGQEALSQTT ISWAPFQDTS EYIISCHPVG TDEEPLQFRV PGTSTSATLT
2170 2180 2190 2200 2210 2220 2230 2240
GLTRGATYNI IVEALKDQQR HKVREEVVTV GNSVNEGLNQ PTDDSCFDPY TVSHYAVGDE WERMSESGFK LLCQCLGFGS
2250 2260 2270 2280 2290 2300 2310 2320
GHFRCDSSRW CHDNGVNYKI GEKWDRQGEN GQMMSCTCLG NGKGEFKCDP HEATCYDDGK TYHVGEQWQK EYLGAICSCT
2330 2340 2350 2360 2370 2380 2390
CFGGQRGWRC DNCRRPGGEP SPEGTTGQSY NQYSQRYHQR TNTNVNCPIE CFMPLDVQAD REDSRE

b

10	20	30	40	50	60	70	80
MLRGPGPGLL	LLAVQCLGTA	VPSTGASKSK	RQAQQMVQPQ	SPVAVSQSKP	GCYDNGKHYQ	INQQWERTYL	GNALVCTCYG
90	100	110	120	130	140	150	160
GSRGFNCESK	PEAEETCFDK	YTGNTYRVGD	TYERPKDSMI	WDCTCIGAGR	GRISCTIANR	CHEGGQSYKI	GDTWRRPHET
170	180	190	200	210	220	230	240
GGYMLECVCL	GNGKGEWTCK	PIAEKCFDHA	AGTSYVVGET	WEKPYQGWMM	VDCTCLGEGS	GRITCTSRNR	CNDQDTRTSY
250	260	270	280	290	300	310	320
RIGDTWSKKD	NRGNLLQCIC	TGNGRGEWKC	ERHTSVQTTS	SGSGPFTDVR	AAVYQPQPHP	QPPPYGHCVT	DSGVVYSVGM
330	340	350	360	370	380	390	400
QWLKTQGNKQ	MLCTCLGNGV	SCQETAVTQT	YGGNSNGEPC	VLPFTYNGRT	FYSCTTEGRQ	DGHLWCSTTS	NYEQDQKYSF
410	420	430	440	450	460	470	480
CTDHTVLVQT	QGGNSNGALC	HFPFLYNNHN	YTDCTSEGRR	DNMKWCGTTQ	NYDADQKFGF	CPMAAHEEIC	TTNEGVMYRI
490	500	510	520	530	540	550	560
GDQWDKQHDM	GHMMRCTCVG	NGRGEWTCIA	YSQLRDQCIV	DDITYNVNDT	FHKRHEEGHM	LNCTCFGQGR	GRWKCDPVDQ
570	580	590	600	610	620	630	640
CQDSETGTFY	QIGDSWEKYV	HGVRYQCYCY	GRGIGEWHCQ	PLQTYPSSSG	PVEVFITETP	SQPNSHPIQW	NAPQPSHISK
650	660	670	680	690	700	710	720
YILRWRPKNS	VGRWKEATIP	GHLNSYTIKG	LKPGVVYEGQ	LISIQQYGHQ	EVTRFDFTTT	STSTPVTSNT	VTGETTPFSP
730	740	750	760	770	780	790	800
LVATSESVTE	ITASSFVVSW	VSASDTVSGF	RVEYELSEEG	DEPQYLDLPS	TATSVNIPDL	LPGRKYIVNV	YQISEDGEQS
810	820	830	840	850	860	870	880
LILSTSQTTA	PDAPPDPTVD	QVDDTSIVVR	WSRPQAPITG	YRIVYSPSVE	GSSTELNLPE	TANSVTLSDL	QPGVQYNITI
890	900	910	920	930	940	950	960
YAVEENQEST	PVVIQQETTG	TPRSDTVPSP	RDLQFVEVTD	VKVTIMWTPP	ESAVTGYRVD	VIPVNLPGEH	GQRLPISRNT
970	980	990	1000	1010	1020	1030	1040
FAEVTGLSPG	VTYYFKVFAV	SHGRESKPLT	AQQTTKLDAP	TNLQFVNETD	STVLVRWTPP	RAQITGYRLT	VGLTRRGQPR
1050	1060	1070	1080	1090	1100	1110	1120
QYNVGPSVSK	YPLRNLQPAS	EYTVSLVAIK	GNQESPKATG	VFTTLQPGSS	IPPYNTEVTE	TTIVITWTPA	PRIGFKLGVR
1130	1140	1150	1160	1170	1180	1190	1200
PSQGGEAPRE	VTSDSGSIVV	SGLTPGVEYV	YTIQVLRDGQ	ERDAPIVNKV	VTPLSPPTNL	HLEANPDTGV	LTVSWERSTT
1210	1220	1230	1240	1250	1260	1270	1280
PDITGYRITT	TPTNGQQGNS	LEEVVHADQS	SCTFDNLSPG	LEYNVSVYTV	KDDKESVPIS	DTIIPAVPPP	TDLRFTNIGP
1290	1300	1310	1320	1330	1340	1350	1360
DTMRVTWAPP	PSIDLTNFLV	RYSPVKNEED	VAELSISPSD	NAVVLTNLLP	GTEYVVSVSS	VYEQHESTPL	RGRQKTGLDS
1370	1380	1390	1400	1410	1420	1430	1440
PTGIDFSDIT	ANSFTVHWIA	PRATITGYRI	RHHPEHFSGR	PREDRVPHSR	NSITLTNLTP	GTEYVVSIVA	LNGREESPLL
1450	1460	1470	1480	1490	1500	1510	1520
IGQQSTVSDV	PRDLEVVAAT	PTSLLISWDA	PAVTVRYYRI	TYGETGGNSP	VQEFTVPGSK	STATISGLKP	GVDYTITVYA
1530	1540	1550	1560	1570	1580	1590	1600
VTGRGDSPAS	SKPISINYRT	EIDKPSQMQV	TDVQDNSISV	KWLPSSSPVT	GYRVTTTPKN	GPGPTKTKTA	GPDQTEMTIE
1610	1620	1630	1640	1650	1660	1670	1680
GLQPTVEYVV	SVYAQNPSGE	SQPLVQTAVT	NIDRPKGLAF	TDVDVDSIKI	AWESPQGQVS	RYRVTYSSPE	DGIHELFPAP
1690	1700	1710	1720	1730	1740	1750	1760
DGEEDTAELQ	GLRPGSEYTV	SVVALHDDME	SQPLIGTQST	AIPAPTDLKF	TQVTPTSLSA	QWTPPNVQLT	GYRVRVTPKE
1770	1780	1790	1800	1810	1820	1830	1840
KTGPMKEINL	APDSSSVVVS	GLMVATKYEV	SVYALKDTLT	SRPAQGVVTT	LENVSPPRRA	RVTDATETTI	TISWRTKTET
1850	1860	1870	1880	1890	1900	1910	1920
ITGFQVDAVP	ANGQTPIQRT	IKPDVRSYTI	TGLQPGTDYK	IYLYTLNDNA	RSSPVVIDAS	TAIDAPSNLR	FLATTPNSLL
1930	1940	1950	1960	1970	1980	1990	2000
VSWQPPRARI	TGYIIKYEKP	GSPPREVVPR	PRPGVTEATI	TGLEPGTEYT	IYVIALKNNQ	KSEPLIGRKK	TDELPQLVTL
2010	2020	2030	2040	2050	2060	2070	2080
PHPNLHGPEI	LDVPSTVQKT	PFVTHPGYDT	GNGIQLPGTS	GQQPSVGQQM	IFEEHGFRRT	TPPTTATPIR	HRPRPYPPNV
2090	2100	2110	2120	2130	2140	2150	2160
GEEIQIGHIP	REDVDYHLYP	HGPGLNPNAS	TGQEALSQTT	ISWAPFQDTS	EYIISCHPVG	TDEEPLQFRV	PGTSTSATLT
2170	2180	2190	2200	2210	2220	2230	2240
GLTRGATYNI	IVEALKDQQR	HKVREEVVTV	GNSVNEGLNQ	PTDDSCFDPY	TVSHYAVGDE	WERMSESGFK	LLCQCLGFGS
2250	2260	2270	2280	2290	2300	2310	2320
GHFRCDSSRW	CHDNGVNYKI	GEKWDRQGEN	GQMMSCTCLG	NGKGEFKCDP	HEATCYDDGK	TYHVGEQWQK	EYLGAICSCT
2330	2340	2350	2360	2370	2380	2390	
CFGGQRGWRC	DNCRRPGGEP	SPEGTTGQSY	NQYSQRYHQR	TNTNVNCPIE	CFMPLDVQAD	REDSRE	

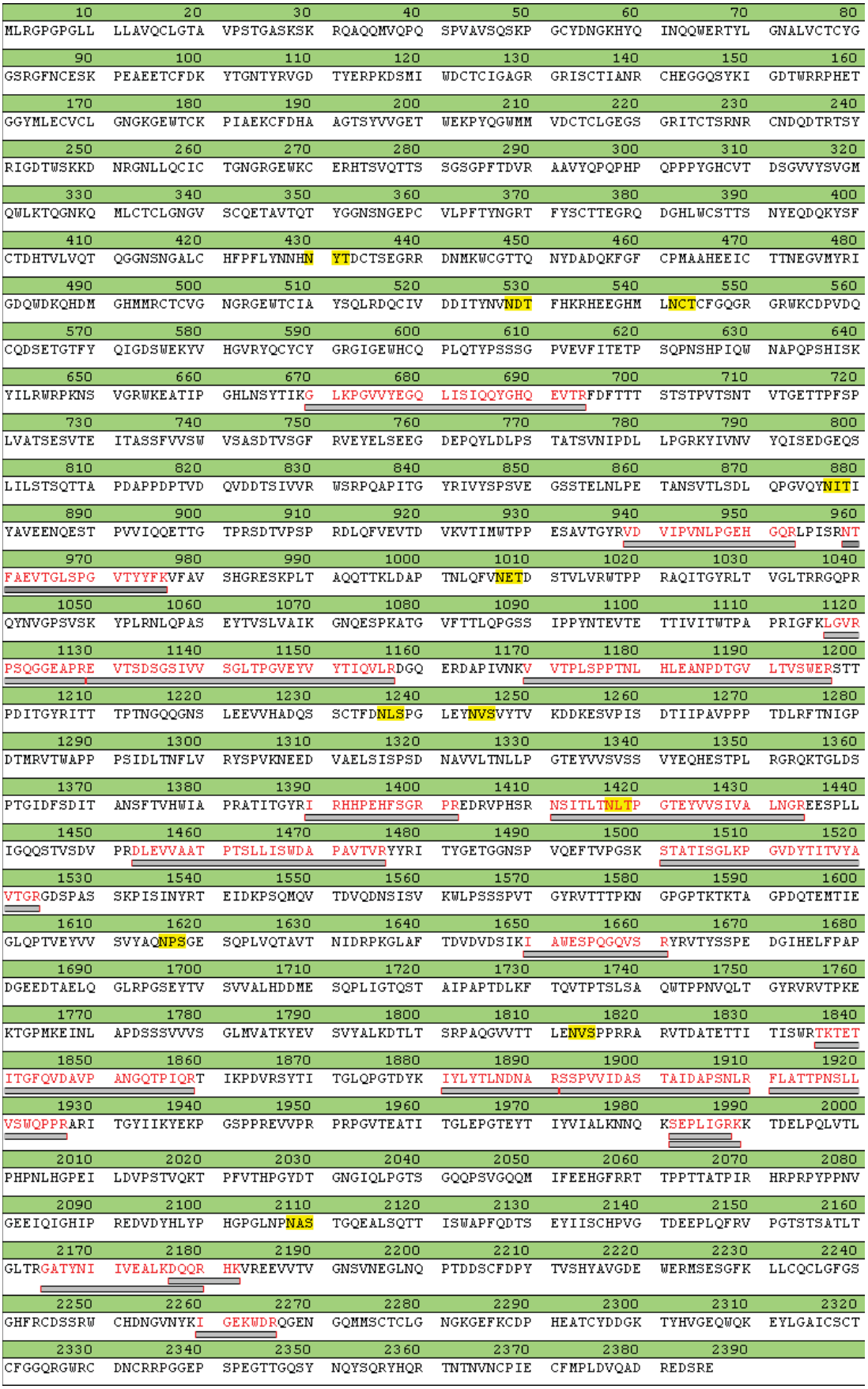

```
      10         20         30         40         50         60         70         80
MLRGPGPGLL LLAVQCLGTA VPSTGASKSK RQAQQMVQPQ SPVAVSQSKP GCYDNGKHYQ INQQWERTYL GNALVCTCYG

      90        100        110        120        130        140        150        160
GSRGFNCESK PEAEETCFDK YTGNTYRVGD TYERPKDSMI WDCTCIGAGR GRISCTIANR CHEGGQSYKI GDTWRRPHET

     170        180        190        200        210        220        230        240
GGYMLECVCL GNGKGEWTCK PIAEKCFDHA AGTSYVVVGET WEKPYQGWMM VDCTCLGEGS GRITCTSRNR CNDQDTRTSY

     250        260        270        280        290        300        310        320
RIGDTWSKKD NRGNLLQCIC TGNGRGEWKC ERHTSVQTTS SGSGPFTDVR AAVYQPQPHP QPPPYGHCVT DSGVVYSVGM

     330        340        350        360        370        380        390        400
QWLKTQGNKQ MLCTCLGNGV SCQETAVTQT YGGNSNGEPC VLPFTYNGRT FYSCTTEGRQ DGHLWCSTTS NYEQDQKYSF

     410        420        430        440        450        460        470        480
CTDHTVLVQT QGGNSNGALC HFPFLYNNHN YTDCTSEGRR DNMKWCGTTQ NYDADQKFGF CPMAAHEEIC TTNEGVMYRI

     490        500        510        520        530        540        550        560
GDQWDKQHDM GHMMRCTCVG NGRGEWTCIA YSQLRDQCIV DDITYNVNDT FHKRHEEGHM LNCTCFGQGR GRWKCDPVDQ

     570        580        590        600        610        620        630        640
CQDSETGTFY QIGDSWEKYV HGVRYQCYCY GRGIGEWHCQ PLQTYPSSSG PVEVFITETP SQPNSHPIQW NAPQPSHISK

     650        660        670        680        690        700        710        720
YILRWRPKNS VGRWKEATIP GHLNSYTIKG LKPGVVYEGQ LISIQQYGHQ EVTRFDFTTT STSTPVTSNT VTGETTPFSP

     730        740        750        760        770        780        790        800
LVATSESVTE ITASSFVVSW VSASDTVSGF RVEYELSEEG DEPQYLDLPS TATSVNIPDL LPGRKYIVNV YQISEDGEQS

     810        820        830        840        850        860        870        880
LILSTSQTTA PDAPPDPTVD QVDDTSIVVR WSRPQAPITG YRIVYSPSVE GSSTELNLPE TANSVTLSDL QPGVQYNITI

     890        900        910        920        930        940        950        960
YAVEENQEST PVVIQQETTG TPRSDTVPSP RDLQFVEVTD VKVTIMWTPP ESAVTGYRVD VIPVNLPGEH GQRLPISRNT

     970        980        990       1000       1010       1020       1030       1040
FAEVTGLSPG VTYYFKVFAV SHGRESKPLT AQQTTKLDAP TNLQFVNETD STVLVRWTPP RAQITGYRLT VGLTRRGQPR

    1050       1060       1070       1080       1090       1100       1110       1120
QYNVGPSVSK YPLRNLQPAS EYTVSLVAIK GNQESPKATG VFTTLQPGSS IPPYNTEVTE TTIVITWTPA PRIGFKLGVR

    1130       1140       1150       1160       1170       1180       1190       1200
PSQGGEAPRE VTSDSGSIVV SGLTPGVEYV YTIQVLRDGQ ERDAPIVNKV VTPLSPPTNL HLEANPDTGV LTVSWERSTT

    1210       1220       1230       1240       1250       1260       1270       1280
PDITGYRITT TPTNGQQGNS LEEVVHADQS SCTFDNLSPG LEYNVSVYTV KDDKESVPIS DTIIPAVPPP TDLRFTNIGP

    1290       1300       1310       1320       1330       1340       1350       1360
DTMRVTWAPP PSIDLTNFLV RYSPVKNEED VAELSISPSD NAVVLTNLLP GTEYVVSVSS VYEQHESTPL RGRQKTGLDS

    1370       1380       1390       1400       1410       1420       1430       1440
PTGIDFSDIT ANSFTVHWIA PRATITGYRI RHHPEHFSGR PREDRVPHSR NSITLTNLTP GTEYVVSIVA LNGREESPLL

    1450       1460       1470       1480       1490       1500       1510       1520
IGQQSTVSDV PRDLEVVAAT PTSLLISWDA PAVTVRYYRI TYGETGGNSP VQEFTVPGSK STATISGLKP GVDYTITVYA

    1530       1540       1550       1560       1570       1580       1590       1600
VTGRGDSPAS SKPISINYRT EIDKPSQMQV TDVQDNSISV KWLPSSSPVT GYRVTTTPKN GPGPTKTKTA GPDQTEMTIE

    1610       1620       1630       1640       1650       1660       1670       1680
GLQPTVEYVV SVYAQNPSGE SQPLVQTAVT NIDRPKGLAF TDVDVDSIKI AWESPQGQVS RYRVTYSSPE DGIHELFPAP

    1690       1700       1710       1720       1730       1740       1750       1760
DGEEDTAELQ GLRPGSEYTV SVVALHDDME SQPLIGTQST AIPAPTDLKF TQVTPTSLSA QWTPPNVQLT GYRVRVTPKE

    1770       1780       1790       1800       1810       1820       1830       1840
KTGPMKEINL APDSSSVVVS GLMVATKYEV SVYALKDTLT SRPAQGVVTT LENVSPPRRA RVTDATETTI TISWRTKTET

    1850       1860       1870       1880       1890       1900       1910       1920
ITGFQVDAVP ANGQTPIQRT IKPDVRSYTI TGLQPGTDYK IYLYTLNDNA RSSPVVIDAS TAIDAPSNLR FLATTPNSLL

    1930       1940       1950       1960       1970       1980       1990       2000
VSWQPPRARI TGYIIKYEKP GSPPREVVPR PRPGVTEATI TGLEPGTEYT IYVIALKNNQ KSEPLIGRKK TDELPQLVTL

    2010       2020       2030       2040       2050       2060       2070       2080
PHPNLHGPEI LDVPSTVQKT PFVTHPGYDT GNGIQLPGTS GQQPSVGQQM IFEEHGFRRT TPPTTATPIR HRPRPYPPNV

    2090       2100       2110       2120       2130       2140       2150       2160
GEEIQIGHIP REDVDYHLYP HGPGLNPNAS TGQEALSQTT ISWAPFQDTS EYIISCHPVG TDEEPLQFRV PGTSTSATLT

    2170       2180       2190       2200       2210       2220       2230       2240
GLTRGATYNI IVEALKDQQR HKVREEVVTV GNSVNEGLNQ PTDDSCFDPY TVSHYAVGDE WERMSESGFK LLCQCLGFGS

    2250       2260       2270       2280       2290       2300       2310       2320
GHFRCDSSRW CHDNGVNYKI GEKWDRQGEN GQMMSCTCLG NGKGEFKCDP HEATCYDDGK TYHVGEQWQK EYLGAICSCT

    2330       2340       2350       2360       2370       2380       2390
CFGGQRGWRC DNCRRPGGEP SPEGTTGQSY NQYSQRYHQR TNTNVNCPIE CFMPLDVQAD REDSRE
```

c

10	20	30	40	50	60	70	80
MLRGPGPGLL	LLAVQCLGTA	VPSTGASKSK	RQAQQMVQPQ	SPVAVSQSKP	GCYDNGKHYQ	INQQWERTYL	GNALVCTCYG
90	100	110	120	130	140	150	160
GSRGFNCESK	PEAEETCFDK	YTGNTYRVGD	TYERPKDSMI	WDCTCIGAGR	GRISCTIANR	CHEGGQSYKI	GDTWRRPHET
170	180	190	200	210	220	230	240
GGYMLECVCL	GNGKGEWTCK	PIAEKCFDHA	AGTSYVVGET	WEKPYQGWMM	VDCTCLGEGS	GRITCTSRNR	CNDQDTRTSY
250	260	270	280	290	300	310	320
RIGDTWSKKD	NRGNLLQCIC	TGNGRGEWKC	ERHTSVQTTS	SGSGPFTDVR	AAVYQPQPHP	QPPPYGHCVT	DSGVVYSVGM
330	340	350	360	370	380	390	400
QWLKTQGNKQ	MLCTCLGNGV	SCQETAVTQT	YGGNSNGEPC	VLPFTYNGRT	FYSCTTEGRQ	DGHLWCSTTS	NYEQDQKYSF
410	420	430	440	450	460	470	480
CTDHTVLVQT	QGGNSNGALC	HFPFLYNNHN	YTDCTSEGRR	DNMKWCGTTQ	NYDADQKFGF	CPMAAHEEIC	TTNEGVMYRI
490	500	510	520	530	540	550	560
GDQWDKQHDM	GHMMRCTCVG	NGRGEWTCIA	YSQLRDQCIV	DDITYNVNDT	FHKRHEEGHM	LNCTCFGQGR	GRWKCDPVDQ
570	580	590	600	610	620	630	640
CQDSETGTFY	QIGDSWEKYV	HGVRYQCYCY	GRGIGEWHCQ	PLQTYPSSSG	PVEVFITETP	SQPNSHPIQW	NAPQPSHISK
650	660	670	680	690	700	710	720
YILRWRPKNS	VGRWKEATIP	GHLNSYTIKG	LKPGVVYEGQ	LISIQQYGHQ	EVTRFDFTTT	STSTPVTSNT	VTGETTPFSP
730	740	750	760	770	780	790	800
LVATSESVTE	ITASSFVVSW	VSASDTVSGF	RVEYELSEEG	DEPQYLDLPS	TATSVNIPDL	LPGRKYIVNV	YQISEDGEQS
810	820	830	840	850	860	870	880
LILSTSQTTA	PDAPPDPTVD	QVDDTSIVVR	WSRPQAPITG	YRIVYSPSVE	GSSTELNLPE	TANSVTLSDL	QPGVQYNITI
890	900	910	920	930	940	950	960
YAVEENQEST	PVVIQQETTG	TPRSDTVPSP	RDLQFVEVTD	VKVTIMWTPP	ESAVTGYRVD	VIPVNLPGEH	GQRLPISRNT
970	980	990	1000	1010	1020	1030	1040
FAEVTGLSPG	VTYYFKVFAV	SHGRESKPLT	AQQTTKLDAP	TNLQFVNETD	STVLVRWTPP	RAQITGYRLT	VGLTRRGQPR
1050	1060	1070	1080	1090	1100	1110	1120
QYNVGPSVSK	YPLRNLQPAS	EYTVSLVAIK	GNQESPKATG	VFTTLQPGSS	IPPYNTEVTE	TTIVITWTPA	PRIGFKLGVR
1130	1140	1150	1160	1170	1180	1190	1200
PSQGGEAPRE	VTSDSGSIVV	SGLTPGVEYV	YTIQVLRDGQ	ERDAPIVNKV	VTPLSPPTNL	HLEANPDTGV	LTVSWERSTT
1210	1220	1230	1240	1250	1260	1270	1280
PDITGYRITT	TPTNGQQGNS	LEEVVHADQS	SCTFDNLSPG	LEYNVSVYTV	KDDKESVPIS	DTIIPAVPPP	TDLRFTNIGP
1290	1300	1310	1320	1330	1340	1350	1360
DTMRVTWAPP	PSIDLTNFLV	RYSPVKNEED	VAELSISPSD	NAVVLTNLLP	GTEYVVSVSS	VYEQHESTPL	RGRQKTGLDS
1370	1380	1390	1400	1410	1420	1430	1440
PTGIDFSDIT	ANSFTVHWIA	PRATITGYRI	RHHPEHFSGR	PREDRVPHSR	NSITLTNLTP	GTEYVVSIVA	LNGREESPLL
1450	1460	1470	1480	1490	1500	1510	1520
IGQQSTVSDV	PRDLEVVAAT	PTSLLISWDA	PAVTVRYYRI	TYGETGGNSP	VQEFTVPGSK	STATISGLKP	GVDYTITVYA
1530	1540	1550	1560	1570	1580	1590	1600
VTGRGDSPAS	SKPISINYRT	EIDKPSQMQV	TDVQDNSISV	KWLPSSSPVT	GYRVTTTPKN	GPGPTKTKTA	GPDQTEMTIE
1610	1620	1630	1640	1650	1660	1670	1680
GLQPTVEYVV	SVYAQNPSGE	SQPLVQTAVT	NIDRPKGLAF	TDVDVDSIKI	AWESPQGQVS	RYRVTYSSPE	DGIHELFPAP
1690	1700	1710	1720	1730	1740	1750	1760
DGEEDTAELQ	GLRPGSEYTV	SVVALHDDME	SQPLIGTQST	AIPAPTDLKF	TQVTPTSLSA	QWTPPNVQLT	GYRVRVTPKE
1770	1780	1790	1800	1810	1820	1830	1840
KTGPMKEINL	APDSSSVVVS	GLMVATKYEV	SVYALKDTLT	SRPAQGVVTT	LENVSPPRRA	RVTDATETTI	TISWRTKTET
1850	1860	1870	1880	1890	1900	1910	1920
ITGFQVDAVP	ANGQTPIQRT	IKPDVRSYTI	TGLQPGTDYK	IYLYTLNDNA	RSSPVVIDAS	TAIDAPSNLR	FLATTPNSLL
1930	1940	1950	1960	1970	1980	1990	2000
VSWQPPRARI	TGYIIKYEKP	GSPPREVVPR	PRPGVTEATI	TGLEPGTEYT	IYVIALKNNQ	KSEPLIGRKK	TDELPQLVTL
2010	2020	2030	2040	2050	2060	2070	2080
PHPNLHGPEI	LDVPSTVQKT	PFVTHPGYDT	GNGIQLPGTS	GQQPSVGQQM	IFEEHGFRRT	TPPTTATPIR	HRPRPYPPNV
2090	2100	2110	2120	2130	2140	2150	2160
GEEIQIGHIP	REDVDYHLYP	HGPGLNPNAS	TGQEALSQTT	ISWAPFQDTS	EYIISCHPVG	TDEEPLQFRV	PGTSTSATLT
2170	2180	2190	2200	2210	2220	2230	2240
GLTRGATYNI	IVEALKDQQR	HKVREEVVTV	GNSVNEGLNQ	PTDDSCFDPY	TVSHYAVGDE	WERMSESGFK	LLCQCLGFGS
2250	2260	2270	2280	2290	2300	2310	2320
GHFRCDSSRW	CHDNGVNYKI	GEKWDRQGEN	GQMMSCTCLG	NGKGEFKCDP	HEATCYDDGK	TYHVGEQWQK	EYLGAICSCT
2330	2340	2350	2360	2370	2380	2390	
CFGGQRGWRC	DNCRRPGGEP	SPEGTTGQSY	NQYSQRYHQR	TNTNVNCPIE	CFMPLDVQAD	REDSRE	

Figure A.1. *Peptide fingerprinting for Fibronectin produced during peritoneal-ovarian cancer cell co-culture.*

Letters in red indicate peptides that were detected during MS (a) Protein identified in Table 2.1 (sample A1) as intact 440 kDa fibronectin produced by LP-9 cells alone (b) Protein identified in Table 2.1 (sample A2) as cleaved 220 kDa fibronectin produced by LP-9 cells alone (c) Protein identified in Table 2.1 (sample A7) as cleaved 120 kDa fibronectin (d) Protein identified in Table 2.1 (sample A8) as cleaved 70 kDa fibronectin.

a

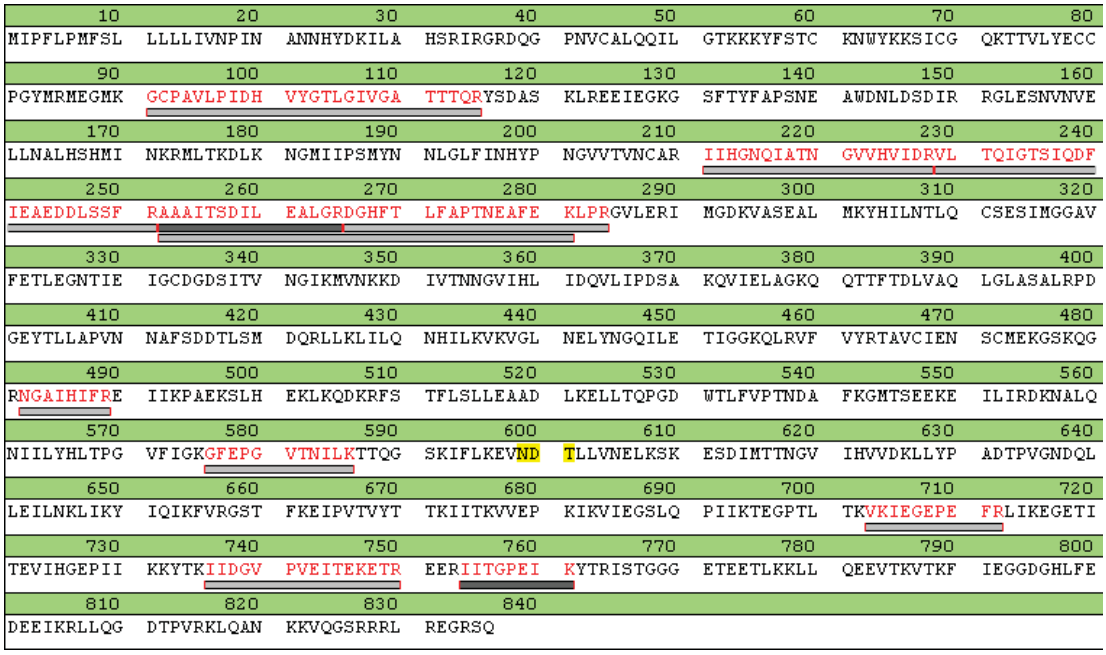

10	20	30	40	50	60	70	80
MIPFLPMFSL	LLLLIVNPIN	ANNHYDKILA	HSRIRGRDQG	PNVCALQQIL	GTKKKYFSTC	KNWYKKSICG	QKTTVLYECC
90	100	110	120	130	140	150	160
PGYMRMEGMK	GCPAVLPIDH	VYGTLGIVGA	TTTQRYSDAS	KLREEIEGKG	SFTYFAPSNE	AWDNLDSDIR	RGLESNVNVE
170	180	190	200	210	220	230	240
LLNALHSHMI	NKRMLTKDLK	NGMIIPSMYN	NLGLFINHYP	NGVVTVNCAR	IIHGNQIATN	GVVHVIDRVL	TQIGTSIQDF
250	260	270	280	290	300	310	320
IEAEDDLSSF	RAAAITSDIL	EALGRDGHFT	LFAPTNEAFE	KLPRGVLERI	MGDKVASEAL	MKYHILNTLQ	CSESIMGGAV
330	340	350	360	370	380	390	400
FETLEGNTIE	IGCDGDSITV	NGIKMVNKKD	IVTNNGVIHL	IDQVLIPDSA	KQVIELAGKQ	QTTFTDLVAQ	LGLASALRPD
410	420	430	440	450	460	470	480
GEYTLLAPVN	NAFSDDTLSM	DQRLLKLILQ	NHILKVKVGL	NELYNGQILE	TIGGKQLRVF	VYRTAVCIEN	SCMEKGSKQG
490	500	510	520	530	540	550	560
RNGAIHIFRE	IIKPAEKSLH	EKLKQDKRFS	TFLSLLEAAD	LKELLTQPGD	WTLFVPTNDA	FKGMTSEEKE	ILIRDKNALQ
570	580	590	600	610	620	630	640
NIILYHLTPG	VFIGKGFEPG	VTNILKTTQG	SKIFLKEVND	TLLVNELKSK	ESDIMTTNGV	IHVVDKLLYP	ADTPVGNDQL
650	660	670	680	690	700	710	720
LEILNKLIKY	IQIKFVRGST	FKEIPVTVYT	TKIITKVVEP	KIKVIEGSLQ	PIIKTEGPTL	TKVKIEGEPE	FRLIKEGETI
730	740	750	760	770	780	790	800
TEVIHGEPII	KKYTKIIDGV	PVEITEKETR	EERIITGPEI	KYTRISTGGG	ETEETLKKLL	QEEVTKVTKF	IEGGDGHLFE
810	820	830	840				
DEEIKRLLQG	DTPVRKLQAN	KKVQGSRRRL	REGRSQ				

Figure A.2. Peptide fingerprinting for Periostin produced during peritoneal-ovarian cancer cell co-culture.

Protein identified in Table 2.1**Table 2.1** (sample A3) as intact 90 kDa periostin produced by LP-9 cells alone.

a

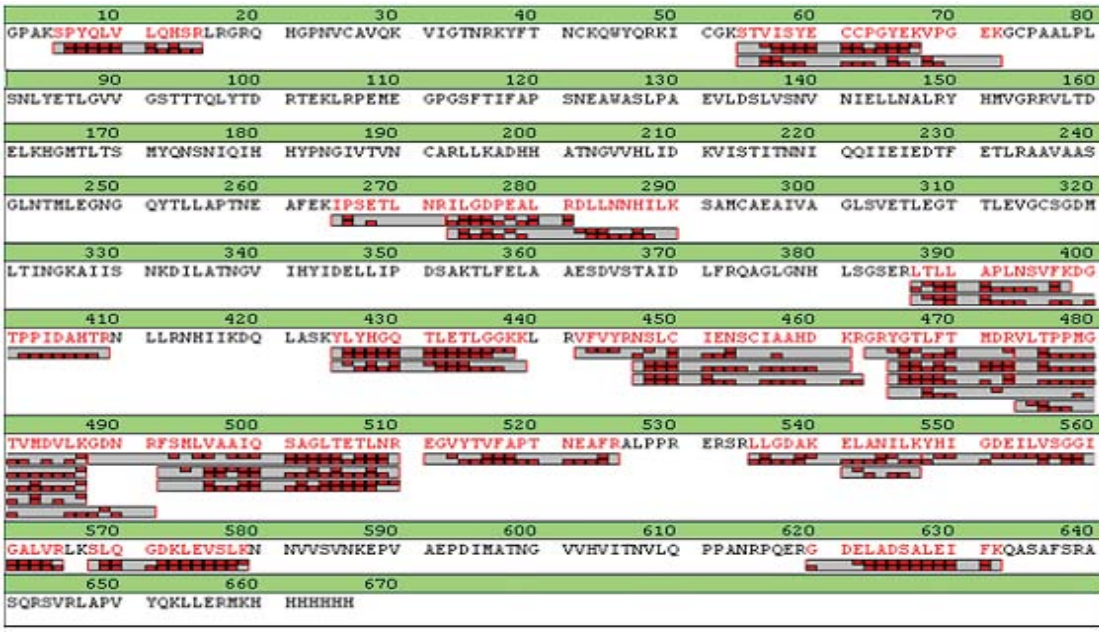
10 20 30 40 50 60 70 80
GPAKSPYQLV LQHSRLRGRQ HGPNVCAVQK VIGTNRKYFT NCKQWYQRKI CGKSTVISYE CCPGYEKVPG EKGCPAALPL
90 100 110 120 130 140 150 160
SNLYETLGVV GSTTTQLYTD RTEKLRPEME GPGSFTIFAP SNEAWASLPA EVLDSLVSNV NIELLNALRY HMVGRRVLTD
170 180 190 200 210 220 230 240
ELKHGMTLTS MYQNSNIQIH HYPNGIVTVN CARLLKADHH ATNGVVHLID KVISTITNNI QQIIEIEDTF ETLRAAVAAS
250 260 270 280 290 300 310 320
GLNTMLEGNG QYTLLAPTNE AFEKIPSETL NRILGDPEAL RDLLNNHILK SAMCAEAIVA GLSVETLEGT TLEVGCSGDM
330 340 350 360 370 380 390 400
LTINGKAIIS NKDILATNGV IHYIDELLIP DSAKTLFELA AESDVSTAID LFRQAGLGNH LSGSERLTLL APLNSVFKDG
410 420 430 440 450 460 470 480
TPPIDAHTRN LLRNHIIKDQ LASKYLYHGQ TLETLGGKKL RVFVYRNSLC IENSCIAAHD KRGRYGTLFT MDRVLTPPMG
490 500 510 520 530 540 550 560
TVMDVLKGDN RFSMLVAAIQ SAGLTETLNR EGVYTVFAPT NEAFRALPPR ERSRLLGDAK ELANILKYHI GDEILVSGGI
570 580 590 600 610 620 630 640
GALVRLKSLQ GDKLEVSLKN NVVSVNKEPV AEPDIMATNG VVHVITNVLQ PPANRPQERG DELADSALEI FKQASAFSRA
650 660 670
SQRSVRLAPV YQKLLERMKH HHHHHH

b

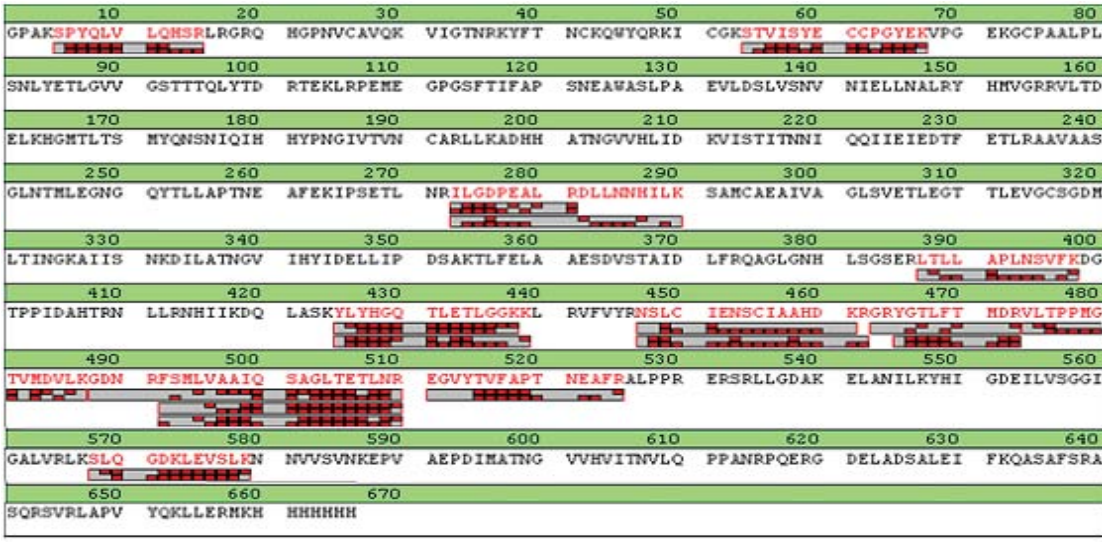
10 20 30 40 50 60 70 80
GPAKSPYQLV LQHSRLRGRQ HGPNVCAVQK VIGTNRKYFT NCKQWYQRKI CGKSTVISYE CCPGYEKVPG EKGCPAALPL
90 100 110 120 130 140 150 160
SNLYETLGVV GSTTTQLYTD RTEKLRPEME GPGSFTIFAP SNEAWASLPA EVLDSLVSNV NIELLNALRY HMVGRRVLTD
170 180 190 200 210 220 230 240
ELKHGMTLTS MYQNSNIQIH HYPNGIVTVN CARLLKADHH ATNGVVHLID KVISTITNNI QQIIEIEDTF ETLRAAVAAS
250 260 270 280 290 300 310 320
GLNTMLEGNG QYTLLAPTNE AFEKIPSETL NRILGDPEAL RDLLNNHILK SAMCAEAIVA GLSVETLEGT TLEVGCSGDM
330 340 350 360 370 380 390 400
LTINGKAIIS NKDILATNGV IHYIDELLIP DSAKTLFELA AESDVSTAID LFRQAGLGNH LSGSERLTLL APLNSVFKDG
410 420 430 440 450 460 470 480
TPPIDAHTRN LLRNHIIKDQ LASKYLYHGQ TLETLGGKKL RVFVYRNSLC IENSCIAAHD KRGRYGTLFT MDRVLTPPMG
490 500 510 520 530 540 550 560
TVMDVLKGDN RFSMLVAAIQ SAGLTETLNR EGVYTVFAPT NEAFRALPPR ERSRLLGDAK ELANILKYHI GDEILVSGGI
570 580 590 600 610 620 630 640
GALVRLKSLQ GDKLEVSLKN NVVSVNKEPV AEPDIMATNG VVHVITNVLQ PPANRPQERG DELADSALEI FKQASAFSRA
650 660 670
SQRSVRLAPV YQKLLERMKH HHHHHH

c

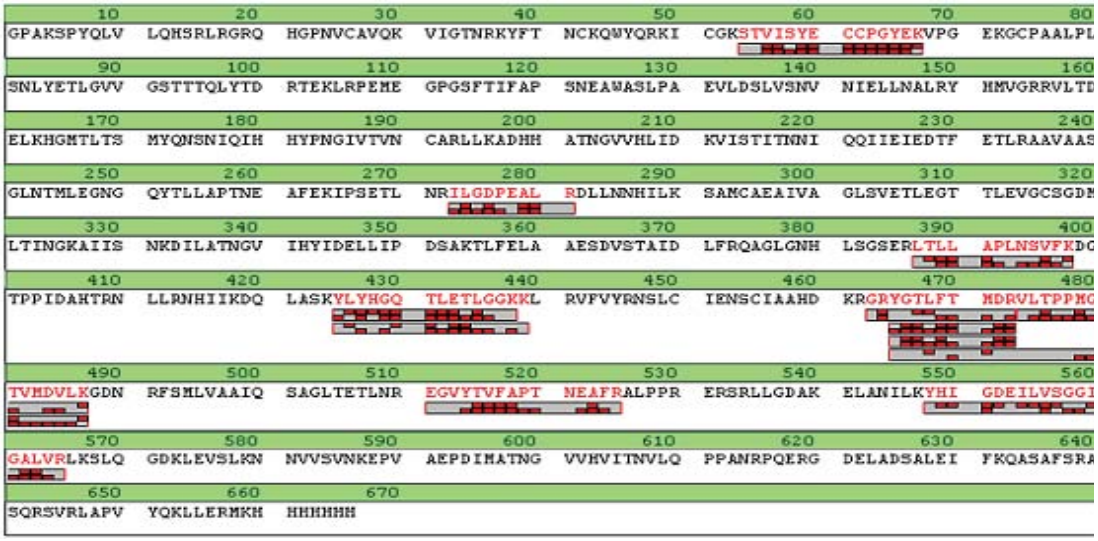

Figure A.3. Peptide fingerprinting for TGFBIp produced during peritoneal-ovarian cancer cell co-culture.

(a) Protein identified in Table 2.1 (sample A4) as intact 68 kDa TGFBIp produced by LP-9 cells alone. (b) Protein identified in Figure 3.8a (band 3) as cleaved 68 kDa TGFBIp (c) Protein identified in Figure 3.8a (band 4) as cleaved 68 kDa TGFBIp.

a

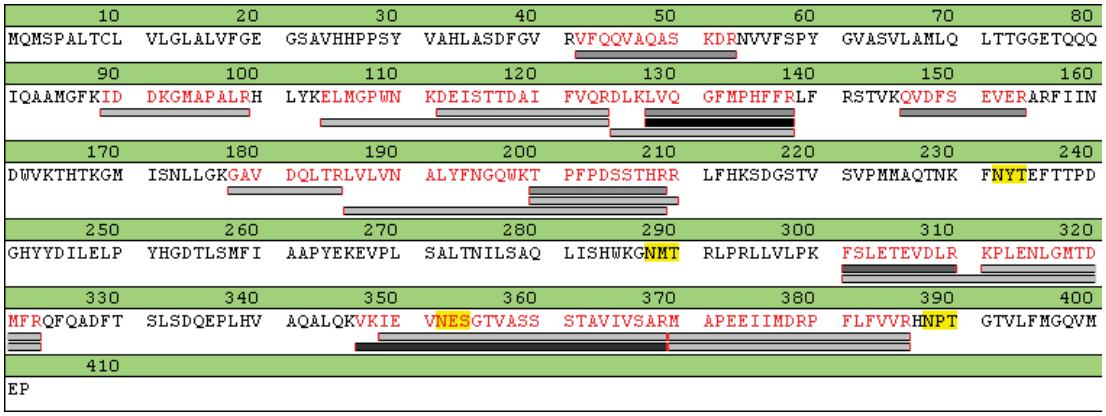
10 20 30 40 50 60 70 80
MQMSPALTCL VLGLALVFGE GSAVHHPPSY VAHLASDFGV RVFQQVAQAS KDRNVVFSPY GVASVLAMLQ LTTGGETQQQ
90 100 110 120 130 140 150 160
IQAAMGFKID DKGMAPALRH LYKELMGPWN KDEISTTDAI FVQRDLKLVQ GFMPHFFRLF RSTVKQVDFS EVERARFIIN
170 180 190 200 210 220 230 240
DWVKTHTKGM ISNLLGKGAV DQLTRLVLVN ALYFNGQWKT PFPDSSTHRR LFHKSDGSTV SVPMMAQTNK FNYTEFTTPD
250 260 270 280 290 300 310 320
GHYYDILELP YHGDTLSMFI AAPYEKEVPL SALTNILSAQ LISHWKGNMT RLPRLLVLPK FSLETEVDLR KPLENLGMTD
330 340 350 360 370 380 390 400
MFRQFQADFT SLSDQEPLHV AQALQKVKIE VNESGTVASS STAVIVSARM APEEIIMDRP FLFVVRHNPT GTVLFMGQVM
410
EP

b


10 20 30 40 50 60 70 80
MQMSPALTCL VLGLALVFGE GSAVHHPPSY VAHLASDFGV RVFQQVAQAS KDRNVVFSPY GVASVLAMLQ LTTGGETQQQ
90 100 110 120 130 140 150 160
IQAAMGFKID DKGMAPALRH LYKELMGPWN KDEISTTDAI FVQRDLKLVQ GFMPHFFRLF RSTVKQVDFS EVERARFIIN
170 180 190 200 210 220 230 240
DWVKTHTKGM ISNLLGKGAV DQLTRLVLVN ALYFNGQWKT PFPDSSTHRR LFHKSDGSTV SVPMMAQTNK FNYTEFTTPD
250 260 270 280 290 300 310 320
GHYYDILELP YHGDTLSMFI AAPYEKEVPL SALTNILSAQ LISHWKGNMT RLPRLLVLPK FSLETEVDLR KPLENLGMTD
330 340 350 360 370 380 390 400
MFRQFQADFT SLSDQEPLHV AQALQKVKIE VNESGTVASS STAVIVSARM APEEIIMDRP FLFVVRHNPT GTVLFMGQVM
410
EP

c

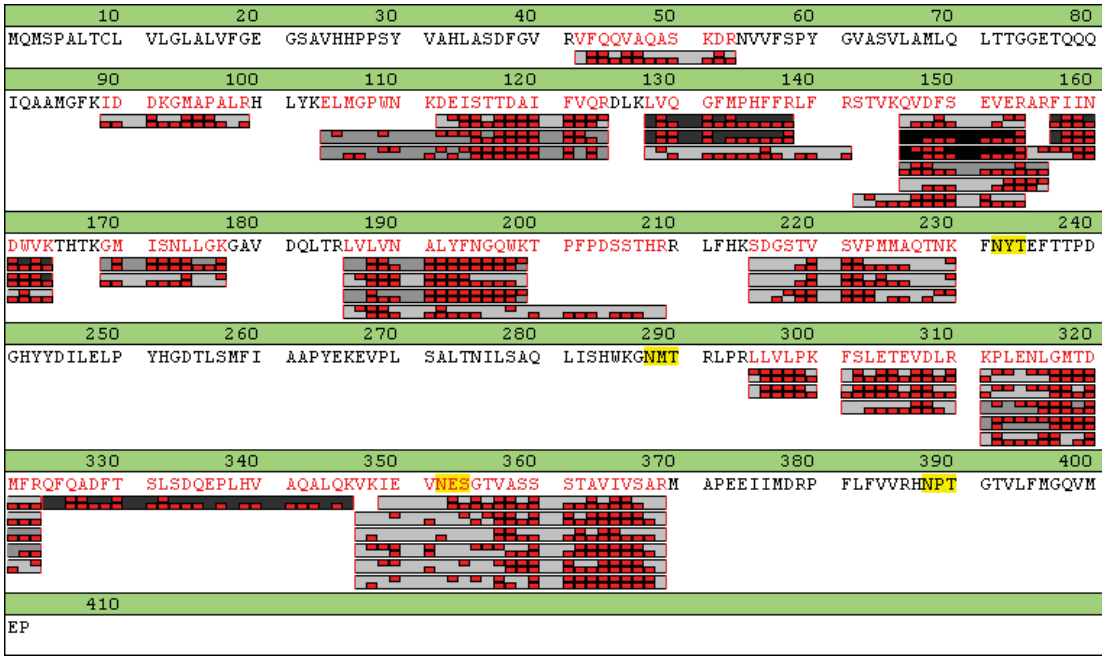

Figure A.4. Peptide fingerprinting for PAI-1 produced during peritoneal-ovarian cancer cell co-culture.

(a) Protein identified in Table 2.1 (sample A5) as intact 45 kDa PAI-1 produced by Lp-9 cells alone (b) Protein identified in Table 2.2 (sample B4) as cleaved 44 kDa PAI-1 (c) Protein identified in Table 2.3 (Sample C4) as cleaved 44 kDa PAI-1

a

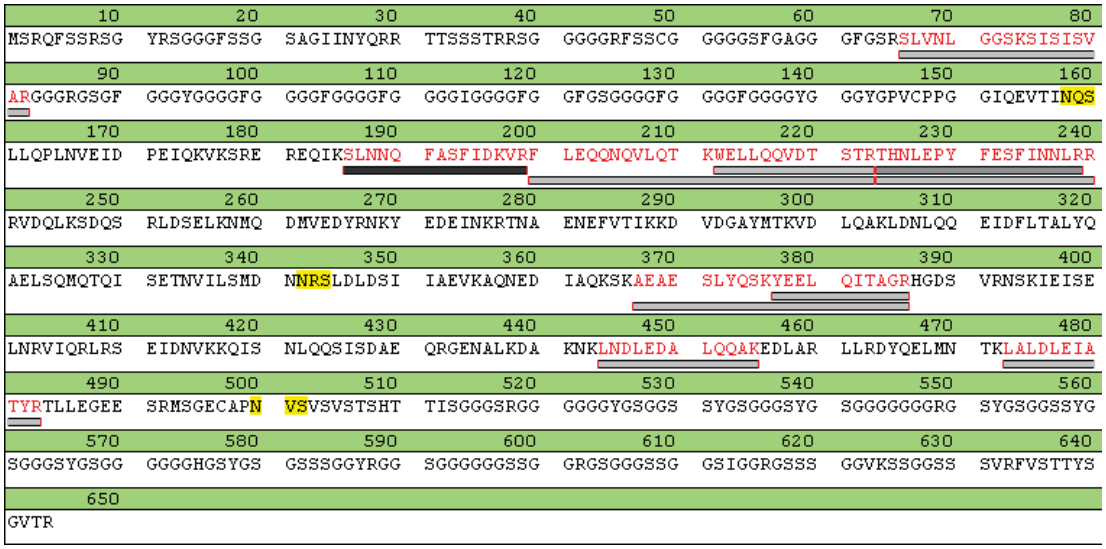
10 20 30 40 50 60 70 80
MSRQFSSRSG YRSGGGFSSG SAGIINYQRR TTSSSTRRSG GGGGRFSSCG GGGGSFGAGG GFGSRSLVNL GGSKSISISV
90 100 110 120 130 140 150 160
ARGGGRGSGF GGGYGGGGFG GGGFGGGGFG GGGIGGGGFG GFGSGGGGFG GGGFGGGGYG GGYGPVCPPG GIQEVTINQS
170 180 190 200 210 220 230 240
LLQPLNVEID PEIQKVKSRE REQIKSLNNQ FASFIDKVRF LEQQNQVLQT KWELLQQVDT STRTHNLEPY FESFINNLRR
250 260 270 280 290 300 310 320
RVDQLKSDQS RLDSELKNMQ DMVEDYRNKY EDEINKRTNA ENEFVTIKKD VDGAYMTKVD LQAKLDNLQQ EIDFLTALYQ
330 340 350 360 370 380 390 400
AELSQMQTQI SETNVILSMD NNRSLDLDSI IAEVKAQNED IAQKSKAEAE SLYQSKYEEL QITAGRHGDS VRNSKIEISE
410 420 430 440 450 460 470 480
LNRVIQRLRS EIDNVKKQIS NLQQSISDAE QRGENALKDA KNKLNDLEDA LQQAKEDLAR LLRDYQELMN TKLALDLEIA
490 500 510 520 530 540 550 560
TYRTLLEGEE SRMSGECAPN VSVSVSTSHT TISGGGSRGG GGGGYGSGGS SYGSGGGSYG SGGGGGGGRG SYGSGGSSYG
570 580 590 600 610 620 630 640
SGGGSYGSGG GGGGHGSYGS GSSSGGYRGG SGGGGGGSSG GRGSGGGSSG GSIGGRGSSS GGVKSSGGSS SVRFVSTTYS
650
GVTR

b

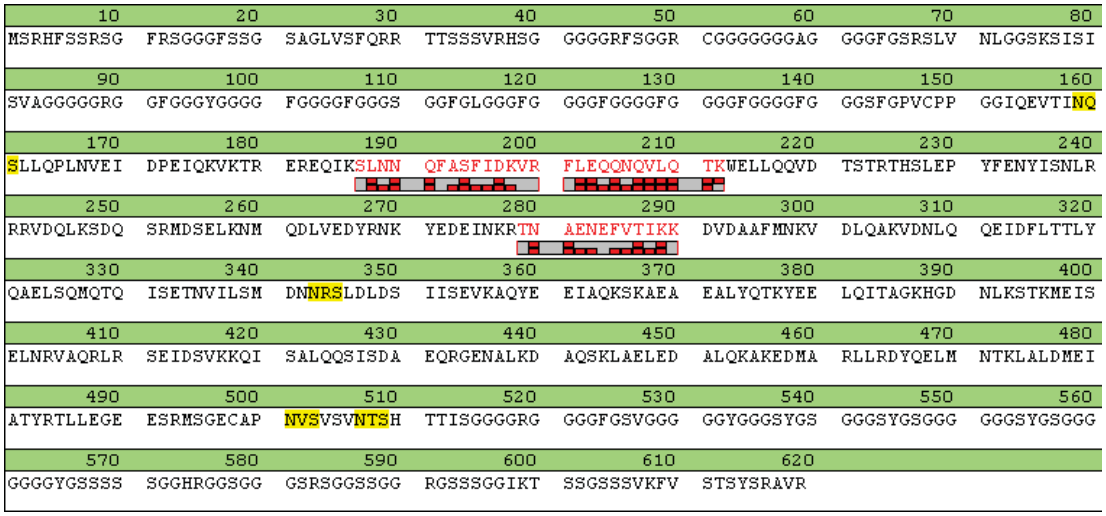
10 20 30 40 50 60 70 80
MSRHFSSRSG FRSGGGFSSG SAGLVSFQRR TTSSSVRHSG GGGGRFSGGR CGGGGGGGAG GGGFGSRSLV NLGGSKSISI
90 100 110 120 130 140 150 160
SVAGGGGGRG GFGGGYGGGG FGGGGFGGGS GGFGLGGGFG GGGFGGGGFG GGGFGGGGFG GGSFGPVCPP GGIQEVTINQ
170 180 190 200 210 220 230 240
SLLQPLNVEI DPEIQKVKTR EREQIKSLNN QFASFIDKVR FLEQQNQVLQ TKWELLQQVD TSTRTHSLEP YFENYISNLR
250 260 270 280 290 300 310 320
RRVDQLKSDQ SRMDSELKNM QDLVEDYRNK YEDEINKRTN AENEFVTIKK DVDAAFMNKV DLQAKVDNLQ QEIDFLTTLY
330 340 350 360 370 380 390 400
QAELSQMQTQ ISETNVILSM DNNRSLDLDS IISEVKAQYE EIAQKSKAEA EALYQTKYEE LQITAGKHGD NLKSTKMEIS
410 420 430 440 450 460 470 480
ELNRVAQRLR SEIDSVKKQI SALQQSISDA EQRGENALKD AQSKLAELED ALQKAKEDMA RLLRDYQELM NTKLALDMEI
490 500 510 520 530 540 550 560
ATYRTLLEGE ESRMSGECAP NVSVSVNTSH TTISGGGGRG GGGFGSVGGG GGYGGGSYGS GGGSYGSGGG GGGSYGSGGG
570 580 590 600 610 620
GGGGYGSSSS SGGHRGGSGG GSRSGGSSGG RGSSSGGIKT SSGSSSVKFV STSYSRAVR

c

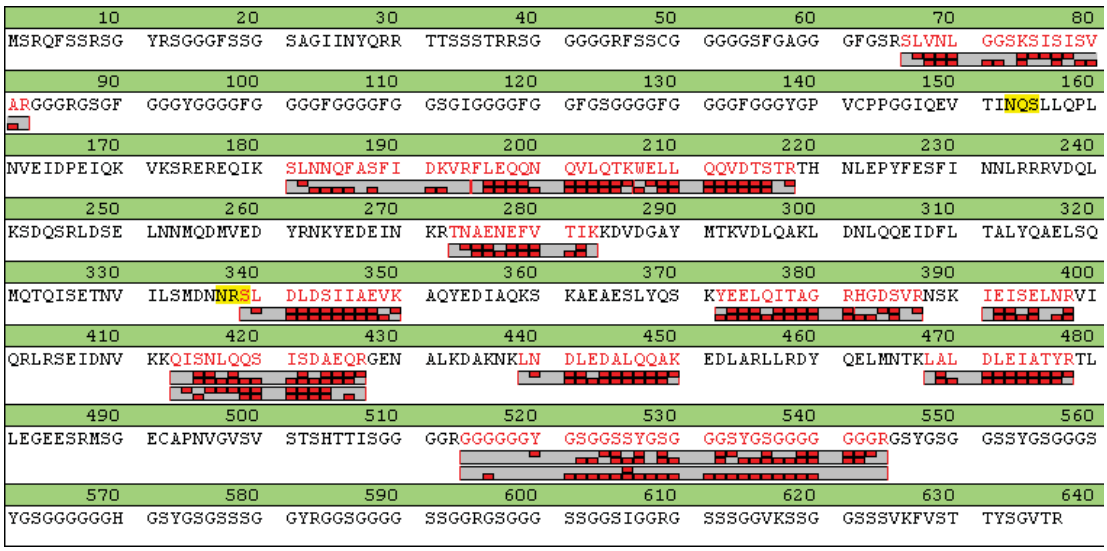
10 20 30 40 50 60 70 80
MSRQFSSRSG YRSGGGFSSG SAGIINYQRR TTSSSTRRSG GGGGRFSSCG GGGGSFGAGG GFGSRSLVNL GGSKSISISV
90 100 110 120 130 140 150 160
ARGGGRGSGF GGGYGGGGFG GGGFGGGGFG GSGIGGGGFG GFGSGGGGFG GGGFGGGYGP VCPPGGIQEV TINQSLLQPL
170 180 190 200 210 220 230 240
NVEIDPEIQK VKSREREQIK SLNNQFASFI DKVRFLEQQN QVLQTKWELL QQVDTSTRTH NLEPYFESFI NNLRRRVDQL
250 260 270 280 290 300 310 320
KSDQSRLDSE LNNMQDMVED YRNKYEDEIN KRTNAENEFV TIKKDVDGAY MTKVDLQAKL DNLQQEIDFL TALYQAELSQ
330 340 350 360 370 380 390 400
MQTQISETNV ILSMDNNRSL DLDSIIAEVK AQYEDIAQKS KAEAESLYQS KYEELQITAG RHGDSVRNSK IEISELNRVI
410 420 430 440 450 460 470 480
QRLRSEIDNV KKQISNLQQS ISDAEQRGEN ALKDAKNKLN DLEDALQQAK EDLARLLRDY QELMNTKLAL DLEIATYRTL
490 500 510 520 530 540 550 560
LEGEESRMSG ECAPNVGVSV STSHTTISGG GGRGGGGGGY GSGGSSYGSG GGSYGSGGGG GGGRGSYGSG GSSYGSGGGS
570 580 590 600 610 620 630 640
YGSGGGGGGH GSYGSGSSSG GYRGGSGGGG SSGGRGSGGG SSGGSIGGRG SSSGGVKSSG GSSSVKFVST TYSGVTR

d

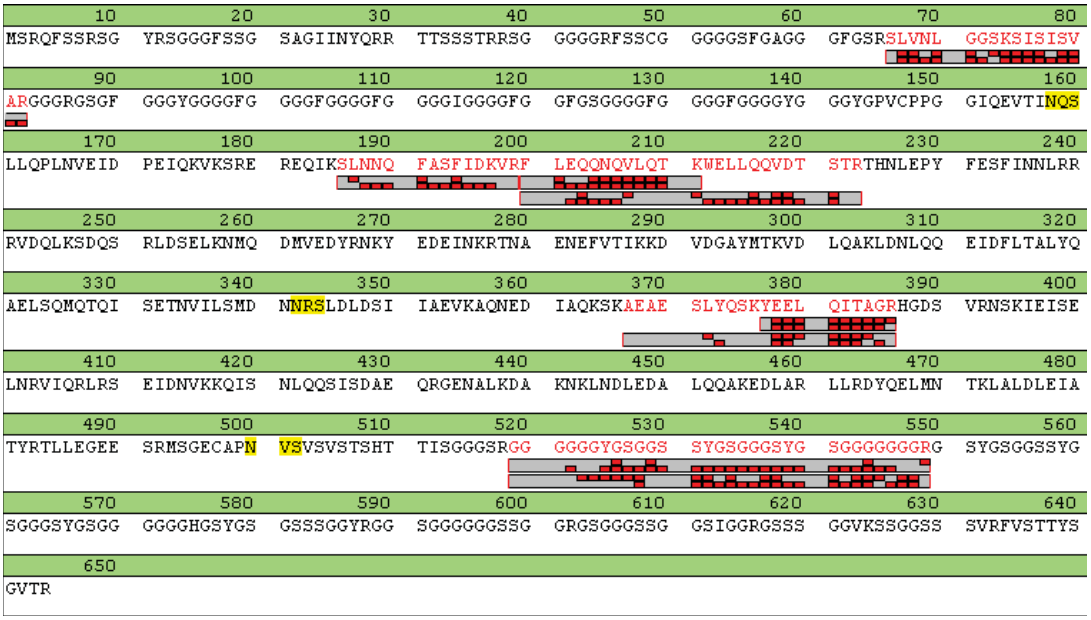
10 20 30 40 50 60 70 80
MSRQFSSRSG YRSGGGFSSG SAGIINYQRR TTSSSTRRSG GGGGRFSSCG GGGGSFGAGG GFGSRSLVNL GGSKSISISV
90 100 110 120 130 140 150 160
ARGGGRGSGF GGGYGGGGFG GGGFGGGGFG GGGIGGGGFG GFGSGGGGFG GGGFGGGGYG GGYGPVCPPG GIQEVTINQS
170 180 190 200 210 220 230 240
LLQPLNVEID PEIQKVKSRE REQIKSLNNQ FASFIDKVRF LEQQNQVLQT KWELLQQVDT STRTHNLEPY FESFINNLRR
250 260 270 280 290 300 310 320
RVDQLKSDQS RLDSELKNMQ DMVEDYRNKY EDEINKRTNA ENEFVTIKKD VDGAYMTKVD LQAKLDNLQQ EIDFLTALYQ
330 340 350 360 370 380 390 400
AELSQMQTQI SETNVILSMD NNRSLDLDSI IAEVKAQNED IAQKSKAEAE SLYQSKYEEL QITAGRHGDS VRNSKIEISE
410 420 430 440 450 460 470 480
LNRVIQRLRS EIDNVKKQIS NLQQSISDAE QRGENALKDA KNKLNDLEDA LQQAKEDLAR LLRDYQELMN TKLALDLEIA
490 500 510 520 530 540 550 560
TYRTLLEGEE SRMSGECAPN VSVSVSTSHT TISGGGSRGG GGGGYGSGGS SYGSGGGSYG SGGGGGGGRG SYGSGGSSYG
570 580 590 600 610 620 630 640
SGGGSYGSGG GGGGHGSYGS GSSSGGYRGG SGGGGGGSSG GRGSGGGSSG GSIGGRGSSS GGVKSSGGSS SVRFVSTTYS
650
GVTR

e

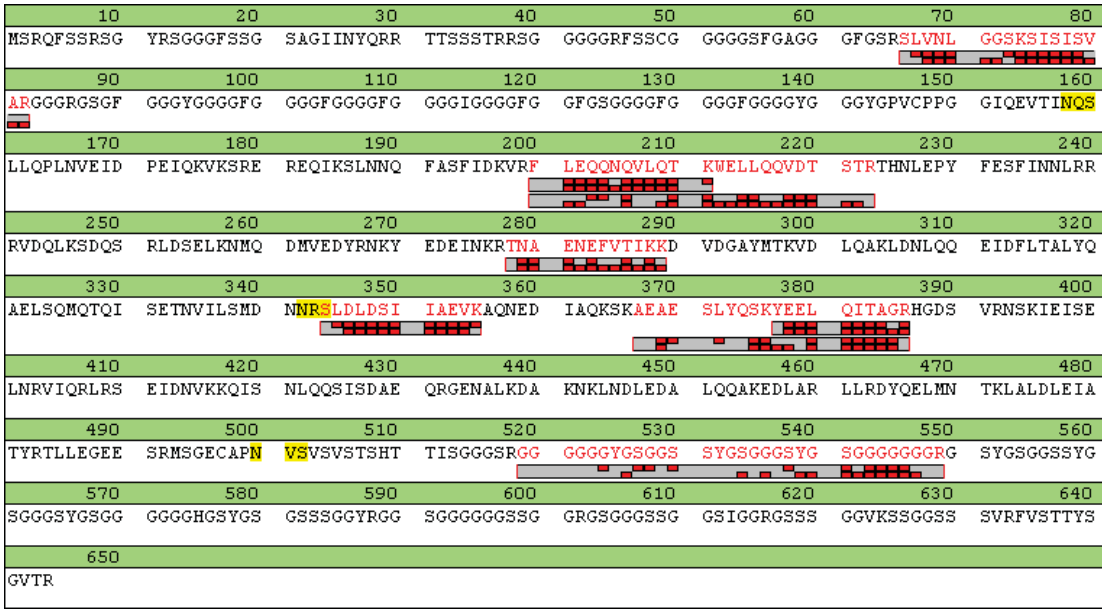
10 20 30 40 50 60 70 80
MSRQFSSRSG YRSGGGFSSG SAGIINYQRR TTSSSTRRSG GGGGRFSSCG GGGGSFGAGG GFGSRSLVNL GGSKSISISV
90 100 110 120 130 140 150 160
ARGGGRGSGF GGGYGGGGFG GGGFGGGGFG GGGIGGGGFG GFGSGGGGFG GGGFGGGGYG GGYGPVCPPG GIQEVTINQS
170 180 190 200 210 220 230 240
LLQPLNVEID PEIQKVKSRE REQIKSLNNQ FASFIDKVRF LEQQNQVLQT KWELLQQVDT STRTHNLEPY FESFINNLRR
250 260 270 280 290 300 310 320
RVDQLKSDQS RLDSELKNMQ DMVEDYRNKY EDEINKRTNA ENEFVTIKKD VDGAYMTKVD LQAKLDNLQQ EIDFLTALYQ
330 340 350 360 370 380 390 400
AELSQMQTQI SETNVILSMD NNRSLDLDSI IAEVKAQNED IAQKSKAEAE SLYQSKYEEL QITAGRHGDS VRNSKIEISE
410 420 430 440 450 460 470 480
LNRVIQRLRS EIDNVKKQIS NLQQSISDAE QRGENALKDA KNKLNDLEDA LQQAKEDLAR LLRDYQELMN TKLALDLEIA
490 500 510 520 530 540 550 560
TYRTLLEGEE SRMSGECAPN VSVSVSTSHT TISGGGSRGG GGGGYGSGGS SYGSGGGSYG SGGGGGGGRG SYGSGGSSYG
570 580 590 600 610 620 630 640
SGGGSYGSGG GGGGHGSYGS GSSSGGYRGG SGGGGGGSSG GRGSGGGSSG GSIGGRGSSS GGVKSSGGSS SVRFVSTTYS
650
GVTR

f

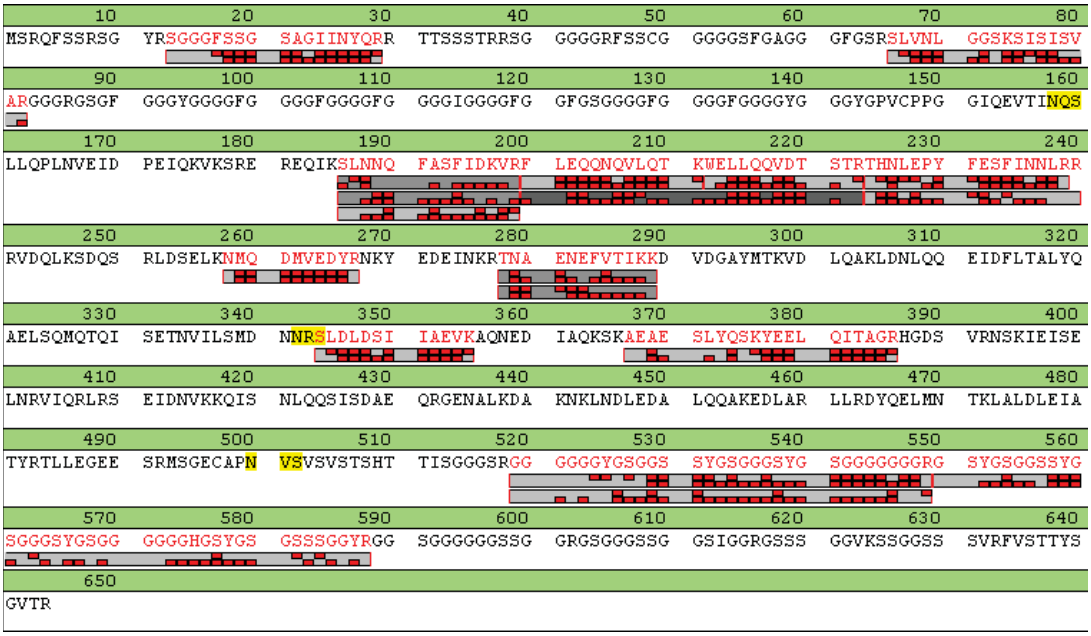
10 20 30 40 50 60 70 80
MSRQFSSRSG YRSGGGFSSG SAGIINYQRR TTSSSTRRSG GGGGRFSSCG GGGGSFGAGG GFGSRSLVNL GGSKSISISV
90 100 110 120 130 140 150 160
ARGGGRGSGF GGGYGGGGFG GGGFGGGGFG GGGIGGGGFG GFGSGGGGFG GGGFGGGGYG GGYGPVCPPG GIQEVTINQS
170 180 190 200 210 220 230 240
LLQPLNVEID PEIQKVKSRE REQIKSLNNQ FASFIDKVRF LEQQNQVLQT KWELLQQVDT STRTHNLEPY FESFINNLRR
250 260 270 280 290 300 310 320
RVDQLKSDQS RLDSELKNMQ DMVEDYRNKY EDEINKRTNA ENEFVTIKKD VDGAYMTKVD LQAKLDNLQQ EIDFLTALYQ
330 340 350 360 370 380 390 400
AELSQMQTQI SETNVILSMD NNRSLDLDSI IAEVKAQNED IAQKSKAEAE SLYQSKYEEL QITAGRHGDS VRNSKIEISE
410 420 430 440 450 460 470 480
LNRVIQRLRS EIDNVKKQIS NLQQSISDAE QRGENALKDA KNKLNDLEDA LQQAKEDLAR LLRDYQELMN TKLALDLEIA
490 500 510 520 530 540 550 560
TYRTLLEGEE SRMSGECAPN VSVSVSTSHT TISGGGSRGG GGGGYGSGGS SYGSGGGSYG SGGGGGGGRG SYGSGGSSYG
570 580 590 600 610 620 630 640
SGGGSYGSGG GGGGHGSYGS GSSSGGYRGG SGGGGGGSSG GRGSGGGSSG GSIGGRGSSS GGVKSSGGSS SVRFVSTTYS
650
GVTR

g

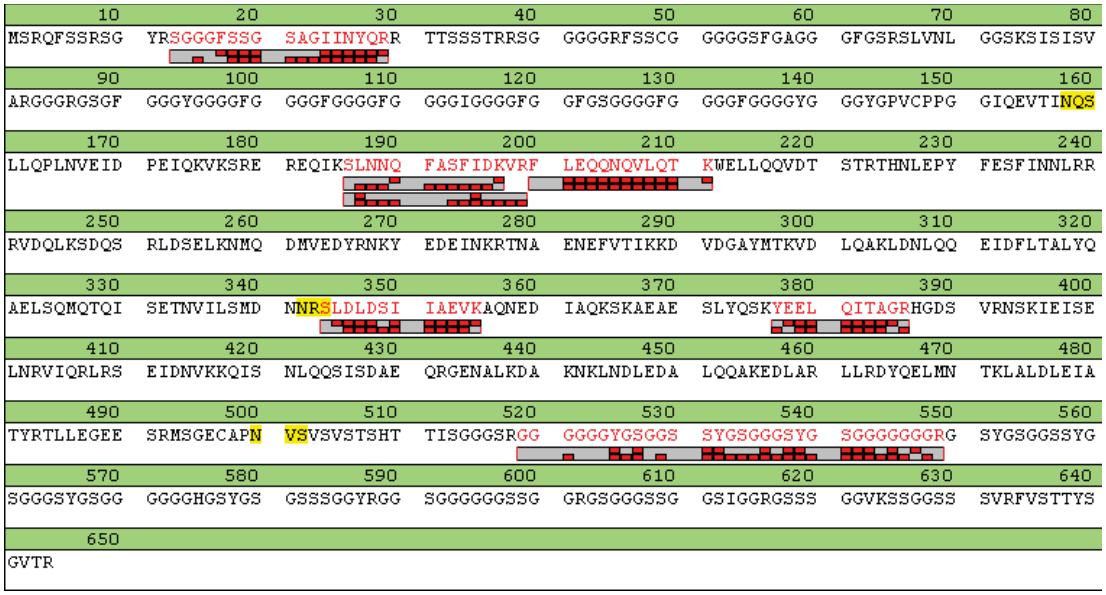
10 20 30 40 50 60 70 80
MSRQFSSRSG YRSGGGFSSG SAGIINYQRR TTSSSTRRSG GGGGRFSSCG GGGGSFGAGG GFGSRSLVNL GGSKSISISV
90 100 110 120 130 140 150 160
ARGGGRGSGF GGGYGGGGFG GGGFGGGGFG GGGIGGGGFG GFGSGGGGFG GGGFGGGGYG GGYGPVCPPG GIQEVTINQS
170 180 190 200 210 220 230 240
LLQPLNVEID PEIQKVKSRE REQIKSLNNQ FASFIDKVRF LEQQNQVLQT KWELLQQVDT STRTHNLEPY FESFINNLRR
250 260 270 280 290 300 310 320
RVDQLKSDQS RLDSELKNMQ DMVEDYRNKY EDEINKRTNA ENEFVTIKKD VDGAYMTKVD LQAKLDNLQQ EIDFLTALYQ
330 340 350 360 370 380 390 400
AELSQMQTQI SETNVILSMD NNRSLDLDSI IAEVKAQNED IAQKSKAEAE SLYQSKYEEL QITAGRHGDS VRNSKIEISE
410 420 430 440 450 460 470 480
LNRVIQRLRS EIDNVKKQIS NLQQSISDAE QRGENALKDA KNKLNDLEDA LQQAKEDLAR LLRDYQELMN TKLALDLEIA
490 500 510 520 530 540 550 560
TYRTLLEGEE SRMSGECAPN VSVSVSTSHT TISGGGSRGG GGGGYGSGGS SYGSGGGSYG SGGGGGGGRG SYGSGGSSYG
570 580 590 600 610 620 630 640
SGGGSYGSGG GGGGHGSYGS GSSSGGYRGG SGGGGGGSSG GRGSGGGSSG GSIGGRGSSS GGVKSSGGSS SVRFVSTTYS
650
GVTR

h

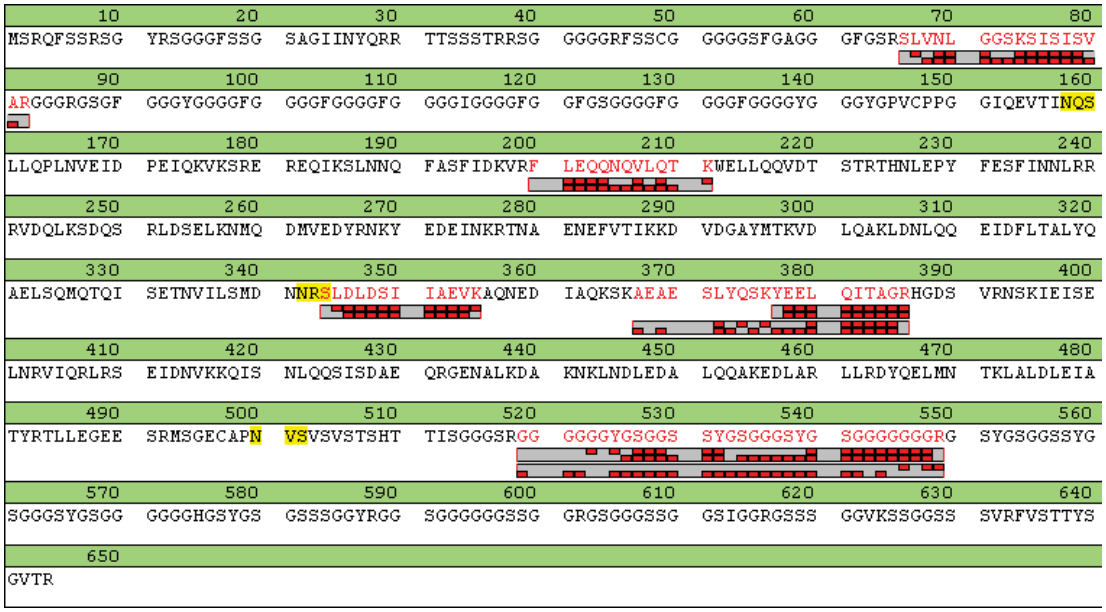
10 20 30 40 50 60 70 80
MSRQFSSRSG YRSGGGFSSG SAGIINYQRR TTSSSTRRSG GGGGRFSSCG GGGGSFGAGG GFGSRSLVNL GGSKSISISV
90 100 110 120 130 140 150 160
ARGGGRGSGF GGGYGGGGFG GGGFGGGGFG GGGIGGGGFG GFGSGGGGFG GGGFGGGGYG GGYGPVCPPG GIQEVTINQS
170 180 190 200 210 220 230 240
LLQPLNVEID PEIQKVKSRE REQIKSLNNQ FASFIDKVRF LEQQNQVLQT KWELLQQVDT STRTHNLEPY FESFINNLRR
250 260 270 280 290 300 310 320
RVDQLKSDQS RLDSELKNMQ DMVEDYRNKY EDEINKRTNA ENEFVTIKKD VDGAYMTKVD LQAKLDNLQQ EIDFLTALYQ
330 340 350 360 370 380 390 400
AELSQMQTQI SETNVILSMD NNRSLDLDSI IAEVKAQNED IAQKSKAEAE SLYQSKYEEL QITAGRHGDS VRNSKIEISE
410 420 430 440 450 460 470 480
LNRVIQRLRS EIDNVKKQIS NLQQSISDAE QRGENALKDA KNKLNDLEDA LQQAKEDLAR LLRDYQELMN TKLALDLEIA
490 500 510 520 530 540 550 560
TYRTLLEGEE SRMSGECAPN VSVSVSTSHT TISGGGSRGG GGGGYGSGGS SYGSGGGSYG SGGGGGGGRG SYGSGGSSYG
570 580 590 600 610 620 630 640
SGGGSYGSGG GGGGHGSYGS GSSSGGYRGG SGGGGGGSSG GRGSGGGSSG GSIGGRGSSS GGVKSSGGSS SVRFVSTTYS
650
GVTR

i

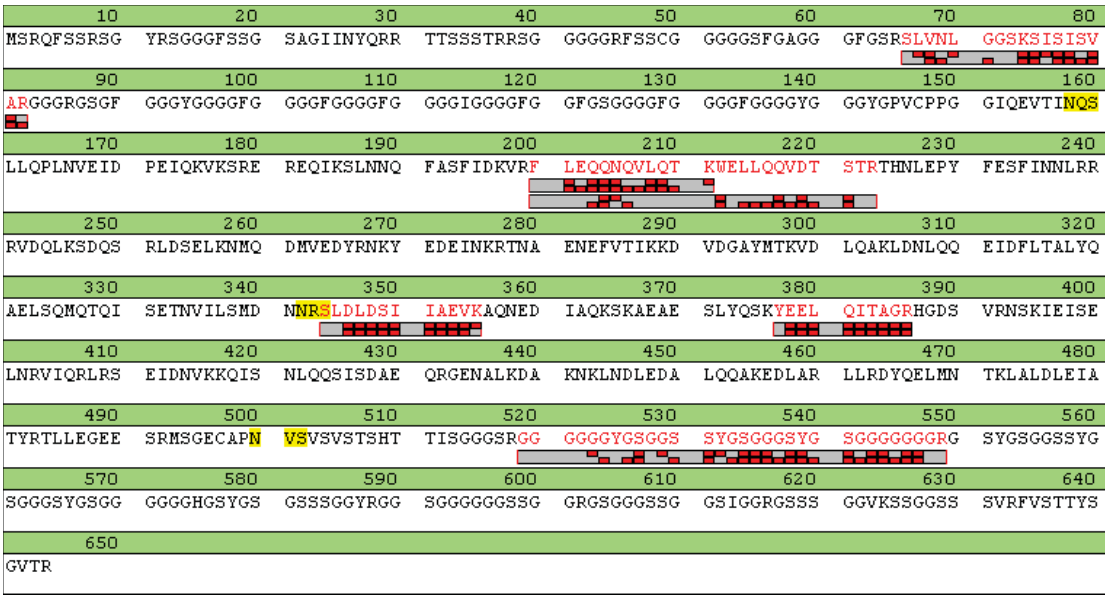
10 20 30 40 50 60 70 80
MSRQFSSRSG YRSGGGFSSG SAGIINYQRR TTSSSTRRSG GGGGRFSSCG GGGGSFGAGG GFGSRSLVNL GGSKSISISV
90 100 110 120 130 140 150 160
ARGGGRGSGF GGGYGGGGFG GGGFGGGGFG GGGIGGGGFG GFGSGGGGFG GGGFGGGGYG GGYGPVCPPG GIQEVTINQS
170 180 190 200 210 220 230 240
LLQPLNVEID PEIQKVKSRE REQIKSLNNQ FASFIDKVRF LEQQNQVLQT KWELLQQVDT STRTHNLEPY FESFINNLRR
250 260 270 280 290 300 310 320
RVDQLKSDQS RLDSELKNMQ DMVEDYRNKY EDEINKRTNA ENEFVTIKKD VDGAYMTKVD LQAKLDNLQQ EIDFLTALYQ
330 340 350 360 370 380 390 400
AELSQMQTQI SETNVILSMD NNRSLDLDSI IAEVKAQNED IAQKSKAEAE SLYQSKYEEL QITAGRHGDS VRNSKIEISE
410 420 430 440 450 460 470 480
LNRVIQRLRS EIDNVKKQIS NLQQSISDAE QRGENALKDA KNKLNDLEDA LQQAKEDLAR LLRDYQELMN TKLALDLEIA
490 500 510 520 530 540 550 560
TYRTLLEGEE SRMSGECAPN VSVSVSTSHT TISGGGSRGG GGGGYGSGGS SYGSGGGSYG SGGGGGGGRG SYGSGGSSYG
570 580 590 600 610 620 630 640
SGGGSYGSGG GGGGHGSYGS GSSSGGYRGG SGGGGGGSSG GRGSGGGSSG GSIGGRGSSS GGVKSSGGSS SVRFVSTTYS
650
GVTR

j

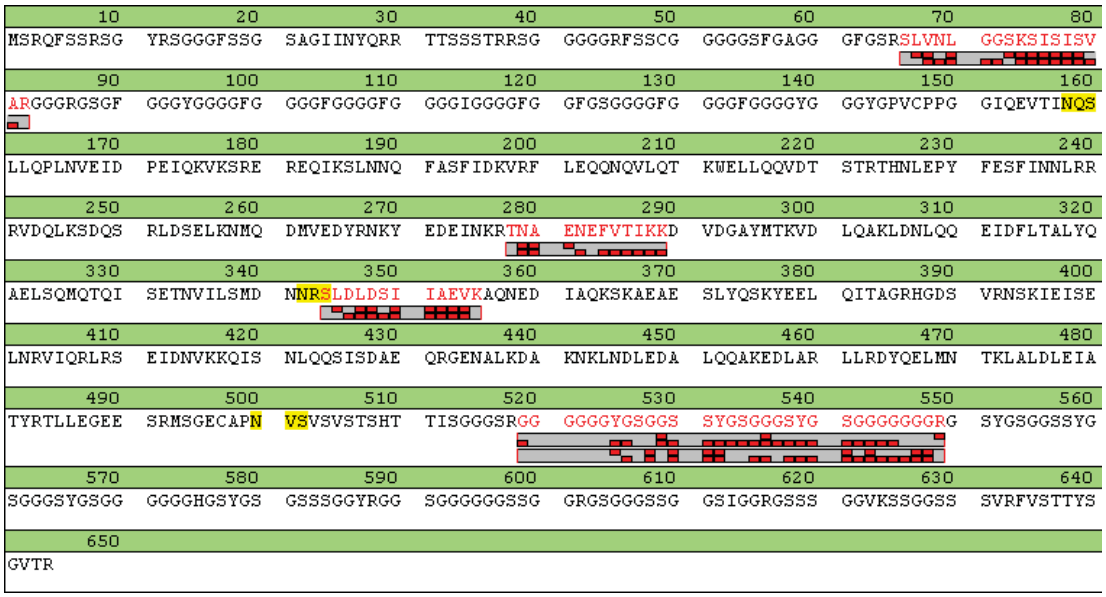

Figure A.5. Peptide fingerprinting for CK-1 produced during peritoneal-ovarian cancer cell co-culture.

(a) Protein identified in Table 2.1 (sample A6) as a likely 120 kDa CK-1 dimer (b) Protein identified in Table 2.2 (sample B3) as cleaved 50 kDa CK-1 (c) Protein identified in Table 2.2 (Sample B8) as cleaved 34 kDa CK-1 (d) Protein identified in Table 2.2. (Sample B9) as cleaved 33 kDa CK-1 (e) Protein identified in Table 2.3 (Sample C2) as cleaved 55 kDa CK-1 (f) Protein identified in Table 2.3 (Sample C4) as cleaved 48 kDa CK-1 (g) Protein identified in Table 2.3 (Sample C5) as cleaved 44 kDa CK-1 (hr) Protein identified in Table 2.3 (Sample C9) as cleaved 35 kDa CK-1 (i) Protein identified in Table 2.3 (Sample C10) as cleaved 35 kDa CK-1 (j) Protein identified in Table 2.3 (Sample C11) as cleaved 34 kDa CK-1.

a

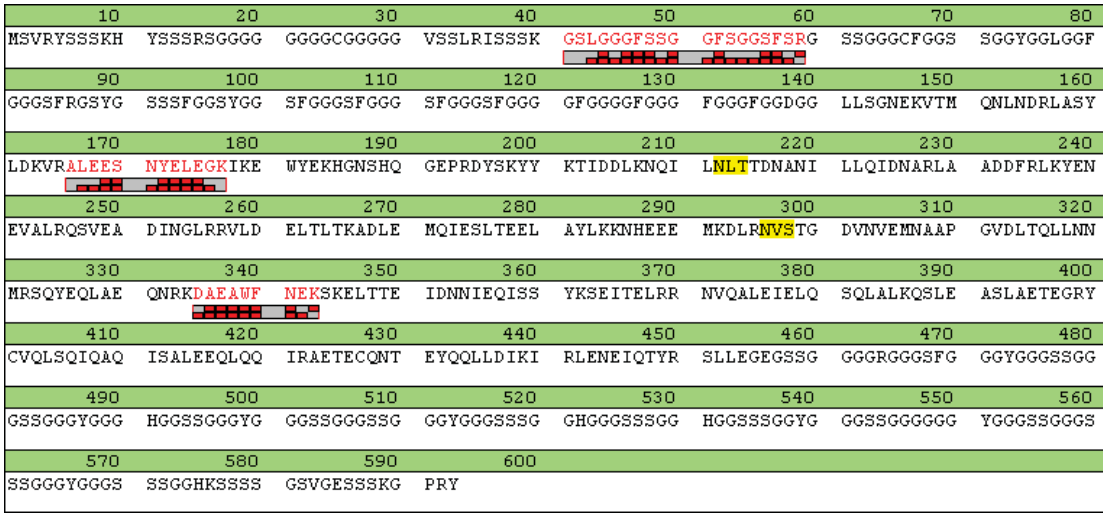
10 20 30 40 50 60 70 80
MSVRYSSSKH YSSSRSGGGG GGGGCGGGGG VSSLRISSSK GSLGGGFSSG GFSGGSFSRG SSGGGCFGGS SGGYGGLGGF
90 100 110 120 130 140 150 160
GGGSFRGSYG SSSFGGSYGG SFGGGSFGGG SFGGGSFGGG GFGGGGFGGG FGGGFGGDGG LLSGNEKVTM QNLNDRLASY
170 180 190 200 210 220 230 240
LDKVRALEES NYELEGKIKE WYEKHGNSHQ GEPRDYSKYY KTIDDLKNQI LNLTTDNANI LLQIDNARLA ADDFRLKYEN
250 260 270 280 290 300 310 320
EVALRQSVEA DINGLRRVLD ELTLTKADLE MQIESLTEEL AYLKKNHEEE MKDLRNVSTG DVNVEMNAAP GVDLTQLLNN
330 340 350 360 370 380 390 400
MRSQYEQLAE QNRKDAEAWF NEKSKELTTE IDNNIEQISS YKSEITELRR NVQALEIELQ SQLALKQSLE ASLAETEGRY
410 420 430 440 450 460 470 480
CVQLSQIQAQ ISALEEQLQQ IRAETECQNT EYQQLLDIKI RLENEIQTYR SLLEGEGSSG GGGRGGGSFG GGYGGGSSGG
490 500 510 520 530 540 550 560
GSSGGGYGGG HGGSSGGGYG GGSSGGGSSG GGYGGGSSSG GHGGGSSSGG HGGSSSGGYG GGSSGGGGGG YGGGSSGGGS
570 580 590 600
SSGGGYGGGS SSGGHKSSSS GSVGESSSKG PRY

b

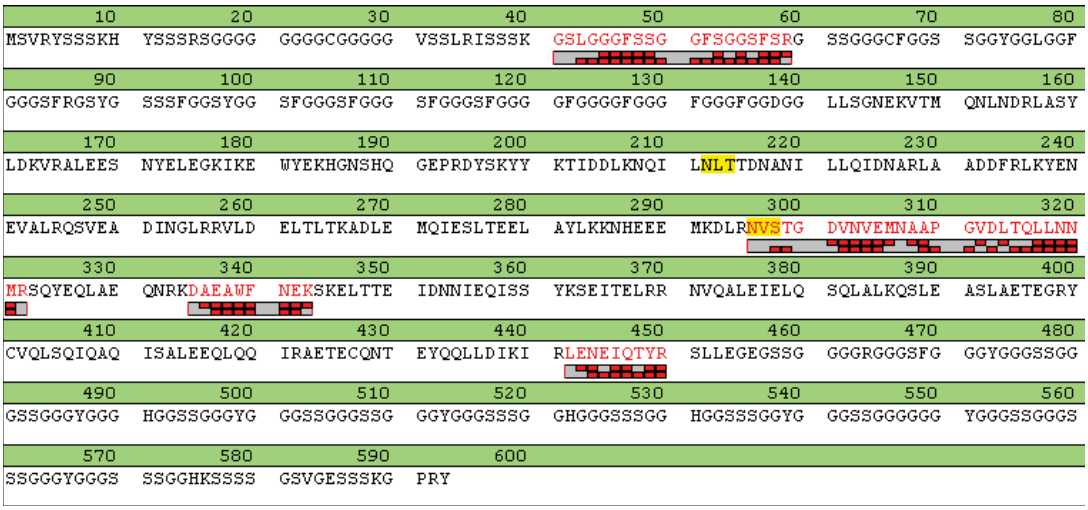
10 20 30 40 50 60 70 80
MSVRYSSSKH YSSSRSGGGG GGGGCGGGGG VSSLRISSSK GSLGGGFSSG GFSGGSFSRG SSGGGCFGGS SGGYGGLGGF
90 100 110 120 130 140 150 160
GGGSFRGSYG SSSFGGSYGG SFGGGSFGGG SFGGGSFGGG GFGGGGFGGG FGGGFGGDGG LLSGNEKVTM QNLNDRLASY
170 180 190 200 210 220 230 240
LDKVRALEES NYELEGKIKE WYEKHGNSHQ GEPRDYSKYY KTIDDLKNQI LNLTTDNANI LLQIDNARLA ADDFRLKYEN
250 260 270 280 290 300 310 320
EVALRQSVEA DINGLRRVLD ELTLTKADLE MQIESLTEEL AYLKKNHEEE MKDLRNVSTG DVNVEMNAAP GVDLTQLLNN
330 340 350 360 370 380 390 400
MRSQYEQLAE QNRKDAEAWF NEKSKELTTE IDNNIEQISS YKSEITELRR NVQALEIELQ SQLALKQSLE ASLAETEGRY
410 420 430 440 450 460 470 480
CVQLSQIQAQ ISALEEQLQQ IRAETECQNT EYQQLLDIKI RLENEIQTYR SLLEGEGSSG GGGRGGGSFG GGYGGGSSGG
490 500 510 520 530 540 550 560
GSSGGGYGGG HGGSSGGGYG GGSSGGGSSG GGYGGGSSSG GHGGGSSSGG HGGSSSGGYG GGSSGGGGGG YGGGSSGGGS
570 580 590 600
SSGGGYGGGS SSGGHKSSSS GSVGESSSKG PRY

c

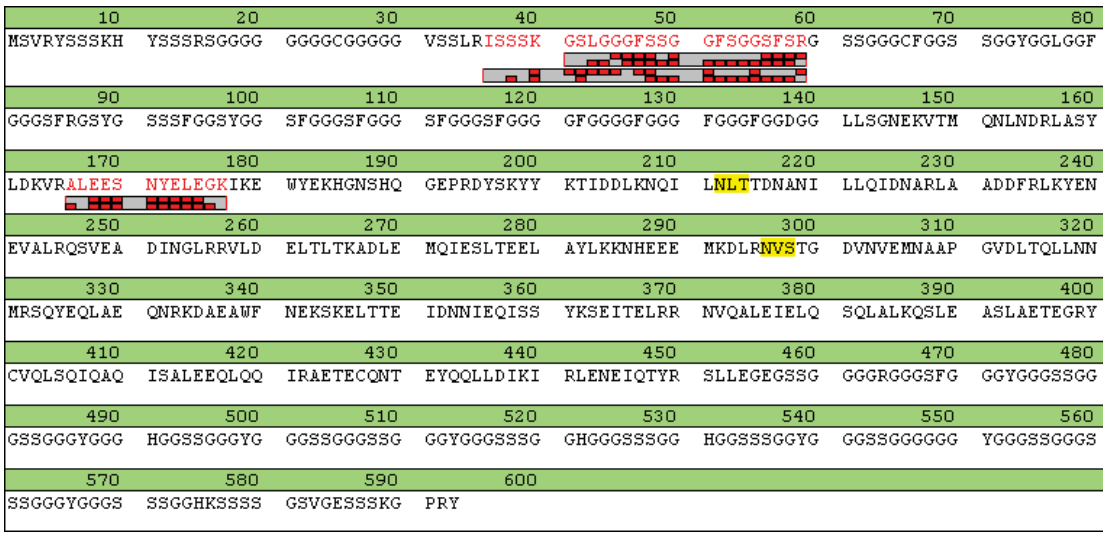
10 20 30 40 50 60 70 80
MSVRYSSSKH YSSSRSGGGG GGGGCGGGGG VSSLRISSSK GSLGGGFSSG GFSGGSFSRG SSGGGCFGGS SGGYGGLGGF
90 100 110 120 130 140 150 160
GGGSFRGSYG SSSFGGSYGG SFGGGSFGGG SFGGGSFGGG GFGGGGFGGG FGGGFGGDGG LLSGNEKVTM QNLNDRLASY
170 180 190 200 210 220 230 240
LDKVRALEES NYELEGKIKE WYEKHGNSHQ GEPRDYSKYY KTIDDLKNQI LNLTTDNANI LLQIDNARLA ADDFRLKYEN
250 260 270 280 290 300 310 320
EVALRQSVEA DINGLRRVLD ELTLTKADLE MQIESLTEEL AYLKKNHEEE MKDLRNVSTG DVNVEMNAAP GVDLTQLLNN
330 340 350 360 370 380 390 400
MRSQYEQLAE QNRKDAEAWF NEKSKELTTE IDNNIEQISS YKSEITELRR NVQALEIELQ SQLALKQSLE ASLAETEGRY
410 420 430 440 450 460 470 480
CVQLSQIQAQ ISALEEQLQQ IRAETECQNT EYQQLLDIKI RLENEIQTYR SLLEGEGSSG GGGRGGGSFG GGYGGGSSGG
490 500 510 520 530 540 550 560
GSSGGGYGGG HGGSSGGGYG GGSSGGGSSG GGYGGGSSSG GHGGGSSSGG HGGSSSGGYG GGSSGGGGGG YGGGSSGGGS
570 580 590 600
SSGGGYGGGS SSGGHKSSSS GSVGESSSKG PRY

d

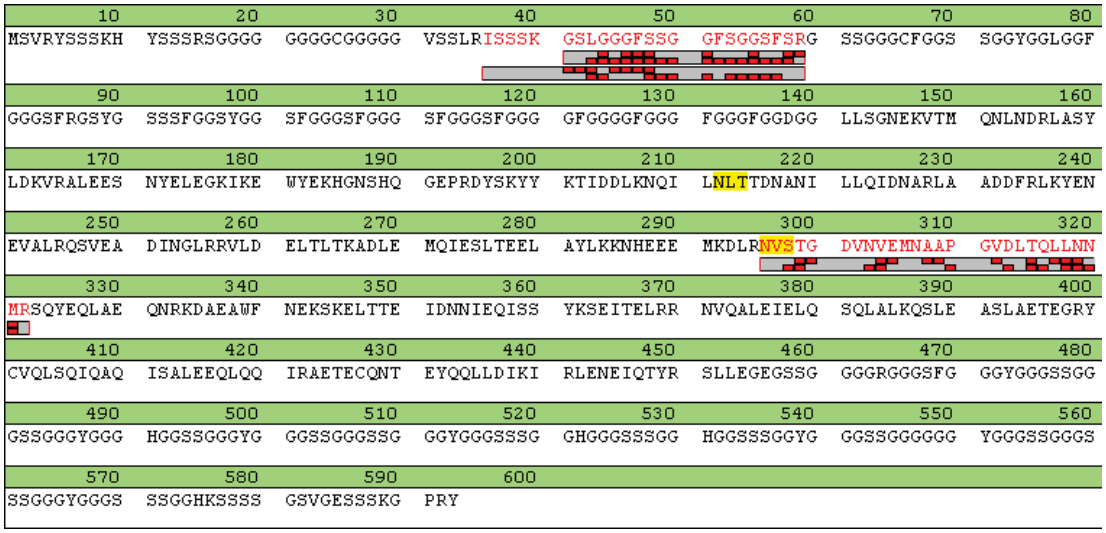

Figure A.6. Peptide fingerprinting for CK-10 produced during peritoneal-ovarian cancer cell co-culture.

(a) Protein identified in Table 2.2 (sample B3) as cleaved 50 kDa CK-10 (b) Protein identified in Table 2.3 (sample C2) as cleaved 55 kDa CK-10 (c) Protein identified in Table 2.3 (Sample C5) as cleaved 44 kDa CK-10 (d) Protein identified in Table 2.3 (Sample C11) as cleaved 34 kDa CK-10.

a

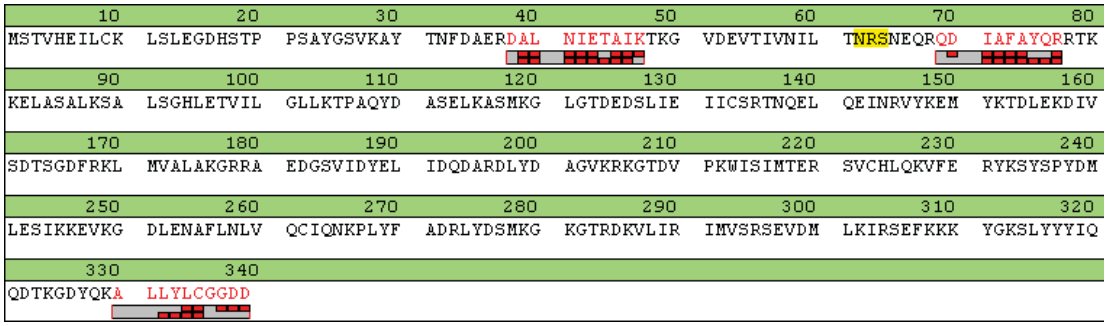
10 20 30 40 50 60 70 80
MSTVHEILCK LSLEGDHSTP PSAYGSVKAY TNFDAERDAL NIETAIKTKG VDEVTIVNIL TNRSNEQRQD IAFAYQRRTK
90 100 110 120 130 140 150 160
KELASALKSA LSGHLETVIL GLLKTPAQYD ASELKASMKG LGTDEDSLIE IICSRTNQEL QEINRVYKEM YKTDLEKDIV
170 180 190 200 210 220 230 240
SDTSGDFRKL MVALAKGRRA EDGSVIDYEL IDQDARDLYD AGVKRKGTDV PKWISIMTER SVCHLQKVFE RYKSYSPYDM
250 260 270 280 290 300 310 320
LESIKKEVKG DLENAFLNLV QCIQNKPLYF ADRLYDSMKG KGTRDKVLIR IMVSRSEVDM LKIRSEFKKK YGKSLYYYIQ
330 340
QDTKGDYQKA LLYLCGGDD

b

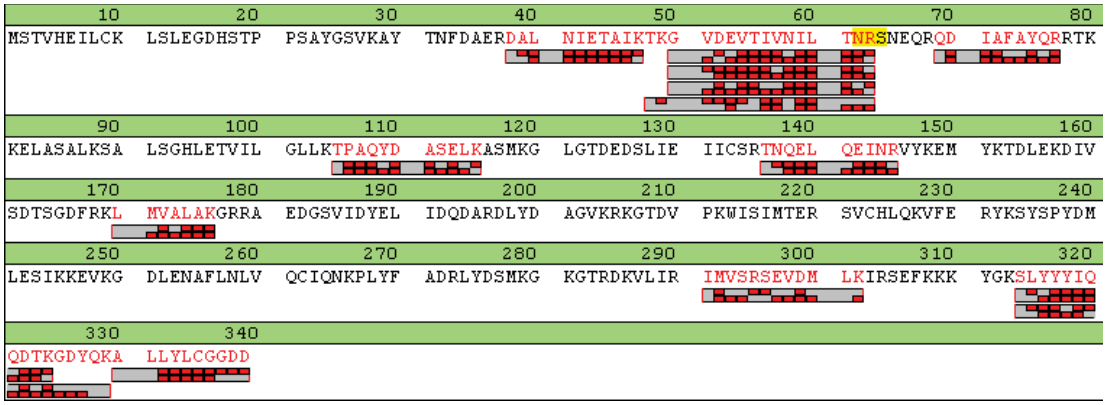
10 20 30 40 50 60 70 80
MSTVHEILCK LSLEGDHSTP PSAYGSVKAY TNFDAERDAL NIETAIKTKG VDEVTIVNIL TNRSNEQRQD IAFAYQRRTK
90 100 110 120 130 140 150 160
KELASALKSA LSGHLETVIL GLLKTPAQYD ASELKASMKG LGTDEDSLIE IICSRTNQEL QEINRVYKEM YKTDLEKDIV
170 180 190 200 210 220 230 240
SDTSGDFRKL MVALAKGRRA EDGSVIDYEL IDQDARDLYD AGVKRKGTDV PKWISIMTER SVCHLQKVFE RYKSYSPYDM
250 260 270 280 290 300 310 320
LESIKKEVKG DLENAFLNLV QCIQNKPLYF ADRLYDSMKG KGTRDKVLIR IMVSRSEVDM LKIRSEFKKK YGKSLYYYIQ
330 340
QDTKGDYQKA LLYLCGGDD

c

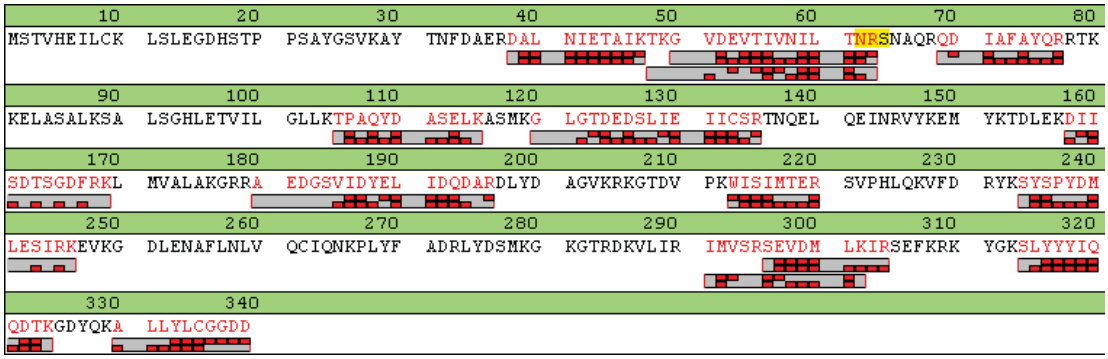
10 20 30 40 50 60 70 80
MSTVHEILCK LSLEGDHSTP PSAYGSVKAY TNFDAERDAL NIETAIKTKG VDEVTIVNIL TNRSNAQRQD IAFAYQRRTK
90 100 110 120 130 140 150 160
KELASALKSA LSGHLETVIL GLLKTPAQYD ASELKASMKG LGTDEDSLIE IICSRTNQEL QEINRVYKEM YKTDLEKDII
170 180 190 200 210 220 230 240
SDTSGDFRKL MVALAKGRRA EDGSVIDYEL IDQDARDLYD AGVKRKGTDV PKWISIMTER SVPHLQKVFD RYKSYSPYDM
250 260 270 280 290 300 310 320
LESIRKEVKG DLENAFLNLV QCIQNKPLYF ADRLYDSMKG KGTRDKVLIR IMVSRSEVDM LKIRSEFKRK YGKSLYYYIQ
330 340
QDTKGDYQKA LLYLCGGDD

d

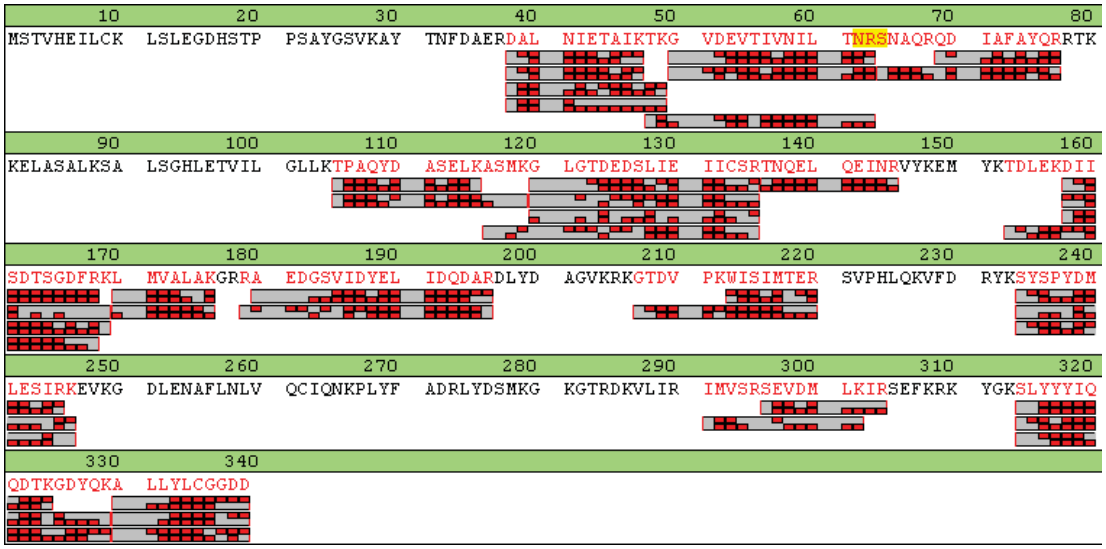

Figure A.7. Peptide fingerprinting for annexin A2 produced during peritoneal-ovarian cancer cell co-culture.

(a) Protein identified in Table 2.1 (sample B7) as cleaved 34 kDa Anx A2 (b) Protein identified in Table 2.2 (sample B8) as cleaved 34 kDa Anx A2 (c) Protein identified in Table 2.3 (Sample C9) as cleaved 34 kDa Anx A2 (d) Protein identified in Table 2.3 (Sample C10) as cleaved 34 kDa Anx A2.

a

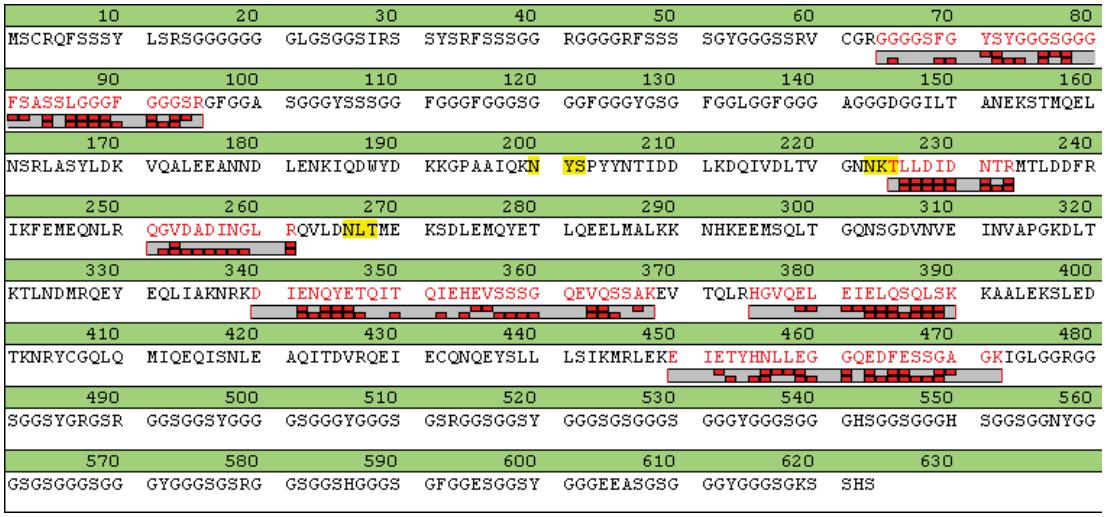
10 20 30 40 50 60 70 80
MSCRQFSSSY LSRSGGGGGG GLGSGGSIRS SYSRFSSSGG RGGGGRFSSS SGYGGGSSRV CGRGGGGSFG YSYGGGSGGG
90 100 110 120 130 140 150 160
FSASSLGGGF GGGSRGFGGA SGGGYSSSGG FGGGFGGGSG GGFGGGYGSG FGGLGGFGGG AGGGDGGILT ANEKSTMQEL
170 180 190 200 210 220 230 240
NSRLASYLDK VQALEEANND LENKIQDWYD KKGPAAIQKN YSPYYNTIDD LKDQIVDLTV GNNKTLLDID NTRMTLDDFR
250 260 270 280 290 300 310 320
IKFEMEQNLR QGVDADINGL RQVLDNLTME KSDLEMQYET LQEELMALKK NHKEEMSQLT GQNSGDVNVE INVAPGKDLT
330 340 350 360 370 380 390 400
KTLNDMRQEY EQLIAKNRKD IENQYETQIT QIEHEVSSSG QEVQSSAKEV TQLRHGVQEL EIELQSQLSK KAALEKSLED
410 420 430 440 450 460 470 480
TKNRYCGQLQ MIQEQISNLE AQITDVRQEI ECQNQEYSLL LSIKMRLEKE IETYHNLLEG GQEDFESSGA GKIGLGGRGG
490 500 510 520 530 540 550 560
SGGSYGRGSR GGSGGSYGGG GSGGGYGGGS GSRGGSGGSY GGGSGSGGGS GGGYGGGSGG GHSGGSGGGH SGGSGGNYGG
570 580 590 600 610 620 630
GSGSGGGSGG GYGGGSGSRG GSGGSHGGGS GFGGESGGSY GGGEEASGSG GGYGGGSGKS SHS

b

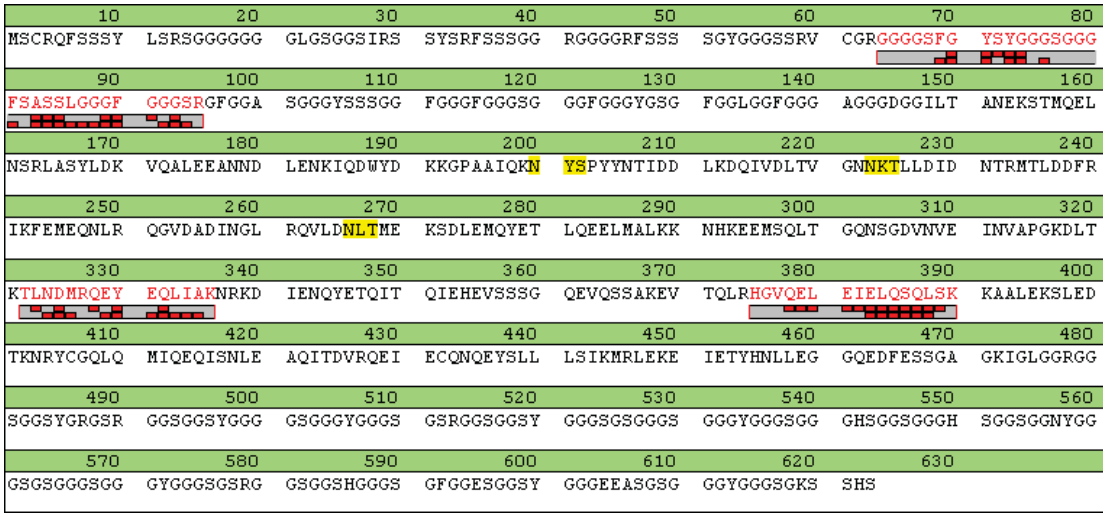
10 20 30 40 50 60 70 80
MSCRQFSSSY LSRSGGGGGG GLGSGGSIRS SYSRFSSSGG RGGGGRFSSS SGYGGGSSRV CGRGGGGSFG YSYGGGSGGG
90 100 110 120 130 140 150 160
FSASSLGGGF GGGSRGFGGA SGGGYSSSGG FGGGFGGGSG GGFGGGYGSG FGGLGGFGGG AGGGDGGILT ANEKSTMQEL
170 180 190 200 210 220 230 240
NSRLASYLDK VQALEEANND LENKIQDWYD KKGPAAIQKN YSPYYNTIDD LKDQIVDLTV GNNKTLLDID NTRMTLDDFR
250 260 270 280 290 300 310 320
IKFEMEQNLR QGVDADINGL RQVLDNLTME KSDLEMQYET LQEELMALKK NHKEEMSQLT GQNSGDVNVE INVAPGKDLT
330 340 350 360 370 380 390 400
KTLNDMRQEY EQLIAKNRKD IENQYETQIT QIEHEVSSSG QEVQSSAKEV TQLRHGVQEL EIELQSQLSK KAALEKSLED
410 420 430 440 450 460 470 480
TKNRYCGQLQ MIQEQISNLE AQITDVRQEI ECQNQEYSLL LSIKMRLEKE IETYHNLLEG GQEDFESSGA GKIGLGGRGG
490 500 510 520 530 540 550 560
SGGSYGRGSR GGSGGSYGGG GSGGGYGGGS GSRGGSGGSY GGGSGSGGGS GGGYGGGSGG GHSGGSGGGH SGGSGGNYGG
570 580 590 600 610 620 630
GSGSGGGSGG GYGGGSGSRG GSGGSHGGGS GFGGESGGSY GGGEEASGSG GGYGGGSGKS SHS

c

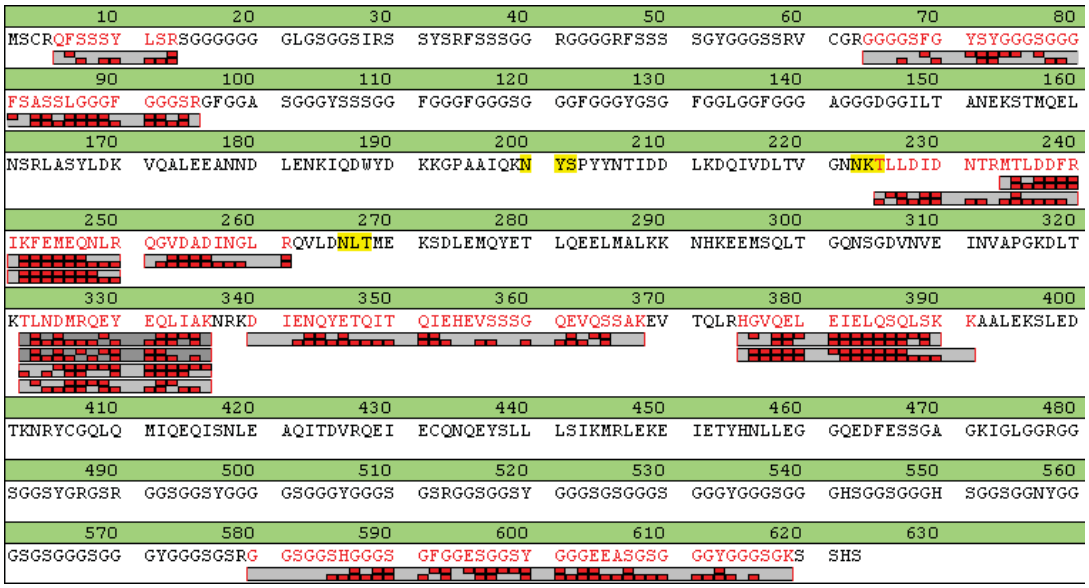
10 20 30 40 50 60 70 80
MSCRQFSSSY LSRSGGGGGG GLGSGGSIRS SYSRFSSSGG RGGGGRFSSS SGYGGGSSRV CGRGGGGSFG YSYGGGSGGG
90 100 110 120 130 140 150 160
FSASSLGGGF GGGSRGFGGA SGGGYSSSGG FGGGFGGGSG GGFGGGYGSG FGGLGGFGGG AGGGDGGILT ANEKSTMQEL
170 180 190 200 210 220 230 240
NSRLASYLDK VQALEEANND LENKIQDWYD KKGPAAIQKN YSPYYNTIDD LKDQIVDLTV GNNKTLLDID NTRMTLDDFR
250 260 270 280 290 300 310 320
IKFEMEQNLR QGVDADINGL RQVLDNLTME KSDLEMQYET LQEELMALKK NHKEEMSQLT GQNSGDVNVE INVAPGKDLT
330 340 350 360 370 380 390 400
KTLNDMRQEY EQLIAKNRKD IENQYETQIT QIEHEVSSSG QEVQSSAKEV TQLRHGVQEL EIELQSQLSK KAALEKSLED
410 420 430 440 450 460 470 480
TKNRYCGQLQ MIQEQISNLE AQITDVRQEI ECQNQEYSLL LSIKMRLEKE IETYHNLLEG GQEDFESSGA GKIGLGGRGG
490 500 510 520 530 540 550 560
SGGSYGRGSR GGSGGSYGGG GSGGGYGGGS GSRGGSGGSY GGGSGSGGGS GGGYGGGSGG GHSGGSGGGH SGGSGGNYGG
570 580 590 600 610 620 630
GSGSGGGSGG GYGGGSGSRG GSGGSHGGGS GFGGESGGSY GGGEEASGSG GGYGGGSGKS SHS

d

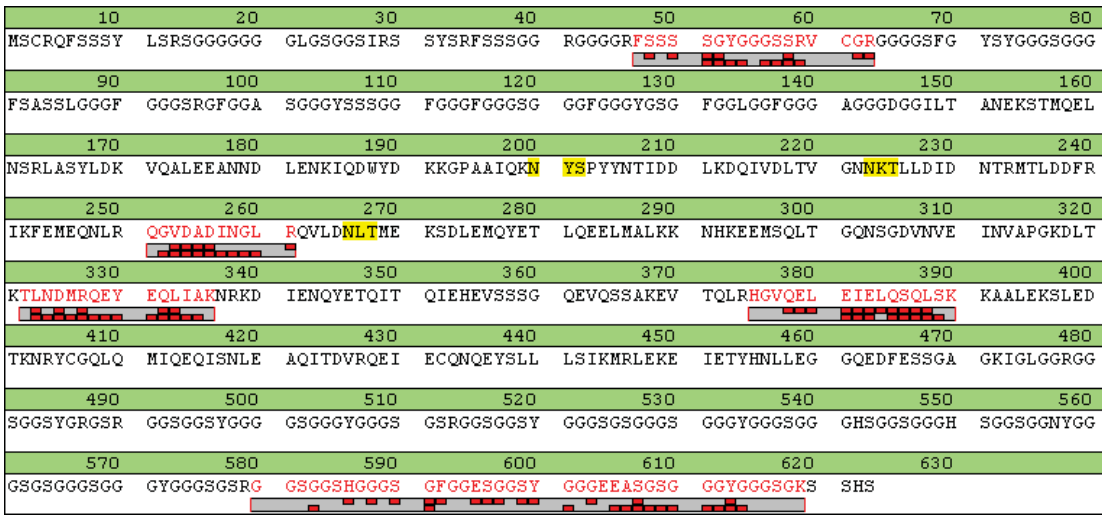

Figure A.8. Peptide fingerprinting for CK-9 produced during peritoneal-ovarian cancer cell co-culture.

(a) Protein identified in Table 2.2 (sample B8) as cleaved 34 kDa CK-9 (b) Protein identified in Table 2.2 (sample B10) as cleaved 28 kDa CK-9 (c) Protein identified in Table 2.3 (Sample C4) as cleaved 48 kDa CK-9 (d) Protein identified in Table 2.3 (Sample C10) as cleaved 35 kDa CK-9.

a

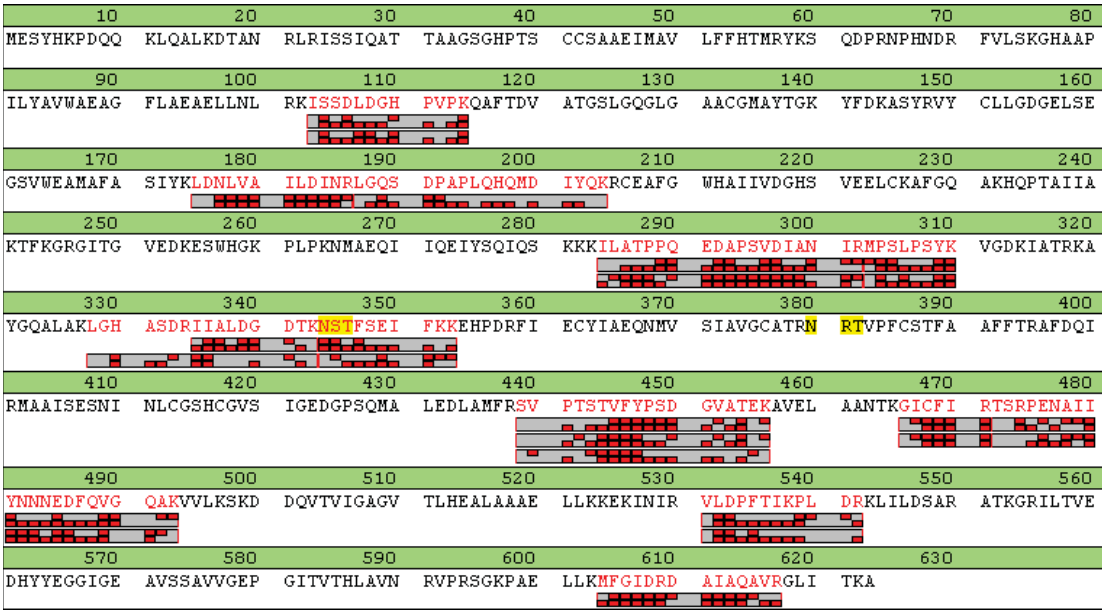

b

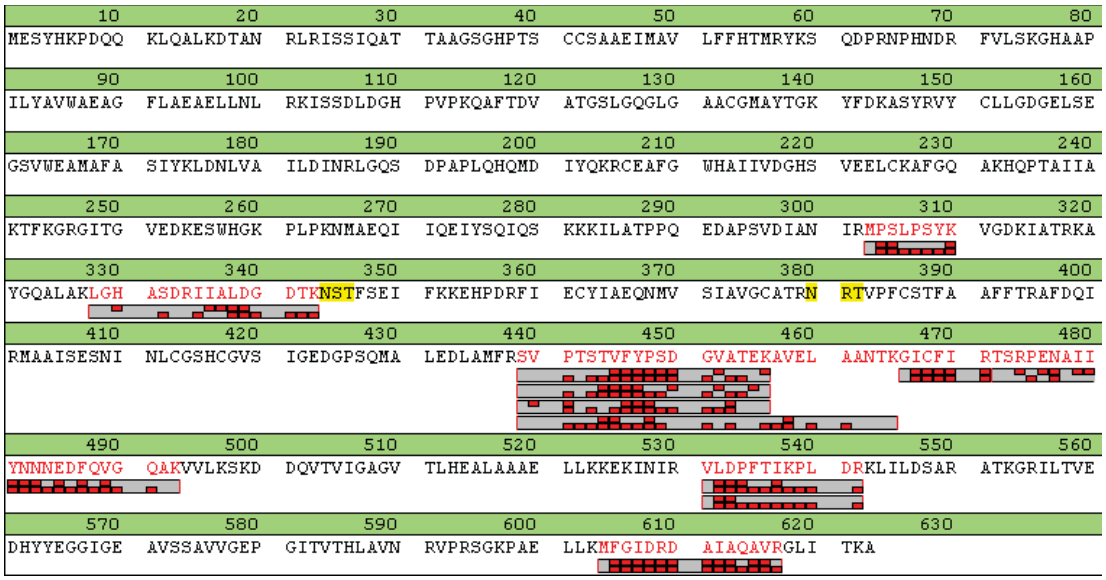

Figure A.9. Peptide fingerprinting for Transketolase produced during peritoneal-ovarian cancer cell co-culture.

(a) Protein identified in Table 2.3 (sample C1) as larger than expected 80 kDa TKT (b) Protein identified in Table 2.3 (sample C6) as cleaved 43 kDa TKT.

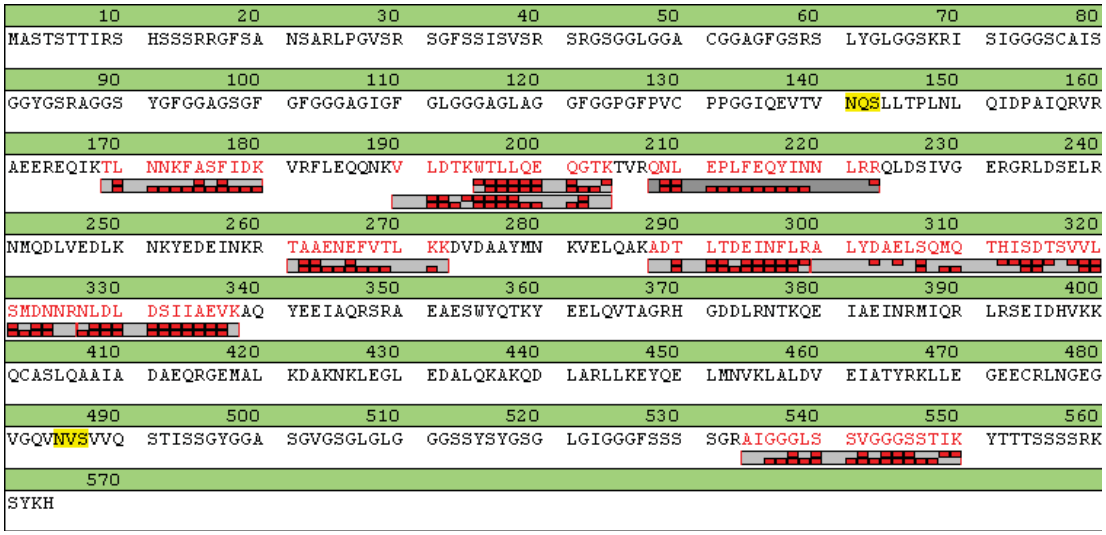

Figure A. 10. *Peptide fingerprinting for CK-6C produced during peritoneal-ovarian cancer cell co-culture.*

Protein identified in Table 2.3 (sample C4) as cleaved 48 kDa CK-6C.

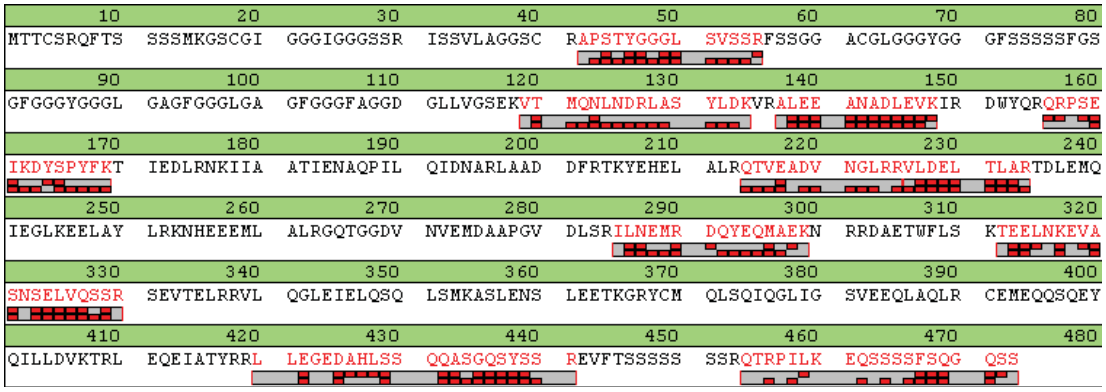

Figure A. 11. *Peptide fingerprinting for CK-16 produced during peritoneal-ovarian cancer cell co-culture.*

Protein identified in Table 2.3 (sample C4) as cleaved 48 kDa CK-16.

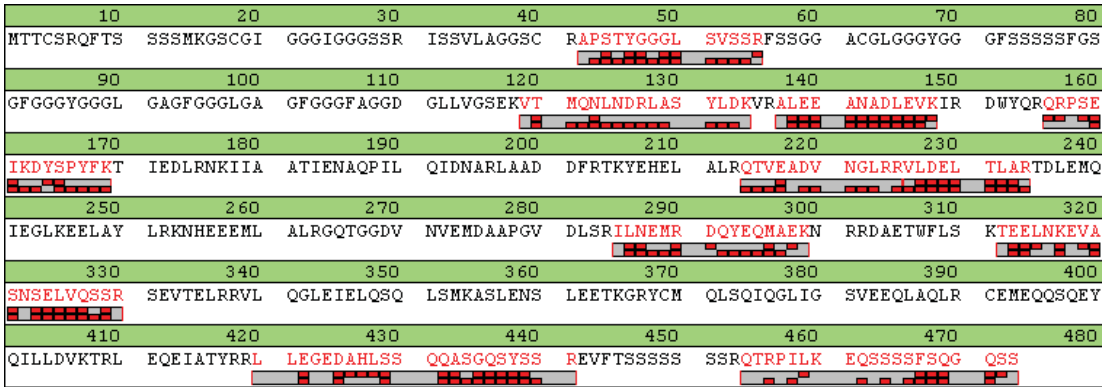

Figure A. 12. *Peptide fingerprinting for CK-14 produced during peritoneal-ovarian cancer cell co-culture.*

Protein identified in Table 2.3 (sample C4) as cleaved 48 kDa CK-14.

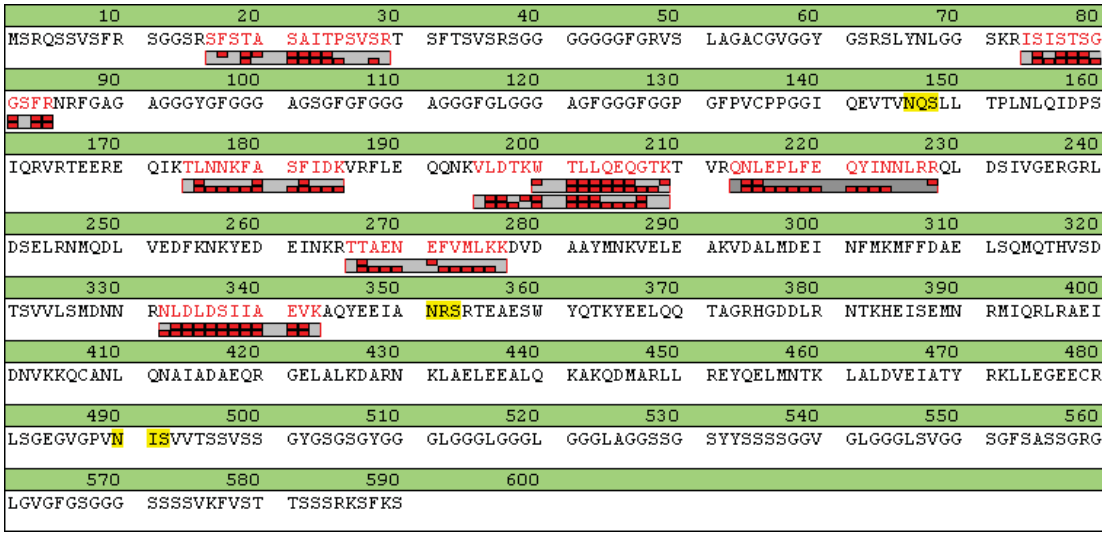

Figure A. 13. *Peptide fingerprinting for CK-5 produced during peritoneal-ovarian cancer cell co-culture.*

Protein identified in Table 2.3 (sample C4) as cleaved 48 kDa CK-5.

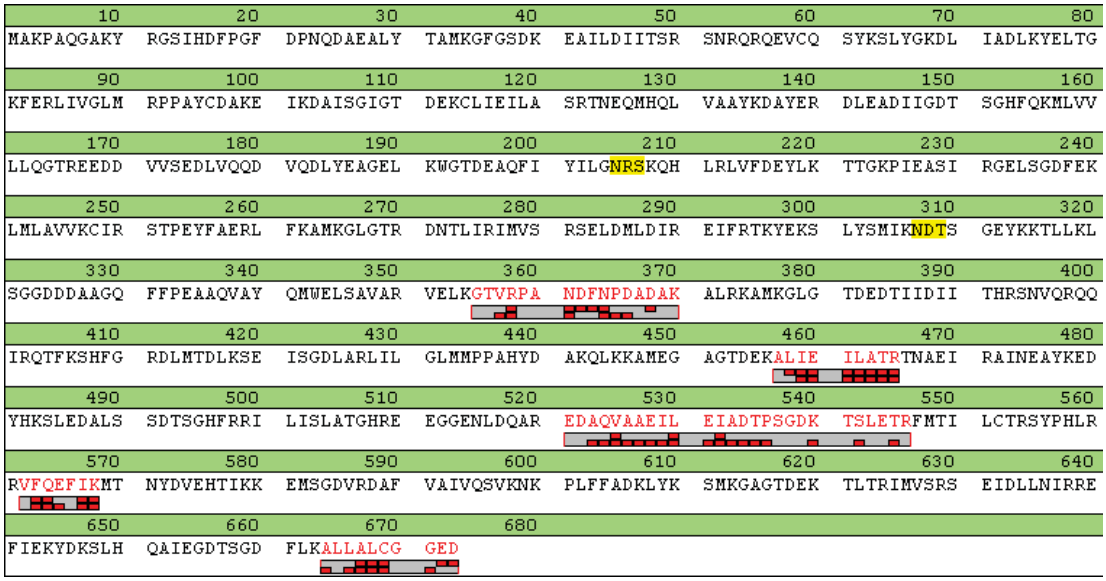

Figure A.14. *Peptide fingerprinting for annexin A6 produced during peritoneal-ovarian cancer cell co-culture.*

Protein identified in Table 2.3 (sample C8) as cleaved 36 kDa Anx A6.

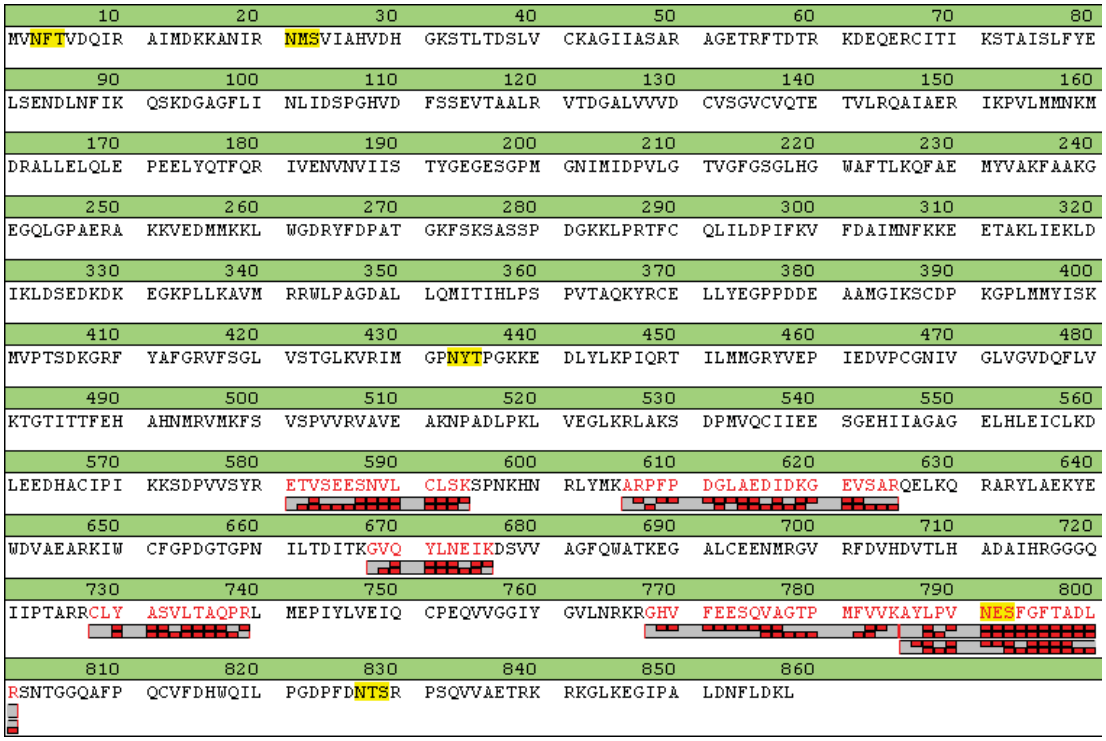

Figure A.15. *Peptide fingerprinting for Elongation Factor-2 produced during peritoneal-ovarian cancer cell co-culture.*

Protein identified in Table 2.3 (sample C11) as cleaved 34 kDa EEF-2.

Table A. 1. *The one letter codes used in amino acid sequencing.*

1 LETTER CODE	AMINO ACID
A	Alanine
C	Cysteine
D	Aspartic Acid/Asparagine
E	Glutamic Acid
F	Phenylalanine
G	Glycine
H	Histidine
I	Isoleucine
L	Leucine
K	Lysine
M	Methionine
N	Asparagine
O	Pyrrolysine
P	Proline
Q	Glutamine
R	Arginine
S	Serine
T	Threonine
U	Selenocysteine
V	Valine
W	Tryptophan
Y	Tyrosine

PUBLICATIONS ARISING FROM THIS THESIS (ENTIRE ARTICLES)

Accepted to IJC on the 12th May, to be updated to their printable version once *available*

Ween, M.P., Lokman, N.A., Hoffmann, P., Rodgers, R.J., Ricciardelli, C., and Oehler, M.K. (2011) Transforming growth factor-beta-induced protein secreted by peritoneal cells increases the metastatic potential of ovarian cancer cells.
International Journal of Cancer, v.128 (7), pp. 1570-1584, April 2011

NOTE: This publication is included in the print copy of the thesis held in the University of Adelaide Library.

It is also available online to authorised users at:

http://dx.doi.org/10.1002/ijc.25494

REFERENCES

REFERENCES

1. AIHW, A.I.o.H.a. and Welfare, *Cancer in Australia*, H.a. Welfare, Editor. 2008, Media and Publishing Unit, Australian Institute of Health and Welfare.

2. Morrison, J., *Advances in the understanding and treatment of ovarian cancer.* J Br Menopause Soc, 2005. **11**(2): p. 66-71.

3. Kaku, T., et al., *Histological classification of ovarian cancer.* Med Electron Microsc, 2003. **36**(1): p. 9-17.

4. Scully, R.E., *Ovarian tumors. A review.* Am J Pathol, 1977. **87**(3): p. 686-720.

5. Herbst, A.L., *The epidemiology of ovarian carcinoma and the current status of tumor markers to detect disease.* Am J Obstet Gynecol, 1994. **170**(4): p. 1099-105; discussion 1105-7.

6. Auersperg, N., et al., *The biology of ovarian cancer.* Semin Oncol, 1998. **25**(3): p. 281-304.

7. Fredrickson, T.N., *Ovarian tumors of the hen.* Environ Health Perspect, 1987. **73**: p. 35-51.

8. Van Niekerk, C.C., et al., *Changes in expression of differentiation markers between normal ovarian cells and derived tumors.* Am J Pathol, 1993. **142**(1): p. 157-77.

9. Hopkins, P.J., *Ovarian Cancer- Diagnosis and treatment*. 2001, John Hopkins University.

10. Oncology, C. *Ovarian cancer types*. 1999 14-10-2007; Available from: http://www.oncologychannel.com/ovariancancer/types.shtml.

11. Ricciardelli, C. and M.K. Oehler, *Diverse molecular pathways in ovarian cancer and their clinical significance.* Maturitas, 2009. **62**(3): p. 270-5.

12. Bell, D.A., M.A. Weinstock, and R.E. Scully, *Peritoneal implants of ovarian serous borderline tumors. Histologic features and prognosis.* Cancer, 1988. **62**(10): p. 2212-22.

13. Kurman, R.J., et al., *Early detection and treatment of ovarian cancer: shifting from early stage to minimal volume of disease based on a new model of carcinogenesis.* Am J Obstet Gynecol, 2008. **198**(4): p. 351-6.

14. Shih Ie, M. and R.J. Kurman, *Ovarian tumorigenesis: a proposed model based on morphological and molecular genetic analysis.* Am J Pathol, 2004. **164**(5): p. 1511-8.

15. Purdie, D., et al., *Reproductive and other factors and risk of epithelial ovarian cancer: an Australian case-control study. Survey of Women's Health Study Group.* Int J Cancer, 1995. **62**(6): p. 678-84.

16. Soegaard, M., et al., *Risk of ovarian cancer in women with first-degree relatives with cancer.* Acta Obstet Gynecol Scand, 2009. **88**(4): p. 449-56.

17. Miki, Y., et al., *A strong candidate for the breast and ovarian cancer susceptibility gene BRCA1.* Science, 1994. **266**(5182): p. 66-71.

18. Wooster, R., et al., *Identification of the breast cancer susceptibility gene BRCA2.* Nature, 1995. **378**(6559): p. 789-92.

19. Modan, B., et al., *Parity, oral contraceptives, and the risk of ovarian cancer among carriers and noncarriers of a BRCA1 or BRCA2 mutation.* N Engl J Med, 2001. **345**(4): p. 235-40.

20. Gayther, S.A., et al., *Rapid detection of regionally clustered germ-line BRCA1 mutations by multiplex heteroduplex analysis. UKCCCR Familial Ovarian Cancer Study Group.* Am J Hum Genet, 1996. **58**(3): p. 451-6.

21. Anand, N., et al., *Protein elongation factor EEF1A2 is a putative oncogene in ovarian cancer.* Nat Genet, 2002. **31**(3): p. 301-5.

22. Schuijer, M. and E.M. Berns, *TP53 and ovarian cancer.* Hum Mutat, 2003. **21**(3): p. 285-91.

23. Sellar, G.C., et al., *OPCML at 11q25 is epigenetically inactivated and has tumor-suppressor function in epithelial ovarian cancer.* Nat Genet, 2003. **34**(3): p. 337-43.

24. Shayesteh, L., et al., *PIK3CA is implicated as an oncogene in ovarian cancer.* Nat Genet, 1999. **21**(1): p. 99-102.

25. Lancaster, J.M., et al., *Microsomal epoxide hydrolase polymorphism as a risk factor for ovarian cancer.* Mol Carcinog, 1996. **17**(3): p. 160-2.

26. Berchuck, A., et al., *The p53 tumor suppressor gene frequently is altered in gynecologic cancers.* Am J Obstet Gynecol, 1994. **170**(1 Pt 1): p. 246-52.

27. Tashiro, H., et al., *c-myc over-expression in human primary ovarian tumours: its relevance to tumour progression.* Int J Cancer, 1992. **50**(5): p. 828-33.

28. Berchuck, A., et al., *Overexpression of HER-2/neu is associated with poor survival in advanced epithelial ovarian cancer.* Cancer Res, 1990. **50**(13): p. 4087-91.

29. Kacinski, B.M., et al., *Oncogene expression in vivo by ovarian adenocarcinomas and mixed-mullerian tumors.* Yale J Biol Med, 1989. **62**(4): p. 379-92.

30. Kohler, M., et al., *The expression of EGF receptors, EGF-like factors and c-myc in ovarian and cervical carcinomas and their potential clinical significance.* Anticancer Res, 1989. **9**(6): p. 1537-47.

31. Li, X.L., et al., *[Association of SNPs in the promoter of MMP-2 and TIMP-2 genes with epithelial ovarian cancer].* Yi Chuan, 2008. **30**(4): p. 455-62.

32. Li, Y., et al., *The functional polymorphisms on promoter region of matrix metalloproteinase-12, -13 genes may alter the risk of epithelial ovarian carcinoma in Chinese.* Int J Gynecol Cancer, 2009. **19**(1): p. 129-33.

33. Leite, D.B., et al., *Progesterone receptor (PROGINS) polymorphism and the risk of ovarian cancer.* Steroids, 2008. **73**(6): p. 676-80.

34. Gleeson, D., et al., *Androgen associated hepatocellular carcinoma with an aggressive course.* Gut, 1991. **32**(9): p. 1084-6.

35. Brawer, M.K., et al., *Androgen deprivation and other treatments for advanced prostate cancer.* Rev Urol, 2001. **3 Suppl 2**: p. S59-68.

36. Rakha, E.A., et al., *Prognostic markers in triple-negative breast cancer.* Cancer, 2007. **109**(1): p. 25-32.

37. Goodman, M.T., et al., *Association of two common single-nucleotide polymorphisms in the CYP19A1 locus and ovarian cancer risk.* Endocr Relat Cancer, 2008. **15**(4): p. 1055-60.

38. Chan, J.K., et al., *Prognostic factors for high-risk early-stage epithelial ovarian cancer: a Gynecologic Oncology Group study.* Cancer, 2008. **112**(10): p. 2202-10.

39. Risch, H.A., *Hormonal etiology of epithelial ovarian cancer, with a hypothesis concerning the role of androgens and progesterone.* J Natl Cancer Inst, 1998. **90**(23): p. 1774-86.

40. Shoham, Z., *Epidemiology, etiology, and fertility drugs in ovarian epithelial carcinoma: where are we today?* Fertil Steril, 1994. **62**(3): p. 433-48.

41. Whittemore, A.S., R. Harris, and J. Itnyre, *Characteristics relating to ovarian cancer risk: collaborative analysis of 12 US case-control studies. IV. The pathogenesis of epithelial ovarian cancer. Collaborative Ovarian Cancer Group.* Am J Epidemiol, 1992. **136**(10): p. 1212-20.

42. Rosenberg, L., et al., *A case-control study of oral contraceptive use and invasive epithelial ovarian cancer.* Am J Epidemiol, 1994. **139**(7): p. 654-61.

43. Adami, H.O., et al., *Parity, age at first childbirth, and risk of ovarian cancer.* Lancet, 1994. **344**(8932): p. 1250-4.

44. Booth, M., V. Beral, and P. Smith, *Risk factors for ovarian cancer: a case-control study.* Br J Cancer, 1989. **60**(4): p. 592-8.

45. Hankinson, S.E., et al., *A prospective study of reproductive factors and risk of epithelial ovarian cancer.* Cancer, 1995. **76**(2): p. 284-90.

46. Reeves, G.K., et al., *Cancer incidence and mortality in relation to body mass index in the Million Women Study: cohort study.* BMJ, 2007. **335**(7630): p. 1134.

47. Lahmann, P.H., et al., *Anthropometric measures and epithelial ovarian cancer risk in the european prospective investigation into cancer and nutrition.* Int J Cancer, 2009.

48. Olsen, C.M., et al., *Body size and risk of epithelial ovarian and related cancers: a population-based case-control study.* Int J Cancer, 2008. **123**(2): p. 450-6.

49. Kobayashi, H., et al., *Ovarian endometrioma--risks factors of ovarian cancer development.* Eur J Obstet Gynecol Reprod Biol, 2008. **138**(2): p. 187-93.

50. Key, T.J., et al., *Cancer incidence in British vegetarians.* Br J Cancer, 2009. **101**(1): p. 192-7.

51. Vickers, M.R., et al., *Main morbidities recorded in the women's international study of long duration oestrogen after menopause (WISDOM): a randomised controlled trial of hormone replacement therapy in postmenopausal women.* Bmj, 2007. **335**(7613): p. 239.

52. Arpaci, A., et al., *Investigation of PON1 192 and PON1 55 polymorphisms in ovarian cancer patients in Turkish population.* In Vivo, 2009. **23**(3): p. 421-4.

53. Cramer, D.W., et al., *Over-the-counter analgesics and risk of ovarian cancer.* Lancet, 1998. **351**(9096): p. 104-7.

54. Fritsche, H.A. and R.C. Bast, *CA 125 in ovarian cancer: advances and controversy.* Clin Chem, 1998. **44**(7): p. 1379-80.

55. Tuxen, M.K., G. Soletormos, and P. Dombernowsky, *Tumor markers in the management of patients with ovarian cancer.* Cancer Treat Rev, 1995. **21**(3): p. 215-45.

56. Markman, M., *Optimizing primary chemotherapy in ovarian cancer.* Hematol Oncol Clin North Am, 2003. **17**(4): p. 957-68, viii.

57. Kryczek, I., et al., *B7-H4 expression identifies a novel suppressive macrophage population in human ovarian carcinoma.* J Exp Med, 2006. **203**(4): p. 871-81.

58. Simon, I., et al., *B7-H4 is over-expressed in early-stage ovarian cancer and is independent of CA125 expression.* Gynecol Oncol, 2007. **106**(2): p. 334-41.

59. Ghadersohi, A., et al., *Prostate-derived Ets transcription factor as a favorable prognostic marker in ovarian cancer patients.* Int J Cancer, 2008. **123**(6): p. 1376-84.

60. Tan, X.J., et al., *[Correlation of preoperative serum vascular endothelial growth factor level with CA125 level in patients with epithelial ovarian cancer and its prognostic value].* Zhonghua Fu Chan Ke Za Zhi, 2008. **43**(1): p. 9-12.

61. McSorley, M.A., et al., *Prediagnostic circulating follicle stimulating hormone concentrations and ovarian cancer risk.* Int J Cancer, 2009. **125**(3): p. 674-9.

62. Ferrandina, G., et al., *Prognostic role of topoisomerase-IIalpha in advanced ovarian cancer patients.* Br J Cancer, 2008. **98**(12): p. 1910-5.

63. Steffensen, K.D., et al., *Protein levels and gene expressions of the epidermal growth factor receptors, HER1, HER2, HER3 and HER4 in benign and malignant ovarian tumors.* Int J Oncol, 2008. **33**(1): p. 195-204.

64. Tanner, B., et al., *ErbB-3 predicts survival in ovarian cancer.* J Clin Oncol, 2006. **24**(26): p. 4317-23.

65. Gilmour, L.M., et al., *Expression of erbB-4/HER-4 growth factor receptor isoforms in ovarian cancer.* Cancer Res, 2001. **61**(5): p. 2169-76.

66. Clinton, G.M. and W. Hua, *Estrogen action in human ovarian cancer.* Crit Rev Oncol Hematol, 1997. **25**(1): p. 1-9.

67. Rao, B.R. and B.J. Slotman, *Endocrine factors in common epithelial ovarian cancer.* Endocr Rev, 1991. **12**(1): p. 14-26.

68. Harding, M., et al., *Estrogen and progesterone receptors in ovarian cancer.* Cancer, 1990. **65**(3): p. 486-91.

69. Burges, A., et al., *Prognostic significance of estrogen receptor alpha and beta expression in human serous carcinomas of the ovary.* Arch Gynecol Obstet, 2010. **281**(3): p. 511-7.

70. Hempling, R.E., et al., *Progesterone receptor status is a significant prognostic variable of progression-free survival in advanced epithelial ovarian cancer.* Am J Clin Oncol, 1998. **21**(5): p. 447-51.

71. Kountourakis, P., et al., *Expression and prognostic significance of kallikrein-related peptidase 8 protein levels in advanced ovarian cancer by using automated quantitative analysis.* Thromb Haemost, 2009. **101**(3): p. 541-6.

72. White, N.M., et al., *KLK6 and KLK13 predict tumor recurrence in epithelial ovarian carcinoma.* Br J Cancer, 2009. **101**(7): p. 1107-13.

73. Dong, Y., et al., *Kallikrein-Related Peptidase 7 Promotes Multicellular Aggregation via the {alpha}5{beta}1 Integrin Pathway and Paclitaxel Chemoresistance in Serous Epithelial Ovarian Carcinoma.* Cancer Res, 2010. **70**(7): p. 2624-33.

74. Dong, Y., et al., *Human kallikrein 4 (KLK4) is highly expressed in serous ovarian carcinomas.* Clin Cancer Res, 2001. **7**(8): p. 2363-71.

75. Dong, Y., et al., *Differential splicing of KLK5 and KLK7 in epithelial ovarian cancer produces novel variants with potential as cancer biomarkers.* Clin Cancer Res, 2003. **9**(5): p. 1710-20.

76. Baba, T., et al., *Trophinin is a potent prognostic marker of ovarian cancer involved in platinum sensitivity.* Biochem Biophys Res Commun, 2007. **360**(2): p. 363-9.

77. Pinke, D.E., et al., *The prognostic significance of elongation factor eEF1A2 in ovarian cancer.* Gynecol Oncol, 2008. **108**(3): p. 561-8.

78. Yang, G.F., et al., *Expression and clinical significance of YKL-40 protein in epithelial ovarian cancer tissues.* Ai Zheng, 2009. **28**(2): p. 142-5.

79. Kim, H.S., et al., *In vitro extreme drug resistance assay to taxanes or platinum compounds for the prediction of clinical outcomes in epithelial ovarian cancer: a prospective cohort study.* J Cancer Res Clin Oncol, 2009. **135**(11): p. 1513-20.

80. Hoskins, W.J., *Surgical staging and cytoreductive surgery of epithelial ovarian cancer.* Cancer, 1993. **71**(4 Suppl): p. 1534-40.

81. Amadori, D., E. Sansoni, and A. Amadori, *Ovarian cancer: natural history and metastatic pattern.* Front Biosci, 1997. **2**: p. g8-10.

82. Buy, J.N., et al., *Peritoneal implants from ovarian tumors: CT findings.* Radiology, 1988. **169**(3): p. 691-4.

83. Carmignani, C.P., et al., *Intraperitoneal cancer dissemination: mechanisms of the patterns of spread.* Cancer Metastasis Rev, 2003. **22**(4): p. 465-72.

84. Meyers, M.A., et al., *The peritoneal ligaments and mesenteries: pathways of intraabdominal spread of disease.* Radiology, 1987. **163**(3): p. 593-604.

85. Andren, O., et al., *How well does the Gleason score predict prostate cancer death? A 20-year followup of a population based cohort in Sweden.* J Urol, 2006. **175**(4): p. 1337-40.

86. Burleson, K.M., L.K. Hansen, and A.P. Skubitz, *Ovarian carcinoma spheroids disaggregate on type I collagen and invade live human mesothelial cell monolayers.* Clin Exp Metastasis, 2004. **21**(8): p. 685-97.

87. Strobel, T. and S.A. Cannistra, *Beta1-integrins partly mediate binding of ovarian cancer cells to peritoneal mesothelium in vitro.* Gynecol Oncol, 1999. **73**(3): p. 362-7.

88. Cannistra, S.A., et al., *Binding of ovarian cancer cells to peritoneal mesothelium in vitro is partly mediated by CD44H.* Cancer Res, 1993. **53**(16): p. 3830-8.

89. Greimel, E.R., et al., *Randomized study of the Arbeitsgemeinschaft Gynaekologische Onkologie Ovarian Cancer Study Group comparing quality of life in patients with ovarian cancer treated with cisplatin/paclitaxel versus carboplatin/paclitaxel.* J Clin Oncol, 2006. **24**(4): p. 579-86.

90. Norway, C.i., *Cancer Registry of Norway*. 2000, Norway: Institute of Population-based Cancer research: Oslo.

91. Ting, A.Y., et al., *Tamoxifen prevents premalignant changes of breast, but not ovarian, cancer in rats at high risk for both diseases.* Cancer Prev Res (Phila Pa), 2008. **1**(7): p. 546-53.

92. Kang, H., et al., *Phase II study of combination chemotherapy with etoposide and ifosfamide in patients with heavily pretreated recurrent or persistent epithelial ovarian cancer.* J Korean Med Sci, 2009. **24**(5): p. 945-50.

93. de Jong, R.S., et al., *Effect of low-dose oral etoposide on serum CA-125 in patients with advanced epithelial ovarian cancer.* Gynecol Oncol, 1997. **66**(2): p. 197-201.

94. Kang, H., et al., *Topotecan combined with carboplatin in recurrent epithelial ovarian cancer: results of a single-institutional phase II study.* Gynecol Oncol, 2009. **114**(2): p. 210-4.

95. Nielsen, H.A., D. Nielsen, and S.A. Engelholm, *Effect of topotecan on serum CA-125 in patients with advanced epithelial ovarian cancer.* Gynecol Oncol, 2000. **77**(3): p. 383-8.

96. Le, T., et al., *Prospective evaluation of weekly topotecan in recurrent platinum-resistant epithelial ovarian cancer.* Int J Gynecol Cancer, 2008. **18**(3): p. 428-31.

97. Gore, M., et al., *Clinical evidence for topotecan-paclitaxel non--cross-resistance in ovarian cancer.* J Clin Oncol, 2001. **19**(7): p. 1893-900.

98. ten Bokkel Huinink, W., et al., *Topotecan versus paclitaxel for the treatment of recurrent epithelial ovarian cancer.* J Clin Oncol, 1997. **15**(6): p. 2183-93.

99. Gore, M., et al., *A randomised trial of oral versus intravenous topotecan in patients with relapsed epithelial ovarian cancer.* Eur J Cancer, 2002. **38**(1): p. 57-63.

100. Kaye, S.B., et al., *Phase II trials of docetaxel (Taxotere) in advanced ovarian cancer--an updated overview.* Eur J Cancer, 1997. **33**(13): p. 2167-70.

101. Vasey, P.A., et al., *Phase III randomized trial of docetaxel-carboplatin versus paclitaxel-carboplatin as first-line chemotherapy for ovarian carcinoma.* J Natl Cancer Inst, 2004. **96**(22): p. 1682-91.

102. Wang, J., et al., *[Therapeutic effect of docetaxel combined with oxaliplatin for treatment of recurrent epithelial ovarian cancer.].* Nan Fang Yi Ke Da Xue Xue Bao, 2009. **29**(11): p. 2319-20.

103. Vasey, P.A., et al., *A phase Ib trial of docetaxel, carboplatin and erlotinib in ovarian, fallopian tube and primary peritoneal cancers.* Br J Cancer, 2008. **98**(11): p. 1774-80.

104. Wilhelm, S.M., et al., *BAY 43-9006 exhibits broad spectrum oral antitumor activity and targets the RAF/MEK/ERK pathway and receptor tyrosine kinases involved in tumor progression and angiogenesis.* Cancer Res, 2004. **64**(19): p. 7099-109.

105. Panka, D.J., et al., *The Raf inhibitor BAY 43-9006 (Sorafenib) induces caspase-independent apoptosis in melanoma cells.* Cancer Res, 2006. **66**(3): p. 1611-9.

106. Lyons, J.F., et al., *Discovery of a novel Raf kinase inhibitor.* Endocr Relat Cancer, 2001. **8**(3): p. 219-25.

107. Singer, G., et al., *Mutations in BRAF and KRAS characterize the development of low-grade ovarian serous carcinoma.* J Natl Cancer Inst, 2003. **95**(6): p. 484-6.

108. Yu, C., et al., *The role of Mcl-1 downregulation in the proapoptotic activity of the multikinase inhibitor BAY 43-9006.* Oncogene, 2005. **24**(46): p. 6861-9.

109. Siu, L.L., et al., *Phase I trial of sorafenib and gemcitabine in advanced solid tumors with an expanded cohort in advanced pancreatic cancer.* Clin Cancer Res, 2006. **12**(1): p. 144-51.

110. Burger, R.A., et al., *Phase II trial of bevacizumab in persistent or recurrent epithelial ovarian cancer or primary peritoneal cancer: a Gynecologic Oncology Group Study.* J Clin Oncol, 2007. **25**(33): p. 5165-71.

111. Cannistra, S.A., et al., *Phase II study of bevacizumab in patients with platinum-resistant ovarian cancer or peritoneal serous cancer.* J Clin Oncol, 2007. **25**(33): p. 5180-6.

112. Cohn, D.E., et al., *Bevacizumab and weekly taxane chemotherapy demonstrates activity in refractory ovarian cancer.* Gynecol Oncol, 2006. **102**(2): p. 134-9.

113. Penson, R.T., et al., *Phase II Study of Carboplatin, Paclitaxel, and Bevacizumab With Maintenance Bevacizumab As First-Line Chemotherapy for Advanced Mullerian Tumors.* J Clin Oncol, 2009.

114. Mabuchi, S., et al., *Maintenance treatment with bevacizumab prolongs survival in an in vivo ovarian cancer model.* Clin Cancer Res, 2008. **14**(23): p. 7781-9.

115. Freeburg, E.M., et al., *Resistance to cisplatin does not affect sensitivity of human ovarian cancer cell lines to mifepristone cytotoxicity.* Cancer Cell Int, 2009. **9**: p. 4.

116. Freeburg, E.M., A.A. Goyeneche, and C.M. Telleria, *Mifepristone abrogates repopulation of ovarian cancer cells in between courses of cisplatin treatment.* Int J Oncol, 2009. **34**(3): p. 743-55.

117. Goyeneche, A.A., R.W. Caron, and C.M. Telleria, *Mifepristone inhibits ovarian cancer cell growth in vitro and in vivo.* Clin Cancer Res, 2007. **13**(11): p. 3370-9.

118. Rocereto, T.F., et al., *A phase II evaluation of mifepristone in the treatment of recurrent or persistent epithelial ovarian, fallopian or primary peritoneal cancer: A gynecologic oncology group study.* Gynecol Oncol, 2009.

119. Li, Y.F., et al., *Aromatase inhibitors in ovarian cancer: is there a role?* Int J Gynecol Cancer, 2008. **18**(4): p. 600-14.

120. Armstrong, D.K., et al., *Intraperitoneal cisplatin and paclitaxel in ovarian cancer.* N Engl J Med, 2006. **354**(1): p. 34-43.

121. Bankhead, C., *Intraperitoneal therapy for advanced ovarian cancer: will it become standard care?* J Natl Cancer Inst, 2006. **98**(8): p. 510-2.

122. Rothenberg, M.L., et al., *Combined intraperitoneal and intravenous chemotherapy for women with optimally debulked ovarian cancer: results from an intergroup phase II trial.* J Clin Oncol, 2003. **21**(7): p. 1313-9.

123. Trimble, E.L., et al., *Intraperitoneal chemotherapy for women with epithelial ovarian cancer.* Oncologist, 2008. **13**(4): p. 403-9.

124. Tiersten, A.D., et al., *Phase II evaluation of neoadjuvant chemotherapy and debulking followed by intraperitoneal chemotherapy in women with stage III and IV epithelial ovarian, fallopian tube or primary peritoneal cancer: Southwest Oncology Group Study S0009.* Gynecol Oncol, 2009. **112**(3): p. 444-9.

125. Lu, Z., et al., *Tumor-penetrating microparticles for intraperitoneal therapy of ovarian cancer.* J Pharmacol Exp Ther, 2008. **327**(3): p. 673-82.

126. Knudson, C.B. and W. Knudson, *Hyaluronan-binding proteins in development, tissue homeostasis, and disease.* FASEB J., 1993. **7**(13): p. 1233-1241.

127. Orkin, R.W., C.B. Underhill, and B.P. Toole, *Hyaluronate degradation in 3T3 and simian virus-transformed 3T3 cells.* J Biol Chem, 1982. **257**(10): p. 5821-6.

128. Zhang, L., C.B. Underhill, and L. Chen, *Hyaluronan on the surface of tumor cells is correlated with metastatic behavior.* Cancer Res, 1995. **55**(2): p. 428-33.

129. Knudson, W., *The role of CD44 as a cell surface hyaluronan receptor during tumor invasion of connective tissue.* Front Biosci., 1998. **3**: p. D604-D615.

130. Yeo, T.K., et al., *Increased hyaluronan at sites of attachment to mesentery by CD44-positive mouse ovarian and breast tumor cells.* Am J Pathol, 1996. **148**(6): p. 1733-40.

131. Day, A.J. and G.D. Prestwich, *Hyaluronan-binding proteins: tying up the giant.* J Biol Chem, 2002. **277**(7): p. 4585-8.

132. Tammi, M.I., A.J. Day, and E.A. Turley, *Hyaluronan and homeostasis: A balancing act.* J.Biol.Chem., 2001.

133. Boregowda, R.K., et al., *Expression of hyaluronan in human tumor progression.* J Carcinog, 2006. **5**: p. 2.

134. Sercu, S., et al., *Interaction of extracellular matrix protein 1 with extracellular matrix components: ECM1 is a basement membrane protein of the skin.* J Invest Dermatol, 2008. **128**(6): p. 1397-408.

135. Ricciardelli, C., et al., *Formation of hyaluronan- and versican-rich pericellular matrix by prostate cancer cells promotes cell motility.* J Biol Chem, 2007. **282**(14): p. 10814-25.

136. Evanko, S.P., J.C. Angello, and T.N. Wight, *Formation of hyaluronan- and versican-rich pericellular matrix is required for proliferation and migration of vascular smooth muscle cells.* Arterioscler.Thromb.Vasc.Biol., 1999. **19**(4): p. 1004-1013.

137. Evanko, S.P., et al., *Hyaluronan-dependent pericellular matrix.* Adv Drug Deliv Rev, 2007. **59**(13): p. 1351-65.

138. Platt, V.M. and F.C. Szoka, Jr., *Anticancer therapeutics: targeting macromolecules and nanocarriers to hyaluronan or CD44, a hyaluronan receptor.* Mol Pharm, 2008. **5**(4): p. 474-86.

139. Auvinen, P., et al., *Hyaluronan in peritumoral stroma and malignant cells associates with breast cancer spreading and predicts survival.* Am J Pathol, 2000. **156**(2): p. 529-36.

140. Anttila, M.A., et al., *High levels of stromal hyaluronan predict poor disease outcome in epithelial ovarian cancer.* Cancer Res, 2000. **60**(1): p. 150-5.

141. Lipponen, P., et al., *High stromal hyaluronan level is associated with poor differentiation and metastasis in prostate cancer.* Eur.J.Cancer, 2001. **37**(7): p. 849-856.

142. Posey, J.T., et al., *Evaluation of the prognostic potential of hyaluronic acid and hyaluronidase (HYAL1) for prostate cancer.* Cancer Res, 2003. **63**(10): p. 2638-44.

143. Pirinen, R., et al., *Prognostic value of hyaluronan expression in non-small-cell lung cancer: Increased stromal expression indicates unfavorable outcome in patients with adenocarcinoma.* Int J Cancer, 2001. **95**(1): p. 12-7.

144. Ropponen, K., et al., *Tumor cell-associated hyaluronan as an unfavorable prognostic factor in colorectal cancer.* Cancer Res, 1998. **58**(2): p. 342-7.

145. Afify, A., et al., *Expression of CD44s, CD44v6, and hyaluronan across the spectrum of normal-hyperplasia-carcinoma in breast.* Appl Immunohistochem Mol Morphol, 2008. **16**(2): p. 121-7.

146. Suwiwat, S., et al., *Expression of extracellular matrix components versican, chondroitin sulfate, tenascin, and hyaluronan, and their association with disease outcome in node-negative breast cancer.* Clin Cancer Res, 2004. **10**(7): p. 2491-8.

147. Delpech, B., et al., *Hyaluronan and hyaluronectin in the extracellular matrix of human brain tumour stroma.* Eur J Cancer, 1993. **29A**(7): p. 1012-7.

148. Kinzler, K.W. and B. Vogelstein, *Landscaping the cancer terrain.* Science, 1998. **280**(5366): p. 1036-7.

149. Hanahan, D. and R.A. Weinberg, *The hallmarks of cancer.* Cell, 2000. **100**(1): p. 57-70.

150. Toole, B.P., C. Biswas, and J. Gross, *Hyaluronate and invasiveness of the rabbit V2 carcinoma.* Proc Natl Acad Sci U S A, 1979. **76**(12): p. 6299-303.

151. Jojovic, M., et al., *Expression of hyaluronate and hyaluronate synthase in human primary tumours and their metastases in scid mice.* Cancer Lett, 2002. **188**(1-2): p. 181-9.

152. Kosaki, R., K. Watanabe, and Y. Yamaguchi, *Overproduction of hyaluronan by expression of the hyaluronan synthase Has2 enhances anchorage-independent growth and tumorigenicity.* Cancer Res, 1999. **59**(5): p. 1141-5.

153. Liu, N., et al., *Hyaluronan synthase 3 overexpression promotes the growth of TSU prostate cancer cells.* Cancer Res, 2001. **61**(13): p. 5207-14.

154. Itano, N., et al., *Relationship between hyaluronan production and metastatic potential of mouse mammary carcinoma cells.* Cancer Res, 1999. **59**(10): p. 2499-504.

155. Udabage, L., et al., *Antisense-mediated suppression of hyaluronan synthase 2 inhibits the tumorigenesis and progression of breast cancer.* Cancer Res, 2005. **65**(14): p. 6139-50.

156. Yabushita, H., et al., *Hyaluronan synthase expression in ovarian cancer.* Oncol Rep, 2004. **12**(4): p. 739-43.

157. Deed, R., et al., *Early-response gene signalling is induced by angiogenic oligosaccharides of hyaluronan in endothelial cells. Inhibition by non-angiogenic, high-molecular-weight hyaluronan.* Int J Cancer, 1997. **71**(2): p. 251-6.

158. Rooney, P., et al., *The role of hyaluronan in tumour neovascularization (review).* Int J Cancer, 1995. **60**(5): p. 632-6.

159. Sugahara, K.N., et al., *Tumor cells enhance their own CD44 cleavage and motility by generating hyaluronan fragments.* J Biol Chem, 2006. **281**(9): p. 5861-8.

160. Fujisaki, T., et al., *CD44 stimulation induces integrin-mediated adhesion of colon cancer cell lines to endothelial cells by up-regulation of integrins and c-Met and activation of integrins.* Cancer Res, 1999. **59**(17): p. 4427-34.

161. Sugahara, K.N., et al., *Hyaluronan oligosaccharides induce CD44 cleavage and promote cell migration in CD44-expressing tumor cells.* J Biol Chem, 2003. **278**(34): p. 32259-65.

162. Liu, D., et al., *Expression of hyaluronidase by tumor cells induces angiogenesis in vivo.* Proc Natl Acad Sci U S A, 1996. **93**(15): p. 7832-7.

163. West, D.C., et al., *Angiogenesis induced by degradation products of hyaluronic acid.* Science, 1985. **228**(4705): p. 1324-6.

164. Sattar, A., et al., *Application of angiogenic oligosaccharides of hyaluronan increases blood vessel numbers in rat skin.* J Invest Dermatol, 1994. **103**(4): p. 576-9.

165. Lokeshwar, V.B., et al., *Tumor-associated hyaluronic acid: a new sensitive and specific urine marker for bladder cancer.* Cancer Res, 1997. **57**(4): p. 773-7.

166. Lokeshwar, V.B., et al., *Urinary hyaluronic acid and hyaluronidase: markers for bladder cancer detection and evaluation of grade.* J Urol, 2000. **163**(1): p. 348-56.

167. Droller, M.J., *Tumor-derived hyaluronidase: a diagnostic urine marker for high-grade bladder cancer.* J Urol, 1998. **160**(2): p. 619-20.

168. Ho, S.M. and R.Y. Cheng, *A promising bladder cancer detection assay: the HA-HAase test.* J Urol, 2004. **172**(3): p. 824-5.

169. Hautmann, S., et al., *Immunocyt and the HA-HAase urine tests for the detection of bladder cancer: a side-by-side comparison.* Eur Urol, 2004. **46**(4): p. 466-71.

170. Kumar, S., et al., *Sera of children with renal tumours contain low-molecular-mass hyaluronic acid.* Int J Cancer, 1989. **44**(3): p. 445-8.

171. Hasselbalch, H., et al., *Serum hyaluronan is increased in malignant lymphoma.* Am J Hematol, 1995. **50**(4): p. 231-3.

172. Thylen, A., J. Wallin, and G. Martensson, *Hyaluronan in serum as an indicator of progressive disease in hyaluronan-producing malignant mesothelioma.* Cancer, 1999. **86**(10): p. 2000-5.

173. Obayashi, Y., et al., *Role of serum-derived hyaluronan-associated protein-hyaluronan complex in ovarian cancer.* Oncol Rep, 2008. **19**(5): p. 1245-51.

174. Aruffo, A., et al., *CD44 is the principal cell surface receptor for hyaluronate.* Cell, 1990. **61**(7): p. 1303-13.

175. Bourguignon, L.Y., D. Zhu, and H. Zhu, *CD44 isoform-cytoskeleton interaction in oncogenic signaling and tumor progression.* Front Biosci, 1998. **3**: p. d637-49.

176. Jalkanen, S. and M. Jalkanen, *Lymphocyte CD44 binds the COOH-terminal heparin-binding domain of fibronectin.* J Cell Biol, 1992. **116**(3): p. 817-25.

177. Skoudy, A., et al., *CD44 binds to the Shigella IpaB protein and participates in bacterial invasion of epithelial cells.* Cell Microbiol, 2000. **2**(1): p. 19-33.

178. Malkar, N.B., et al., *Modulation of triple-helical stability and subsequent melanoma cellular responses by single-site substitution of fluoroproline derivatives.* Biochemistry, 2002. **41**(19): p. 6054-64.

179. Screaton, G.R., et al., *Genomic structure of DNA encoding the lymphocyte homing receptor CD44 reveals at least 12 alternatively spliced exons.* Proc Natl Acad Sci U S A, 1992. **89**(24): p. 12160-4.

180. Naor, D., et al., *CD44 in cancer.* Crit Rev Clin Lab Sci, 2002. **39**(6): p. 527-79.

181. Ponta, H., L. Sherman, and P.A. Herrlich, *CD44: from adhesion molecules to signalling regulators.* Nat Rev Mol Cell Biol, 2003. **4**(1): p. 33-45.

182. Stickeler, E., et al., *Expression of CD44 standard and variant isoforms v5, v6 and v7 in human ovarian cancer cell lines.* Anticancer Res, 1997. **17**(3C): p. 1871-6.

183. Coradini and Perbellini, *Hyaluronan: a suitable carrier for an histone deacetylase inhibitor in the treatment of human solid tumors.* Cancer Therapy, 2004. **2**: p. 201-216.

184. Buess, M., et al., *Tumor-endothelial interaction links the CD44(+)/CD24(-) phenotype with poor prognosis in early-stage breast cancer.* Neoplasia, 2009. **11**(10): p. 987-1002.

185. Okayama, H., et al., *CD44v6, MMP-7 and nuclear Cdx2 are significant biomarkers for prediction of lymph node metastasis in primary gastric cancer.* Oncol Rep, 2009. **22**(4): p. 745-55.

186. Kawano, T., et al., *Expression of E-cadherin, and CD44s and CD44v6 and its association with prognosis in head and neck cancer.* Auris Nasus Larynx, 2004. **31**(1): p. 35-41.

187. Lee, S.M., et al., *Prognostic significance of CD44s expression in biliary tract cancers.* Ann Surg Oncol, 2008. **15**(4): p. 1155-60.

188. Gu, H., P. Shang, and C. Zhou, *[Expression of CD44v6 and E-cadherin in prostate carcinoma and metastasis of prostate carcinoma].* Zhonghua Nan Ke Xue, 2004. **10**(1): p. 32-4, 38.

189. Zhu, D. and L.Y. Bourguignon, *Interaction between CD44 and the repeat domain of ankyrin promotes hyaluronic acid-mediated ovarian tumor cell migration.* J Cell Physiol, 2000. **183**(2): p. 182-95.

190. Bourguignon, L.Y., et al., *Interaction between the adhesion receptor, CD44, and the oncogene product, p185HER2, promotes human ovarian tumor cell activation.* J Biol Chem, 1997. **272**(44): p. 27913-8.

191. Cannistra, S.A., et al., *CD44 variant expression is a common feature of epithelial ovarian cancer: lack of association with standard prognostic factors.* J Clin Oncol, 1995. **13**(8): p. 1912-21.

192. Bourguignon, L.Y., et al., *CD44 interaction with c-Src kinase promotes cortactin-mediated cytoskeleton function and hyaluronic acid-dependent ovarian tumor cell migration.* J Biol Chem, 2001. **276**(10): p. 7327-36.

193. Bourguignon, L.Y., et al., *Ankyrin-Tiam1 interaction promotes Rac1 signaling and metastatic breast tumor cell invasion and migration.* J Cell Biol, 2000. **150**(1): p. 177-91.

194. Strobel, T., L. Swanson, and S.A. Cannistra, *In vivo inhibition of CD44 limits intra-abdominal spread of a human ovarian cancer xenograft in nude mice: a novel role for CD44 in the process of peritoneal implantation.* Cancer Res, 1997. **57**(7): p. 1228-32.

195. Lessan, K., et al., *CD44 and beta1 integrin mediate ovarian carcinoma cell adhesion to peritoneal mesothelial cells.* Am J Pathol, 1999. **154**(5): p. 1525-37.

196. Kim, Y., et al., *CD44-epidermal growth factor receptor interaction mediates hyaluronic acid-promoted cell motility by activating protein kinase C signaling involving Akt, Rac1, Phox, reactive oxygen species, focal adhesion kinase, and MMP-2.* J Biol Chem, 2008. **283**(33): p. 22513-28.

197. Bourguignon, L.Y., W. Xia, and G. Wong, *Hyaluronan-mediated CD44 interaction with p300 and SIRT1 regulates beta-catenin signaling and NFkappaB-specific transcription activity leading to MDR1 and Bcl-xL gene expression and chemoresistance in breast tumor cells.* J Biol Chem, 2009. **284**(5): p. 2657-71.

198. Harrell, J.C., et al., *Estrogen receptor positive breast cancer metastasis: altered hormonal sensitivity and tumor aggressiveness in lymphatic vessels and lymph nodes.* Cancer Res, 2006. **66**(18): p. 9308-15.

199. Jones, L.M., et al., *Hyaluronic acid secreted by mesothelial cells: a natural barrier to ovarian cancer cell adhesion.* Clin Exp Metastasis, 1995. **13**(5): p. 373-80.

200. Zagorianakou, N., et al., *CD44s expression, in benign, borderline and malignant tumors of ovarian surface epithelium. Correlation with p53, steroid receptor status, proliferative indices (PCNA, MIB1) and survival.* Anticancer Res, 2004. **24**(3a): p. 1665-70.

201. Rodriguez-Rodriguez, L., et al., *The CD44 receptor is a molecular predictor of survival in ovarian cancer.* Med Oncol, 2003. **20**(3): p. 255-63.

202. Sillanpaa, S., et al., *CD44 expression indicates favorable prognosis in epithelial ovarian cancer.* Clin Cancer Res, 2003. **9**(14): p. 5318-24.

203. Wegrowski, Y. and F.X. Maquart, *Involvement of stromal proteoglycans in tumour progression.* Crit Rev Oncol Hematol, 2004. **49**(3): p. 259-68.

204. Chung, I.M., et al., *Enhanced extracellular matrix accumulation in restenosis of coronary arteries after stent deployment.* J Am Coll Cardiol, 2002. **40**(12): p. 2072-81.

205. Ito, K., et al., *Multiple forms of mouse PG-M, a large chondroitin sulfate proteoglycan generated by alternative splicing.* J.Biol.Chem., 1995. **270**(2): p. 958-965.

206. Kischel, P., et al., *Versican overexpression in human breast cancer lesions: known and new isoforms for stromal tumor targeting.* Int J Cancer, 2010. **126**(3): p. 640-50.

207. Suwan, K., et al., *Versican/PG-M Assembles Hyaluronan into Extracellular Matrix and Inhibits CD44-mediated Signaling toward Premature Senescence in Embryonic Fibroblasts.* J Biol Chem, 2009. **284**(13): p. 8596-604.

208. Koyama, H., et al., *Hyperproduction of hyaluronan in neu-induced mammary tumor accelerates angiogenesis through stromal cell recruitment: possible involvement of versican/PG-M.* Am J Pathol, 2007. **170**(3): p. 1086-99.

209. Ricciardelli, C., et al., *The biological role and regulation of versican levels in cancer.* Cancer Metastasis Rev, 2009.

210. Wu, Y.J., et al., *The interaction of versican with its binding partners.* Cell Res, 2005. **15**(7): p. 483-94.

211. Cattaruzza, S., et al., *Distribution of PG-M/versican variants in human tissues and de novo expression of isoform V3 upon endothelial cell activation, migration, and neoangiogenesis in vitro.* J Biol Chem, 2002. **277**(49): p. 47626-35.

212. Perissinotto, D., et al., *Avian neural crest cell migration is diversely regulated by the two major hyaluronan-binding proteoglycans PG-M/versican and aggrecan.* Development, 2000. **127**(13): p. 2823-2842.

213. Sheng, W., et al., *The roles of versican V1 and V2 isoforms in cell proliferation and apoptosis.* Mol Biol Cell, 2005. **16**(3): p. 1330-40.

214. Wu, Y., et al., *Versican V1 isoform induces neuronal differentiation and promotes neurite outgrowth.* Mol Biol Cell, 2004. **15**(5): p. 2093-104.

215. Schmalfeldt, M., et al., *Brain derived versican V2 is a potent inhibitor of axonal growth.* J.Cell Sci., 2000. **113 (Pt 5)**: p. 807-816.

216. Sakko, A.J., et al., *Versican accumulation in human prostatic fibroblast cultures is enhanced by prostate cancer cell-derived transforming growth factor beta1.* Cancer Res., 2001. **61**(3): p. 926-930.

217. Ricciardelli, C., et al., *Regulation of stromal versican expression by breast cancer cells and importance to relapse-free survival in patients with node-negative primary breast cancer.* Clin Cancer Res, 2002. **8**(4): p. 1054-60.

218. Nikitovic, D., et al., *Transforming growth factor-beta as a key molecule triggering the expression of versican isoforms v0 and v1, hyaluronan synthase-2 and synthesis of hyaluronan in malignant osteosarcoma cells.* IUBMB Life, 2006. **58**(1): p. 47-53.

219. Arslan, F., et al., *The role of versican isoforms V0/V1 in glioma migration mediated by transforming growth factor-beta2.* Br J Cancer, 2007. **96**(10): p. 1560-8.

220. Touab, M., et al., *Versican is differentially expressed in human melanoma and may play a role in tumor development.* Am J Pathol, 2002. **160**(2): p. 549-57.

221. Sakko, A.J., et al., *Modulation of Prostate Cancer Cell Attachment to Matrix by Versican.* Cancer Res, 2003. **63**(16): p. 4786-4791.

222. Lemire, J.M., et al., *Overexpression of the V3 variant of versican alters arterial smooth muscle cell adhesion, migration, and proliferation in vitro.* J.Cell Physiol, 2002. **190**(1): p. 38-45.

223. Serra, M., et al., *V3 versican isoform expression alters the phenotype of melanoma cells and their tumorigenic potential.* Int J Cancer, 2005. **114**(6): p. 879-86.

224. Miquel-Serra, L., et al., *V3 versican isoform expression has a dual role in human melanoma tumor growth and metastasis.* Lab Invest, 2006. **86**(9): p. 889-901.

225. Perides, G., et al., *Glial hyaluronate-binding protein: a product of metalloproteinase digestion of versican?* Biochem.J., 1995. **312 (Pt 2)**: p. 377-384.

226. Saarialho-Kere, U., et al., *Accumulation of matrilysin (MMP-7) and macrophage metalloelastase (MMP-12) in actinic damage.* J.Invest Dermatol., 1999. **113**(4): p. 664-672.

227. Passi, A., et al., *The sensitivity of versican from rabbit lung to gelatinase A (MMP-2) and B (MMP-9) and its involvement in the development of hydraulic lung edema.* FEBS Lett., 1999. **456**(1): p. 93-96.

228. Kuno, K., et al., *The exon/intron organization and chromosomal mapping of the mouse ADAMTS-1 gene encoding an ADAM family protein with TSP motifs.* Genomics, 1997. **46**(3): p. 466-71.

229. Sandy, J.D., et al., *Versican V1 proteolysis in human aorta in vivo occurs at the Glu441-Ala442 bond, a site that is cleaved by recombinant ADAMTS-1 and ADAMTS-4.* J.Biol.Chem., 2001. **276**(16): p. 13372-13378.

230. Somerville, R.P., et al., *Characterization of ADAMTS-9 and ADAMTS-20 as a distinct ADAMTS subfamily related to Caenorhabditis elegans GON-1.* J Biol Chem, 2003. **278**(11): p. 9503-13.

231. Boerboom, D., et al., *Regulation of transcripts encoding ADAMTS-1 (a disintegrin and metalloproteinase with thrombospondin-like motifs-1) and progesterone receptor by human chorionic gonadotropin in equine preovulatory follicles.* J Mol Endocrinol, 2003. **31**(3): p. 473-85.

232. Matsumoto, K., et al., *Distinct interaction of versican/PG-M with hyaluronan and link protein.* J Biol Chem, 2003. **278**(42): p. 41205-12.

233. LeBaron, R.G., *Versican.* Perspect.Dev.Neurobiol., 1996. **3**(4): p. 261-271.

234. Zhang, Y., et al., *The G3 domain of versican enhances cell proliferation via epidermial growth factor-like motifs.* J.Biol.Chem., 1998. **273**(33): p. 21342-21351.

235. Yang, B.L., et al., *Cell adhesion and proliferation mediated through the G1 domain of versican.* J.Cell Biochem., 1999. **72**(2): p. 210-220.

236. Zheng, P.S., et al., *Versican/PG-M G3 domain promotes tumor growth and angiogenesis.* Faseb J, 2004. **18**: p. 754-760.

237. Cattaruzza, S., et al., *The globular domains of PGM/versican modulate the proliferation-apoptosis equilibrium and invasive capabilities of tumor cells.* Faseb J, 2004. **18**: p. 779-781.

238. Ang, L.C., et al., *Versican enhances locomotion of astrocytoma cells and reduces cell adhesion through its G1 domain.* J.Neuropathol.Exp.Neurol., 1999. **58**(6): p. 597-605.

239. Paris, S., et al., *Hyaluronectin modulation of lung metastasis in nude mice.* Eur J Cancer, 2006. **42**(18): p. 3253-9.

240. Yee, A.J., et al., *The effect of versican G3 domain on local breast cancer invasiveness and bony metastasis.* Breast Cancer Res, 2007. **9**(4): p. R47.

241. Creighton, C.J., et al., *Analysis of tumor-host interactions by gene expression profiling of lung adenocarcinoma xenografts identifies genes involved in tumor formation.* Mol Cancer Res, 2005. **3**(3): p. 119-29.

242. LaPierre, D.P., et al., *The ability of versican to simultaneously cause apoptotic resistance and sensitivity.* Cancer Res, 2007. **67**(10): p. 4742-50.

243. Brown, L.F., et al., *Vascular stroma formation in carcinoma in situ, invasive carcinoma, and metastatic carcinoma of the breast.* Clin.Cancer Res., 1999. **5**(5): p. 1041-1056.

244. Kodama, J., et al., *Versican expression in human cervical cancer.* Eur J Cancer, 2007. **43**(9): p. 1460-6.

245. Kodama, J., et al., *Prognostic significance of stromal versican expression in human endometrial cancer.* Ann Oncol, 2007. **18**(2): p. 269-74.

246. Voutilainen, K., et al., *Versican in epithelial ovarian cancer: Relation to hyaluronan, clinicopathologic factors and prognosis.* Int J Cancer, 2003. **107**(3): p. 359-64.

247. Lancaster, J.M., et al., *Identification of genes associated with ovarian cancer metastasis using microarray expression analysis.* Int J Gynecol Cancer, 2006. **16**(5): p. 1733-45.

248. Casey, R.C., et al., *Cell membrane glycosylation mediates the adhesion, migration, and invasion of ovarian carcinoma cells.* Clin Exp Metastasis, 2003. **20**(2): p. 143-52.

249. Casey, M.J., et al., *Histology of prophylactically removed ovaries from BRCA1 and BRCA2 mutation carriers compared with noncarriers in hereditary breast ovarian cancer syndrome kindreds.* Gynecol Oncol, 2000. **78**(3 Pt 1): p. 278-87.

250. Casey, R.C., et al., *Establishment of an in vitro assay to measure the invasion of ovarian carcinoma cells through mesothelial cell monolayers.* Clin Exp Metastasis, 2003. **20**(4): p. 343-56.

251. Gardner, M.J., et al., *Human ovarian tumour cells can bind hyaluronic acid via membrane CD44: a possible step in peritoneal metastasis.* Clin Exp Metastasis, 1996. **14**(4): p. 325-34.

252. Knudson, W., E. Bartnik, and C.B. Knudson, *Assembly of pericellular matrices by COS-7 cells transfected with CD44 lymphocyte-homing receptor genes.* Proc.Natl.Acad.Sci.U.S.A, 1993. **90**(9): p. 4003-4007.

253. Hayen, W., et al., *Hyaluronan stimulates tumor cell migration by modulating the fibrin fiber architecture.* J Cell Sci, 1999. **112 (Pt 13)**: p. 2241-51.

254. Lee, H., K. Lee, and T.G. Park, *Hyaluronic acid-paclitaxel conjugate micelles: synthesis, characterization, and antitumor activity.* Bioconjug Chem, 2008. **19**(6): p. 1319-25.

255. Banzato, A., et al., *A paclitaxel-hyaluronan bioconjugate targeting ovarian cancer affords a potent in vivo therapeutic activity.* Clin Cancer Res, 2008. **14**(11): p. 3598-606.

256. Auzenne, E., et al., *Hyaluronic acid-paclitaxel: antitumor efficacy against CD44(+) human ovarian carcinoma xenografts.* Neoplasia, 2007. **9**(6): p. 479-86.

257. Gibbs, P., et al., *Hyaluronan-Irinotecan improves progression-free survival in 5-fluorouracil refractory patients with metastatic colorectal cancer: a randomized phase II trial.* Cancer Chemother Pharmacol, 2010.

258. He, M., et al., *Hyaluronic acid coated poly(butyl cyanoacrylate) nanoparticles as anticancer drug carriers.* Int J Pharm, 2009. **373**(1-2): p. 165-73.

259. Cohen, M.S., et al., *A novel intralymphatic nanocarrier delivery system for cisplatin therapy in breast cancer with improved tumor efficacy and lower systemic toxicity in vivo.* Am J Surg, 2009. **198**(6): p. 781-6.

260. Prada, P.J., et al., *Transperineal injection of hyaluronic acid in the anterior perirectal fat to decrease rectal toxicity from radiation delivered with low-dose-rate brachytherapy for prostate cancer patients.* Brachytherapy, 2009. **8**(2): p. 210-7.

261. Bartusik, D., et al., *Combined treatment of human MCF-7 breast carcinoma with antibody, cationic lipid and hyaluronic acid using ex vivo assays.* J Pharm Biomed Anal, 2010. **51**(1): p. 192-201.

262. Sun, X., et al., *Positive hyaluronan/PEI/DNA complexes as a target-specific intracellular delivery to malignant breast cancer.* Drug Deliv, 2009. **16**(7): p. 357-62.

263. Jiang, G., et al., *Target specific intracellular delivery of siRNA/PEI-HA complex by receptor mediated endocytosis.* Mol Pharm, 2009. **6**(3): p. 727-37.

264. Chono, S., et al., *An efficient and low immunostimulatory nanoparticle formulation for systemic siRNA delivery to the tumor.* J Control Release, 2008. **131**(1): p. 64-9.

265. Lee, S.O., et al., *Silibinin suppresses PMA-induced MMP-9 expression by blocking the AP-1 activation via MAPK signaling pathways in MCF-7 human breast carcinoma cells.* Biochem Biophys Res Commun, 2007. **354**(1): p. 165-71.

266. Mateen, S., et al., *Silibinin inhibits human nonsmall cell lung cancer cell growth through cell-cycle arrest by modulating expression and function of key cell-cycle regulators.* Mol Carcinog, 2009.

267. Kaur, M., et al., *Silibinin suppresses growth and induces apoptotic death of human colorectal carcinoma LoVo cells in culture and tumor xenograft.* Mol Cancer Ther, 2009. **8**(8): p. 2366-74.

268. Handorean, A.M., et al., *Silibinin suppresses CD44 expression in prostate cancer cells.* Am J Transl Res, 2009. **1**(1): p. 80-6.

269. Wallach-Dayan, S.B., et al., *DNA vaccination with CD44 variant isoform reduces mammary tumor local growth and lung metastasis.* Mol Cancer Ther, 2008. **7**(6): p. 1615-23.

270. Hong, S.P., et al., *CD44-positive cells are responsible for gemcitabine resistance in pancreatic cancer cells.* Int J Cancer, 2009. **125**(10): p. 2323-31.

271. Jin, L., et al., *Targeting of CD44 eradicates human acute myeloid leukemic stem cells.* Nat Med, 2006. **12**(10): p. 1167-74.

272. Subramaniam, V., et al., *Suppression of human colon cancer tumors in nude mice by siRNA CD44 gene therapy.* Exp Mol Pathol, 2007. **83**(3): p. 332-40.

273. Xie, Z., et al., *Inhibition of CD44 expression in hepatocellular carcinoma cells enhances apoptosis, chemosensitivity, and reduces tumorigenesis and invasion.* Cancer Chemother Pharmacol, 2008. **62**(6): p. 949-57.

274. Li, C.Z., et al., *Inhibition of CD44 expression by small interfering RNA to suppress the growth and metastasis of ovarian cancer cells in vitro and in vivo.* Folia Biol (Praha), 2008. **54**(6): p. 180-6.

275. Wiranowska, M., et al., *Modulation of Hyaluronan production by CD44 positive Glioma cells.* Int J Cancer, 2009.

276. Yoshida, M., et al., *Induction of apoptosis by anti-CD44 antibody in human chondrosarcoma cell line SW1353.* Biomed Res, 2008. **29**(1): p. 47-52.

277. Marangoni, E., et al., *CD44 targeting reduces tumour growth and prevents post-chemotherapy relapse of human breast cancers xenografts.* Br J Cancer, 2009. **100**(6): p. 918-22.

278. Afify, A., P. Purnell, and L. Nguyen, *Role of CD44s and CD44v6 on human breast cancer cell adhesion, migration, and invasion.* Exp Mol Pathol, 2009. **86**(2): p. 95-100.

279. Guo, Y., et al., *Inhibition of human melanoma growth and metastasis in vivo by anti-CD44 monoclonal antibody.* Cancer Res, 1994. **54**(6): p. 1561-5.

280. Draffin, J.E., et al., *CD44 potentiates the adherence of metastatic prostate and breast cancer cells to bone marrow endothelial cells.* Cancer Res, 2004. **64**(16): p. 5702-11.

281. S. E. Hahn, L.A.d.C., D. Sayegh, A. Ferry, K. O'Reilly, D. S. Pereira, D. B. Rubinstein, H. Findlay, D. S. Young, *2007 ASCO Annual Meeting Proceedings Part I.* Journal of Clinical Oncology, 2007. **25**(18S): p. 13510.

282. Herrera-Gayol, A. and S. Jothy, *CD44 modulates Hs578T human breast cancer cell adhesion, migration, and invasiveness.* Exp Mol Pathol, 1999. **66**(1): p. 99-108.

283. Riechelmann, H., et al., *Phase I trial with the CD44v6-targeting immunoconjugate bivatuzumab mertansine in head and neck squamous cell carcinoma.* Oral Oncol, 2008. **44**(9): p. 823-9.

284. Rupp, U., et al., *Safety and pharmacokinetics of bivatuzumab mertansine in patients with CD44v6-positive metastatic breast cancer: final results of a phase I study.* Anticancer Drugs, 2007. **18**(4): p. 477-85.

285. Tijink, B.M., et al., *A phase I dose escalation study with anti-CD44v6 bivatuzumab mertansine in patients with incurable squamous cell carcinoma of the head and neck or esophagus.* Clin Cancer Res, 2006. **12**(20 Pt 1): p. 6064-72.

286. Schonherr, E., M.G. Kinsella, and T.N. Wight, *Genistein selectively inhibits platelet-derived growth factor-stimulated versican biosynthesis in monkey arterial smooth muscle cells.* Arch.Biochem.Biophys., 1997. **339**(2): p. 353-361.

287. Syrokou, A., et al., *Proteoglycans in human malignant mesothelioma. Stimulation of their synthesis induced by epidermal, insulin and platelet-derived growth factors involves receptors with tyrosine kinase activity.* Biochimie, 1999. **81**(7): p. 733-744.

288. Burgess, J.K., et al., *A phosphodiesterase 4 inhibitor inhibits matrix protein deposition in airways in vitro.* J Allergy Clin Immunol, 2006. **118**(3): p. 649-57.

289. Todorova, L., et al., *Lung fibroblast proteoglycan production induced by serum is inhibited by budesonide and formoterol.* Am J Respir Cell Mol Biol, 2006. **34**(1): p. 92-100.

290. Potter-Perigo, S., et al., *Regulation of proteoglycan synthesis by leukotriene d4 and epidermal growth factor in bronchial smooth muscle cells.* Am J Respir Cell Mol Biol, 2004. **30**(1): p. 101-8.

291. Nakamura, J.L., D.A. Haas-Kogan, and R.O. Pieper, *Glioma invasiveness responds variably to irradiation in a co-culture model.* Int J Radiat Oncol Biol Phys, 2007. **69**(3): p. 880-6.

292. Almholt, K., et al., *Metastasis is strongly reduced by the matrix metalloproteinase inhibitor Galardin in the MMTV-PymT transgenic breast cancer model.* Mol Cancer Ther, 2008. **7**(9): p. 2758-67.

293. Vankemmelbeke, M.N., et al., *Selective inhibition of ADAMTS-1, -4 and -5 by catechin gallate esters.* Eur J Biochem, 2003. **270**(11): p. 2394-403.

294. Knudson, W. and C.B. Knudson, *Assembly of a chondrocyte-like pericellular matrix on non-chondrogenic cells. Role of the cell surface hyaluronan receptors in the assembly of a pericellular matrix.* J.Cell Sci., 1991. **99 (Pt 2)**: p. 227-235.

295. Zeng, C., et al., *Inhibition of tumor growth in vivo by hyaluronan oligomers.* Int J Cancer, 1998. **77**(3): p. 396-401.

296. Heng, B.C., et al., *Hyaluronan binding to link module of TSG-6 and to G1 domain of aggrecan is differently regulated by pH.* J Biol Chem, 2008. **283**(47): p. 32294-301.

297. Hosono, K., et al., *Hyaluronan oligosaccharides inhibit tumorigenicity of osteosarcoma cell lines MG-63 and LM-8 in vitro and in vivo via perturbation of hyaluronan-rich pericellular matrix of the cells.* Am J Pathol, 2007. **171**(1): p. 274-86.

298. Alaniz, L., et al., *Low molecular weight hyaluronan inhibits colorectal carcinoma growth by decreasing tumor cell proliferation and stimulating immune response.* Cancer Lett, 2009. **278**(1): p. 9-16.

299. Cui, X., et al., *Reversal effects of hyaluronan oligosaccharides on adriamycin resistance of K562/A02 cells.* Anticancer Drugs, 2009. **20**(9): p. 800-6.

300. Slomiany, M.G., et al., *Abrogating drug resistance in malignant peripheral nerve sheath tumors by disrupting hyaluronan-CD44 interactions with small hyaluronan oligosaccharides.* Cancer Res, 2009. **69**(12): p. 4992-8.

301. Molpus, K.L., et al., *Characterization of a xenograft model of human ovarian carcinoma which produces intraperitoneal carcinomatosis and metastases in mice.* Int J Cancer, 1996. **68**(5): p. 588-95.

302. Kokenyesi, R., *Ovarian carcinoma cells synthesize both chondroitin sulfate and heparan sulfate cell surface proteoglycans that mediate cell adhesion to interstitial matrix.* J Cell Biochem, 2001. **83**(2): p. 259-70.

303. Kleinman, H.K., et al., *Isolation and characterization of type IV procollagen, laminin, and heparan sulfate proteoglycan from the EHS sarcoma.* Biochemistry, 1982. **21**(24): p. 6188-93.

304. Andersen, J.S. and M. Mann, *Functional genomics by mass spectrometry.* FEBS Lett, 2000. **480**(1): p. 25-31.

305. Pandey, A. and M. Mann, *Proteomics to study genes and genomes.* Nature, 2000. **405**(6788): p. 837-46.

306. Anderson, N.G. and N.L. Anderson, *Twenty years of two-dimensional electrophoresis: past, present and future.* Electrophoresis, 1996. **17**(3): p. 443-53.

307. Wasinger, V.C., et al., *Progress with gene-product mapping of the Mollicutes: Mycoplasma genitalium.* Electrophoresis, 1995. **16**(7): p. 1090-4.

308. Paweletz, C.P., et al., *Proteomic patterns of nipple aspirate fluids obtained by SELDI-TOF: potential for new biomarkers to aid in the diagnosis of breast cancer.* Dis Markers, 2001. **17**(4): p. 301-7.

309. Liu, M., et al., *Differential expression of proteomics models of colorectal cancer, colorectal benign disease and healthy controls.* Proteome Sci, 2010. **8**(1): p. 16.

310. Tsunemi, S., et al., *Proteomics-based identification of a tumor-associated antigen and its corresponding autoantibody in gastric cancer.* Oncol Rep, 2010. **23**(4): p. 949-56.

311. Borgia, B., et al., *A proteomic approach for the identification of vascular markers of liver metastasis.* Cancer Res, 2010. **70**(1): p. 309-18.

312. Davidson, B., et al., *Proteomic analysis of malignant ovarian cancer effusions as a tool for biologic and prognostic profiling.* Clin Cancer Res, 2006. **12**(3 Pt 1): p. 791-9.

313. Gortzak-Uzan, L., et al., *A proteome resource of ovarian cancer ascites: integrated proteomic and bioinformatic analyses to identify putative biomarkers.* J Proteome Res, 2008. **7**(1): p. 339-51.

314. Cicchillitti, L., et al., *Comparative proteomic analysis of paclitaxel sensitive A2780 epithelial ovarian cancer cell line and its resistant counterpart A2780TC1 by 2D-DIGE: the role of ERp57.* J Proteome Res, 2009. **8**(4): p. 1902-12.

315. Chen, J.Y., et al., *A systems biology approach to the study of cisplatin drug resistance in ovarian cancers.* J Bioinform Comput Biol, 2007. **5**(2a): p. 383-405.

316. Maloney, A., et al., *Gene and protein expression profiling of human ovarian cancer cells treated with the heat shock protein 90 inhibitor 17-allylamino-17-demethoxygeldanamycin.* Cancer Res, 2007. **67**(7): p. 3239-53.

317. Conrads, T.P., et al., *High-resolution serum proteomic features for ovarian cancer detection.* Endocr Relat Cancer, 2004. **11**(2): p. 163-78.

318. Zhang, Z., et al., *Three biomarkers identified from serum proteomic analysis for the detection of early stage ovarian cancer.* Cancer Res, 2004. **64**(16): p. 5882-90.

319. Li, X.Q., et al., *Proteomic identification of tumor-associated protein in ovarian serous cystadenocarinoma.* Cancer Lett, 2009. **275**(1): p. 109-16.

320. Kuk, C., et al., *Mining the ovarian cancer ascites proteome for potential ovarian cancer biomarkers.* Mol Cell Proteomics, 2009. **8**(4): p. 661-9.

321. Petri, A.L., et al., *Three new potential ovarian cancer biomarkers detected in human urine with equalizer bead technology.* Acta Obstet Gynecol Scand, 2009. **88**(1): p. 18-26.

322. Jackson, D., et al., *Proteomic profiling identifies afamin as a potential biomarker for ovarian cancer.* Clin Cancer Res, 2007. **13**(24): p. 7370-9.

323. Bengtsson, S., et al., *Large-scale proteomics analysis of human ovarian cancer for biomarkers.* J Proteome Res, 2007. **6**(4): p. 1440-50.

324. Wu, S.P., et al., *SELDI-TOF MS profiling of plasma proteins in ovarian cancer.* Taiwan J Obstet Gynecol, 2006. **45**(1): p. 26-32.

325. Su, F., et al., *Validation of candidate serum ovarian cancer biomarkers for early detection.* Biomark Insights, 2007. **2**: p. 369-75.

326. Koomen, J.M., et al., *Proteomic contributions to personalized cancer care.* Mol Cell Proteomics, 2008. **7**(10): p. 1780-94.

327. Lee, J.H., et al., *Expression of the CD44 adhesion molecule in primary and metastatic gynecologic malignancies and their cell lines.* Int J Gynecol Cancer, 1995. **5**(3): p. 193-199.

328. Gardner, M.J., et al., *Expression of cell adhesion molecules on ovarian tumour cell lines and mesothelial cells, in relation to ovarian cancer metastasis.* Cancer Lett, 1995. **91**(2): p. 229-34.

329. Hashimoto, M., et al., *Unstable expression of E-cadherin adhesion molecules in metastatic ovarian tumor cells.* Jpn J Cancer Res, 1989. **80**(5): p. 459-63.

330. Slack-Davis, J.K., et al., *Vascular cell adhesion molecule-1 is a regulator of ovarian cancer peritoneal metastasis.* Cancer Res, 2009. **69**(4): p. 1469-76.

331. Roomi, M.W., et al., *In vitro modulation of MMP-2 and MMP-9 in human cervical and ovarian cancer cell lines by cytokines, inducers and inhibitors.* Oncol Rep, 2010. **23**(3): p. 605-14.

332. Dolo, V., et al., *Matrix-degrading proteinases are shed in membrane vesicles by ovarian cancer cells in vivo and in vitro.* Clin Exp Metastasis, 1999. **17**(2): p. 131-40.

333. Zohny, S.F. and S.T. Fayed, *Clinical utility of circulating matrix metalloproteinase-7 (MMP-7), CC chemokine ligand 18 (CCL18) and CC chemokine ligand 11 (CCL11) as markers for diagnosis of epithelial ovarian cancer.* Med Oncol, 2009.

334. Graves, P.R. and T.A. Haystead, *Molecular biologist's guide to proteomics.* Microbiol Mol Biol Rev, 2002. **66**(1): p. 39-63; table of contents.

335. Romberger, D.J., *Fibronectin.* Int J Biochem Cell Biol, 1997. **29**(7): p. 939-43.

336. Kenny, H.A., et al., *The initial steps of ovarian cancer cell metastasis are mediated by MMP-2 cleavage of vitronectin and fibronectin.* J Clin Invest, 2008. **118**(4): p. 1367-79.

337. Nagai, T., et al., *Monoclonal antibody characterization of two distant sites required for function of the central cell-binding domain of fibronectin in cell adhesion, cell migration, and matrix assembly.* J Cell Biol, 1991. **114**(6): p. 1295-305.

338. Ruoslahti, E., et al., *Alignment of biologically active domains in the fibronectin molecule.* J Biol Chem, 1981. **256**(14): p. 7277-81.

339. Hayashi, M. and K.M. Yamada, *Domain structure of the carboxyl-terminal half of human plasma fibronectin.* J Biol Chem, 1983. **258**(5): p. 3332-40.

340. Zardi, L., et al., *Elution of fibronectin proteolytic fragments from a hydroxyapatite chromatography column. A simple procedure for the purification of fibronectin domains.* Eur J Biochem, 1985. **146**(3): p. 571-9.

341. Akiyama, S.K., et al., *The interaction of fibronectin fragments with fibroblastic cells.* J Biol Chem, 1985. **260**(24): p. 13256-60.

342. Yamada, K.M. and D.W. Kennedy, *Dualistic nature of adhesive protein function: fibronectin and its biologically active peptide fragments can autoinhibit fibronectin function.* J Cell Biol, 1984. **99**(1 Pt 1): p. 29-36.

343. Pierschbacher, M.D. and E. Ruoslahti, *Cell attachment activity of fibronectin can be duplicated by small synthetic fragments of the molecule.* Nature, 1984. **309**(5963): p. 30-3.

344. Wachtfogel, Y.T., et al., *Fibronectin degradation products containing the cytoadhesive tetrapeptide stimulate human neutrophil degranulation.* J Clin Invest, 1988. **81**(5): p. 1310-6.

345. Quigley, J.P., et al., *Limited cleavage of cellular fibronectin by plasminogen activator purified from transformed cells.* Proc Natl Acad Sci U S A, 1987. **84**(9): p. 2776-80.

346. Horowitz, J.C., et al., *Plasminogen activation induced pericellular fibronectin proteolysis promotes fibroblast apoptosis.* Am J Respir Cell Mol Biol, 2008. **38**(1): p. 78-87.

347. Al-Hazmi, N., et al., *The 120 kDa cell-binding fragment of fibronectin up-regulates migration of alphavbeta6-expressing cells by increasing matrix metalloproteinase-2 and -9 secretion.* Eur J Oral Sci, 2007. **115**(6): p. 454-8.

348. Wilhelm, S.M., et al., *Matrix metalloproteinase-3 (stromelysin-1). Identification as the cartilage acid metalloprotease and effect of pH on catalytic properties and calcium affinity.* J Biol Chem, 1993. **268**(29): p. 21906-13.

349. Stracke, J.O., et al., *Biochemical characterization of the catalytic domain of human matrix metalloproteinase 19. Evidence for a role as a potent basement membrane degrading enzyme.* J Biol Chem, 2000. **275**(20): p. 14809-16.

350. Ohuchi, E., et al., *Membrane type 1 matrix metalloproteinase digests interstitial collagens and other extracellular matrix macromolecules.* J Biol Chem, 1997. **272**(4): p. 2446-51.

351. Quantin, B., G. Murphy, and R. Breathnach, *Pump-1 cDNA codes for a protein with characteristics similar to those of classical collagenase family members.* Biochemistry, 1989. **28**(13): p. 5327-34.

352. Ramani, V.C. and R.S. Haun, *The extracellular matrix protein fibronectin is a substrate for kallikrein 7.* Biochem Biophys Res Commun, 2008. **369**(4): p. 1169-73.

353. Takeshita, S., et al., *Osteoblast-specific factor 2: cloning of a putative bone adhesion protein with homology with the insect protein fasciclin I.* Biochem J, 1993. **294 (Pt 1)**: p. 271-8.

354. Horiuchi, K., et al., *Identification and characterization of a novel protein, periostin, with restricted expression to periosteum and periodontal ligament and increased expression by transforming growth factor beta.* J Bone Miner Res, 1999. **14**(7): p. 1239-49.

355. Kruzynska-Frejtag, A., et al., *Periostin (an osteoblast-specific factor) is expressed within the embryonic mouse heart during valve formation.* Mech Dev, 2001. **103**(1-2): p. 183-8.

356. Kruzynska-Frejtag, A., et al., *Periostin is expressed within the developing teeth at the sites of epithelial-mesenchymal interaction.* Dev Dyn, 2004. **229**(4): p. 857-68.

357. Norris, R.A., et al., *Periostin regulates collagen fibrillogenesis and the biomechanical properties of connective tissues.* J Cell Biochem, 2007. **101**(3): p. 695-711.

358. Kikuchi, Y., et al., *Periostin is expressed in pericryptal fibroblasts and cancer-associated fibroblasts in the colon.* J Histochem Cytochem, 2008. **56**(8): p. 753-64.

359. Sasaki, H., et al., *Expression of Periostin, homologous with an insect cell adhesion molecule, as a prognostic marker in non-small cell lung cancers.* Jpn J Cancer Res, 2001. **92**(8): p. 869-73.

360. Kim, C.J., et al., *Periostin is down-regulated in high grade human bladder cancers and suppresses in vitro cell invasiveness and in vivo metastasis of cancer cells.* Int J Cancer, 2005. **117**(1): p. 51-8.

361. Shao, R., et al., *Acquired expression of periostin by human breast cancers promotes tumor angiogenesis through up-regulation of vascular endothelial growth factor receptor 2 expression.* Mol Cell Biol, 2004. **24**(9): p. 3992-4003.

362. Yoshioka, N., et al., *Suppression of anchorage-independent growth of human cancer cell lines by the TRIF52/periostin/OSF-2 gene.* Exp Cell Res, 2002. **279**(1): p. 91-9.

363. Ruan, K., S. Bao, and G. Ouyang, *The multifaceted role of periostin in tumorigenesis.* Cell Mol Life Sci, 2009. **66**(14): p. 2219-30.

364. Puppin, C., et al., *High periostin expression correlates with aggressiveness in papillary thyroid carcinomas.* J Endocrinol, 2008. **197**(2): p. 401-8.

365. Puglisi, F., et al., *Expression of periostin in human breast cancer.* J Clin Pathol, 2008. **61**(4): p. 494-8.

366. Li, J.S., et al., *Expression of periostin and its clinicopathological relevance in gastric cancer.* World J Gastroenterol, 2007. **13**(39): p. 5261-6.

367. Sasaki, H., et al., *Serum level of the periostin, a homologue of an insect cell adhesion molecule, in thymoma patients.* Cancer Lett, 2001. **172**(1): p. 37-42.

368. Tilman, G., et al., *Human periostin gene expression in normal tissues, tumors and melanoma: evidences for periostin production by both stromal and melanoma cells.* Mol Cancer, 2007. **6**: p. 80.

369. Tai, I.T., M. Dai, and L.B. Chen, *Periostin induction in tumor cell line explants and inhibition of in vitro cell growth by anti-periostin antibodies.* Carcinogenesis, 2005. **26**(5): p. 908-15.

370. Baril, P., et al., *Periostin promotes invasiveness and resistance of pancreatic cancer cells to hypoxia-induced cell death: role of the beta4 integrin and the PI3k pathway.* Oncogene, 2007. **26**(14): p. 2082-94.

371. Ben, Q.W., et al., *Circulating levels of periostin may help identify patients with more aggressive colorectal cancer.* Int J Oncol, 2009. **34**(3): p. 821-8.

372. Sasaki, H., et al., *Elevated serum periostin levels in patients with bone metastases from breast but not lung cancer.* Breast Cancer Res Treat, 2003. **77**(3): p. 245-52.

373. Gillan, L., et al., *Periostin secreted by epithelial ovarian carcinoma is a ligand for alpha(V)beta(3) and alpha(V)beta(5) integrins and promotes cell motility.* Cancer Res, 2002. **62**(18): p. 5358-64.

374. Reich, E., *molecular basis of biological degradative processes*, ed. R.D. Berlin, Henman, L., Lepow, I. H., Tanzer, J. M.,. 1980, New York: Academic Press.

375. Dano, K., et al., *Plasminogen activators, tissue degradation, and cancer.* Adv Cancer Res, 1985. **44**: p. 139-266.

376. Saksela, O., *Plasminogen activation and regulation of pericellular proteolysis.* Biochim Biophys Acta, 1985. **823**(1): p. 35-65.

377. van Mourik, J.A., D.A. Lawrence, and D.J. Loskutoff, *Purification of an inhibitor of plasminogen activator (antiactivator) synthesized by endothelial cells.* J Biol Chem, 1984. **259**(23): p. 14914-21.

378. Adams, D.S., et al., *A synthetic DNA encoding a modified human urokinase resistant to inhibition by serum plasminogen activator inhibitor.* J Biol Chem, 1991. **266**(13): p. 8476-82.

379. Shakespeare, M. and P. Wolf, *The demonstration of urokinase antigen in whole blood.* Thromb Res, 1979. **14**(6): p. 825-35.

380. Astedt, B. and L. Holmberg, *Immunological identity of urokinase and ovarian carcinoma plasminogen activator released in tissue culture.* Nature, 1976. **261**(5561): p. 595-7.

381. Schmalfeldt, B., et al., *Primary tumor and metastasis in ovarian cancer differ in their content of urokinase-type plasminogen activator, its receptor, and inhibitors types 1 and 2.* Cancer Res, 1995. **55**(18): p. 3958-63.

382. Kuhn, W., et al., *Urokinase (uPA) and PAI-1 predict survival in advanced ovarian cancer patients (FIGO III) after radical surgery and platinum-based chemotherapy.* Gynecol Oncol, 1994. **55**(3 Pt 1): p. 401-9.

383. Keski-Oja, J., et al., *Regulation of mRNAs for type-1 plasminogen activator inhibitor, fibronectin, and type I procollagen by transforming growth factor-beta. Divergent responses in lung fibroblasts and carcinoma cells.* J Biol Chem, 1988. **263**(7): p. 3111-5.

384. Hirashima, Y., et al., *Transforming growth factor-beta1 produced by ovarian cancer cell line HRA stimulates attachment and invasion through an up-regulation of plasminogen activator inhibitor type-1 in human peritoneal mesothelial cells.* J Biol Chem, 2003. **278**(29): p. 26793-802.

385. Mikolajczyk, S.D., et al., *Prostatic human kallikrein 2 inactivates and complexes with plasminogen activator inhibitor-1.* Int J Cancer, 1999. **81**(3): p. 438-42.

386. Shih Ie, M., et al., *Ovarian cancer specific kallikrein profile in effusions.* Gynecol Oncol, 2007. **105**(2): p. 501-7.

387. Traub, P. and R.L. Shoeman, *Intermediate filament proteins: cytoskeletal elements with gene-regulatory function?* Int Rev Cytol, 1994. **154**: p. 1-103.

388. Steinert, P.M. and D.R. Roop, *Molecular and cellular biology of intermediate filaments.* Annu Rev Biochem, 1988. **57**: p. 593-625.

389. Zhao, Y., et al., *Assembly and activation of HK-PK complex on endothelial cells results in bradykinin liberation and NO formation.* Am J Physiol Heart Circ Physiol, 2001. **280**(4): p. H1821-9.

390. Lucas, S.D., et al., *Aberrantly expressed cytokeratin 1, a tumor-associated autoantigen in papillary thyroid carcinoma.* Int J Cancer, 1997. **73**(2): p. 171-7.

391. Barboro, P., et al., *Differential proteomic analysis of nuclear matrix in muscle-invasive bladder cancer: potential to improve diagnosis and prognosis.* Cell Oncol, 2008. **30**(1): p. 13-26.

392. Hasan, A.A., T. Zisman, and A.H. Schmaier, *Identification of cytokeratin 1 as a binding protein and presentation receptor for kininogens on endothelial cells.* Proc Natl Acad Sci U S A, 1998. **95**(7): p. 3615-20.

393. Shariat-Madar, Z., F. Mahdi, and A.H. Schmaier, *Mapping binding domains of kininogens on endothelial cell cytokeratin 1.* J Biol Chem, 1999. **274**(11): p. 7137-45.

394. Colman, R.W., et al., *Binding of high molecular weight kininogen to human endothelial cells is mediated via a site within domains 2 and 3 of the urokinase receptor.* J Clin Invest, 1997. **100**(6): p. 1481-7.

395. Motta, G., et al., *High molecular weight kininogen regulates prekallikrein assembly and activation on endothelial cells: a novel mechanism for contact activation.* Blood, 1998. **91**(2): p. 516-28.

396. Odya, C.E., et al., *Purification and properties of prolylcarboxypeptidase (angiotensinase C) from human kidney.* J Biol Chem, 1978. **253**(17): p. 5927-31.

397. Presland, R.B. and R.J. Jurevic, *Making sense of the epithelial barrier: what molecular biology and genetics tell us about the functions of oral mucosal and epidermal tissues.* J Dent Educ, 2002. **66**(4): p. 564-74.

398. van der Velden, L.A., et al., *Expression of intermediate filament proteins in benign lesions of the oral mucosa.* Eur Arch Otorhinolaryngol, 1999. **256**(10): p. 514-9.

399. Lee, W.Y., L. Cheng, and T.W. Chang, *High grade adenosquamous carcinoma of the breast diagnosed by fine needle aspiration cytology.* Acta Cytol, 1999. **43**(2): p. 323-5.

400. Markey, A.C., et al., *Keratin expression in basal cell carcinomas.* Br J Dermatol, 1992. **126**(2): p. 154-60.

401. Abrahams, N.A., A.H. Ormsby, and J. Brainard, *Validation of cytokeratin 5/6 as an effective substitute for keratin 903 in the differentiation of benign from malignant glands in prostate needle biopsies.* Histopathology, 2002. **41**(1): p. 35-41.

402. Wang, W., A. Bergh, and J.E. Damber, *Morphological transition of proliferative inflammatory atrophy to high-grade intraepithelial neoplasia and cancer in human prostate.* Prostate, 2009. **69**(13): p. 1378-86.

403. Mohammadizadeh, F., et al., *Expression of basal and luminal cytokeratins in breast cancer and their correlation with clinicopathological prognostic variables.* Indian J Med Sci, 2009. **63**(4): p. 152-62.

404. Ribeiro-Silva, A., et al., *p63 correlates with both BRCA1 and cytokeratin 5 in invasive breast carcinomas: further evidence for the pathogenesis of the basal phenotype of breast cancer.* Histopathology, 2005. **47**(5): p. 458-66.

405. Kim, D.S., et al., *Primary malignant mesothelioma developed in liver.* Hepatogastroenterology, 2008. **55**(84): p. 1081-4.

406. Moran, C.A., J. Albores-Saavedra, and S. Suster, *Primary peritoneal mesotheliomas in children: a clinicopathological and immunohistochemical study of eight cases.* Histopathology, 2008. **52**(7): p. 824-30.

407. Ismail, H.M., et al., *Pleural mesothelioma: diagnostic problems and evaluation of prognostic factors.* J Egypt Natl Canc Inst, 2006. **18**(4): p. 303-10.

408. Miettinen, M. and M. Sarlomo-Rikala, *Expression of calretinin, thrombomodulin, keratin 5, and mesothelin in lung carcinomas of different types: an immunohistochemical analysis of 596 tumors in comparison with epithelioid mesotheliomas of the pleura.* Am J Surg Pathol, 2003. **27**(2): p. 150-8.

409. Chu, P.G. and L.M. Weiss, *Expression of cytokeratin 5/6 in epithelial neoplasms: an immunohistochemical study of 509 cases.* Mod Pathol, 2002. **15**(1): p. 6-10.

410. Grin, A., F.P. O'Malley, and A.M. Mulligan, *Cytokeratin 5 and estrogen receptor immunohistochemistry as a useful adjunct in identifying atypical papillary lesions on breast needle core biopsy.* Am J Surg Pathol, 2009. **33**(11): p. 1615-23.

411. Pintens, S., et al., *Triple negative breast cancer: a study from the point of view of basal CK5/6 and HER-1.* J Clin Pathol, 2009. **62**(7): p. 624-8.

412. Tse, G.M., et al., *Breast cancer in the elderly: a histological assessment.* Histopathology, 2009. **55**(4): p. 441-51.

413. van de Rijn, M., et al., *Expression of cytokeratins 17 and 5 identifies a group of breast carcinomas with poor clinical outcome.* Am J Pathol, 2002. **161**(6): p. 1991-6.

414. Hicks, D.G., et al., *Breast cancers with brain metastases are more likely to be estrogen receptor negative, express the basal cytokeratin CK5/6, and overexpress HER2 or EGFR.* Am J Surg Pathol, 2006. **30**(9): p. 1097-104.

415. van Leenders, G.J., et al., *Expression of basal cell keratins in human prostate cancer metastases and cell lines.* J Pathol, 2001. **195**(5): p. 563-70.

416. Ring, B.Z., et al., *A novel five-antibody immunohistochemical test for subclassification of lung carcinoma.* Mod Pathol, 2009. **22**(8): p. 1032-43.

417. Ko, C.J., D.J. Leffell, and J.M. McNiff, *Adenosquamous carcinoma: a report of nine cases with p63 and cytokeratin 5/6 staining.* J Cutan Pathol, 2009. **36**(4): p. 448-52.

418. Khayyata, S., et al., *Value of P63 and CK5/6 in distinguishing squamous cell carcinoma from adenocarcinoma in lung fine-needle aspiration specimens.* Diagn Cytopathol, 2009. **37**(3): p. 178-83.

419. Cury, P.M., et al., *Value of the mesothelium-associated antibodies thrombomodulin, cytokeratin 5/6, calretinin, and CD44H in distinguishing epithelioid pleural*

mesothelioma from adenocarcinoma metastatic to the pleura. Mod Pathol, 2000. **13**(2): p. 107-12.

420. Shield, P.W. and K. Koivurinne, *The value of calretinin and cytokeratin 5/6 as markers for mesothelioma in cell block preparations of serous effusions.* Cytopathology, 2008. **19**(4): p. 218-23.

421. Pons, M., et al., *Activation of Raf-1 is defective in annexin 6 overexpressing Chinese hamster ovary cells.* FEBS Lett, 2001. **501**(1): p. 69-73.

422. Dejmek, J.S. and A. Dejmek, *The reactivity to CK5/6 antibody in tumor cells from non-small cell lung cancers shed into pleural effusions predicts survival.* Oncol Rep, 2006. **15**(3): p. 583-7.

423. Deavers, M.T., et al., *Ovarian sex cord-stromal tumors: an immunohistochemical study including a comparison of calretinin and inhibin.* Mod Pathol, 2003. **16**(6): p. 584-90.

424. Barboro, P., et al., *Proteomic analysis of the nuclear matrix in the early stages of rat liver carcinogenesis: identification of differentially expressed and MAR-binding proteins.* Exp Cell Res, 2009. **315**(2): p. 226-39.

425. Ostergaard, M., et al., *Proteome profiling of bladder squamous cell carcinomas: identification of markers that define their degree of differentiation.* Cancer Res, 1997. **57**(18): p. 4111-7.

426. Freedberg, I.M., et al., *Keratins and the keratinocyte activation cycle.* J Invest Dermatol, 2001. **116**(5): p. 633-40.

427. Kawasaki, S., et al., *Up-regulated gene expression in the conjunctival epithelium of patients with Sjogren's syndrome.* Exp Eye Res, 2003. **77**(1): p. 17-26.

428. Knapp, A.C., et al., *Cytokeratin No. 9, an epidermal type I keratin characteristic of a special program of keratinocyte differentiation displaying body site specificity.* J Cell Biol, 1986. **103**(2): p. 657-67.

429. Moll, I., et al., *Distribution of a special subset of keratinocytes characterized by the expression of cytokeratin 9 in adult and fetal human epidermis of various body sites.* Differentiation, 1987. **33**(3): p. 254-65.

430. Larkin, A., et al., *Monoclonal antibody 5C3 raised against formalin fixed paraffin-embedded invasive breast tumour tissue: characterisation of its reactive antigen via immunoprecipitation and internal sequencing.* J Immunol Methods, 2005. **303**(1-2): p. 53-65.

431. Fu, B.S., et al., *[Serum proteomic analysis on metastasis-associated proteins of hepatocellular carcinoma.].* Nan Fang Yi Ke Da Xue Xue Bao, 2009. **29**(9): p. 1775-8.

432. He, X.S., et al., *[Combined total hepatectomy, orthotopic liver transplantation and pancreatoduodenectomy for unresectable hilar bile duct carcinoma].* Zhonghua Wai Ke Za Zhi, 2006. **44**(5): p. 302-5.

433. Fuchs, E., *Keratins and the skin.* Annu Rev Cell Dev Biol, 1995. **11**: p. 123-53.

434. Maddox, P., et al., *Cytokeratin expression and acetowhite change in cervical epithelium.* J Clin Pathol, 1994. **47**(1): p. 15-7.

435. Hamakawa, H., et al., *Cytokeratin expression in squamous cell carcinoma of the lung and oral cavity: an immunohistochemical study with possible clinical relevance.* Oral Surg Oral Med Oral Pathol Oral Radiol Endod, 1998. **85**(4): p. 438-43.

436. Metcalfe, M.J., D.M. Baker, and G. Burnstock, *Purinoceptor expression on keratinocytes reflects their function on the epidermis during chronic venous insufficiency.* Arch Dermatol Res, 2006. **298**(6): p. 301-7.

437. Peschen, M., et al., *Changes of cytokeratin expression in the epidermis with chronic venous insufficiency.* Vasa, 1997. **26**(2): p. 76-80.

438. Wetzels, R.H., et al., *Laminin and type VII collagen distribution in different types of human lung carcinoma: correlation with expression of keratins 14, 16, 17 and 18.* Histopathology, 1992. **20**(4): p. 295-303.

439. Kurokawa, I., et al., *Cytokeratin expression in subungual squamous cell carcinoma.* J Int Med Res, 2006. **34**(4): p. 441-3.

440. Uehara, F., et al., *[Immunohistochemical localization of MUC 1 and keratin 14 in the invasive regions of malignant eyelid tumors].* Nippon Ganka Gakkai Zasshi, 1997. **101**(11): p. 866-73.

441. Ivanyi, D., et al., *Keratin subtypes in carcinomas of the uterine cervix: implications for histogenesis and differential diagnosis.* Cancer Res, 1990. **50**(16): p. 5143-52.

442. Chu, P.G., M.H. Lyda, and L.M. Weiss, *Cytokeratin 14 expression in epithelial neoplasms: a survey of 435 cases with emphasis on its value in differentiating squamous cell carcinomas from other epithelial tumours.* Histopathology, 2001. **39**(1): p. 9-16.

443. Tse, G.M., et al., *The role of immunohistochemistry for smooth-muscle actin, p63, CD10 and cytokeratin 14 in the differential diagnosis of papillary lesions of the breast.* J Clin Pathol, 2007. **60**(3): p. 315-20.

444. Yamada, A., et al., *Expression of cytokeratin 7 predicts survival in stage I/IIA/IIB squamous cell carcinoma of the esophagus.* Oncol Rep, 2008. **20**(5): p. 1021-7.

445. Boone, J., et al., *Validation of tissue microarray technology in squamous cell carcinoma of the esophagus.* Virchows Arch, 2008. **452**(5): p. 507-14.

446. de Araujo, V.C., et al., *Salivary duct carcinoma: cytokeratin 14 as a marker of in-situ intraductal growth.* Histopathology, 2002. **41**(3): p. 244-9.

447. Wu, P.C., et al., *Hepatocellular carcinoma expressing both hepatocellular and biliary markers also expresses cytokeratin 14, a marker of bipotential progenitor cells.* J Hepatol, 1999. **31**(5): p. 965-6.

448. Tsubokawa, F., et al., *Heterogeneity of expression of cytokeratin subtypes in squamous cell carcinoma of the lung: with special reference to CK14 overexpression in cancer of high-proliferative and lymphogenous metastatic potential.* Pathol Int, 2002. **52**(4): p. 286-93.

449. Shores, C.G., et al., *Clinical evaluation of a new molecular method for detection of micrometastases in head and neck squamous cell carcinoma.* Arch Otolaryngol Head Neck Surg, 2004. **130**(8): p. 937-42.

450. Becker, M.T., et al., *Molecular assay to detect metastatic head and neck squamous cell carcinoma.* Arch Otolaryngol Head Neck Surg, 2004. **130**(1): p. 21-7.

451. Tammen, H., et al., *Expression profiling of breast cancer cells by differential peptide display.* Breast Cancer Res Treat, 2003. **79**(1): p. 83-93.

452. Morgan, P.R. and L. Su, *Intermediate filaments in oral neoplasia. I. Oral cancer and epithelial dysplasia.* Eur J Cancer B Oral Oncol, 1994. **30B**(3): p. 160-6.

453. Moll, R., et al., *The catalog of human cytokeratins: patterns of expression in normal epithelia, tumors and cultured cells.* Cell, 1982. **31**(1): p. 11-24.

454. Rose, A., et al., *Comparative gene and protein expression in primary cultures of epithelial cells from benign prostatic hyperplasia and prostate cancer.* Cancer Lett, 2005. **227**(2): p. 213-22.

455. Bongers, V., et al., *Potential early markers of carcinogenesis in the mucosa of the head and neck using exfoliative cytology.* J Pathol, 1996. **178**(3): p. 284-9.

456. Yoshikawa, K., Y. Katagata, and S. Kondo, *Relative amounts of keratin 17 are higher than those of keratin 16 in hair-follicle-derived tumors in comparison with nonfollicular epithelial skin tumors.* J Invest Dermatol, 1995. **104**(3): p. 396-400.

457. Rafiee, P., et al., *Characterization of the cytokeratins of human colonic, pancreatic, and gastric adenocarcinoma cell lines.* Pancreas, 1992. **7**(2): p. 123-31.

458. Smedts, F., et al., *Expression of keratins 1, 6, 15, 16, and 20 in normal cervical epithelium, squamous metaplasia, cervical intraepithelial neoplasia, and cervical carcinoma.* Am J Pathol, 1993. **142**(2): p. 403-12.

459. Bitterlich, N. and J. Schneider, *Cut-off-independent tumour marker evaluation using ROC approximation.* Anticancer Res, 2007. **27**(6C): p. 4305-10.

460. Racker, E., *Alternate pathways of glucose and fructose metabolism.* Adv Enzymol Relat Subj Biochem, 1954. **15**: p. 141-82.

461. Kochetov, G.A. and N.N. Chernov, *Isoforms of baker's yeast transketolase.* Experientia, 1970. **26**(10): p. 1067-8.

462. Basu, T.K. and J.W. Dickerson, *The thiamin status of early cancer patients with particular reference to those with breast and bronchial carcinomas.* Oncology, 1976. **33**(5-6): p. 250-2.

463. Ayre, J.E. and W.A. Bauld, *Thiamine Deficiency and High Estrogen Findings in Uterine Cancer and in Menorrhagia.* Science, 1946. **103**(2676): p. 441-445.

464. Robinson, D., et al., *A tyrosine kinase profile of prostate carcinoma.* Proc Natl Acad Sci U S A, 1996. **93**(12): p. 5958-62.

465. Vizan, P., et al., *Modulation of pentose phosphate pathway during cell cycle progression in human colon adenocarcinoma cell line HT29.* Int J Cancer, 2009. **124**(12): p. 2789-96.

466. Trebukhina, R.V., et al., *[Transketolase activity and thiamine diphosphate content in oncological patients].* Vopr Med Khim, 1983. **29**(5): p. 100-3.

467. Rubporn, A., et al., *Comparative proteomic analysis of lung cancer cell line and lung fibroblast cell line.* Cancer Genomics Proteomics, 2009. **6**(4): p. 229-37.

468. Sun, J.Y., et al., *[Analysis of differentially expressed lung metastasis-associated proteins in adenoid cystic carcinoma cell lines].* Zhonghua Kou Qiang Yi Xue Za Zhi, 2004. **39**(2): p. 114-7.

469. An, J., et al., *Proteomics analysis of differentially expressed metastasis-associated proteins in adenoid cystic carcinoma cell lines of human salivary gland.* Oral Oncol, 2004. **40**(4): p. 400-8.

470. Corona, G., et al., *Differential proteomic analysis of hepatocellular carcinoma.* Int J Oncol, 2010. **36**(1): p. 93-9.

471. Liu, S., et al., *High-performance liquid chromatography/nano-electrospray ionization tandem mass spectrometry, two-dimensional difference in-gel electrophoresis and gene microarray identification of lymphatic metastasis-associated biomarkers.* Rapid Commun Mass Spectrom, 2008. **22**(20): p. 3172-8.

472. Rais, B., et al., *Oxythiamine and dehydroepiandrosterone induce a G1 phase cycle arrest in Ehrlich's tumor cells through inhibition of the pentose cycle.* FEBS Lett, 1999. **456**(1): p. 113-8.

473. Thomas, A.A., et al., *Synthesis, in vitro and in vivo activity of thiamine antagonist transketolase inhibitors.* Bioorg Med Chem Lett, 2008. **18**(6): p. 2206-10.

474. Paoletti, F., A. Mocali, and D. Tombaccini, *Cysteine proteinases are responsible for characteristic transketolase alterations in Alzheimer fibroblasts.* J Cell Physiol, 1997. **172**(1): p. 63-8.

475. Mai, J., D.M. Waisman, and B.F. Sloane, *Cell surface complex of cathepsin B/annexin II tetramer in malignant progression.* Biochim Biophys Acta, 2000. **1477**(1-2): p. 215-30.

476. Gerke, V. and S.E. Moss, *Annexins: from structure to function.* Physiol Rev, 2002. **82**(2): p. 331-71.

477. Hayes, M.J., et al., *Regulation of actin dynamics by annexin 2.* EMBO J, 2006. **25**(9): p. 1816-26.

478. Cesarman, G.M., C.A. Guevara, and K.A. Hajjar, *An endothelial cell receptor for plasminogen/tissue plasminogen activator (t-PA). II. Annexin II-mediated enhancement of t-PA-dependent plasminogen activation.* J Biol Chem, 1994. **269**(33): p. 21198-203.

479. Kassam, G., et al., *The role of annexin II tetramer in the activation of plasminogen.* J Biol Chem, 1998. **273**(8): p. 4790-9.

480. Balch, C. and J.R. Dedman, *Annexins II and V inhibit cell migration.* Exp Cell Res, 1997. **237**(2): p. 259-63.

481. Diaz, V.M., et al., *Specific interaction of tissue-type plasminogen activator (t-PA) with annexin II on the membrane of pancreatic cancer cells activates plasminogen and promotes invasion in vitro.* Gut, 2004. **53**(7): p. 993-1000.

482. Ling, Q., et al., *Annexin II regulates fibrin homeostasis and neoangiogenesis in vivo.* J Clin Invest, 2004. **113**(1): p. 38-48.

483. Kassam, G., et al., *The p11 subunit of the annexin II tetramer plays a key role in the stimulation of t-PA-dependent plasminogen activation.* Biochemistry, 1998. **37**(48): p. 16958-66.

484. Sharma, M.R., et al., *Angiogenesis-associated protein annexin II in breast cancer: selective expression in invasive breast cancer and contribution to tumor invasion and progression.* Exp Mol Pathol, 2006. **81**(2): p. 146-56.

485. Duncan, R., et al., *Characterisation and protein expression profiling of annexins in colorectal cancer.* Br J Cancer, 2008. **98**(2): p. 426-33.

486. Shiozawa, Y., et al., *Annexin II/annexin II receptor axis regulates adhesion, migration, homing, and growth of prostate cancer.* J Cell Biochem, 2008. **105**(2): p. 370-80.

487. Tchagang, A.B., et al., *Early detection of ovarian cancer using group biomarkers.* Mol Cancer Ther, 2008. **7**(1): p. 27-37.

488. Sodek, K.L., et al., *Identification of pathways associated with invasive behavior by ovarian cancer cells using multidimensional protein identification technology (MudPIT).* Mol Biosyst, 2008. **4**(7): p. 762-73.

489. Shiozawa, Y., et al., *Annexin II/annexin II receptor axis regulates adhesion, migration, homing, and growth of prostate cancer.* J Cell Biochem, 2008. **105**(2): p. 370-80.

490. Sharma, M.R., et al., *Antibody-directed targeting of angiostatin's receptor annexin II inhibits Lewis Lung Carcinoma tumor growth via blocking of plasminogen activation: possible biochemical mechanism of angiostatin's action.* Exp Mol Pathol, 2006. **81**(2): p. 136-45.

491. Brownstein, C., et al., *A mediator of cell surface-specific plasmin generation.* Ann N Y Acad Sci, 2001. **947**: p. 143-55; discussion 155-6.

492. Tatenhorst, L., et al., *Knockdown of annexin 2 decreases migration of human glioma cells in vitro.* Neuropathol Appl Neurobiol, 2006. **32**(3): p. 271-7.

493. Nedjadi, T., et al., *S100A6 binds to annexin 2 in pancreatic cancer cells and promotes pancreatic cancer cell motility.* Br J Cancer, 2009. **101**(7): p. 1145-54.

494. Bao, H., et al., *Overexpression of Annexin II affects the proliferation, apoptosis, invasion and production of proangiogenic factors in multiple myeloma.* Int J Hematol, 2009. **90**(2): p. 177-85.

495. Bellagamba, C., et al., *Tyrosine phosphorylation of annexin II tetramer is stimulated by membrane binding.* J Biol Chem, 1997. **272**(6): p. 3195-9.

496. Gould, K.L., et al., *The protein-tyrosine kinase substrate p36 is also a substrate for protein kinase C in vitro and in vivo.* Mol Cell Biol, 1986. **6**(7): p. 2738-44.

497. Laumonnier, Y., et al., *Identification of the annexin A2 heterotetramer as a receptor for the plasmin-induced signaling in human peripheral monocytes.* Blood, 2006. **107**(8): p. 3342-9.

498. Tsunezumi, J., et al., *Matrilysin (matrix metalloprotease-7) cleaves membrane-bound annexin II and enhances binding of tissue-type plasminogen activator to cancer cell surfaces.* Febs J, 2008. **275**(19): p. 4810-23.

499. Clifton, J.G., et al., *Identification of members of the annexin family in the detergent-insoluble fraction of rat Morris hepatoma plasma membranes.* J Chromatogr A, 2006. **1123**(2): p. 205-11.

500. Jung, Y., et al., *Annexin II expressed by osteoblasts and endothelial cells regulates stem cell adhesion, homing, and engraftment following transplantation.* Blood, 2007. **110**(1): p. 82-90.

501. Kube, E., et al., *Protein-protein interaction studied by site-directed mutagenesis. Characterization of the annexin II-binding site on p11, a member of the S100 protein family.* J Biol Chem, 1992. **267**(20): p. 14175-82.

502. Gerke, V., C.E. Creutz, and S.E. Moss, *Annexins: linking Ca2+ signalling to membrane dynamics.* Nat Rev Mol Cell Biol, 2005. **6**(6): p. 449-61.

503. Davies, A.A., et al., *Nonidet P-40 extraction of lymphocyte plasma membrane. Characterization of the insoluble residue.* Biochem J, 1984. **219**(1): p. 301-8.

504. Owens, R.J. and M.J. Crumpton, *Isolation and characterization of a novel 68,000-Mr Ca2+-binding protein of lymphocyte plasma membrane.* Biochem J, 1984. **219**(1): p. 309-16.

505. Owens, R.J., C.J. Gallagher, and M.J. Crumpton, *Cellular distribution of p68, a new calcium-binding protein from lymphocytes.* Embo J, 1984. **3**(5): p. 945-52.

506. Shadle, P.J., V. Gerke, and K. Weber, *Three Ca2+-binding proteins from porcine liver and intestine differ immunologically and physicochemically and are distinct in Ca2+ affinities.* J Biol Chem, 1985. **260**(30): p. 16354-60.

507. Doubell, A.F., et al., *Identification and immunolocalisation of annexins V and VI, the major cardiac annexins, in rat heart.* Cardiovasc Res, 1993. **27**(7): p. 1359-67.

508. Luckcuck, T., P.J. Trotter, and J.H. Walker, *Localization of annexin VI in the adult and neonatal heart.* Cell Biol Int, 1998. **22**(3): p. 199-205.

509. Babiychuk, E.B. and A. Draeger, *Annexins in cell membrane dynamics. Ca(2+)-regulated association of lipid microdomains.* J Cell Biol, 2000. **150**(5): p. 1113-24.

510. Schmitz-Peiffer, C., et al., *Activated protein kinase C alpha associates with annexin VI from skeletal muscle.* Biochem J, 1998. **330 (Pt 2)**: p. 675-81.

511. Grewal, T., et al., *Annexin A6 stimulates the membrane recruitment of p120GAP to modulate Ras and Raf-1 activity.* Oncogene, 2005. **24**(38): p. 5809-20.

512. Bode, G., et al., *Interaction between S100A8/A9 and annexin A6 is involved in the calcium-induced cell surface exposition of S100A8/A9.* J Biol Chem, 2008. **283**(46): p. 31776-84.

513. Francia, G., et al., *Identification by differential display of annexin-VI, a gene differentially expressed during melanoma progression.* Cancer Res, 1996. **56**(17): p. 3855-8.

514. Theobald, J., et al., *Expression of annexin VI in A431 carcinoma cells suppresses proliferation: a possible role for annexin VI in cell growth regulation.* Biochim Biophys Acta, 1994. **1223**(3): p. 383-90.

515. Hawkins, T.E., et al., *Immunological development and cardiovascular function are normal in annexin VI null mutant mice.* Mol Cell Biol, 1999. **19**(12): p. 8028-32.

516. Rodriguez-Ariza, A., et al., *Altered protein expression and protein nitration pattern during d-galactosamine-induced cell death in human hepatocytes: a proteomic analysis.* Liver Int, 2005. **25**(6): p. 1259-69.

517. Ryazanov, A.G. and A.S. Spirin, *Phosphorylation of elongation factor 2: a key mechanism regulating gene expression in vertebrates.* New Biol, 1990. **2**(10): p. 843-50.

518. Marzouki, A., et al., *Effect of ADP-ribosylation and phosphorylation on the interaction of elongation factor 2 with guanylic nucleotides.* Biochimie, 1991. **73**(7-8): p. 1151-6.

519. White, S.J., et al., *Doxorubicin generates a proapoptotic phenotype by phosphorylation of elongation factor 2.* Free Radic Biol Med, 2007. **43**(9): p. 1313-21.

520. Nakamura, J., et al., *Overexpression of eukaryotic elongation factor eEF2 in gastrointestinal cancers and its involvement in G2/M progression in the cell cycle.* Int J Oncol, 2009. **34**(5): p. 1181-9.

521. Agnelli, L., et al., *Molecular classification of multiple myeloma: a distinct transcriptional profile characterizes patients expressing CCND1 and negative for 14q32 translocations.* J Clin Oncol, 2005. **23**(29): p. 7296-306.

522. Yim, E.K., et al., *Genomic and proteomic expression patterns in HPV-16 E6 gene transfected stable human carcinoma cell lines.* DNA Cell Biol, 2004. **23**(12): p. 826-35.

523. Pavlides Stephanos, T.A., Vera Iset, Flomenberg Neal, Frank Philippe G., Casimiro Mathew C., Wang Chenguang, Pestell Richard G., Ubaldo E.Martinez-Outschoorn, Howell Anthony, Sotgia Federica, and Lisanti Michael P., *Transcriptional evidence for the "Reverse Warburg Effect" in human breast cancer tumor stroma and metastasis: Similarities with oxidative stress, inflammation, Alzheimer's disease, and "Neuron-Glia Metabolic Coupling"* Aging, 2010. **2**(4): p. 133-149.

524. Fernandez-Madrid, F., et al., *Autoantibodies to Annexin XI-A and Other Autoantigens in the Diagnosis of Breast Cancer.* Cancer Res, 2004. **64**(15): p. 5089-96.

525. Li, L., et al., *Identification of hepatocellular-carcinoma-associated antigens and autoantibodies by serological proteome analysis combined with protein microarray.* J Proteome Res, 2008. **7**(2): p. 611-20.

526. Suzuki, A., et al., *Identification of melanoma antigens using a Serological Proteome Approach (SERPA).* Cancer Genomics Proteomics, 2010. **7**(1): p. 17-23.

527. Li, S.L., et al., *Quantitative proteome analysis of multidrug resistance in human ovarian cancer cell line.* J Cell Biochem, 2010. **109**(4): p. 625-33.

528. Nilsson, L. and O. Nygard, *Structural and functional studies of the interaction of the eukaryotic elongation factor EF-2 with GTP and ribosomes.* Eur J Biochem, 1988. **171**(1-2): p. 293-9.

529. Skonier, J., et al., *cDNA cloning and sequence analysis of beta ig-h3, a novel gene induced in a human adenocarcinoma cell line after treatment with transforming growth factor-beta.* DNA Cell Biol, 1992. **11**(7): p. 511-22.

530. Gibson, M.A., J.S. Kumaratilake, and E.G. Cleary, *Immunohistochemical and ultrastructural localization of MP78/70 (betaig-h3) in extracellular matrix of developing and mature bovine tissues.* J Histochem Cytochem, 1997. **45**(12): p. 1683-96.

531. Hashimoto, K., et al., *Characterization of a cartilage-derived 66-kDa protein (RGD-CAP/beta ig-h3) that binds to collagen.* Biochim Biophys Acta, 1997. **1355**(3): p. 303-14.

532. Munier, F.L., et al., *Kerato-epithelin mutations in four 5q31-linked corneal dystrophies.* Nat Genet, 1997. **15**(3): p. 247-51.

533. Gibson, M.A., J.S. Kumaratilake, and E.G. Cleary, *The protein components of the 12-nanometer microfibrils of elastic and nonelastic tissues.* J Biol Chem, 1989. **264**(8): p. 4590-8.

534. Schorderet, D.F., et al., *Genomic characterization and embryonic expression of the mouse Bigh3 (Tgfbi) gene.* Biochem Biophys Res Commun, 2000. **274**(2): p. 267-74.

535. Ohno, S., et al., *RGD-CAP ((beta)ig-h3) enhances the spreading of chondrocytes and fibroblasts via integrin alpha(1)beta(1).* Biochim Biophys Acta, 1999. **1451**(1): p. 196-205.

536. Kim, J.E., et al., *Identification of motifs for cell adhesion within the repeated domains of transforming growth factor-beta-induced gene, betaig-h3.* J Biol Chem, 2000. **275**(40): p. 30907-15.

537. Park, S.W., et al., *Beta ig-h3 promotes renal proximal tubular epithelial cell adhesion, migration and proliferation through the interaction with alpha3beta1 integrin.* Exp Mol Med, 2004. **36**(3): p. 211-9.

538. Nam, J.O., et al., *Identification of the alphavbeta3 integrin-interacting motif of betaig-h3 and its anti-angiogenic effect.* J Biol Chem, 2003. **278**(28): p. 25902-9.

539. Nam, E.J., et al., *Up-regulated transforming growth factor beta-inducible gene h3 in rheumatoid arthritis mediates adhesion and migration of synoviocytes through alpha v beta3 integrin: Regulation by cytokines.* Arthritis Rheum, 2006. **54**(9): p. 2734-44.

540. Thapa, N., K.B. Kang, and I.S. Kim, *Beta ig-h3 mediates osteoblast adhesion and inhibits differentiation.* Bone, 2005. **36**(2): p. 232-42.

541. Lee, B.H., et al., *betaig-h3 triggers signaling pathways mediating adhesion and migration of vascular smooth muscle cells through alphavbeta5 integrin.* Exp Mol Med, 2006. **38**(2): p. 153-61.

542. Kim, J.E., et al., *Identification of motifs in the fasciclin domains of the transforming growth factor-beta-induced matrix protein betaig-h3 that interact with the alphavbeta5 integrin.* J Biol Chem, 2002. **277**(48): p. 46159-65.

543. Kim, M.O., et al., *Transforming growth factor-beta-inducible gene-h3 (beta(ig)-h3) promotes cell adhesion of human astrocytoma cells in vitro: implication of alpha6beta4 integrin.* Neurosci Lett, 2003. **336**(2): p. 93-6.

544. Ferguson, J.W., et al., *The extracellular matrix protein betaIG-H3 is expressed at myotendinous junctions and supports muscle cell adhesion.* Cell Tissue Res, 2003. **313**(1): p. 93-105.

545. Dokmanovic, M., et al., *Retinoid-induced growth arrest of breast carcinoma cells involves co-activation of multiple growth-inhibitory genes.* Cancer Biol Ther, 2002. **1**(1): p. 24-7.

546. Gratchev, A., et al., *Alternatively activated macrophages differentially express fibronectin and its splice variants and the extracellular matrix protein betaIG-H3.* Scand J Immunol, 2001. **53**(4): p. 386-92.

547. Skonier, J., et al., *beta ig-h3: a transforming growth factor-beta-responsive gene encoding a secreted protein that inhibits cell attachment in vitro and suppresses the growth of CHO cells in nude mice.* DNA Cell Biol, 1994. **13**(6): p. 571-84.

548. Yun, S.J., et al., *Induction of TGF-beta-inducible gene-h3 (betaig-h3) by TGF-beta1 in astrocytes: implications for astrocyte response to brain injury.* Brain Res Mol Brain Res, 2002. **107**(1): p. 57-64.

549. Schneider, D., et al., *Induction and expression of betaig-h3 in pancreatic cancer cells.* Biochim Biophys Acta, 2002. **1588**(1): p. 1-6.

550. Walker, G., et al., *Estrogen-regulated gene expression predicts response to endocrine therapy in patients with ovarian cancer.* Gynecol Oncol, 2007. **106**(3): p. 461-8.

551. Ahmed, A.A., et al., *The extracellular matrix protein TGFBI induces microtubule stabilization and sensitizes ovarian cancers to paclitaxel.* Cancer Cell, 2007. **12**(6): p. 514-27.

552. Gilbert, R.E., et al., *Renal expression of transforming growth factor-beta inducible gene-h3 (beta ig-h3) in normal and diabetic rats.* Kidney Int, 1998. **54**(4): p. 1052-62.

553. Lee, S.H., et al., *Expression of TGF-beta-induced matrix protein betaig-h3 is up-regulated in the diabetic rat kidney and human proximal tubular epithelial cells treated with high glucose.* Kidney Int, 2003. **64**(3): p. 1012-21.

554. Billings, P.C., et al., *The transforming growth factor-beta-inducible matrix protein (beta)ig-h3 interacts with fibronectin.* J Biol Chem, 2002. **277**(31): p. 28003-9.

555. Wang, M., et al., *TGFBI gene transcript is transforming growth factor-beta1-responsive and cell density-dependent in a human corneal epithelial cell line.* Ophthalmic Genet, 2002. **23**(4): p. 237-45.

556. Ha, S.W., et al., *TGF-beta-induced protein beta ig-h3 is upregulated by high glucose in vascular smooth muscle cells.* J Cell Biochem, 2003. **88**(4): p. 774-82.

557. Bae, J.S., et al., *Betaig-h3 supports keratinocyte adhesion, migration, and proliferation through alpha3beta1 integrin.* Biochem Biophys Res Commun, 2002. **294**(5): p. 940-8.

558. Katz, A.B. and L.B. Taichman, *A partial catalog of proteins secreted by epidermal keratinocytes in culture.* J Invest Dermatol, 1999. **112**(5): p. 818-21.

559. LeBaron, R.G., et al., *Beta IG-H3, a novel secretory protein inducible by transforming growth factor-beta, is present in normal skin and promotes the adhesion and spreading of dermal fibroblasts in vitro.* J Invest Dermatol, 1995. **104**(5): p. 844-9.

560. Hanssen, E., B. Reinboth, and M.A. Gibson, *Covalent and non-covalent interactions of betaig-h3 with collagen VI. Beta ig-h3 is covalently attached to the amino-terminal region of collagen VI in tissue microfibrils.* J Biol Chem, 2003. **278**(27): p. 24334-41.

561. Reinboth, B., et al., *Beta ig-h3 interacts directly with biglycan and decorin, promotes collagen VI aggregation, and participates in ternary complexing with these macromolecules.* J Biol Chem, 2006. **281**(12): p. 7816-24.

562. Ha, S.W., et al., *Elevation of urinary betaig-h3, transforming growth factor-beta-induced protein in patients with type 2 diabetes and nephropathy.* Diabetes Res Clin Pract, 2004. **65**(2): p. 167-73.

563. Bjornson Granqvist, A., et al., *Podocyte proteoglycan synthesis is involved in the development of nephrotic syndrome.* Am J Physiol Renal Physiol, 2006. **291**(4): p. F722-30.

564. Thapa, N., B.H. Lee, and I.S. Kim, *TGFBIp/betaig-h3 protein: a versatile matrix molecule induced by TGF-beta.* Int J Biochem Cell Biol, 2007. **39**(12): p. 2183-94.

565. Kim, H.J. and I.S. Kim, *Transforming growth factor-beta-induced gene product, as a novel ligand of integrin alphaMbeta2, promotes monocytes adhesion, migration and chemotaxis.* Int J Biochem Cell Biol, 2008. **40**(5): p. 991-1004.

566. O'Brien, E.R., et al., *Beta ig-h3, a transforming growth factor-beta-inducible gene, is overexpressed in atherosclerotic and restenotic human vascular lesions.* Arterioscler Thromb Vasc Biol, 1996. **16**(4): p. 576-84.

567. Dieudonne, S.C., et al., *Differential display of human marrow stromal cells reveals unique mRNA expression patterns in response to dexamethasone.* J Cell Biochem, 1999. **76**(2): p. 231-43.

568. Monticone, M., et al., *Gene expression profile of human bone marrow stromal cells determined by restriction fragment differential display analysis.* J Cell Biochem, 2004. **92**(4): p. 733-44.

569. Rawe, I.M., et al., *Beta-ig. Molecular cloning and in situ hybridization in corneal tissues.* Invest Ophthalmol Vis Sci, 1997. **38**(5): p. 893-900.

570. Li, C., et al., *Inhibitory effect of pravastatin on transforming growth factor beta1-inducible gene h3 expression in a rat model of chronic cyclosporine nephropathy.* Am J Nephrol, 2005. **25**(6): p. 611-20.

571. Uekita, T., et al., *Dynamics of betaig-h3 mRNA expression during pregnancy in the uterus and the placenta of the mouse: a possible regulatory factor for trophoblastic invasion.* J Reprod Dev, 2003. **49**(3): p. 243-52.

572. Carson, D.D., et al., *Changes in gene expression during the early to mid-luteal (receptive phase) transition in human endometrium detected by high-density microarray screening.* Mol Hum Reprod, 2002. **8**(9): p. 871-9.

573. Hedegaard, C.J., et al., *Transforming growth factor beta induced protein accumulation in granular corneal dystrophy type III (Reis-Bucklers dystrophy). Identification by mass spectrometry in 15 year old two-dimensional protein gels.* Mol Vis, 2003. **9**: p. 355-9.

574. Konishi, M., et al., *Immunohistology of kerato-epithelin in corneal stromal dystrophies associated with R124 mutations of the BIGH3 gene.* Curr Eye Res, 2000. **21**(5): p. 891-6.

575. Korvatska, E., et al., *On the role of kerato-epithelin in the pathogenesis of 5q31-linked corneal dystrophies.* Invest Ophthalmol Vis Sci, 1999. **40**(10): p. 2213-9.

576. Streeten, B.W., et al., *Immunolocalization of beta ig-h3 protein in 5q31-linked corneal dystrophies and normal corneas.* Arch Ophthalmol, 1999. **117**(1): p. 67-75.

577. Cha, D.R., et al., *Urinary concentration of transforming growth factor-beta-inducible gene-h3(beta ig-h3) in patients with Type 2 diabetes mellitus.* Diabet Med, 2005. **22**(1): p. 14-20.

578. Calaf, G.M., et al., *BigH3 protein expression as a marker for breast cancer.* Int J Mol Med, 2008. **21**(5): p. 561-8.

579. Sasaki, H., et al., *Beta IGH3, a TGF-beta inducible gene, is overexpressed in lung cancer.* Jpn J Clin Oncol, 2002. **32**(3): p. 85-9.

580. Ivanov, S.V., et al., *Two novel VHL targets, TGFBI (BIGH3) and its transactivator KLF10, are up-regulated in renal clear cell carcinoma and other tumors.* Biochem Biophys Res Commun, 2008. **370**(4): p. 536-40.

581. Yamanaka, M., et al., *BIGH3 is overexpressed in clear cell renal cell carcinoma.* Oncol Rep, 2008. **19**(4): p. 865-74.

582. Hourihan, R.N., G.C. O'Sullivan, and J.G. Morgan, *Transcriptional gene expression profiles of oesophageal adenocarcinoma and normal oesophageal tissues.* Anticancer Res, 2003. **23**(1A): p. 161-5.

583. Kitahara, O., et al., *Alterations of gene expression during colorectal carcinogenesis revealed by cDNA microarrays after laser-capture microdissection of tumor tissues and normal epithelia.* Cancer Res, 2001. **61**(9): p. 3544-9.

584. Golembieski, W.A. and S.A. Rempel, *cDNA array analysis of SPARC-modulated changes in glioma gene expression.* J Neurooncol, 2002. **60**(3): p. 213-26.

585. Aitkenhead, M., et al., *Identification of endothelial cell genes expressed in an in vitro model of angiogenesis: induction of ESM-1, (beta)ig-h3, and NrCAM.* Microvasc Res, 2002. **63**(2): p. 159-71.

586. Zajchowski, D.A., et al., *Identification of gene expression profiles that predict the aggressive behavior of breast cancer cells.* Cancer Res, 2001. **61**(13): p. 5168-78.

587. Zhao, Y., M. El-Gabry, and T.K. Hei, *Loss of Betaig-h3 protein is frequent in primary lung carcinoma and related to tumorigenic phenotype in lung cancer cells.* Mol Carcinog, 2006. **45**(2): p. 84-92.

588. Shao, G., et al., *Epigenetic inactivation of Betaig-h3 gene in human cancer cells.* Cancer Res, 2006. **66**(9): p. 4566-73.

589. Zhao, Y.L., C.Q. Piao, and T.K. Hei, *Downregulation of Betaig-h3 gene is causally linked to tumorigenic phenotype in asbestos treated immortalized human bronchial epithelial cells.* Oncogene, 2002. **21**(49): p. 7471-7.

590. Zhao, Y.L., C.Q. Piao, and T.K. Hei, *Overexpression of Betaig-h3 gene downregulates integrin alpha5beta1 and suppresses tumorigenicity in radiation-induced tumorigenic human bronchial epithelial cells.* Br J Cancer, 2002. **86**(12): p. 1923-8.

591. Becker, J., et al., *Keratoepithelin suppresses the progression of experimental human neuroblastomas.* Cancer Res, 2006. **66**(10): p. 5314-21.

592. Jeong, H.W. and I.S. Kim, *TGF-beta1 enhances betaig-h3-mediated keratinocyte cell migration through the alpha3beta1 integrin and PI3K.* J Cell Biochem, 2004. **92**(4): p. 770-80.

593. Kim, J.E., et al., *RGD peptides released from beta ig-h3, a TGF-beta-induced cell-adhesive molecule, mediate apoptosis.* Oncogene, 2003. **22**(13): p. 2045-53.

594. Zamilpa, R., et al., *C-terminal fragment of transforming growth factor beta-induced protein (TGFBIp) is required for apoptosis in human osteosarcoma cells.* Matrix Biol, 2009.

595. Park, S.J., et al., *Conformational resemblance between the structures of integrin-activating pentapetides derived from betaig-h3 and RGD peptide analogues in a membrane environment.* Peptides, 2004. **25**(2): p. 199-205.

596. Tang, J., et al., *BetaIg-h3 is involved in the HAb18G/CD147-mediated metastasis process in human hepatoma cells.* Exp Biol Med (Maywood), 2007. **232**(3): p. 344-52.

597. Ma, C., et al., *Extracellular matrix protein {beta}ig-h3/TGFBI promotes metastasis of colon cancer by enhancing cell extravasation.* Genes Dev, 2008. **22**(3): p. 308-21.

598. Tang, J., et al., *Betaig-h3 interacts with alpha3beta1 integrin to promote adhesion and migration of human hepatoma cells.* Exp Biol Med (Maywood), 2009. **234**(1): p. 35-9.

599. Galardy, R.E., et al., *Low molecular weight inhibitors in corneal ulceration.* Ann N Y Acad Sci, 1994. **732**: p. 315-23.

600. Ricciardelli, C., et al., *Androgen receptor levels in prostate cancer epithelial and peritumoral stromal cells identify non-organ confined disease.* Prostate, 2005. **63**(1): p. 19-28.

601. Irigoyen, M., et al., *TGFbeta-induced protein mediates lymphatic endothelial cell adhesion to the extracellular matrix under low oxygen conditions.* Cell Mol Life Sci, 2008. **65**(14): p. 2244-55.

602. Andersen, R.B., et al., *Purification and structural characterization of transforming growth factor beta induced protein (TGFBIp) from porcine and human corneas.* Biochemistry, 2004. **43**(51): p. 16374-84.

603. Zhang, Y., et al., *TGFBI deficiency predisposes mice to spontaneous tumor development.* Cancer Res, 2009. **69**(1): p. 37-44.

604. Nam, J.O., et al., *Regulation of tumor angiogenesis by fastatin, the fourth FAS1 domain of betaig-h3, via alphavbeta3 integrin.* Cancer Res, 2005. **65**(10): p. 4153-61.

605. Balic, M., et al., *Most early disseminated cancer cells detected in bone marrow of breast cancer patients have a putative breast cancer stem cell phenotype.* Clin Cancer Res, 2006. **12**(19): p. 5615-21.

606. Clout, N.J. and E. Hohenester, *A model of FAS1 domain 4 of the corneal protein beta(ig)-h3 gives a clearer view on corneal dystrophies.* Mol Vis, 2003. **9**: p. 440-8.

607. Witz, C.A., et al., *Expression of the alpha2beta1 and alpha3beta1 integrins at the surface of mesothelial cells: a potential attachment site of endometrial cells.* Fertil Steril, 2000. **74**(3): p. 579-84.

608. Heyman, L., et al., *Vitronectin and its receptors partly mediate adhesion of ovarian cancer cells to peritoneal mesothelium in vitro.* Tumour Biol, 2008. **29**(4): p. 231-44.

609. Park, Y.H., et al., *Effects of hepatocyte growth factor on the expression of matrix metalloproteinases and their tissue inhibitors during the endometrial cancer invasion in a three-dimensional coculture.* Int J Gynecol Cancer, 2003. **13**(1): p. 53-60.

610. Ahmed, N., et al., *Ascites induces modulation of alpha6beta1 integrin and urokinase plasminogen activator receptor expression and associated functions in ovarian carcinoma.* Br J Cancer, 2005. **92**(8): p. 1475-85.

611. Liotta, L.A. and E.C. Kohn, *The microenvironment of the tumour-host interface.* Nature, 2001. **411**(6835): p. 375-9.

612. Zigrino, P., S. Loffek, and C. Mauch, *Tumor-stroma interactions: their role in the control of tumor cell invasion.* Biochimie, 2005. **87**(3-4): p. 321-8.

613. Ricciardelli, C. and R.J. Rodgers, *Extracellular matrix of ovarian tumors.* Semin Reprod Med, 2006. **24**(4): p. 270-82.

614. He, W., J. Chang, and J. Zhang, *[A research on serum, urine and tumor tissue hyaluronate assays for detecting malignant ovarian tumors].* Zhonghua Fu Chan Ke Za Zhi, 1995. **30**(3): p. 161-3.

615. Ricciardelli, C., et al., *Elevated levels of versican but not decorin predict disease progression in early-stage prostate cancer.* Clin.Cancer Res., 1998. **4**(4): p. 963-971.

616. Hanekamp, E.E., et al., *Consequences of loss of progesterone receptor expression in development of invasive endometrial cancer.* Clin Cancer Res, 2003. **9**(11): p. 4190-9.

617. Pukkila, M.J., et al., *Versican expression in pharyngeal squamous cell carcinoma: an immunohistochemical study.* J Clin Pathol, 2004. **57**(7): p. 735-9.

618. Pirinen, R., et al., *Versican in nonsmall cell lung cancer: relation to hyaluronan, clinicopathologic factors, and prognosis.* Hum Pathol, 2005. **36**(1): p. 44-50.

619. Pukkila, M., et al., *High stromal versican expression predicts unfavourable outcome in oral squamous cell carcinoma.* J Clin Pathol, 2007. **60**(3): p. 267-72.

620. Lu, K.H., et al., *Selection of potential markers for epithelial ovarian cancer with gene expression arrays and recursive descent partition analysis.* Clin Cancer Res, 2004. **10**(10): p. 3291-300.

621. Bast, R.C., *Early Detection of Ovarian Cancer: New Technologies in Pursuit of a Disease that is Neither Common nor Rare.* Trans Am Clin Climatol Assoc, 2004. **115**: p. 233-48.

622. Bignotti, E., et al., *Gene expression profile of ovarian serous papillary carcinomas: identification of metastasis-associated genes.* Am J Obstet Gynecol, 2007. **196**(3): p. 245 e1-11.

623. Knudson, W., et al., *CD44-anchored hyaluronan-rich pericellular matrices: an ultrastructural and biochemical analysis.* Exp.Cell Res., 1996. **228**(2): p. 216-228.

624. Delpech, B., et al., *Serum hyaluronan (hyaluronic acid) in breast cancer patients.* Int J Cancer, 1990. **46**(3): p. 388-90.

625. De Wever, O. and M. Mareel, *Role of tissue stroma in cancer cell invasion.* J Pathol, 2003. **200**(4): p. 429-47.

626. Ronnov-Jessen, L., et al., *Cellular changes involved in conversion of normal to malignant breast: importance of the stromal reaction.* Physiol Rev, 1996. **76**(1): p. 69-125.

627. Tuxhorn, J.A., et al., *Reactive stroma in human prostate cancer: induction of myofibroblast phenotype and extracellular matrix remodeling.* Clin Cancer Res, 2002. **8**(9): p. 2912-23.

628. Soltermann, A., et al., *Prognostic significance of epithelial-mesenchymal and mesenchymal-epithelial transition protein expression in non-small cell lung cancer.* Clin Cancer Res, 2008. **14**(22): p. 7430-7.

629. Reichert, R.A., *Primary ovarian adenofibromatous neoplasms with mucin-containing signet-ring cells: a report of 2 cases.* Int J Gynecol Pathol, 2007. **26**(2): p. 165-72.

630. Brown, T.J., et al., *Activation of SPARC expression in reactive stroma associated with human epithelial ovarian cancer.* Gynecol Oncol, 1999. **75**(1): p. 25-33.

631. Tzuman, Y.C., et al., *Peritoneal adhesion and angiogenesis in ovarian carcinoma are inversely regulated by hyaluronan: the role of gonadotropins.* Neoplasia, 2010. **12**(1): p. 51-60.

632. Stern, R., A.A. Asari, and K.N. Sugahara, *Hyaluronan fragments: an information-rich system.* Eur J Cell Biol, 2006. **85**(8): p. 699-715.

633. Ghatak, S., S. Misra, and B.P. Toole, *Hyaluronan oligosaccharides inhibit anchorage-independent growth of tumor cells by suppressing the phosphoinositide 3-kinase/Akt cell survival pathway.* J Biol Chem, 2002. **277**(41): p. 38013-20.

The supplementary video will not play on some computers which do not have the correct video codecs installed.

If you find you are having difficulties, please search for a VLC media player (VLC program).